VOL. 585 NO. 2 NOVEMBER 1, 1991

JOURNAL OF CHROMATOGRAPHY

INCLUDING ELECTROPHORESIS AND OTHER SEPARATION METHODS

ELSEVIER

JOURNAL OF CHROMATOGRAPHY

INCLUDING ELECTROPHORESIS AND OTHER SEPARATION METHODS

Scope. The *Journal of Chromatography* publishes papers on all aspects of chromatography, electrophoresis and related methods. Contributions consist mainly of research papers dealing with chromatographic theory, instrumental development and their applications. The section *Biomedical Applications*, which is under separate editorship, deals with the following aspects: developments in and applications of chromatographic and electrophoretic techniques related to clinical diagnosis or alterations during medical treatment; screening and profiling of body fluids or tissues with special reference to metabolic disorders; results from basic medical research with direct consequences in clinical practice; drug level monitoring and pharmacokinetic studies; clinical toxicology; analytical studies in occupational medicine.

Submission of Papers. Manuscripts (in English; *four* copies are required) should be submitted to: Editorial Office of *Journal of Chromatography*, P.O. Box 681, 1000 AR Amsterdam, Netherlands, Telefax (+31-20) 5862 304, or to: The Editor of *Journal of Chromatography, Biomedical Applications*, P.O. Box 681, 1000 AR Amsterdam, Netherlands. Review articles are invited or proposed by letter to the Editors. An outline of the proposed review should first be forwarded to the Editors for preliminary discussion prior to preparation. Submission of an article is understood to imply that the article is original and unpublished and is not being considered for publication elsewhere. For copyright regulations, see below.

Publication. The *Journal of Chromatography* (incl. *Biomedical Applications*) has 39 volumes in 1992. The subscription prices for 1992 are:

J. Chromatogr. (incl. *Cum. Indexes, Vols. 551–600*) + *Biomed. Appl.* (Vols. 573–611):
Dfl. 7722.00 plus Dfl. 1209.00 (p.p.h.) (total *ca.* US$ 4421.25)

J. Chromatogr. (incl. *Cum. Indexes, Vols. 551–600*) only (Vols. 585–611):
Dfl. 6210.00 plus Dfl. 837.00 (p.p.h.) (total *ca.* US$ 3488.50)

Biomed. Appl. only (Vols. 573–584):
Dfl. 2760.00 plus Dfl. 372.00 (p.p.h.) (total *ca.* US$ 1550.50).

Subscription Orders. The Dutch guilder price is definitive. The US$ price is subject to exchange-rate fluctuations and is given as a guide. Subscriptions are accepted on a prepaid basis only, unless different terms have been previously agreed upon. Subscriptions orders can be entered only by calender year (Jan.–Dec.) and should be sent to Elsevier Science Publishers, Journal Department, P.O. Box 211, 1000 AE Amsterdam, Netherlands, Tel. (+31-20) 5803 642, Telefax (+31-20) 5803 598, or to your usual subscription agent. Postage and handling charges include surface delivery except to the following countries where air delivery via SAL (Surface Air Lift) mail is ensured: Argentina, Australia, Brazil, Canada, Hong Kong, India, Israel, Japan*, Malaysia, Mexico, New Zealand, Pakistan, PR CHina, Singapore, South Africa, South Korea, Taiwan, Thailand, USA. *For Japan air delivery (SAL) requires 25% additional charge of the normal postage and handling charge. For all other countries airmail rates are available upon request. Claims for missing issues must be made within three months of our publication (mailing) date, otherwise such claims cannot be honoured free of charge. Back volumes of the *Journal of Chromatography* (Vols. 1–572) are available at Dfl. 208.00 (plus postage). Customers in the USA and Canada wishing information on this and other Elsevier journals, please contact Journal Information Center, Elsevier Science Publishing Co. Inc., 655 Avenue of the Americas, New York, NY 10010, USA, Tel. (+1-212) 633 3750, Telefax (+1-212) 633 3990.

Abstracts/Contents Lists published in Analytical Abstracts, Biochemical Abstracts, Biological Abstracts, Chemical Abstracts, Chemical Titles, Chromatography Abstracts, Clinical Chemistry Lookout, Current Contents/Life Sciences, Current Contents/Physical, Chemical & Earth Sciences, Deep-Sea Research/Part B: Oceanographic Literature Review, Excerpta Medica, Index Medicus, Mass Spectrometry Bulletin, PASCAL-CNRS, Pharmaceutical Abstracts, Referativnyi Zhurnal, Research Alert, Science Citation Index and Trends in Biotechnology.

See inside back cover for Publication Schedule, Information for Authors and information on Advertisements.

0021-9673/91/$03.50

Printed in the Netherlands

CONTENTS

(Abstracts/Contents Lists published in Analytical Abstracts, Biochemical Abstracts, Biological Abstracts, Chemical Abstracts, Chemical Titles, Chromatography Abstracts, Current Contents/Life Sciences, Current Contents/Physical, Chemical & Earth Sciences, Deep-Sea Research/Part B: Oceanographic Literature Review, Excerpta Medica, Index Medicus, Mass Spectrometry Bulletin, PASCAL-CRNS, Referativnyi Zhurnal, Research Alert and Science Citation Index)

REGULAR PAPERS

Column Liquid Chromatography

Gas Chromatography

(Continued overleaf)

Electrophoresis

In articles with more than one author, the name of the author to whom correspondence should be addressed is indicated in the article heading by a 6-pointed asterisk (*)

An authoritative review... highly recommended...

Optimization of Chromatographic Selectivity

A Guide to Method Development

by **P. Schoenmakers,** *Philips Research Laboratories, Eindhoven, The Netherlands*

(Journal of Chromatography Library, 35)

"The contents of this book have been put together with great expertise and care, and represent an authoritative review of this very timely topic... highly recommended to practising analytical chemists and to advanced students." (Jnl. of Chromatography)

"...an important contribution by a worker who has been in the field almost from its inception and who understands that field as well as anyone. If one is serious about method development, particularly for HPLC, this book will well reward a careful reading and will continue to be useful for reference purposes." (Mag. of Liquid & Gas Chromatography)

This is the first detailed description of method development in chromatography - the overall process of which may be summarized as: method selection, phase selection, selectivity optimization, and system optimization. All four aspects receive attention in this eminently readable book.

The first chapter describes chromatographic theory and nomenclature and outlines the method development process. Guidelines are then given for method selection and quantitative concepts for characterizing and classifying chromatographic phases. Selective separation methods (from both GC and LC) are given - the main parameters of each method are identified and simple, quantitative relations are sought to describe their effects. Criteria by which to judge the quality of separation are discussed with clear recommendations for different situations. The specific problems involved in the optimization of chromatographic selectivity are explained. Optimization procedures, illustrated by examples, are described and compared on the basis of a number of criteria. Suggestions are made both for the application of different procedures and for further research. The optimization of programmed analysis receives special attention, and the last chapter summarizes the optimization of the chromatographic system, including the optimization of the efficiency, sensitivity and instrumentation.

Those developing chromatographic methods or wishing to improve existing methods will value the detailed, structured way in which the subject is presented. Because optimization procedures and criteria are described as elements of a complete optimization package, the book will help the reader to understand, evaluate and select current and future commercial systems.

Contents: 1. Introduction. 2. Selection of Methods. 3. Parameters Affecting Selectivity. 4. Optimization Criteria. 5. Optimization Procedures. 6. Programmed Analysis. 7. System Optimization. Indexes.

1986 1st repr. 1987 xvi + 346 pages
US$ 110.50 / Dfl. 210.00
ISBN 0-444-42681-7

ELSEVIER SCIENCE PUBLISHERS

P.O. Box 211, 1000 AE Amsterdam, The Netherlands
P.O. Box 882, Madison Square Station, New York, NY 10159, USA

Data Handling in Science and Technology, 4

Advanced Scientific Computing in BASIC with Applications in Chemistry, Biology and Pharmacology

by **P. Valkó** *and* **S. Vajda**

This book gives a practical introduction to numerical methods and presents BASIC subroutines for real-life computations in the areas of chemistry, biology, and pharmacology. The choice of BASIC as the programming language is motivated by its simplicity, its availability on all personal computers and by its power in data acquisition. While most of the scientific packages currently available in BASIC date back to the period of limited memory and speed, the subroutines presented here can handle a broad range of realistic problems with the power and sophistication needed by professionals and with simple, step-by-step instructions for students and beginners. A diskette containing the 37 program modules and 39 sample programs listed in the book is available separately. The main task considered in the book is that of extracting useful information from measurements via modelling, simulation, and statistical data evaluations. Efficient and robust numerical methods have been chosen to solve related problems in numerical algebra, nonlinear equations and optimization, parameter estimation, signal processing, and differential equations. For each class of routines an introduction to the relevant theory and techniques is given, so that the reader will recognise and use the appropriate method for solving his or her particular problem. Simple examples illustrate the use and applicability of each method.

Contents: **1. Computational Linear Algebra.** Basic concepts and methods. Linear programming. LU decomposition. Inversion of symmetric, positive definite matrices. Tridiagonal systems of equations. Eigenvalues and eigenvectors of a symmetric matrix. Accuracy in algebraic computations. Ill-conditioned problems. Applications and further problems. **2. Nonlinear Equations and Extremum Problems.** Nonlinear equations in one variable. Minimum of functions in one dimension. Systems of nonlinear equations. Minimization in multidimensions. Applications and further problems. **3. Parameter Estimation.** Fitting a straight line by weighted linear regression. Mutivariable linear regression. Nonlinear least squares. Linearization, weighting and reparameterization. Ill-conditioned estimation problems. Multiresponse estimation. Equilibrating balance equations. Fitting error-in-variables models. Fitting orthogonal polynomials. Applications and further problems. **4. Signal Processing.** Classical methods. Spline functions in signal processing. Fourier transform spectral methods. Applications and further problems. **5. Dynamical Models.** Numerical solution of ordinary differential equations. Stiff differential equations. Sensitivity analysis. Quasi steady state approximation. Estimation of parameters in differential equations. Identification of linear systems. Determining the input of a linear system by numerical deconvolution. Applications and further problems. **Subject Index**

1989 xvii + 322 pages
Price: US $ 108.50 / Dfl. 190.00
ISBN 0-444-87270-1
5.25" Diskette US $ 63.00 / Dfl. 110.00
ISBN 0-444-87271-X.

Elsevier Science Publishers

P.O. Box 211, 1000 AE Amsterdam, The Netherlands
P.O. Box 882, Madison Square Station, New York, NY 10159, USA

Journal of Chromatography, 585 (1991) 187–193
Elsevier Science Publishers B.V., Amsterdam

CHROM. 23 546

Simplex optimization of liquid chromatography with the function of mutual information as a criterion

Rieko Matsuda, Yuzuru Hayashi*, Takashi Suzuki and Yukio Saito

National Institute of Hygienic Sciences, 1-18-1, Kamiyoga, Setagaya, Tokyo 158 (Japan)

(First received January 29th, 1991; revised manuscript received May 3rd, 1991)

ABSTRACT

This paper demonstrates that the function of mutual information is a valid objective function for the simplex optimization problems in liquid chromatography. The optimum is indicated by the maximum of the function of mutual information over all the examined conditions. When a new peak which is fused with another peak is discovered by an experiment, the function of mutual information increases substantially to make it easy to approach the optimum. The simplex optimization of mobile phase composition (acetonitrile volume fraction) in reversed-phase liquid chromatography for the determination of a mixture of antipyretics (five analytes) is taken as an example.

INTRODUCTION

The simplex optimization has been successfully used, especially in high-performance liquid chromatography [1–7]. Details of the simplex algorithm and concepts can be found elsewhere [8,9].

The most important advantages of the sequential simplex methods are [1,7]: (1) no preconceived model of the retention behavior of solutes is required; (2) the identification or recognition of solutes in individual separations is unnecessary; (3) computational requirements are minimal; (4) any number of independent variables (mobile phase composition X, temperature T, etc.) can be considered.

As pointed out by Berridge [1], a stumbling block of the simplex optimization is the lack of a universally acceptable objective function. Unfortunately, most of the criteria so far proposed for optimization have been acknowledged to suffer to a greater or lesser extent from difficulties in reaching the global optimum or even of reaching the unequivocal definition of the optimum in liquid chromatography [10].

Particularly at the early stage of the simplex optimization, situations can arise where fused peaks occur in a chromatogram and the number of solutes in a sample is unknown. Without knowledge of the number of peaks to be found, the optimal values of some criteria (TOV and CRF) will produce chromatograms comprising fused or strongly overlapped peaks [10]. A prerequisite for an ideal objective function must be as follows: if a subsequent experiment offers further separation and the proof that a peak previously observed is made up of two components, the criterion should give a much better response for this second experiment than for the previous experiment where the coexistence of the two components was not yet recognizable.

This paper demonstrates that the FUnction of Mutual Information, abbreviated as FUMI [11,12], meets the above-mentioned prerequisite for an ideal criterion.

FUMI can be calculated from the peak parameters (area A_j, width σ_j and retention τ_j) for every individual peak and from the noise level $\tilde{a}$ (see Table I). The optimum is defined as the chromatogram which provides the maximum of FUMI among all the examined conditions. Many variables (mobile phase composition X, column length L, wavelength λ, flow-rate v, the amount of added

0021-9673/91/$03.50

TABLE I

FUMI AND ITS RELATED FUNCTIONS

σ_j denotes the width (standard deviation) of Gaussian peak j; A_j is peak area; $\tilde{a}$ is the power spectrum intensity of the filtered white noise [11]; $\kappa_f(j)$ and $\kappa_{f'}(j)$ are the filter-off points [16]; τ_q is the retention time of the last peak q. Φ denotes the total information of a multi (q)-component chromatogram.

$\phi_j = \psi_j - \delta\phi_j$	FUMI for a peak
$\psi_j = \frac{1}{2}\log\left(\frac{A_j^2}{2\pi^{1/2}\sigma_j\tilde{a}}\right)$	Intact information
$\delta\phi_j = -\frac{1}{2}\log\left(\frac{\kappa_f(j)-\tau_j}{\pi^{1/2}\sigma_j} + \frac{\kappa_{f'}(j)-\tau_j}{\pi^{1/2}\sigma_j}\right)$	Information loss
$\Phi = \sum_{j=1}^{q}\phi_j$	FUMI for q peaks

internal standard, etc.) have been simultaneously optimized with FUMI Φ in reversed-phase liquid chromatography [11].

To scientists who are familiar with the traditional optimization methodology, FUMI Φ might seem to be far different from the traditional strategies for separation. On the contrary, the theory of FUMI has been proven to involve as a special case the concepts of commonly used optimization criteria based on the resolution R_s [13]. Only if peak j strongly overlaps with another (*e.g.*, $R_s < 1.5$) is the increase in FUMI ϕ_j for peak j equivalent to the increase in the resolution R_s except for coefficient C (>0) [13]:

$$\frac{\partial\phi_j}{\partial Z} = C\frac{\partial R_s}{\partial Z} \tag{1}$$

where Z denotes a chromatographic variable (X, L, λ, etc.). However, another equation derived from FUMI holds for sufficiently or unduly separated peaks (*e.g.*, $R_s > 1.5$). In this situation, FUMI involves the sensitivity function s_j proposed by Snyder *et al.* [14] and also corresponds to the R_s minimum method under a special condition [13,15].

THEORY

FUMI ϕ_j for peak j is expressed as the subtraction of the information loss $\delta\phi_j$ due to peak overlap from the intact information ψ_j which is inherent to the peak shape itself (see Table I). For simplicity, two peaks are considered. The total information Φ for a chromatogram is described as the sum of the individual peak information ϕ_j:

$$\Phi = \phi_j + \phi_{j+1} \tag{2}$$

If the peaks separate sufficiently ($\delta\phi_j = 0$ and $\phi_j \approx \psi_j$) and if they have almost the same information ϕ_j ($\psi_j \approx \psi_{j+1}$; almost the same area A_j and width σ_j), then Φ takes the simple form:

$$\Phi \approx 2\psi_j \tag{3}$$

If the peaks fuse, $\Phi = 0$ (see below).

If the fused peaks are treated as a single peak of doubled area $2A_j$, the apparent total information Φ^* can be calculated as:

$$\Phi^* \approx \psi_j + \log 2 \tag{4}$$

Eqn. 4 can be derived by substituting $2A_j$ into A_j of ψ_j.

Often, in practice [8], $\psi_j \approx 8$. Then, $\Phi \approx 16$ (eqn. 3) and $\Phi^* \approx 8.7$ (eqn. 4) ($\log 2 \approx 0.693$). Note that $\Phi \gg \Phi^*$.

Calculation of FUMI and simplex

The algorithm of FUMI was described in detail previously [11,12]. The arbitrary constant β involved in FUMI was set at 5.25, which means that the optimal peak resolution (R_s) is about 1.5 if the peak areas are the same [11,16].

A peak-search routine was used to detect individual peaks and calculate Φ^* (eqn. 4). Only if R_s exceeds 0.25 can the two peaks be recognized by the routine. The following terminology is used: the peaks (a) fuse, if $R_s < 0.25$; (b) strongly overlap, if $0.25 \leqslant R_s < 1.5$; (c) separate, if $R_s \geqslant 1.5$. The peak-search routine recognizes the fused peaks (j and $j+1$) not as "two" but as "one" peak. In this case, Φ^* is calculated from the apparent peak parameters (*e.g.*, $2A_j$ and σ_j in eqn. 4) of the apparently single peak. The apparent FUMI Φ^* is used as a criterion of the simplex optimization in this paper.

On the other hand, calculation of the exact FUMI Φ requires all the exact peak parameters A_j, σ_j and τ_j of every individual solute to be known before optimization. The fused peaks should be identified as being "two" peaks for the calculation of Φ. If all the values of Φ can be predicted over the

experimental conditions to be examined, then the optimum (the maximum of Φ) can easily be found, as shown by our previous papers [11,12,15,16]. This is called an interpretive method, and the simplex optimization is a sequential method [2].

For analytical purposes (precision Φ or efficiency ϑ of analysis), the optimum can be defined as the chromatogram which provides the maximum of FUMI Φ or the maximal transmission rate ϑ of the information FUMI [11,12]. In this paper, the Φ optimum (the maximal Φ) is focused, because the Φ optimum coincides with the ϑ optimum (the maximum of ϑ), especially in the optimization of mobile phase composition X in reversed-phase liquid chromatography [12].

The super-modified simplex (SMS) was used to determine the optimum of the variable X (mobile phase composition). FUMI ϕ_j represents the data-processing error relative standard deviation (R.S.D.) for peak j, which depends on the peak shape (A_j and σ_j), overlap (τ_{j-1}, τ_j, τ_{j+1}, A_{j-1}, etc.) and noise level $\tilde{a}$. Then, the experiments of SMS were finished when the difference in the R.S.D. values of the updated vertices was less than 0.1%. SMS has been described in detail [9].

The simplex optimization was simulated on a PC9801 T laptop computer (NEC) and the language used was Quick BASIC.

Simplex optimization with FUMI

Fig. 1 shows the model dependence of the apparent total information Φ^* on the volume fraction X of an organic modifier in reversed-phase liquid chromatography. Two peaks are considered in Figs. 1 and 2 for the purpose of demonstration. The elution order is reversed at $X \approx 18\%$. The logarithm of the capacity factor k_j for peak j is assumed to be linearly related to X according to the proposition of Snyder *et al.* [14] (see the legend of Fig. 1). This log (k_j) –X relationship is illustrated in Fig. 2 of ref. 17. Throughout this paper, peak area A_j is assumed to be invariable in the optimization of X.

The typical chromatograms A–E in Fig. 1 are illustrated in Fig. 2 with the same letters. The values of Φ^* and Φ for chromatograms A–E are listed in Table II. The exact FUMI Φ takes the minimum (zero) in the X range from 16 to 20% (see chromatograms B, C and D and Table II). This means that no precise measurements can be obtained by chromatography in the above region because of the strong peak overlap or fusion ($R_s < 1.5$). The success of the chromatographic quantitation is ensured by the large amount of Φ (see chromatograms A and E) which is located in the X range except for around the elution reversal.

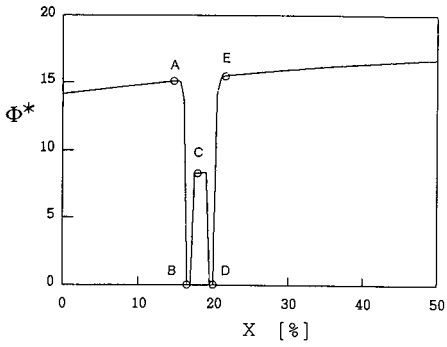

Fig 1. Dependence of the apparent total information Φ^* on the mobile phase composition X for two peaks. $A_j = 10\,000$; $\tilde{a} = 1$; $N = 10\,000$; $\beta = 5.25$; $\tau_0 = 100$ s. The linear log (k_j)–X relationship is assumed: log (k_j) = log (k_{wj}) – S_jX where S_j denotes the solvent strength for peak j [11]. $S_1 = 3.6$; log $(k_{w1}) = 1.4$. $S_2 = 2.5$; log $(k_{w2}) = 1.2$. This linear relationship is illustrated in Fig. 2 of ref. 17.

The apparent FUMI Φ^* takes a different value

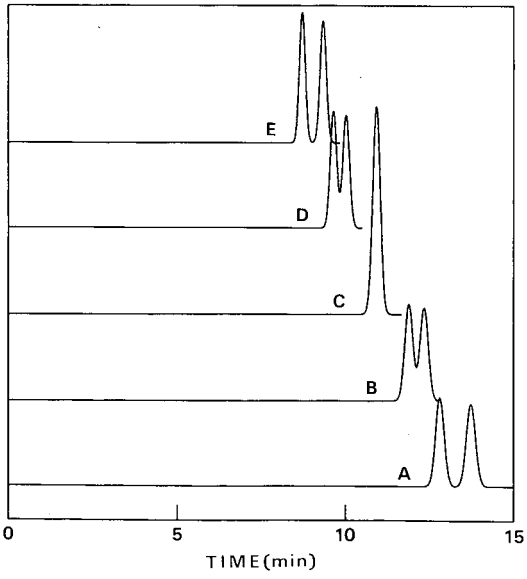

Fig. 2. Chromatograms indicated in Fig. 1. Chromatograms A–E take the information Φ^* indicated with the same letters A–E in Fig. 1. For Φ^* and R_s, see Table II.

TABLE II

Φ^* AND Φ OF CHROMATOGRAMS A–E IN FIG. 1

Chromatogram (X)	Type of resolution (R_s)	Φ^*	Φ
A (15%)	Separated (1.76)	15.08	15.08
B (16.5%)	Strongly overlapped (0.92)	0	0
C (18.2%)	Fused (0)	8.31	0
D (20%)	Strongly overlapped (0.96)	0	0
E (21.5%)	Separated (1.71)	15.47	15.47

only for the fused peaks ($R_s < 0.25$; see chromatogram C). That is, Φ^* and Φ take the same values as long as the peak-search routine can recognize the individual peaks ($R_s \geqslant 0.25$). The value of Φ^* for the fused peaks in chromatogram C is much larger than that of Φ ($=0$) because the peak-search routine cannot recognize the individual peaks and Φ^* is calculated by regarding the almost fused peaks as a large single-component peak (see eqn. 4). This recognition of the apparent FUMI Φ^* is clearly not true. However, Φ^* must be a simple criterion for the simplex optimization in which the number of components in a sample is unknown.

This paper demonstrates the successful application of the apparent FUMI Φ^* to the simplex optimization. Again, we should note that Φ^* gives false values only if peaks fuse ($R_s < 0.25$). Then, Φ^* takes an exact value for the optimum ($\Phi^* = \Phi$).

The false recognition of the fused peaks (C) produces the hillock in the Φ^*–X line around $X = 18\%$ (see Fig. 1). There is no hillock in the response surface of the exact FUMI Φ. The Φ–X line can easily be imagined from Fig. 1 and Table II and was given previously in Fig. 2 of ref. 17.

The hillock in Fig. 1 would have caused the most serious problem in using FUMI Φ^* as a simplex criterion if the probability that the top of the hillock (chromatogram C) was selected as the optimum by the simplex procedure was high. However, the information Φ^* at the top of the hillock is even lower than Φ^* at the high ridge where the optimum should be located and the above-mentioned probability can be concluded to be negligibly low (see below).

The most favorable property of FUMI for the simplex optimization is that FUMI Φ^* has a tendency to increase greatly when a new peak is discovered by an experiment with superior separation conditions (compare chromatogram C with A or E and their Φ^* values in Table II). Chromatograms A and E take almost the same resolution R_s, but FUMI indicates that chromatogram E is in terms of information theoretically superior to A because of the greater amount of information Φ^* ($=\Phi$) that E provides compared with A. This difference in Φ^* arises from the distinguishable peak shape (mainly σ_j).

Fig. 3 shows the influence of the acetonitrile volume fraction X in water on FUMI for the reversed-phase liquid chromatographic analysis of a mixture of antipyretics [18]. The analytes were acetaminophen (S1), caffeine (S2), salicylamide (S4), guaifenesin (S5, as internal standard) and ethenz-

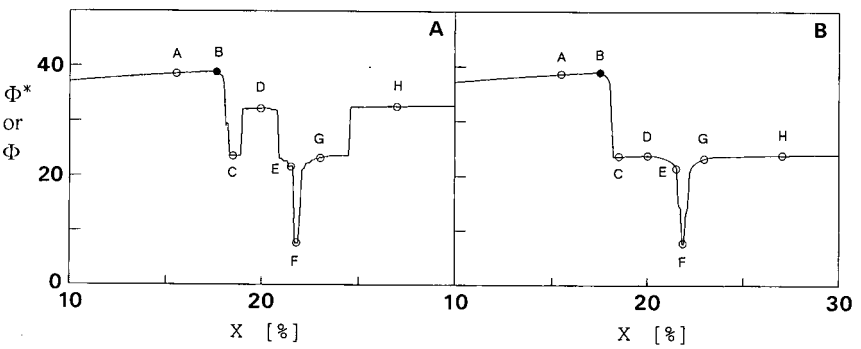

Fig. 3. Influence of the volume fraction X of acetonitrile in water on the apparent FUMI Φ^* (A) and the exact FUMI Φ^* (B). Analytes: acetaminophen (S1); caffeine (S2); salicylamide (S4); guaifenesin (S5, as internal standard); ethenzamide (S6). ● = The optimum (the maximum of Φ). The capacity factor k_j and peak width σ_j (standard deviation) were approximated by the simple model of Fritz and Scott [18,19]. The log (k_j)–X profiles (observed) are illustrated in Fig. 1 of ref. 18. The column used was Inertsil ODS (150 × 4.6 mm I.D.; Gasukuro Kogyo), the temperature was 35°C and the detector was set at 290 nm [18].

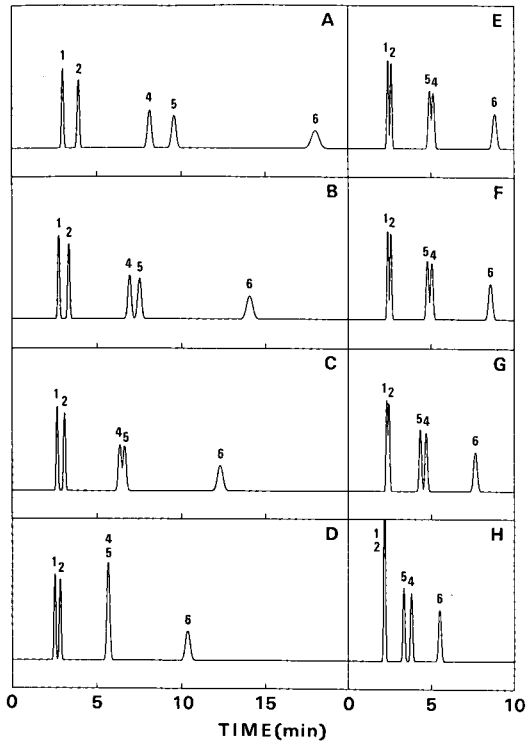

Fig. 4. Chromatograms of different information. Chromatograms A–H of this figure are indicated by the same letters in Fig. 3. X, Φ^*, Φ: (A) 15.5, 38.58, 38.58; (B) 17.4, 38.96, 38.96; (C) 18.5, 23.61, 23.61; (D) 20.0, 32.25, 23.73; (E) 21.5, 21.68, 21.62; (F) 21.8, 7.65, 7.65; (G) 23.0, 23.36, 23.22; (H) 27.0, 32.66, 23.8. Capital letter S is omitted.

amide (S6) (called mixture B in ref. 18). The retention behaviors of these analytes against X are illustrated in Fig. 1 of ref. 18.

The response surface of Fig. 3A denotes the apparent total information Φ^* and that of Fig. 3B is the exact information Φ. The hillocks inherent to Φ^* appear around letters D and H. The chromatograms indicated with letters A–H in Fig. 3 are illustrated in Fig. 4 with the same letters.

As X increases from 10 to 17.4% (point B), the information Φ^* increases gently because of the increase in peak sharpness under the conditions of the complete peak separation (compare Fig. 4A and B). The value of X at point B ($=17.4\%$) is the optimum (the maximum of FUMI).

Slightly above the optimum (point B), FUMI decreases abruptly because of the strong overlap of peaks S4 and S5 (Fig. 4C). When these peaks fuse into one and are not recognizable by the peak-searching routine, FUMI Φ^*, for Fig. 4D takes more information than for Fig. 4C, but is still much less than FUMI for the optimum (Fig. 4B).

In Fig. 4E, the elution order of peaks S4 and S5 is reversed. Although these peaks overlap strongly, they can be recognized individually. Peaks S1 and S2 weakly overlap and suffer from a slight information loss.

The strong overlaps of peak pairs of S1 and S2 and of S4 and S5 cause FUMI to decrease substantially (see Fig. 4F). The relaxation of the strong overlap of peaks S4 and S5 increases the information, as shown in Fig. 3G. When peaks S1 and S2 fuse (Fig. 4H), the apparent FUMI Φ^* takes a greater value ($\Phi^* = 32.7$), which is also much less than the maximal information ($\Phi = 39.0$) at point B.

Fig. 5A shows the evolution of FUMI Φ^* during the simulated simplex optimization (RUN 1). When a bad condition is selected, FUMI takes a low value

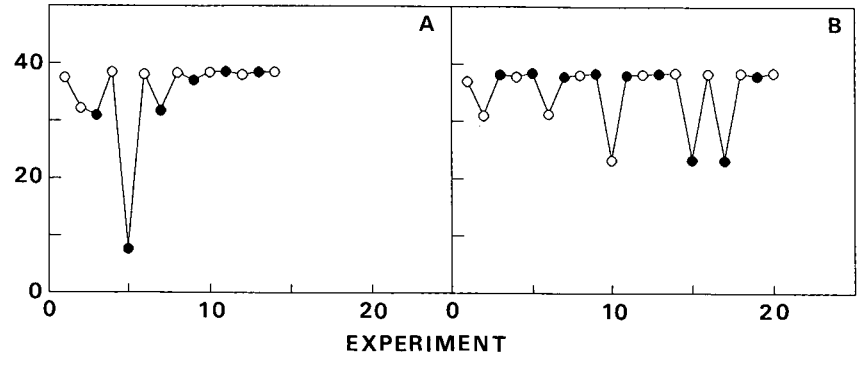

Fig. 5. Progress of the simplex Φ. A = RUN 1; B = RUN 2. The reflection points are denoted with closed circles. FUMI Φ^* was calculated. The detailed values of Φ^* and X are listed in Tables III and IV. Simulation is based on the log (k_j)–X profiles of Fig. 1 of ref. 18.

TABLE III

RESULTS OF THE SIMPLEX OPTIMIZATION WITH FUMI Φ^* (RUN 1)

Experiment	X	Φ^*	Simplex movement
1	12.0	37.5	Initial
2	28.0	32.2	Initial
3	20.0	31.0	Reflection
4	16.8	38.5	Vertex
5	21.6	7.6	Reflection
6	14.6	38.1	Vertex
7	19.1	31.7	Reflection
8	15.8	38.3	Vertex
9	17.8	37.0	Reflection
10	16.4	38.4	Vertex
11	17.2	38.5	Reflection
12	17.6	38.0	Vertex
13	16.8	38.5	Reflection
14	17.0	38.5	Vertex

and the simplex proceeds further. Table III gives the experimental conditions and value of Φ^* at each experiment of the simplex (RUN 1). The chromatograms corresponding to the experiments can be imagined from the typical chromatograms of Fig. 4 and the information FUMI. The simplex was terminated after the large amount of FUMI was obtained.

TABLE IV

RESULTS OF THE SIMPLEX OPTIMIZATION WITH FUMI Φ^* (RUN 2)

Experiment	X	Φ^*	Simplex movement
1	10.0	37.0	Initial
2	20.0	31.0	Initial
3	15.0	38.2	Reflection
4	13.2	37.8	Vertex
5	16.4	38.4	Reflection
6	19.6	31.2	Vertex
7	13.2	37.8	Reflection
8	14.8	38.1	Vertex
9	16.4	38.4	Reflection
10	18.0	23.3	Vertex
11	14.8	38.1	Reflection
12	15.6	38.3	Vertex
13	16.4	38.4	Reflection
14	17.2	38.5	Vertex
15	18.8	23.3	Reflection
16	16.5	38.4	Vertex
17	18.0	23.2	Reflection
18	16.8	38.5	Vertex
19	17.6	38.0	Reflection
20	17.1	38.1	Vertrex

As long as the initial conditions of X (two points) take a wide range in the simplex algorithm, evolution of FUMI similar to Fig. 5A can be obtained for this problem (see Fig. 5B and Table IV for RUN 2). The range of initial conditions for RUN 2 is narrower than for RUN 1 and the required number of experiments is larger for RUN 2.

Experiments 2, 3 and 7 are located on the hillocks of Φ^* (see Table III). Nevertheless, the simplex with FUMI is not at all thwarted by the hillocks. This holds true even if one of the initial conditions of the simplex falls on the hillock (see experiment 2 in Table IV and Fig. 5B).

DISCUSSION

The simplex with FUMI was terminated not after a good separation was obtained, as is the case for the traditional methods [7], but after a large amount of Shannon information was obtained. FUMI contains the concept of R_s in the information loss $\delta\phi_j$ and the sensitivity function s_j [14] in the intact information ψ_j as demonstrated by previous papers [13,17]. In other words, FUMI depends not only on the peak overlap (described by $\delta\phi_j$) but also on the peak shape itself (described by ψ_j and involving area A_j and width σ_j). Therefore, FUMI defines the optimal chromatogram as comprising the peaks of largest possible A_j and smallest possible σ_j without overlap. Of course, a small noise level $\tilde{a}$ is preferred (see Table I).

Simplex is a hill-climbing method and is susceptible to the well known, important problem of locating the local, rather than the global, optimum [1]. FUMI cannot circumvent this problem, which is inherent to the mathematics of the simplex optimization.

FUMI Φ^* can overcome the problem produced by itself (the hillock in Figs. 1 and 3). On the other hand, the exact FUMI Φ has been proved to be a reliable criterion in the optimization of liquid chromatography [11,12]. As evident from Fig. 3A and B, given knowledge on a number of solutes, FUMI can provide smoother response surfaces (Fig. 3B) and will enable more rapid and less disturbed advance of the simplex optimization than the simplex presented in this paper (Fig. 3A). The

currently available multi-channel detectors will be useful for the disclosure of fused peaks [1]. The most significant advantage of FUMI is that Φ^* increases greatly when a new peak is discovered by chromatographic experiments.

Fig. 4G was proposed to be the optimum in previous papers [16,18]. This optimum is suitable for a data processor of excellent peak-resolving powers, such as the Kalman filter ($\beta = 3.25$ and $R_s \approx 1$ for the optimal peak separation). The optimal chromatogram presented here (Fig. 3B) consists of peaks of R_s greater than 1.5 ($\beta = 5.25$) and precise quantitative data can be collected with a data processor of inferior peak-resolving powers, such as perpendicular dropping.

The simulation in this paper involves a problem which has been considered difficult in chromatographic optimization, *i.e.*, the reversion of elution order. In the X region below 10%, the observation time becomes more than 1 h. Most of the peaks overlap strongly or fuse in the X range of more than 30%. If the initial conditions are X of 0 and 100%, then the result will be the same as the 10–30% of this paper. However, the initial conditions of 20–40% may not reach the global optimum. The simulation (RUN 1 and RUN 2) will suffice for the aim of this paper, which is to demonstrate the applicability of FUMI to the simplex optimization of liquid chromatography.

CONCLUSION

The authors and their colleagues have studied the applicability of FUMI to the total chromatographic optimization (TOCO) of many variables [11] and to theoretical interpretation, in terms of information, of the analytical roles of chromatographic variables [12,13,17]. This paper has further expanded the dimension of FUMI to the simplex optimization..

REFERENCES

1 J. C. Berridge, *J. Chromatogr.*, 485 (1989) 3.
2 P. J. Schoenmakers, *Optimization of Chromatographic Selectivity*, Elsevier, Amsterdam, 1986.
3 A. G. Wright, A. F. Fell and J. C. Berridge, *J. Chromatogr.*, 458 (1988) 335.
4 A. G. Wright, A. F. Fell and J. C. Berridge, *J. Chromatogr.*, 464 (1989) 27.
5 J. C. Berridge, *J. Chromatogr.*, 485 (1989) 3.
6 S. N. Deming, J. M. Palasota, J. Lee and L. Sun, *J. Chromatogr.*, 485 (1989) 15.
7 J. A. Crow and J. P. Foley, *Anal. Chem.*, 62 (1990) 378.
8 J. A. Nelder and R. Mead, *Comput. J.*, 7 (1965) 308.
9 M. W. Routh, P. A. Swartz and M. B. Denton, *Anal. Chem.*, 49 (1977) 1422.
10 H. J. G. Debets, B. L. Bajema and D. A. Doornbos, *J. Chromatogr.*, 151 (1983) 131.
11 Y. Hayashi, R. Matsuda and A. Nakamura, *Chromatographia*, 30 (1990) 85.
12 Y. Hayashi and R. Matsuda, *Chromatographia*, 30 (1990) 171.
13 Y. Hayashi and R. Matsuda, *Chromatographia*, 31 (1991) 374.
14 L. R. Snyder, J. W. Dolan and J. R. Gant, *J. Chromatogr.*, 165 (1979) 3.
15 Y. Hayashi and R. Matsuda, *Chromatographia*, 30 (1990) 367.
16 Y. Hayashi and R. Matsuda, *Anal. Chim. Acta*, 222 (1989) 313.
17 Y. Hayashi and R. Matsuda, *Chromatographia*, 31 (1991) 367.
18 R. Matsuda, Y. Hayashi, M. Ishibashi and Y. Takeda, *Anal. Chim. Acta*, 222 (1989) 301.
19 J. S. Fritz and D. M. Scott, *J. Chromatogr.*, 271 (1983) 193.

Journal of Chromatography, 585 (1991) 195–206
Elsevier Science Publishers B.V., Amsterdam

CHROM. 23 537

New chiral covalently bonded, π-donor stationary phases for high-performance liquid chromatography, based on derivatives of optically active 1-(1-naphthyl)ethylamine

Part II☆

Rolf Straub☆☆, Markus Pfister and Hans Arm*

Institute of Organic Chemistry, University of Berne, Freiestrasse 3, CH-3012 Berne (Switzerland)

(Received March 26th, 1991)

ABSTRACT

On the basis of optically active 1-(1-naphthyl)ethylamine as the chiral selector part, several derivatives with different N-acylamide substituents were synthesized and attached to 3-glycidoxypropyl-derived silica to give "brush-type" stationary phases for high-performance liquid chromatography. Their suitability for enantiomer separation was tested with aromatic amide derivatives including two homologous series. The best separations on every phase were found for samples with strong π-acceptor groups, such as the 3,5-dinitrophenyl group.

INTRODUCTION

There has been significant progress in the direct separation of enantiomers by high-performance liquid chromatography (HPLC) in recent years [1], especially with the aid of chiral stationary phases (CSPs) [2,3] with proteins, ligand-exchange sites, helical polymers or chiral cavities [4,5]. Amongst the most successful CSPs are the "brush-type" phases which consist of a silica matrix with covalently bonded chiral groups. The π-acceptor 3,5-dinitrobenzoylphenylglycine CSP developed by Pirkle and co-workers [6,7] is a well known phase of this type, and a great variety of similar CSPs have been reported and in some instances commercialized [8,9].

The mechanistic hypothesis formulated from the study of N-acyl-1-arylalkylamines with these π-acceptor CSPs were instrumental in the design of "reciprocal" CSPs intended to resolve analytes derived with the π-acidic 3,5-dinitrobenzoyl (DNB) group [10,11]. The π-donor 1-arylalkylamide-derived chiral stationary phases are especially interesting from the mechanistic point of view, as they utilize multiple and competing chiral recognition mechanisms depending on the types of analytes and the chiral selector of the CSPs. The proposed model introduces the intercalative and the conflicting non-intercalative process. Chromatographic experiments with suitable homologous series, in which stereochemistry and elution order are correlated, help to distinguish different arrangements of the diatereomeric complex formed out of the chiral selector and the analyte [12].

These or similar "brush-type" CSPs are capable of separating many different enantiomers of phar-

☆ For part I, see ref. 14.
☆☆ This paper is part of the dissertation of R. Straub [19].

0021-9673/91/$03.50

maceutical interest. Preparative-scale separations are also possible if a sufficient amount of the chiral stationary phase is available [13].

In an earlier paper [14] we described chiral stationary phases for HPLC based on optically active 1-(1-naphthyl)ethylamine. (*R*)-4-(N-1-Pivaloylamino-1-ethyl)-1-naphthylamine {(*R*)-2,2-dimethyl-N-[1-(4-amino)naphthylethyl]propanamide} fixed either on a silica support or in a glass capillary showed remarkable separation capabilities for a variety of chiral amides and a broad range of applications in HPLC, supercritical fluid chromatography and gas chromatography [15]. The "brush-type" CSP on a silica matrix has been subject of intense chromatographic and mechanistic investigations during the last few years [16,17]. In subsequent studies computational chemistry was applied to understand the separation mechanism and to design similar CSPs with improved separation capabilities for chiral DNB-amide derivatives [18]. From theoretical calculations (computer-aided molecular modelling, CAMM) [18] and chromatographic data [14,17] it can be deduced that a π-donor naphthyl group and a bulky pivaloylamide substituent attached to the chiral centre of the selector are suitable for enantioseparation. In this paper we examine the chromatographic behaviour of four new π-donor "brush-type" CSPs with different carboxamide substituents on the chiral centre and compare them with the mentioned CSP.

Fig. 1 shows the common basic structure of the phases with amide groups R_i of different rigidity and polarity. To test the separation capabilities of the CSPs we used different chiral amides, shown in Table I.

Homologous series of 1-phenylalkylamides **1a–l** and esters of DNB-amino acids **30a–j**, given in Fig. 2, were used to examine the retention mechanisms which make significant contributions to enantioselectivity.

EXPERIMENTAL

General

Five chiral stationary phases with different N-acyl groups R_i on the chiral selector part were synthesized starting from commercially available (*R*)-1-(1-naphthyl)ethylamine. The preparation of the CSPs was done in five steps according to the procedures described for CSP I (PIV) by Däppen *et al.* [14] and Brügger *et al.* [15] but with different alkyloyl chlorides for the amination step [19]. Cyclohexanecarbonyl chloride was used for CSP II (CYH), adamantanecarbonyl chloride for CSP III

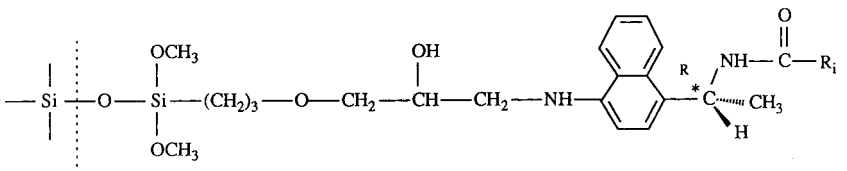

$R_i = R_5 =$ —CF_2—CF_2—CF_3 CSP V (HFP)

Fig. 1. Chiral stationary phases (CSPs) I–V, N-acyl derivatives of (*R*)-4-(N-1-alkyloylamino-1-ethyl)-1-naphthylamine.

TABLE I

SAMPLES **1–29** USED IN CHROMATOGRAPHIC EXPERIMENTS

DNB = 3,5-Dinitrobenzoyl; DNP = 3,5-dinotrophenyl. **8** = DNB amide of cathinone; **9** = DNB amide of merucathinone; **10** = di-DNB derivative of merucathine; **24** = DNB amide of propranolol; **25** = DNB amide of pindolol; **26** = DNB amide of *erythro*-dihydrosphingosine; **27** = DNB amide of *threo*-dihydrosphingosine.

Phenyl-containing samples

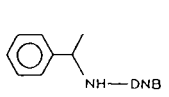

1

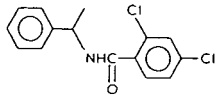

2

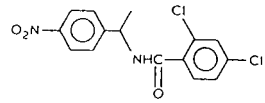

3

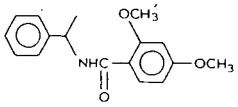

4

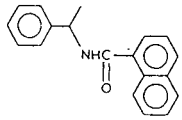

5

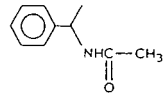

6

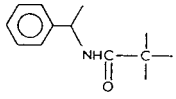

7

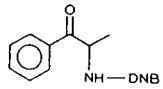

8

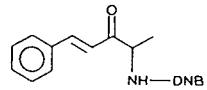

9

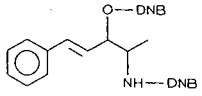

10

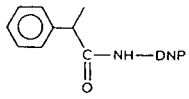

11

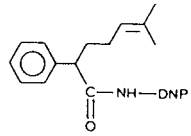

12

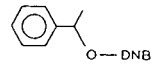

13

Naphthyl- and indolyl-containing samples

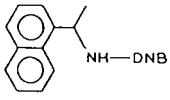

14

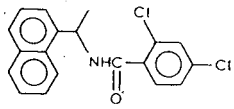

15

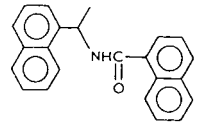

16

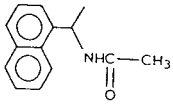

17

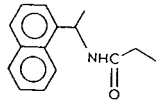

18

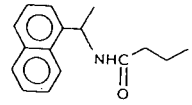

19

(Continued on p. 198)

TABLE I (*continued*)

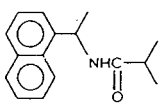

20

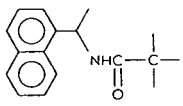

21

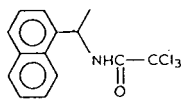

22

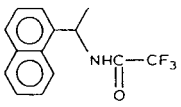

23

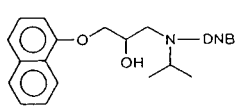

24

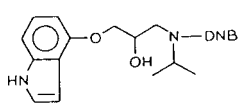

25

Miscellaneous DNB-derived samples

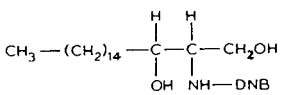

26

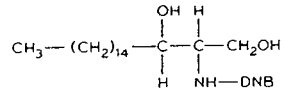

27

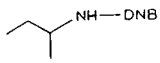

28

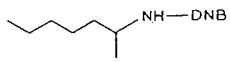

29

(ADA), 3-cyclopentylpropionyl chloride for CSP IV (CPE) and heptafluorobutyryl chloride for CSP V (HFP). The general synthetic procedure for the aromatic nitration of the naphthalene ring in the *para* position, the catalytic reduction of the introduced aromatic nitro group, the bonding procedure to the silica matrix by 3-glycidoxypropyltrimethoxysilane as a spacer and the filling mode into stainless-steel columns were identical for all five CSPs, except for small variations in the purification steps and in the yields. Only the yield, the measured physical parameters of the different intermediates and elemental analysis data of the bonded phases are reported.

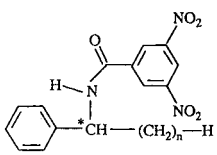

1a-l

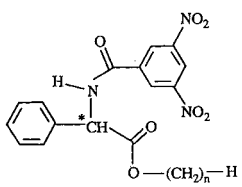

30a-j

Fig. 2. N-3,5-Dinitrobenzoyl (DNB) derived homologous series **1a–l** and **30a–j**.

Materials

For the preparation of CSPs LiChrospher Si 100 (Merck, Darmstadt, Germany) with a particle size of 5 μm and a specific surface area S_{BET} = 264.4 ± 5.4 m^2/g was used. It was dried at 150°C and 0.01 mbar for 6 h prior to the bonding procedure. All chemicals were purchased from Merck (Darmstadt, Germany) or Fluka (Buchs, Switzerland).

Analysis

The NMR data were recorded on a 60-MHz Varian EM 360L NMR spectrometer (Varian, Zug, Switzerland) in [^{2}H]chloroform with tetramethylsilane as internal standard. The polarimetric measurements were done on a Perkin-Elmer Model 241 polarimeter. The IR spectra were recorded on a Perkin-Elmer Model 782 infrared spectrophotometer in chloroform and the UV spectra on a Perkin-Elmer Model 554 UV–VIS spectrophotometer in ethanol (Perkin-Elmer, Überlingen, Germany). The mass spectra were recorded on a Varian MAT CH7 A mass spectrometer (electron impact ionization, 70 eV). Only the mass spectrometric (MS) *m/z* value, the relative intensity of the molecular ion and the base peak are given. The elemental analyses were done with a routine analyser in the Microanalytical Department of Ciba-Geigy, Basle, Switzerland.

Preparation of CSP I (PIV)

(R)-1-(N-1-Pivaloylamino-1-ethyl)naphthalene. This amide was prepared by amination of (*R*)-1-(1-naphthyl)ethylamine in dry dioxane. Yield, 70%; m.p. 133.0–135.0°C; $[\alpha]_D = 39.1°$ ($c = 0.11$ in ethanol, 25°C). ^{1}H NMR (ppm): 8.20–7.68 (m, 3H), 7.68–7.40 (m, 4H), 6.15–5.65 (m, 2H), 1.90 (m, 3H), 1.15 (s, 9H). IR (cm^{-1}): 3460, 3060–2880, 1650, 1600, 1500, 1450. MS: *m/z* 255 (65, M$^{+\cdot}$), 155 (100).

(R)-1-Nitro-4-(N-1-pivaloylamino-1-ethyl)-naphthalene. The nitration of the aromatic ring was done in a mixture of 65% nitric acid and of 98% acetic acid. Yield after several purification steps, 48%; m.p. 152.0–153.0°C; $[\alpha]_D = +50°$ ($c = 0.11$ in ethanol, 25°C). ^{1}H NMR (ppm): 8.65–8.05 (m, 3H), 7.85–7.40 (m, 3H), 6.25–5.65 (m, 2H), 1.65 (d, $J = 6$ Hz, 3H), 1.20 (s, 9H). IR (cm^{-1}): 3460, 3010–2880, 1660, 1600, 1520, 1350. MS: *m/z* 300 (41, M$^{+\cdot}$), 57 (100).

(R)-4-(N-1-Pivaloylamino-1-ethyl)-1-naphthylamine. The aromatic amine was obtained by reduction with hydrazine monohydrate in methanol and a catalytic amount of palladium on activated charcoal. Yield, 63%; m.p., 131.0–131.5°C; $[\alpha]_D = +111.2°$ ($c = 0.107$ in ethanol, 25°C). ^{1}H NMR (ppm): 8.20–7.70 (m, 2H), 6.75 (d, $J = 8$ Hz, 1H), 6.10–5.50 (s, 2H), 4.50–3.65 (s, 2H), 1.65 (d, $J = 6$ Hz, 3H), 1.20 (s, 9H). IR (cm^{-1}): 3460, 3010–2870, 1650, 1625, 1500, 1470-1450. MS: *m/z* 270 (100, M$^{+\cdot}$).

CSP I (PIV). The aromatic amine, 3-glycidoxypropyltrimethoxysilane and dried silica were stirred in methanol. Analysis: found, C 6.99, H 1.51, N 0.69%; calculated, 0.25 mmol of (*R*)-ligand/g stationary phase (based on N) and 0.23 mmol (*R*)-ligand/g stationary phase (based on C).

Preparation of CSP II (CYH)

(R)-1-(N-1-Cyclohexylcarboxamido-1-ethyl)-naphthalene. Yield, 82.3%; m.p., 170.0–170.5°C; $[\alpha]_D = +29.95°$ ($c = 0.177$ in ethanol, 25°C). ^{1}H NMR (ppm): 8.20–7.33 (m, 7H), 6.20–5.50 (m, 2H), 2.20–0.80 (m, 11H), 1.66 (d, $J = 6$ Hz, 3H). IR (cm^{-1}): 3620–2860, 1660, 1600, 1500, 1450. UV–VIS (nm): 288 (sh), 278, 268, 260 (sh), 222. MS: *m/z* 281 (4, M$^{+\cdot}$), 155 (100).

(R)-1-Nitro-4-(N-1-cyclohexylcarboxamido-1-ethyl)naphthalene. Yield, 44.5%; m.p., 193.5–194.5°C; $[\alpha]_D = +44.83°$ ($c = 0.029$ in ethanol, 25°C). ^{1}H NMR (ppm): 8.60–7.90 (m, 3H), 6.20–5.66 (m, 2H), 2.20–0.80 (m, 11H), 1.66 (d, $J = 6$ Hz, 3H). IR (cm^{-1}): 3440, 3000–2860, 1670, 1530, 1500, 1450, 1340. UV–VIS (nm): 328, 246, 220. MS: *m/z* 326 (67, M$^{+\cdot}$), 83 (100).

(R)-4-(N-1-Cyclohexylcarboxamido-1-ethyl)-1-naphthylamine. Yield, 71.66%; m.p., 176.0–176.5°C; $[\alpha]_D = +89.7$ ($c = 0.017$ in ethanol, 25°C). ^{1}H NMR (ppm): 8.16–7.20 (m, 5H), 6.75 (d, 1H), 6.10–5.40 (m, 2H), 4.12 (s, 2H), 2.20–0.70 (m, 11H), 1.66 (d, $J = 6$ Hz, 3H). IR (cm^{-1}): 3010–2860, 1650, 1628, 1500, 1450. UV–VIS (nm): 324, 242, 218. MS: *m/z* 296 (57, M$^{+\cdot}$), 171 (100).

CSP II (CYH). Analysis: found, C 6.43, H 1.34, N 0.63%; calculated, 0.22 mmol (*R*)-ligand/g stationary phase (based on N) and 0.20 mmol (*R*)-ligand/g stationary phases (based on C).

Preparation of CSP III (ADA)

(R)-1-(N-1-Adamantylcarboxamido-1-ethyl)-naphthalene. Yield, 81%; m.p., 189.0–190.0°C; $[\alpha]_D = +5°$ ($c = 0.1$ in ethanol, 25°C). ^{1}H NMR (ppm): 8.16–7.33 (m, 7H), 6.10–5.80 (m, 2H), 2.10–150 (m, 15H), 1.76 (d, $J = 10$ Hz, 3H). IR (cm^{-1}): 3450, 3000, 2910, 2850, 1650, 1600, 1500, 1450. UV–VIS (nm): 290, 278, 268, 260 (sh), 226, 220 (sh). MS: *m/z* 333 (36, M$^{+\cdot}$), 135 (100).

(R)-1-Nitro-4-(N-1-adamantylcarboxamido-1-

ethyl)naphthalene. Yield, 38%; m.p., 201.0–203.0°C (decomposition); $[\alpha]_D = +10°$ ($c = 0.1$ in ethanol, 25°C). ^{1}H NMR (ppm): 8.70–7.40 (m, 6H), 6.10–5.80 (m, 2H), 2.13–1.60 (m, 15H), 1.80 (d, $J = 10$ Hz, 3H). IR (cm^{-1}): 3450, 3000, 2910, 2850, 1660, 1600, 1500, 1450, 1340. UV–VIS (nm): 328, 246, 218. MS: *m/z* 378 (12, M$^{+\cdot}$), 135 (100).

(R)-4-(N-1-Adamantylcarboxamido-1-ethyl)-1-naphthylamine. Yield, 67%; m.p., 191.0°C (decomposition); $[\alpha]_D = +52°$ ($c = 0.1$ in ethanol, 25°C). ^{1}H NMR (ppm): 8.20–7.40 (m, 6H), 6.78 (d, $J = 8$ Hz, 2H), 5.90–5.50 (m, 2H), 2.00–1.10 (m, 15H), 1.75 (d, $J = 10$ Hz, 3H). IR (cm^{-1}): 3630, 3450, 3000, 2910, 2850, 1640, 1500, 1450. UV–VIS (nm): 324, 242, 214. MS: *m/z* 348 (100, M$^{+\cdot}$).

CSP III (ADA). Analysis: found, C 5.75, H 1.04, N 0.3%; calculated, 0.15 mmol (*R*)-ligand/g stationary phase (based on N) and 0.11 mmol (*R*)-ligand/g stationary phase (based on C).

Preparation of CSP IV (CPE)

(R)-1-(N-1-Cyclopentylpropionylamino-1-ethyl)naphthalene. Yield, 94%; m.p., 131.5–132.0°C; $[\alpha]_D = +39°$ ($c = 0.1$ in ethanol, 25°C). ^{1}H NMR (ppm): 7.47–8.23 (m, 7H), 5.97–5.77 (m, 2H), 2.35–0.70 (m, 13H), 1.67 (d, $J = 6$ Hz, 3H). IR (cm^{-1}): 3620, 3440, 3000, 2950, 2870, 1660, 1600, 1500, 1450. UV–VIS (nm): 290 (sh), 278, 268, 226. MS: *m/z* 295 (32 M$^{+\cdot}$), 155 (100).

(R)-1-Nitro-4-(N-1-cyclopentylpropionylamino-1-ethyl)naphthalene. Yield, 47%; m.p., 159.0–160.0°C; $[\alpha]_D = +49°$ ($c = 0.1$ in ethanol, 25°C), ^{1}H NMR (ppm): 8.67–7.53 (m, 6H), 5.93 (s, 2H), 2.30–0.80 (m, 13H), 1.65 (d, $J = 6$ Hz, 3H). IR (cm^{-1}): 3620, 3440, 3000, 2970, 2860, 1670, 1600, 1520, 1500, 1450, 1340. UV–VIS (nm): 334, 246, 222. MS: *m/z* 340 (22, M$^{+\cdot}$), 258 (100).

(R)-4-(N-1-Cyclopentylpropionylamino-1-ethyl)-1-naphthylamine. Yield, 30%; m.p., 156.0–158.0°C; $[\alpha]_D = 106°$ (c) = 0.1 in ethanol, 25°C). ^{1}H NMR (ppm): 8.17–7.40 (m, 6H), 6.73 (d, $J = 8$ Hz), 5.67 (s, 2H), (s, 2H), 2.36–0.82 (m, 13H), 1.62 (d, $J = 6$ Hz, 3 H). IR (cm^{-1}): 3610, 3430, 3000, 2950, 2860, 1650, 1640, 1490, 1450. UV–VIS (nm): 324, 238, 222. MS: *m/z* 310 (31, M$^{+\cdot}$), 171 (100).

CSP IV (CPE). Analysis: found, C 5.98, H 1.10, N 0.5%; calculated, 0.18 mmol (*R*)-ligand/g stationary phase (based on N and C).

Preparation of CSP V (HFP)

(R)-1-(N-1-Heptafluorobutyrylamino-1-ethyl)-naphthalene. Yield, 100%; m.p., 104–105°C; $[\alpha]_D = +40°$ ($c = 0.1$ in ethanol, 20°C). ^{1}H NMR (ppm): 8.17–7.35 (m, 7H), 6.64 (s, 1H), 5.97 (q, 1H), 1.73 (d, $J = 6$ Hz, 3H). IR (cm^{-1}): 3620, 3420, 2970, 1720, 1600, 1520, 1450. UV–VIS (nm): 288 (sh), 278, 269 (sh), 260 (sh), 206. MS: *m/z* 367 (100, M$^{+\cdot}$).

(R)-1-Nitro-4-(N-1-heptafluorobutyrylamino-1-ethyl)-1-naphthalene. Yield, 46%; m.p., 133.0–135.0°C; $[\alpha]_D = +54°$ ($c = 0.1$ in ethanol, 25°C). ^{1}H NMR (ppm): 8.63–7.50 (m, 6H), 6.87 (s, 1H), 6.00 (q, 1H), 1.75 (d, $J = 6$ Hz, 3H). IR (cm^{-1}): 3610, 3420, 2970, 1720, 1520, 1450, 1350. UV–VIS (nm): 324, 242, 218. MS: *m/z* 378 (12, M$^{+\cdot}$), 135 (100).

(R)-4-(N-1-Heptafluorobutyrylamino-1-ethyl)-1-naphthylamine. Yield, 86%; m.p., 137.5–138.5°C; $[\alpha]_D = +95°$ ($c = 0.1$ in ethanol, 25°C), ^{1}H NMR (ppm): 8.00–7.25 (m, 6H), 6.58 (s, 1H), 5.87 (q, 1H), 4.13 (s, 2H), 1.75 (d, $J = 6$ Hz, 3 H). IR (cm^{-1}): 3610, 3420, 2970, 1710, 1620, 1510, 1450. UV–VIS (nm): 306, 222, 198. MS: *m/z* 382 (100, M$^{+\cdot}$).

CSP V (HFP). Analysis: found, C 4.58, H 0.84, N 0.3, F 1.11%; calculated, 0.11 mmol (*R*)-ligand/g stationary phase (based on N) and 0.16 mmol (*R*)-ligand/g stationary phase (based on C).

Liquid chromatography

To eliminate fines the CSPs were sedimented five times in methanol. Stainless-steel tubes (25 cm × 3.2 mm I.D.) were used as columns. A slurry prepared from 1.9 g of the phase and 30 ml of methanol–triethylene glycol (1:9) was filled into the column with a Model 27486-4 air-driven fluid pump (Haskel Engineering and Supply, Burbank, CA, USA) at a pressure of 680 bar. The columns were conditioned with methanol and *n*-hexane.

Chromatography was performed using a Model 110 solvent metering pump (Altex, Berkeley, CA, USA); detector Hitachi Model 100-10 variable-wavelength UV detector (Kontron, Zürich, Switzerland), detection at 254 nm; sampling device, Rheodyne (Berkeley, CA, USA) Model 7125 syringe-loading sample injector with a 20-μl loop; and recording devices, Tarkan W & W recorder 600 (Kontron) and HP 3396 A integrator (Hewlett-Packard, Widen, Switzerland).

The mobile phases used were (a) *n*-hexane–2-pro-

panol (78:22) (b) *n*-hexane–tetrahydrofuran (THF) (75:25) and (c) *n*-hexane–THF (85:15) at a flow-rate of 1 ml/min. The columns and the mobile phase container were maintained at 20°C (Assistant WTE var 3185 thermostat; R.C. Kuhn, Berne, Switzerland).

Toluene as a non-retained standard, dissolved in the appropriate mobile phase, was used to determine the dead time, t_0, and number of theoretical plates, N_0. The measured values were in the range $1.46 \leqslant t_0 \leqslant 1.72$ min and $3300 \leqslant N_0 \leqslant 7600$ for the five phases tested.

RESULTS AND DISCUSSION

Structure of bonded phases

All synthesized phases I–V shown in Fig. 1 are identical except for the bulky aliphatic N-acyl group R_i. The loading density of chiral ligands and the packing quality of the five columns tested are comparable. From the results of elemental analyses we calculated surface densities of *ca.* 0.5–0.7 groups/nm^2, which correspond to only one eighth of the available silanol groups [20]. It was not possible to increase the amount of chiral ligands by using higher reactant concentrations in the bonding procedure. Reasons are the bulkiness of the ligands and the limited reactivity of the Si–OCH_3 group of the spacer molecule used.

Samples

Table II gives the chromatographic results obtained with all samples, different amides, most of them derived with a π-acidic DNB or 3,5-dinitrophenyl (DNP) group for increased charge-transfer (CT) interaction with the naphthalene group of the phases [17]. Every sample contains one or more aromatic groups. Compounds with strong π-acceptors such as DNB or DNP are strongly retained and, in general, sufficient resolution of enantiomers is achieved, as reported previously [14]. On CSP I (PIV), non-aromatic racemates were hardly or not resolved owing to a lack of strong CT interaction between aromatic systems [16]. It was found that a π–π interaction is important for enantiomer separation on all five stationary phases. All have a high selectivity for amides with a π-acidic N-acyl substituent, especially for the DNB-containing compounds **1**, **8**, **9**, **10**, **14**, and **26–29**. The highest separation factors were obtained with compound **14** on all five CSPs; **14** contains a π-basic naphthalene and a DNB-group on the chiral centre. The naphthalene group increases the π-acidity of the DNB group additionally.

Weaker π-acidic aromatic N-acyl substituents lower the ability for chiral recognition, as can be seen with compounds **2** and **15**. Compounds with π-basic or aliphatic N-acyl groups, such as **5–7** and **16–23** have lower separation factors on all five CSPs. Aliphatic N-acyl groups with larger and bulkier alkyl tails are slightly better resolved as shorter tailed homologues. Electronegative substituents increase the acidity of the amide group. The N-trichloro- and N-trifluoroacetyl derivatives are better resolved as the analogous N-acetyl derived amines. The aliphatic N-acyl "tails" increase the hydrophobic character of the samples. This leads to shorter elution times with the same mobile phase in comparison with analogous amines derived with the polar DNB group.

If the π-acidic site of the enantiomers is not fixed to the N-acyl group, as in **3**, chiral recognition is more difficult or even completely lost. The reason may be that several similarly stable diastereomeric complexes between the enantiomers and the chiral selectors are possible.

On CSP V (HFP) all samples have the poorest resolution and also the shortest retention times. Owing to the substitution with fluorine atoms the N-acyl group R_5 is very apolar and relatively small in comparison with the other R_i groups. A change in the polarity of the mobile phase (Table III) increases retention and the separation capability of the stationary phase considerably. Nevertheless, the separation factors for all the tested samples are still smaller than with the other phases.

Correlation experiments

Two homologous series, the racemic 1-phenylalkyl amines **1a–l** and the 1-phenylglycine derivatives **30a–j**, both as DNB derivatives (Fig. 2), were separated with *n*-hexane–2-propanol (78:22) as mobile phase (Tables IV and V and Figs. 3–6).

Chromatographic investigations on other aryl-based π-donor CSPs led to a hypothesis dealing with two competing recognition mechanisms, the non-intercalative and the intercalative process. Hydrogen bonding is an important contribution in the

TABLE II

RESOLUTION OF ENANTIOMERS **1–29** ON STATIONARY PHASES I–V

HPLC conditions: (a) *n*-hexane–2-propanol (78:22); (b) *n*-hexane–tetrahydrofuran (75:25); (c) *n*-hexane–tetrahydrofuran (85:15); flow-rate, 1 ml/min; column, 25 cm × 3.2 mm I.D., 5 μm; detection, UV (254 nm). No. = number of sample given in Table I; k'_1 = capacity factor of the first-eluted enantiomer; α = separation factor; configuration = configuration of last-eluted enantiomer; n.r. = no resolution.

No.	CSP I (PIV)		CSP II (CYH)		CSP III (ADA)		CSP IV (CPE)		CSP V (HFP)		Mobile phase	Configuration
	k'_1	α	k'_1	α	k'_1	α	k'_1	α	k'_1	α		
1	4.92	2.17	5.52	2.34	4.95	2.45	6.95	1.87	0.96	1.33	b	*R*
2	2.51	1.08	3.02	1.06	0.78	1.17	1.43	1.10	0.88	n.r.	b	*R*
3	2.82	1.01	3.56	n.r.	2.50	1.09	3.50	1.08	1.37	n.r.	b	*R*
4	2.51	1.08	3.02	1.06	1.90	1.06	3.19	1.05	3.28	1.05	b	*R*
5	1.44	1.08	1.64	1.07	1.51	1.11	2.80	1.07	2.04	n.r.	b	*R*
6	2.75	1.08	2.91	1.06	5.01	1.05	6.21	1.05	5.48	1.03	b	*R*
7	0.52	1.12	0.59	1.12	0.21	1.47	0.80	1.18	0.66	n.r.	b	*R*
8	3.39	3.46	3.10	3.63	3.92	3.73	3.97	2.72	1.10	1.32	b	*R*
9	4.26	2.57	4.19	2.60	4.39	2.68	5.00	2.09	1.26	1.27	b	*R*
10	8.92	1.32	9.55	1.27	8.45	1.38	12.33	1.31	1.78	1.11	b	3*S*,4*R*
11	10.62	2.28	8.80	2.63	9.57	2.52	12.89	2.53	1.01	1.36	b	
12	9.44	2.16	4.76	2.01	7.43	3.25	9.26	3.14	1.15	n.r.	b	
13	0.61	1.13	0.68	1.08	0.48	1.20	0.84	1.16	0.95	1.14	a	*R*
14	8.19	4.67	7.68	4.84	19.88	4.23	10.33	3.00	3.69	2.83	a	*R*
15	0.94	1.14	1.11	1.08	0.92	1.18	1.63	1.12	0.94	n.r.	b	*R*
16	2.03	1.09	1.73	1.08	1.70	1.14	2.99	1.09	2.11	n.r.	b	*R*
17	5.30	1.05	3.66	1.07	6.02	1.05	7.19	1.04	7.07	n.r.	b	*R*
18	2.95	1.08	3.01	1.05	1.98	1.12	3.16	1.08	2.69	n.r.	b	
19	1.92	1.09	1.97	1.05	1.37	1.58	2.43	1.10	1.98	n.r.	b	
20	3.42	1.12	2.89	1.10	2.91	1.23	3.74	1.17	2.93	n.r.	c	*R*
21	0.50	1.16	0.51	1.16	0.31	1.55	0.82	1.27	0.68	n.r.	b	*R*
22	1.06	1.14	1.05	1.12	0.65	1.41	1.16	1.24	0.61	n.r.	c	*R*
23	1.06	1.14	1.05	1.12	0.64	1.40	1.13	1.22	0.52	n.r.	c	*R*
24	2.97	1.10	3.24	1.09	2.12	1.11	3.52	1.08	1.29	1.06	b	
25	6.66	1.05	7.12	1.05	5.65	1.05	9.63	1.03	2.85	n.r.	b	
26	13.01	1.33	11.27	1.51	14.45	1.63	19.23	1.49	2.69	n.r.	b	
27	11.20	1.41	9.11	1.42	13.07	1.44	15.58	1.44	3.01	n.r.	b	
28	4.03	1.24	5.29	1.26	3.28	1.24	4.71	1.18	0.77	n.r.	b	
29	2.90	1.22	2.82	1.29	2.84	1.29	4.17	1.21	0.49	n.r.	b	

TABLE III

RESOLUTION OF ENANTIOMERS **1–29** ON STATIONARY PHASE V (HFP) WITH MOBILE PHASE *n*-HEXANE–2-PROPANOL

HPLC conditions: *n*-hexane–2-propanol (78:22); flow-rate, 1 ml/min; column, 25 cm × 3.2 mm I.D., 5 μm; detection, UV (254 nm). No. = number of sample given in Table I; k'_1 = capacity factor of the first-eluted enantiomer; α = separation factor; configuration = configuration of the last-eluted enantiomer; n.r. = no resolution.

No.	k'_1	α	Configuration	No.	k'_1	α	Configuration	No.	k'_1	α
1	0.96	1.33	*R*	**14**	3.69	2.83	*R*	**26**	1.24	n.r.
2	1.19	1.07	*R*	**15**	1.49	1.08	*R*	**27**	0.81	n.r.
3	2.26	1.03	*R*	**16**	3.05	1.06	*R*	**28**	0.77	n.r.
4	2.17	1.07	*R*	**17**	2.47	1.04	*R*	**29**	1.83	1.04
5	2.44	1.05	*R*	**18**	1.69	1.04	*R*			
6	1.66	1.04	*R*	**19**	1.41	1.06				
7	0.97	n.r.		**20**	1.29	1.05	*R*			
8	2.96	1.63	*R*	**21**	0.86	1.12	*R*			
9	3.03	1.47	*R*	**22**	0.74	1.13	*R*			
10	2.06	1.13	*R*	**23**	1.35	n.r.				
11	1.78	1.53		**24**	3.02	n.r.				
12	7.83	2.39		**25**	7.84	n.r.				
13	0.95	1.14	*R*							

diastereomeric complex formation for the resolution of alkyl ester derivatives. On the other hand, the homologous N-alkylamide derivatives form a complex with a dominant dipole stacking of the amide dipoles [2,11,12].

If the alkyl chain of the enantiomer intercalates between the strands of the bonded phase and is directed toward the underlying silica support, the separation factor α would diminish with longer alkyl chains more and more owing to unfavourable steric repulsion. If the alkyl chain of the solute is in a more rectangular position relative to the strands of the bonded phase, as in the proposed non-intercalative process, the separation factor α would increase

TABLE IV

RESOLUTION OF N-3,5-DINITROBENZOYL-1-PHENYLALKYLAMINES **1a–l** ON STATIONARY PHASES I–V

HPLC conditions: *n*-hexane–2-propanol (78:22); flow-rate, 1 ml/min; column, 25 cm × 3.2 mm I.D., 5 μm; detection, UV (254 nm). *n* = Number of carbon atoms in the alkyl chain; k'_1 = capacity factor of the first-eluted enantiomer; α = separation factor; configuration = configuration of last-eluted enantiomer.

n	CSP I (PIV)		CSP II (CYH)		CSP III (ADA)		CSP IV (CPE)		CSP V (HFP)		Configuration
	k'_1	α	k'_1	α	k'_1	α	k'_1	α	k'_1	α	
1	9.48	2.08	8.54	2.19	9.82	1.92	6.80	1.80	1.64	1.49	*R*
2	9.94	2.50	8.76	2.61	10.62	1.97	7.44	1.83	1.66	1.56	*R*
3	9.69	2.52	9.08	2.67	10.69	2.36	7.41	2.23	1.42	1.81	*R*
4	10.27	2.38	10.22	2.55	11.70	2.31	7.72	2.15	1.36	1.81	*R*
5	10.29	2.50	10.69	2.64	11.61	2.44	7.51	2.22	1.27	1.87	
7	9.29	2.47	9.62	2.77	10.97	2.51	7.13	2.33	1.12	1.92	
8	8.77	2.52	8.77	2.85	10.33	2.56	6.34	2.35	1.05	1.93	
9	8.43	2.57	8.61	2.94	10.24	2.62	6.49	2.39	1.00	1.95	
10	8.14	2.59	8.56	2.99	9.62	2.61	6.32	2.43	0.94	1.99	
13	7.57	2.67	7.75	3.08	8.56	2.68	6.12	2.45	0.80	2.02	
15	7.00	2.68	7.16	3.14	8.48	2.74	5.46	2.48	0.73	2.11	
17	5.53	2.70	6.96	3.19	6.26	2.76	5.05	2.52	0.68	2.31	

TABLE V

RESOLUTION OF *n*-ALKYL ESTERS OF N-3,5-DINITROBENZOYL-1-PHENYLGLYCINE **30a–j** ON STATIONARY PHASES I–V

HPLC conditions: *n*-hexane–2-propanol (78:22); flow-rate, 1 ml/min; column, 25 cm × 3.2 mm I.D., 5 μm; detection, UV (254 nm). *n* = Number of carbon atoms in the alkoxy chain; k'_1 = capacity factor of the first-eluted enantiomer; α = separation factor; configuration = configuration of last-eluted enantiomer.

n	CSP I (PIV)		CSP II (CYH)		CSP III (ADA)		CSP IV (CPE)		CSP V (HFP)		Configuration
	k'_1	α	k'_1	α	k'_1	α	k'_1	α	k'_1	α	
0	12.05	1.21	10.06	1.16	10.85	1.26	8.47	1.29	7.07	1.11	
1	10.16	1.20	8.02	1.17	8.83	1.29	6.34	1.27	5.69	1.03	*R*
2	7.29	1.20	6.13	1.15	7.14	1.28	5.38	1.27	4.50	1.04	*R*
3	7.13	1.22	5.53	1.16	6.11	1.29	4.63	1.29	3.73	1.06	*R*
4	6.67	1.22	5.23	1.15	5.74	1.30	4.22	1.30	3.35	1.08	
5	6.25	1.23	4.99	1.16	5.62	1.30	4.08	1.31	3.15	1.08	*R*
6	5.63	1.24	4.75	1.16	5.24	1.30	3.74	1.32	2.87	1.09	
8	5.21	1.23	4.68	1.16	5.04	1.31	3.67	1.34	2.56	1.09	
10	4.63	1.23	4.31	1.15	4.64	1.30	3.31	1.35	2.28	1.09	
12	4.34	1.23	4.01	1.15	4.48	1.31	3.09	1.34	2.13	1.09	

with a longer alkyl chain owing to a larger hydrophobic interaction.

For the homologous 1-phenylalkyl amide derivatives **1a–l** (Table IV and Fig. 3), on all five phases there is an increase in the separation factor α with increasing carbon number *n* of the *n*-alkyl "tail". The relative maximization of α at *n* = 2 and the different slopes of the connecting lines between the measured values with *n* < 4 and *n* > 4 point to different arrangements of the solutes in the diastereomeric complex.

Däppen *et al.* [18] calculated four stable complexes with (*R*)-2,2-dimethyl-N-{1-[1-(4-amino)naphthyl]ethyl}propanamide as a model phase and (*R*/*S*)-dinitro-N-(1-phenylethyl)benzamide (**1a**) as test solute. Based on CAMM calculations they pro-

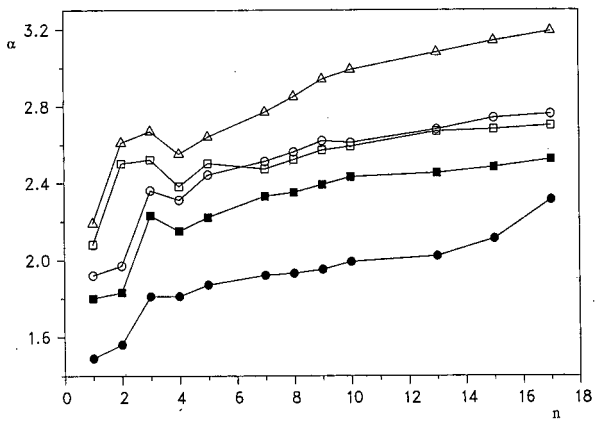

Fig. 3. Separation of phenylalkyl DNB derivatives **1a–l** on CSP I–V using *n*-hexane–2-propanol (78:22) as mobile phase. Separation factor α *versus* carbon number *n*. □ = CSP I (PIV); △ = CSP II (CYH); ○ = CSP III (ADA); ■ = CSP IV (CPE); ● = CSP V (HFP).

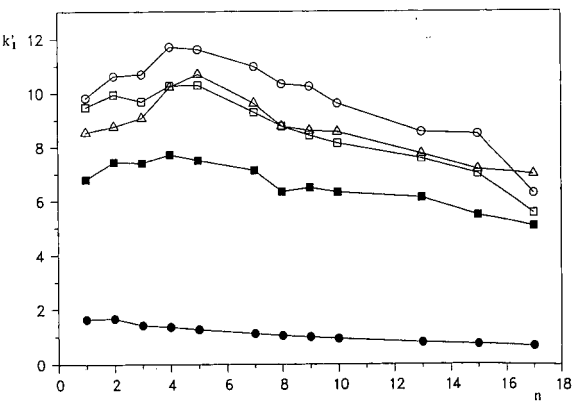

Fig. 4. Separation of phenylalkyl DNB derivatives **1a–l** on CSP I–V using *n*-hexane–2-propanol (78:22) as mobile phase. Capacity factor k'_1 *versus* carbon number *n*. □ = CSP I (PIV); △ = CSP II (CYH); ○ = CSP III (ADA); ■ = CSP IV (CPE); ● = CSP V (HFP).

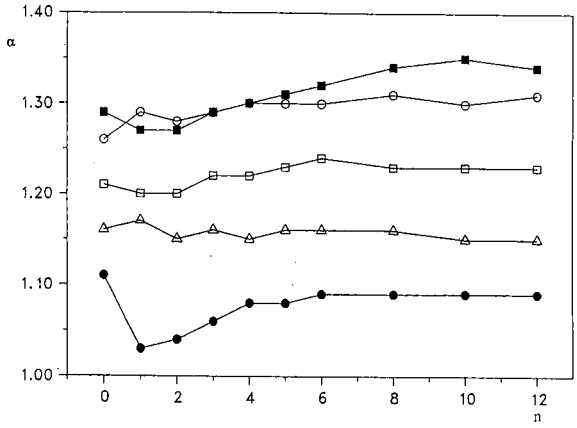

Fig. 5. Separation of phenylglycine DNB derivatives **30a–j** on CSP I–V using *n*-hexane–2-propanol (78:22) as mobile phase. Separation factor α *versus* carbon number *n*. □ = CSP I (PIV); △ = CSP II (CYH); ○ = CSP III (ADA); ■ = CSP IV (CPE); ● = CSP V (HFP).

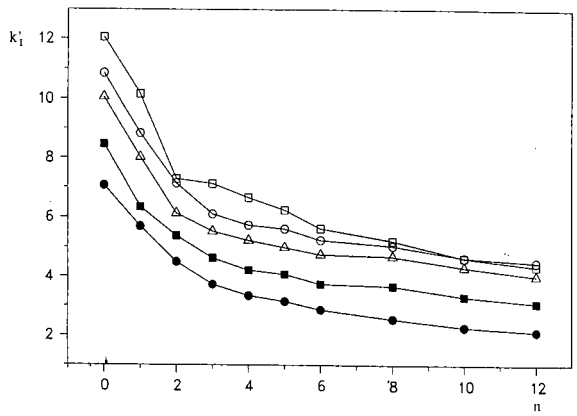

Fig. 6. Separation of phenylglycine DNB derivates **30a–j** on CSP I–V using *n*-hexane–2-propanol (78:22) as mobile phase. Capacity factor k'_1 *versus* carbon number *n*. □ = CSP I (PIV); △ = CSP II (CYH); ○ = CSP III (ADA); ■ = CSP IV (CPE); ● = CSP V (HFP).

posed an arrangement for the most stable complexes without parallel stacking of the aromatic π-donor and the π-acceptor system.

From this result and from our measurements, it is probable that shorter "tailed" enantiomers are capable of attaching with different orientations to the strands of the bonded phase and with partial inclusion between them. However, the short *n*-alkyl chains may not necessarily be directed straight toward the underlying silica support. Against that, solutes with longer alkyl chains have an orientation of the tails almost rectangular to the strands of the bonded phase. The measured α values increase with increasing chain length after $n > 4$ (butyl). This points to a non-intercalative mechanism for these longer "tailed" aryl containing enantiomers.

The *R*-enantiomer usually elutes last, and also there are no signs of inversion of the elution order, although not all pure enantiomers were available to check this completely. For butyl ($n = 4$) or pentyl ($n = 5$) the capacity factors k'_1 go through a maximum on phases I–III. On CSP IV (CPE) this tendency is less pronounced and on CSP V (HFP) the k'_1 values are minimal and nearly constant (Fig. 4).

A homologous series of 1-phenylalkylamine derivatives, **30a–j**, was eluted using hexane–2-propanol (78:22). Table V and Fig. 5 show the relationship between the separation factor α and the carbon number *n* of the analyte's alkyl chain. The corresponding dependence of the capacity factors k'_1 is seen in Fig. 6. For these analytes, the non-intercalative process is initially dominant, presumably because of the added hydrogen-bonding site, the carboalkoxy carbonyl oxygen [2,11,12].

On all five phases the separation factors remain nearly constant and there is a large decrease in the k'_1 values with increasing carbon number *n*. Hence the bulky alkyl "tails" of these samples do not influence the recognition mechanism of all five phases. This behaviour can only be explained with an orientation of the "tails" towards the mobile phase. The smallness of the separation factors is a result of the weaker rotational stability of the molecules, favouring more conformations in the diastereomeric complexes. An explanation for this type of solute was given by Pirkle and co-workers [21,22].

Comparison of bonded phases

All five CSPs show a similar separation behaviour but a different separation performance for chiral amides (Tables II–V, Figs. 3–6). Large differences are found in the magnitude of the separation factors α and in the elution times of the tested analytes. The enantioselectivity of the bonded phases decreases, in general, with the following order of the sterically determinative group: R_2 = cyclohexyl > R_1 = *tert.*-butyl > R_3 = adamantyl > R_4 = cyclopentylethyl ≫ R_5 = heptafluoropropyl. For some types of solutes there are small differences between CSP I, II and III in this general order.

The N-acyl group R_2 of CSP II (CYH) has the same molecular cross-sectional area as R_3 of CSP III (ADA) but no rigid and bulky spherical shape and, therefore, it is able to reach an energetically favourable position by turning of the cyclohexyl ring.

R_3 is the most bulky and rigid N-acyl substituent. R_1 of CSP I (PIV) has a similar volume but more freedom of rotation. This is better for the resolution of short "tailed" enantiomers.

The cyclopentyl ring of CSP IV (CPE) has a smaller diameter than the cyclohexyl ring but its ethyl bridge is freely moveable towards the amide group of the selector. This also allows a more favourable displacement of R_4 in the diastereomeric complex with the analyte. Owing to the smaller dimension of the cyclopentyl ring, the steric interaction site of the chiral selector is smaller than that with the larger R_2.

The CSP V (HFP) with the small and apolar group R_5 shows the poorest resolution and the shortest elution times of all phases. Very polar solutes are badly resolved. With a more hydrophobic analyte a better interaction with the stationary phase is possible owing to a larger extent of dispersional forces.

CONCLUSIONS

Using N-1-(1-naphthyl)ethylamine as starting material, chiral stationary π-donor phases with different separation performances for chiral amine derivatives are accessible. Derivatization of these amines with a strong π-acceptor group such as N-3,5-dinitrobenzoyl or 3,5-dinitrophenyl gives the best results. A variation of the N-acyl substituent of the chiral selector changes the separation performance and the polarity of the bonded phase, indicating a significant contribution of steric interactions in the chiral recognition process.

From correlation experiments with homologous series of analytes, two non-intercalative chiral recognition processes can be assumed. In addition to π–π interactions between aromatic moieties of the solute and the CSP, the steric fit between the molecules within the complex determines the magnitude of the resolution. Bulky but flexible N-acyl groups such as cyclohexylcarbonyl or pivaloyl attached to the chiral centre of the selector increase the discrimination between the two chiral antipodes.

ACKNOWLEDGEMENTS

We thank Mrs. Vera Rätz for valuable assistance with the synthetic and analytical work, the Intercantonal Office for the Control of Medicaments, Berne, for kindly providing samples, Mr. H. Gfeller for mass spectrometric measurements, Dr. W. Padowetz of Ciba Geigy, Basle, for elemental analyses and Mrs. H. Murray for linguistic advice.

REFERENCES

1 S. G. Allenmark, *Chromatographic Enantioseparation, Methods and Applications*, Wiley, New York, 1989.
2 W. H. Pirkle, M. H. Hyun, A. Tsipouras, B. C. Hamper and B. Bank, *J. Pharm. Biomed. Anal.*, 2 (1984) 173.
3 W. Lindner and C. Petterson, in I. W. Wainer (Editor), *Liquid Chromatography in Pharmaceutical Development, an Introduction*, Aster, Springfield, 1985, p. 63.
4 I. W. Wainer, *Trends Anal. Chem.*, 6 (1987) 125.
5 H. Lienne, M. Caude, A. Tambuté and R. Rosset, *Analusis*, 15 (1987) 431.
6 W. H. Pirkle, J. M. Finn, J. L. Schreiner and B. C. Hamper, *J. Am. Chem. Soc.*, 103 (1981) 3964.
7 W. H. Pirkle, J. M. Finn, B. C. Hamper, J. L. Schreiner and J. R. Pribish, *ACS Symp. Ser.*, 185 (1982) 245.
8 R. Däppen, H. Arm and V. Meyer, *J. Chromatogr.*, 373 (1986) 1.
9 A. M. Krstulovic, *J. Pharm. Biomed. Anal.*, 6 (1988) 641.
10 W. H. Pirkle and M. H. Hyun, *J. Org. Chem.*, 49 (1984) 3043.
11 W. H. Pirkle, M. H. Hyun and B. Bank, *J. Chromatogr.*, 316 (1984) 585.
12 W. H. Pirkle and M. H. Hyun, *J. Chromatogr.*, 328 (1985) 1.
13 V. R. Meyer, *Chromatographia*, 24 (1987) 639; and references cited therein.
14 R. Däppen, V. R. Meyer and H. Arm, *J. Chromatogr.*, 361 (1986) 93.
15 R. Brügger, P. Krähenbühl, A. R. Marti, R. Straub and H. Arm, *J. Chromatogr.*, 557 (1991) 163.
16 R. Brügger, A. R. Marti, V. R. Meyer and H. Arm, *J. Chromatogr.*, 440 (1988) 197.
17 R. Däppen, H. R. Karfunkel and F. J. J. Leusen, *J. Chromatogr.*, 469 (1989) 101.
18 R. Däppen, H. R. Karfunkel and F. J. J. Leusen, *J. Comput. Chem.*, 11 (1990) 181.
19 R. Straub, *Dissertation*, University of Berne, Berne, 1990.
20 K. K. Unger, *Porous Silica (Journal of Chromatography Library, Vol. 16)*, Elsevier, Amsterdam, 1979, p. 57.
21 W. H. Pirkle, D. W. House and J. H. Finn, *J. Chromatogr.*, 192 (1980) 143.
22 W. H. Pirkle, C. J. Welch and M. H. Hyun, *J. Org. Chem.*, 48 (1983) 5022.

Journal of Chromatography, 585 (1991) 207–211
Elsevier Science Publishers B.V., Amsterdam

CHROM. 23 544

Fast protein separation by reversed-phase high-performance liquid chromatography on octadecylsilyl-bonded non-porous silica gel

Effect of particle size of column packing on column efficiency

Noriyuki Nimura*, Hiroko Itoh and Toshio Kinoshita

School of Pharmaceutical Sciences, Kitasato University, 9-1 Shirokane-5, Minato-ku, Tokyo 108 (Japan)

Norikazu Nagae and Mitsugu Nomura

Nomura Chemical Co. Ltd., 1-6 Sumire-dai, Seto-City, Aichi 489 (Japan)

(Received May 27th, 1991)

ABSTRACT

The effect of the particle size of column packings on column efficiency in the reversed-phase high-performance liquid chromatographic separation of proteins was studied. Fast protein separations on non-porous octadecylsilyl (C_{18}) spherical silica gels of three different particle diameters (2, 5 and 20 μm) were examined, and five standard proteins were completely resolved within 20 s using a steep gradient elution with 0.1% aqueous trifluoroacetic acid–acetonitrile in all instances. The column efficiencies were approximately the same for all particle sizes. The large-particle (20 μm), non-porous C_{18} column could be operated at room temperature for the fast protein separation. Rapid separations on conventional macroporous C_{18} silica particles of 7 and 20 μm were also examined.

INTRODUCTION

Reversed-phase high-performance liquid chromatography (HPLC) has become a widely used technique for the separation of proteins and peptides. Many kinds of stationary phases have been investigated [1] and silica gel or organic polymer gel-based macroporous supports with hydrophobic surfaces have been developed. Since Unger and coworkers [2–6] presented a chemically bonded non-porous silica gel with particles of 1.5 μm for protein separation, it has been shown that small-particle non-porous supports are more suitable than porous supports for the separation of proteins [7,8]. More recently, fast protein separations within 10 or 20 s [9–12] have been achieved on reversed-phase non-porous packings with particles of less than 2 μm. However, these approaches are generally restricted by the concomitant decrease in column permeability due to excessive pressure. Therefore, the column temperature needs to be maintained at 70–80°C for fast separation.

The mechanisms of protein separation in the reversed-phase gradient elution mode have also been investigated [13–19]. It is thought that the proteins are retained at the column inlet until at some point in the gradient they are desorbed completely. They then move through the column without further in-

0021-9673/91/$03.50

teraction with the stationary phase [15,16]. Protein separation by reversed-phase gradient chromatography is therefore based on a characteristic elution mode which differs from the chromatographic separation of low-molecular-weight compounds. These results prompted the consideration that the particle size of the column packings may not be such an important parameter in the efficiency of the columns in the reversed-phase gradient chromatographic separation of proteins.

In the work reported here, fast protein separation was studied on octadecylsilyl-bonded non-porous silica gels with 2-, 5- and 20-μm particles. Five standard proteins were completely resolved within 20 s on the all column packings and the efficiencies of the columns were approximately the same. The column packed with the 20-μm gel could be operated at room temperature for fast protein separation as a result of its low back-pressure.

EXPERIMENTAL

Reagents

Protein samples, bovine serum albumin, carbonic anhydrase (bovine erythrocytes), cytochrome *c* (horse heart), insulin (bovine pancreas), insulin B chain (bovine insulin), α-lactalbumin (bovine milk) and lysozyme (chicken egg white) were purchased from Sigma (St. Louis, MO, USA). HPLC-grade acetonitrile and trifluoroacetic acid (TFA) were from Wako (Osaka, Japan). The water was purified by passing through a Milli-R/Q system (Millipore, Bedford, MA, USA).

Non-porous silica gels (mean particle diameter 2, 5 and 20 μm) were manufactured by Nomura (Seto-City, Japan) and these materials were chemically bonded with *n*-octadecyldimethylchlorosilane and end-capped with trimethylchlorosilane by conventional methods [20]. The resulting octadecylsilyl-bonded phases were slurry-packed into 30 mm × 4.6 mm I.D. stainless-steel column tubes. For comparison with the separation on the non-porous silica column, the porous silica gels Develosil 300-ODS-7 and -20 (mean pore diameter 30 nm, particle sizes 7 and 20 μm, Nomura) were packed into the same size column tubes.

Instruments

A low-pressure gradient HPLC system consisting of an 880-PU HPLC pump (Jasco, Tokyo, Japan) equipped with an ERC-3510 degasser (Erma, Tokyo, Japan), an 880-SC system controller (Jasco), an 880-02 ternary gradient unit (Jasco), a Model 7125 injector (Rheodyne, Cotati, CA, USA) and an 860-CO column oven (Jasco) was used. The polypeptides were detected with a Shimadzu SPD-2A spectrophotometric detector. The chromatograms were processed by a Model LC100W/F PC workstation equipped with an analogue-to-digital converter (Yokogawa Electric, Tokyo, Japan).

Chromatographic conditions

The following eluent composition was used for gradient elution: A, 0.1% TFA in water; B, 0.1% TFA in 90% aqueous acetonitrile. The gradient programs and flow-rates are given in the text and figure legends. The column temperature was maintained at 75°C or room temperature. The column effluent was monitored at 220 nm.

Each protein was dissolved in eluent A at a concentration of 1 mg/ml and each solution was mixed as an equivalent volume prior to injection. An aliquot of the mixture (5 μl) was injected into the HPLC system. Sample injections coincided with the commencement of the gradient and the actual gradient delay was previously determined by a tracer technique with an acetone-containing eluent. The sample loading capacity of the 20-μm non-porous column, which is the lowest of the columns examined here, was about 10 μg of carbonic anhydrase.

RESULTS AND DISCUSSION

In a preliminary examination, standard proteins were separated on the non-porous C_{18} silica column under conventional gradient elution conditions and the separation was compared with that on a macroporous C_{18} silica column under the same elution conditions. Fig. 1 shows the chromatograms of proteins on the non-porous and macroporous columns. Although the surface areas of the non-porous and macroporous silica were approximately 0.6 and 100 m^2/g, respectively, the retention times on the non-porous silica column were approximately the same as those on the macroporous column, in spite of their greatly different surface areas. This result is consistent with previous studies on protein separation mechanisms such as the on–off mecha-

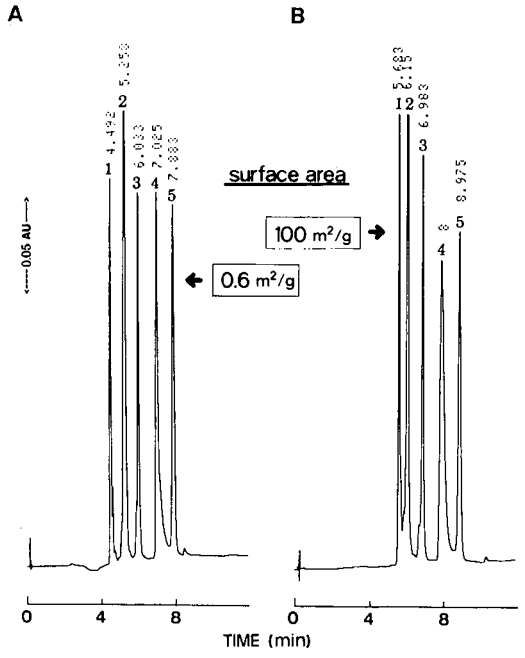

Fig. 1. Chromatograms of proteins on octadecylsilyl (C_{18}-bonded non-porous (NP-C_{18}-5, particle size 5 μm) (A) and macroporous (MP-C_{18}-7, particle size 7 μm) (B) silica columns under conventional gradient elution conditions. Conditions: flow-rate, 2 ml/min; linear gradient, from 10 to 100% eluent B in 20 min; column temperature, ambient. Peaks: 1 = insulin; 2 = cytochrome *c*; 3 = lysozyme; 4 = bovine serum albumin; 5 = carbonic anhydrase.

nism presented by Regnier and co-workers [13,16]. Proteins in the reversed-phase gradient separation would not be repeatedly partitioned on the stationary phase. This suggests that diffusion of the chromatographic peak by repeated adsorption and desorption between the stationary phase and the mobile phase is negligible. Therefore the particle size of the column packings, which is the most important factor in plate theory, would not be such a significant parameter in determining the column efficiency in the reversed-phase gradient chromatographic separation of proteins.

Fig. 2 shows chromatograms of the rapid separation of proteins obtained using columns packed with non-porous C_{18} silica gels of different particle sizes (2, 5 and 20 μm) at a constant flow-rate of 4.0 ml/min. Under this elution condition, as the 2- and 5-μm silica columns showed high back-pressures (over 200 kg/cm^2), all the columns were operated at 75°C.

In all instances the five standard proteins were completely resolved within 20 s and the column efficiencies were determined with the peak widths and resolutions approximately the same. The efficiency achieved by the 20-μm silica column was slightly poorer than those achieved by 2- and 5-μm silica columns. The peak width of carbonic anhydrase on the 20-μm silica column was 1.2 times that on the columns with smaller particles. However, the extent of the decrease of the 20-μm silica column efficiency was negligible small. These results were expected, for the following reasons. Solutes in gradient elution generally disperse not only in a process of repeating partition, but also in a process of non-retention followed by desorption. Especially in protein

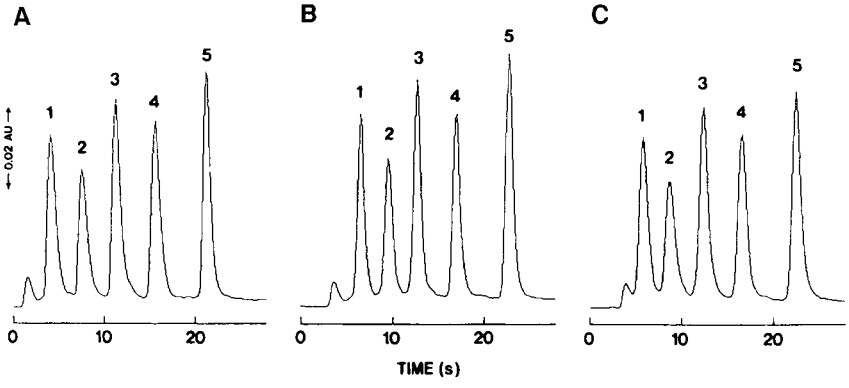

Fig. 2. Fast protein separations on C_{18}-bonded non-porous silica particles of diameter 2 μm (A), 5 μm (B) and 20 μm (C) performed at 75°C. Conditions: flow-rate, 4 ml/min; linear gradient, from 22 to 100% eluent B in 48 s; column temperature, 75°C. Peaks: 1 = insulin B chain; 2 = insulin; 3 = lysozyme; 4 = α-lactalbumin; 5 = carbonic anhydrase.

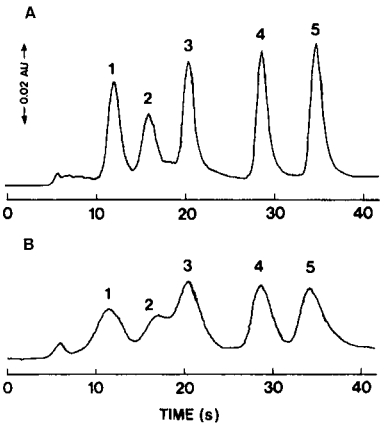

Fig. 3. Fast protein separations on C_{18}-bonded macroporous silica particles of diameter 7 μm (A) and 20 μm (B) performed at 75°C. Conditions: linear gradient, from 34 to 100% eluent B in 48 s. Other conditions and peaks as in Fig. 2.

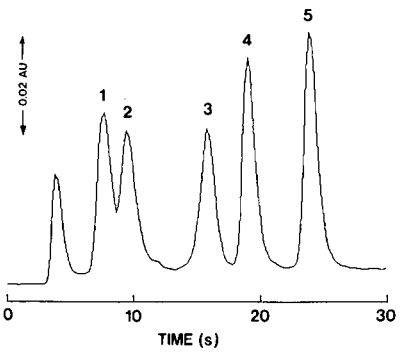

Fig. 4. Fast protein separation at room temperature on non-porous C_{18} particles of diameter 20 μm (NP-C_{18}-20). All conditions as in Fig. 2, except column temperature.

separation, diffusion during the partition process can be neglected as the adsorption-to-desorption transition of proteins [13,16] may only occur once by minute increases in the concentration of the organic solvent in the mobile phase. The proteins then move through the column without further interaction with the bonded phase. Although the dispersion of the unretained solute depends on the particle size of the packing material, this is not a significant factor if the column is small. Slight differences in the peak width dependent on the difference in particle size seem to be caused by such a diffusion factor in these data.

Fig. 3 shows chromatograms of the rapid separation of proteins on the 7- and 20-μm macroporous C_{18} silica particles performed at 75°C. Five proteins were separated within 40 s. The separations were influenced by the particle size. However, the column efficiency should also generally be affected by the distribution of pore size and decreases such as those shown here could be a result of both pore size and particle size distribution.

From these investigations it can been seen that non-porous supports might be favourable for rapid separations with a steep gradient elution because the stream of mobile phase will not become stagnant in pores as is observed on porous supports. Furthermore, a large-particle (20 μm), non-porous silica column can be operated at room temperature because of its low back-pressure. Fig. 4 shows the rapid separation of proteins on the 20-μm non-porous C_{18} column at room temperature. Proteins were satisfactorily separated within 30 s. An unknown peak was observed at the solvent front. This peak might be one of conformers of lysozyme, which is known to unfold reversibly in solution. The conformer concentration increased as the column temperature decreased and with an increasing concentration of acetonitrile at the start of the gradient. As shown previously by Benedek *et al.* [21], lysozyme gave two peaks in the reversed-phase separation; the native peak was more weakly retained than the denatured peak on the bonded phase surface. Therefore the first peak in Fig. 4 might be lysozyme without denaturation; the denatured peak, which was observed at about 15 s, decreased as the native peak increased.

The biological activities of the enzyme protein could often be regained after reversed-phase separation combined with an appropriate treatment such as dilution with a buffer solution [5]. A more rapid and lower temperature operation of the separation therefore allows a higher recovery of the biological activities of proteins. This suggests that the 20-μm non-porous support column may be very useful in the biochemical field.

REFERENCES

1 K. K. Unger, R. Janzen and G. Jilge, *Chromatographia*, 24 (1987) 144.
2 K. K. Unger, J. N. Kinkel. B. Anspach and H. Giesche, *J. Chromatogr.*, 296 (1984) 3.

3 K. K. Unger, G. Jilge, J. N. Kinkel and M. T. W. Hearn, *J. Chromatogr.*, 359 (1986) 61.
4 G. Jilge, R. Janzen, H. Giesche, K. K. Unger, J. N. Kinkel and M. T. W. Hearn, *J. Chromatogr.*, 397 (1987) 71.
5 R. Janzen, K. K. Unger, H. Giesche, J. N. Kinkel and M. T. W. Hearn, *J. Chromatogr.*, 397 (1987) 81.
6 R. Janzen, K. K. Unger, H. Giesche, J. N. Kinkel and M. T. W. Hearn, *J. Chromatogr.*, 397 (1987) 91.
7 L. F. Colwell and R. A. Hartwick, *J. Liq. Chromatogr.*, 10 (1987) 2721.
8 Y. Kato, T. Kitamura, A. Mitsui and T. Hashimoto, *J. Chromatogr.*, 398 (1987) 327.
9 K. Kalghatgi and C. Horvath, *J. Chromatogr.*, 398 (1987) 335.
10 Y.-F. Maa and C. Horvath, *J. Chromatogr.*, 445 (1988) 71.
11 G. P. Rozing and H. Goetz, *J. Chromatogr.*, 476 (1989) 3.
12 K. Kalghatgi, *J. Chromatogr.*, 499 (1990) 267.
13 J. D. Pearson, N. T. Lin and F. D. Regnier, *Anal. Biochem.*, 124 (1982) 217.
14 F. E. Regnier, *Science*, 222 (1983) 245.
15 L. R. Snyder, M. A. Stadalius and M. A. Quarry, *Anal. Chem.*, 55 (1983) 1413A.
16 X. Geng and F. E. Regnier, *J. Chromatogr.*, 296 (1984) 15.
17 D. W. Armstrong and R. E. Boehm, *J. Chromatogr. Sci.*, 22 (1984) 378.
18 M. A. Quarry, M. A. Stadalius, T. H. Mourey and L. R. Snyder, *J. Chromatogr.*, 358 (1986) 1.
19 M. A. Stadalius, M. A. Quarry, T. H. Mourey and L. R. Snyder, *J. Chromatogr.*, 358 (1986) 17.
20 J. N. Kinkel, and K. K. Unger, *J. Chromatogr.*, 316 (1984) 193.
21 K. Benedek, S. Dong and B. L. Karger, *J. Chromatogr.*, 317 (1984) 227.

Journal of Chromatography, 585 (1991) 213–217
Elsevier Science Publishers B.V., Amsterdam

CHROM. 23 513

Rapid electrodialytic clean-up of biological samples for high-performance liquid chromatography

Jeffrey D. Brewster and Edwin G. Piotrowski

US Department of Agriculture, ARS, Eastern Regional Research Center, 600 East Mermaid Lane, Philadelphia, PA 19118 (USA)

(First received October 18th, 1990; revised manuscript received May 14th, 1991)

ABSTRACT

A sample clean-up system employing electrodialysis with size-selective and charge-selective membranes is described. When applied to the treatment of 0.5-ml milk samples containing sulfamethazine, the system produced an undiluted, clear solution in 3 min and eliminated the components in untreated milk that caused column fouling and double peaks. In contrast to conventional liquid- and solid-phase extraction procedures, electrodialytic clean-up is readily automated and uses no organic solvents.

INTRODUCTION

The preparation of biological samples for chromatographic analysis is frequently the slowest and most labor-intensive step in the analytical process. Typical extraction procedures are complex, difficult to automate and entail the expense of handling and disposing of large volumes of organic solvents. Significant improvements in the efficiency and cost of such analyses could be realized by the development of rapid, readily automated sample clean-up procedures. Procedures which also avoid use of organic solvents and provide sufficient sample capacity to allow off-line or on-line concentration would be most effective.

Kok *et al.* [1,2] recently introduced zone electrophoretic sample treatment (ZEST), an on-line electrophoretic technique for the isolation of low-molecular-weight ionic species from complex matrices. While effective in the rapid isolation of analytes from biological matrices, ZEST lacks sufficient sample capacity for trace analysis. In ZEST, a long, narrow sample volume is used in order to maximize sample capacity while suppressing convective mixing and providing efficient removal of Joule heat [1]. Migration occurs parallel to the long axis of the sample volume, so that the analyte must migrate the full length of the sample plug in order to separate from the matrix. Placing a semi-permeable membrane perpendicular to the field permits the use of a different geometry in which migration takes place across the narrow dimension of the sample volume, through the membrane and into a receiving solution. The analyte need only migrate a short distance to achieve complete separation from the matrix, and the increased separation speed permits continuous sample introduction, resulting in much higher throughput. Using appropriate membrane types and configurations, it is possible to remove ions from a feed stream, to concentate an ionic solute or to separate macromolecules and neutral species from small ions. Such electrodialytic systems have long been used on an industrial scale for applications such as desalination of water and concentration of whey [3].

Analytical applications of electrodialysis for the extraction of a number of pharmaceutical compounds [4–6] and metal ions [7] have been described. Although indicating the potential utility of electrophoretic sample treatment, these studies did not demonstrate the capability to isolate rapidly trace levels of analyte from biological samples in volumes compatible with moden chromatographic techniques. The apparatus described here employs

0021-9673/91/$03.50

continuous sample introduction and microliter volumes for the isolation of a charged drug (sulfamethazine) from a complex matrix (skim milk) in less than 5 min. Although the clean-up step was conducted off-line in this work, on-line connection to a high-performance liquid chromatographic (HPLC) system is readily implemented. After completion of this work, a study of electrodialytic sample treatment for amphetamine in serum was published [8].

EXPERIMENTAL

Reagents and solutions

Sulfamethazine (Sigma), Alizarin Red S (National Aniline Division, New York, NY, USA), Procion Blue (Pharmacia), bovine serum albumin (Sigma), tris(hydroxymethyl)aminomethane (Tris), hydrochloric acid, potassium dihydrogenphosphate (Mallinckrodt), non-fat milk (Harbison's Dairies, Bristol, PA, USA), dialysis tubing (Dialya-Por; Thomas Scientific, Philadelphia, PA, USA) and fabric-reinforced cation-exchange membrane type 103QZL386 (Ionics, Watertown, MA, USA) were used as received. Spiked milk was prepared by addition of aqueous stock sulfamethazine to give a concentration of 4 μg/ml and stored at 4°C. Prior to treatment and/or analysis, an aliquot was diluted 1:20 with 0.01 *M* Tris buffer (pH 8.5).

Apparatus

Electrodialysis was conducted in a locally constructed cell shown in Fig. 1. The cell consisted of a stack or "sandwich" of membrane support plates (b,i), membranes (d,f,h) and 0.35-mm fluoropolymer gaskets (e,g), which form the feed and receiving compartments. These stack components were pressed between two 50 × 75 × 9 mm poly(methyl methacrylate) (PMA) blocks (b,j) containing cylindrical holes which formed the anode and cathode compartments. PMA cover plates (a,k) fit over the blocks to seal the electrode compartments. Bolts (omitted for clarity) passed through holes (not shown) around the periphery of the PMA blocks and stack components to compress and seal the stack. Feed and receiving buffers were introduced through 0.5 mm I.D. fluoropolymer tubes which were joined with threaded fittings (m) to one of the PMA blocks. Small holes in each of the stack components allowed fluid to flow from these fittings in-

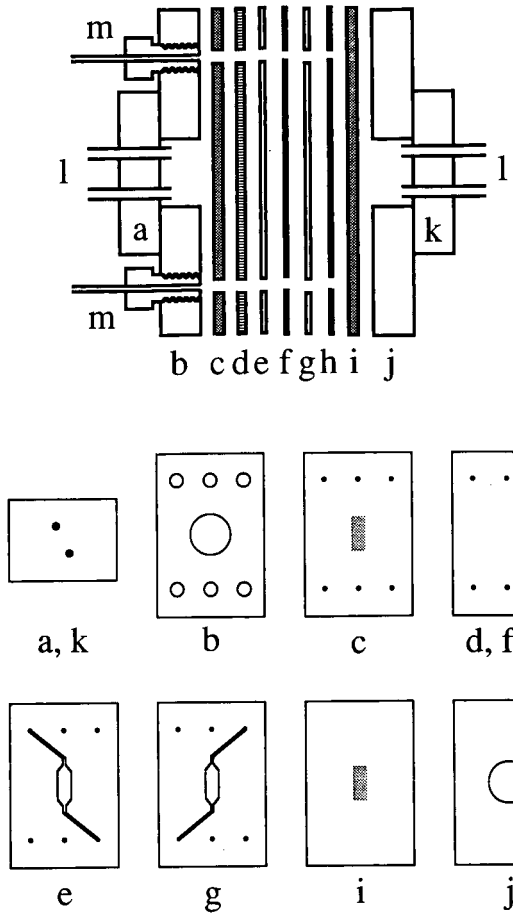

Fig. 1. Electrodialysis cell. a = Anode compartment cover-plate; b = PMA block; c = membrane support plate; d = cation-exchange membrane; e = gasket with receiving compartment; f = dialysis membrane; g = gasket with feed compartment; h = dialysis membrane; i = membrane support plate; j = PMA block; k = cathode compartment cover-plate; l = 3 mm O. D. tubular stainless-steel electrodes; m = threaded fittings for feed and receiving buffer inlet/outlet.

to the feed and receiving compartments. The total volume of each fluid path was *ca.* 100 μl, and the active membrane area was *ca.* 1 cm^2. Electrolyte was pumped through flexible plastic tubing connected to 3 mm O.D. stainless-steel tubes (l) pressed into the electrode compartment cover-plates. These stainless-steel tubes also served as electrodes. The membrane support plates were 1.5-mm rigid plastic sheets perforated with a rectangular array of small holes.

The sample treatment system is shown schematically in Fig. 2. Each of the four fluid streams was fed with a peristaltic pump channel [Manostat (New York, USA) cassette pump]. Sample was introduced into the sample stream by a low-pressure loop injection valve (Rheodyne) with a 0.5-ml injection volume. Treated sample was collected in small test-tubes at the outlet of the cell. A power supply capable of delivering up to 400 V at 100 mA (Heathkit Model IP-32) was used.

The locally assembled HPLC system consisted of an LC-500 syringe pump (Isco), a Model 7125 injector (Rheodyne) with a 100-μl loop, a 250 × 4.6 mm I.D. columns with 5-μm LC18 packing (Supelco) and a Model 115 variable-wavelength UV detector (Gilson) operated at 265 nm. The mobile phase was 0.05 *M* phosphate buffer (pH 6.0)–methanol (70:30) at a flow-rate of 1.5 ml/min [9].

Procedure

Feed, receiving and electrolyte solutions were pumped through the cell and the desired voltage applied. Solutions to be treated were loaded into the loop of the injector and fed into the cell by switching the valve. Recovery (ratio of total analyte in receiving stream to analyte injected) was determined by off-line spectrophotometry of the collected feed and receiving streams following injection of 0.5 ml of sample. The following conditions were used for milk sample treatment: feed flow-rate, 0.29 ml/min; feed buffer, 0.01 *M* Tris (pH 7.4); receiving flow-rate, 0.12 ml/min; receiving buffer, 0.1 *M* Tris (pH 8.5); electrolyte flow-rate, 4.5 ml/min; electrolyte, 0.1 *M* Tris–1 *M* KCl (pH 8.5); applied voltage, 16 V; applied current, 72 mA. The fraction emerging from the receiving side between 2 and 3 min after injection was collected and a 50-μl aliquot was analyzed off-line by HPLC by partially filling the injection loop. Untreated milk was filtered through a 0.2-μm syringe filter prior to HPLC analysis.

RESULTS AND DISCUSSION

The analysis of milk for sulfa drugs is representative of the problems encountered with the HPLC of biological samples. Although there are no chroma-

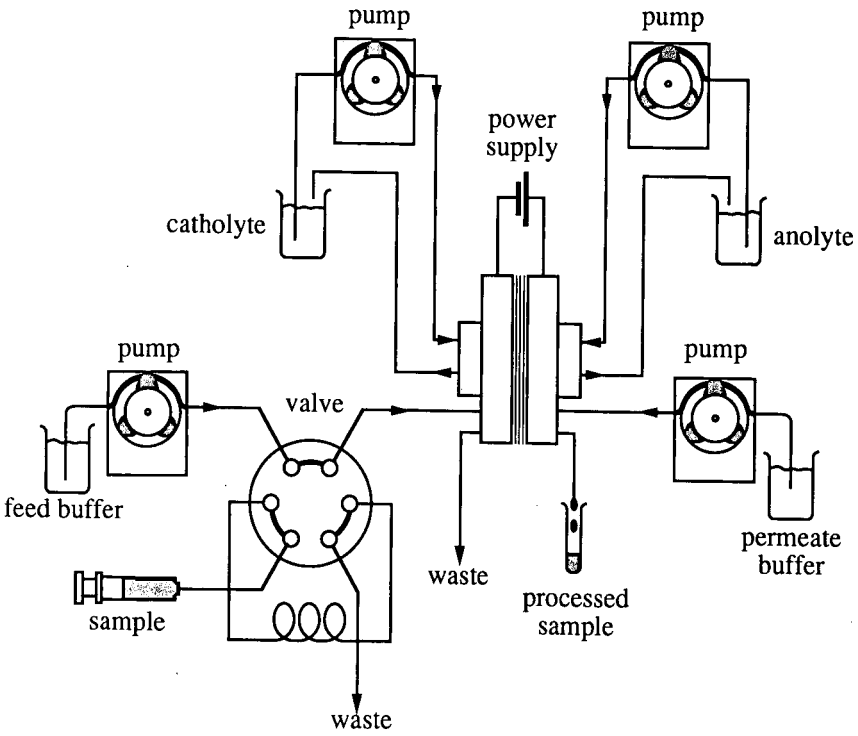

Fig. 2. Electrodialytic sample clean-up system.

tographic interferences from skim milk under the conditions used for this analysis, injection of untreated milk results in rapid degradation of the separation and eventual desctruction of the column, as evidenced by peak broadening, peak splitting and increasing back-pressure. Sample clean-up using solvent extraction [9], solid-phase extraction [10] or dialysis/trace enrichment [11] is typically required in order to remove the sample components which cause these difficulties.

The stack-type electrodialysis cell provides considerable flexibility in membrane configuration and other operating parameters. The physical dimensions of the cell represent a compromise between maximizing the recovery of analyte (large membrane area, short residence times) and minimizing the non-selective transport of matrix constituents (small membrane area, short residence times). Initial studies were conducted with the anionic dye Alizarin Red S (ARS) as a model analyte, and bovine serum albumin covalently labelled with Procion Blue (BSA/PB) as a model matrix. The effects of flow compartment geometry, sample conductivity, applied potential and flow-rate were evaluated. Recovery was measured using 1 mg/ml ARS, and selectivity (ratio of ARS to BSA/PB recoveries) was measured with ARS–BSA/PB mixtures. Selectivity was typically >95:1. Rectangular flow channels gave higher recoveries than circular and serpentine channels, and were more readily cleared of bubbles. In general, recovery was directly proportional to residence time and applied voltage and inversely proportional to sample conductivity and flow-rate. At high applied potential (>18 V) and/or very low flow-rates (< 0.1 ml/min), pH shifts occurred in the cell which reduced the recovery and sometimes resulted in precipitation of solutes. These effects could be minimized, although not eliminated, by main-

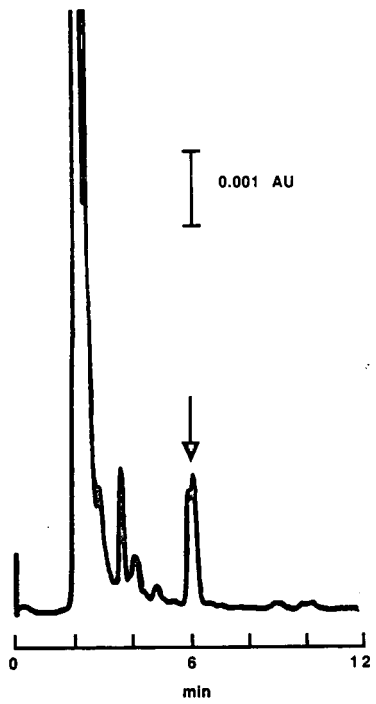

Fig. 3. Chromatogram of untreated, spiked milk (4 μg/ml sulfamethazine, diluted 1:20 with buffer prior to injection). The arrow indicates the sulfamethazine peak. Column, LC18, 250 mm × 4.6 mm I.D. detection, UV absorbance at 265 nm; mobile phase, 0.05 *M* phosphate (pH 6)–methanol (70:30); flow-rate, 1.5 ml/min.

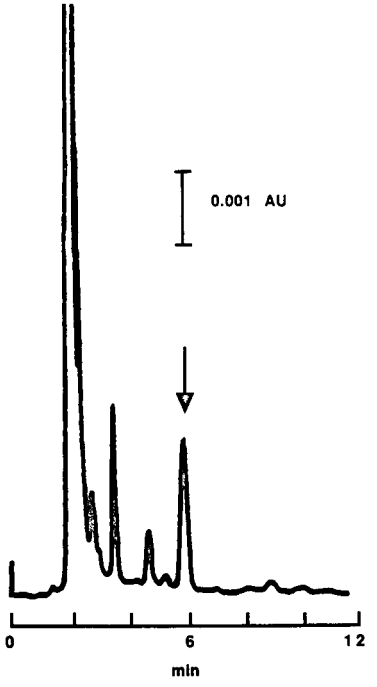

Fig. 4. Chromatogram of electrodialytically treated, spiked milk (4 μg/ml sulfamethazine, diluted 1:20 with buffer prior to treatment). The arrow indicates the sulfamethazine peak. Column, LC18, 250 mm × 4.6 mm I.D.; detection, UV absorbance at 265 nm; mobile phase, 0.05 *M* phosphate (pH 6)–methanol (70:30); flow-rate, 1.5 ml/min. See text for electrodialytic treatment conditions.

taining the flow-rate and buffer strength of the anolyte and catholyte at a high level. The receiving solution could be enriched in analyte by reducing the receiving flow-rate relative to the feed flow-rate, but this concentrating effect was limited to a factor of *ca.* 3 by the need to keep the feed flow at < 0.3 ml/min in order to obtain good recovery and the receiving flow-rate at >0.1 ml/min in order to avoid large pH shifts. Under the conditions used for the treatment of milk samples, enrichment of sulfamethazine in the receiving solution did occur. However, dilution of the sulfamethazine-enriched material as it was pumped out of the cell and into the collection vessel largely negated the enrichment effect, as indicated by the similar peak heights for the treated and untreated samples.

Fig. 3 shows a chromatogram of a sample of filtered, diluted, spiked milk. Injection of this cloudy liquid resulted in reproducible broadening and splitting of the sulfamethazine peak, which was not observed with sulfamethazine standards. Several consecutive injections of untreated sample resulted in a column pressure rise and peak splitting which persisted in subsequent standard injections. Treated milk was a clear liquid which gave a chromatogram (Fig. 4) with sharp peaks and no degradation of column performance on repeated injection.

Electrodialytic sample treatment provided a rapid, solvent-free, readily automated technique for preparing milk samples for HPLC analysis. Extension of the technique to other analytes and biological fluids appears promising and is currently under study.

REFERENCES

1 W. Th. Kok, *Chromatographia*, 24 (1987) 442.
2 W. Th. Kok, K.-P. Hupe and R. W. Frei, *J. Chromatogr.*, 436 (1988) 421.
3 W. A. McRae, in M. Grayson and D. Eckrodt (Editors), *Kirk-Othmer Encyclopedia of Chemical Technology*, Vol. 8, Wiley, New York, 3rd ed., 1979 p. 726.
4 N. Tsunakawa, *Chem. Pharm. Bull.*, 19 (1971) 1164.
5 N. Tsunakawa, *Chem. Pharm. Bull.*, 19 (1971) 2579.
6 N. Tsunakawa, *Chem. Pharm. Bull.*, 19 (1971) 2585.
7 J. A. Cox and R. Carlson, *Anal. Chim. Acta*, 130 (1981) 313.
8 A. J. J. Debets, W. Th. Kok, K.-P- Hupe and U. A. Th. Brinkman, *Chromatographia*, 30 (1990) 361.
9 J. D. Weber and M. D. Smedley, *J. Assoc. Off. Anal. Chem.*, 72 (1989) 445.
10 N. Haagsma and C. van de Water, *J. Chromatogr.*, 333 (1985) 256.
11 M. M. L. Aerts, W. M. J. Beek and U. A. Th. Brinkman, *J. Chromatogr.*, 435 (1988) 97.

Journal of Chromatography, 585 (1991) 219–224
Elsevier Science Publishers B.V., Amsterdam

CHROM. 23 529

Determination of alcohols by high-performance liquid chromatography after pre-column derivatization with 2-(4-carboxyphenyl)-5,6-dimethylbenzimidazole

Masatoki Katayama*, Yuichi Masuda and Hirokazu Taniguchi

Meiji College of Pharmacy, 1-35-23, Nozawa, Setagaya-ku, Tokyo 154 (Japan)

(First received March 20th, 1991; revised manuscript received June 3rd, 1991)

ABSTRACT

A sensitive method for the determination of fatty alcohols using high-performance liquid chromatography with fluorescence detection has been developed. The alcohols were derivatized with 2-(4-carboxyphenyl)-5,6-dimethylbenzimidazole to their esters in the presence of 4-piperidinopyridine and 1-isopropyl-3-(3-dimethylaminopropyl)carbodiimide perchlorate. The resulting esters were extracted with a Sep-Pak ODS cartridge, and then the esters were separated on a reversed-phase column (Zorbax ODS) with methanol–propan-2-ol (85:15, v/v) as the mobile phase. The esters were detected by fluorescence spectrophotometry (excitation 338 nm, emission 428 nm). The limits of detections for alcohols were 0.2–0.4 pg per 20 μl (signal-to-noise ratio of 3) in an acetonitrile solution.

INTRODUCTION

Alipathic alcohols have been determined by gas chromatography [1,2] and high-performance liquid chromatography (HPLC) with derivatization reagents. 3,5-Dinitrobenzoyl chloride [3], phenylisocyanate [4] and trityl chloride [5] were used as pre-column derivatization reagents for the determination of aliphatic alcohols with ultraviolet (UV) detection. 1-Anthroyl and 9-anthroyl nitriles [6], 3-chloroformyl-7-methoxycoumarin [7], 4-diazomethyl-7-methoxycoumarin [8], 7-methoxycoumarin-3- and -4-carbonyl azides [9], 3,4-dihydro-6,7-dimethoxy-4-methyl-3-oxoquinoxaline-2-carbonyl chloride [10] and 3,4-dihydro-6,7-dimethoxy-4-methyl-3-oxoquinoxaline-2-carbonyl azide [11] have been used for the sensitive determination of aliphatic alcohols and hydroxysteroids with fluorimetric detection.

It is established that 2-phenyl-5,6-dimethylbenzimidazoles fluoresce strongly [12,14], and therefore benzimidazole has been used as a labelling reagent for HPLC analysis. The aim of this study was the development of sensitive HPLC methods for the determination of fatty alcohols. The determination of trace amounts of fatty alcohols with chain lengths from 18 to 27 carbon atoms [15,16] and dialkyl glycerols generated from phospholipids [17,18] can give information about lipid contents and the function of membranes. Fatty alcohols with chain lengths from 8 to 20 carbon atoms are used in cosmetics and as raw materials in surfactants [19]. The determination of residual dodecyl alcohols by HPLC with photometric detection was reported by Czichocki *et al.* [20]. The development of sensitive, simple HPLC methods would therefore be useful for the determination of trace amounts of fatty alcohols from tissues or samples from industrial plants and laboratories.

Acid chloride and azide reagents have been reported in many sensitive pre-column derivatization methods [6–11,17,18]. These reagents must be reacted in anhydrous solvents [17,18] at 100°C for 40 min and then at 130°C for 60 min [10,11]. These reagents are unstable and need to be stored under dry and cool conditions [8–10]. As an alternative

0021-9673/91/$03.50

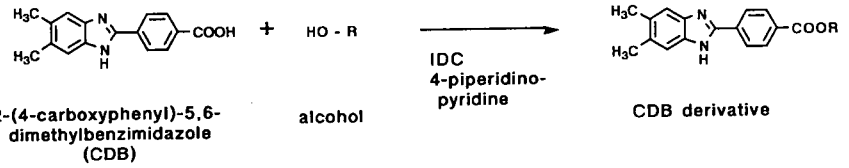

Fig. 1. Derivatization reaction of CBD with alcohol.

reaction condition, it was found that the esterification of fatty acids progressed favourably in the presence of dicyclohexylcarbodiimide and 4-dimethylaminopyridine [21] at room temperature, without the need for an anhydrous solvent. In this work, the analytical reaction proceeded as shown in Fig. 1. Separation conditions for alcohols, cetyl alcohol was selected as a model compound and the reactivities of secondary and tertiary alcohols were also studied.

EXPERIMENTAL

Reagents and materials

A stock solution of alcohol (1000 ng/ml) was prepared by dissolving 10 mg of alcohol (Tokyo Kasei and Nakarai Tesque, Japan) in 0.2 ml of pyridine and diluting to 10 ml with acetonitrile. The 2-(4-carboxyphenyl)-5,6-dimethylbenzimidazole (CDB) solution (0.1%, w/v) was prepared by dissolving 10 mg of the reagent (synthesis given later) in 1.0 ml of pyridine and adding 700 mg of 4-piperidinopyridine (Aldrich) and then diluting to 10 ml with acetonitrile. This solution was stable for 3 days in daylight at room temperature. The 1-isopropyl-3-(3-dimethylaminopropyl)carbodiimide perchlorate (IDC) solution (2.0%) the reagent (Wako, Japan) in 10 ml of acetonitrile. This solution was stable for 8 days in daylight at room temperature. All other reagents were of analytical-reagent grade.

Synthesis of CDB

A 13-g mass of telephthalaldehydic acid dissolved in 400 ml of ethanol was added dropwise to 13 g of 4,5-dimethyl-*o*-phenylenediamine dissolved in 400 ml of ethanol in an ice-bath. After 1 h, the mixture was refluxed for 8 h. After cooling to room temperature, the precipitate was collected and then recrystallized three times from methanol–water (1:1, v/v). A white amorphous product (4 g) was obtained: m.p. over 300°C. Analysis calculated for $C_{16}H_{14}N_2O_2 \cdot 2/3H_2O$: C 72.17, H 5.30, N 10.52; found: C 72.23, H 5.50, N 10.39. IR ν_{max} (cm^{-1}) (KBr): 1705. ^1H NMR dimethylsulphoxide (DMSO)-d_6) δ (ppm): 2.33 (6H, s, $-CH_3$), 7.39 (2H, s, Ar-H), 8.07 (2H, t, Ar-H), 8.04 (2H, t, Ar-H), 12.82 (1H, s, $-COOH$); mass spectrometry (MS) *m/z*: 266 (M^+).

Isolation of CDB esters

Masses of 50 mg of CDB, 500 mg of 4-piperidinopyridine and IDC were successively added to 10 ml of 0.1% cetyl alcohol solution (acetonitrile–pyridine, 9:1) in a screw-capped test-tube. The mixture was heated for 1 h at 80°C in an oil-bath and then the reaction solution was applied to a Sep-Pak ODS cartridge. The column was washed with 20 ml of 50% propan-2-ol. The CDB ester was eluted with 20 ml of propan-2-ol. The eluting solution was evaporated to dryness then the obtained white residue (60 mg) was analysed by IR, ^1H NMR and MS. IR ν_{max} (cm^{-1}) (KBr): 1745 (C=O), 1335 (C–O). ^1H NMR (DMSO-d_6) δ (ppm): 0.88 (3H, t, CH_3), 1.14–1.46 [26H, $(CH_2)_{13}$)], 1.62 (2H, m, $COOCH_2CH_2$), 2.37 (6H, s, 5 and 6 CH_3), 4.05 (2H, t, $COOCH_2$), 7.40 (2H, s, Ar-H), 8.10 and 8.17 (2H each, d each, Ar-H); MS *m/z*: 490 (M^+), 267 ($M^+ - C_{13}H_{27}CHCH=CH_2$).

Apparatus and HPLC conditions

Excitation and emission spectra were measured with a Hitachi 650-10S fluorescence spectrophotometer.

The HPLC apparatus and conditions were as follows: pump, Shimadzu LC-6A liquid chromatograph (Shimadzu, Japan); guard-column, Zorbax ODS (50 × 4.6 mm I.D., 7 μm, DuPont); analytical column, Zorbax ODS (250 × 4.6 mm I.D., 7 μm, DuPont); sample solvent, 20 μl; column temperature, room temperature (about 22°C); detector, Shimadzu RF-530 fluorescence spectrophotometer (excitation 338 nm, emission 428 nm); mobile

phase, methanol–propan-2-ol (85:15); flow-rate, 1.0 ml/min.

Pre-column derivatization of alcohols

A 0.1-ml volume each of the CDB and IDC solutions were added to 1.0 ml of sample solution in a screw-capped test-tube. The mixture was heated at 80°C for 20 min then cooled to room temperature. Volumes of 1.0 ml of water and 2.0 ml of 50% propan-2-ol were added to the reaction solution, which was then applied to the Sep-Pak ODS cartridge. The test-tube was washed with 3.0 ml of 50% propan-2-ol and the washing applied to the column. The column was then washed with 3.0 ml of 50% propan-2-ol and the resultant fluorescence derivatives eluted with 2.0 ml of propan-2-ol. A 20-μl aliquot of the eluate was injected into the HPLC system.

Extraction of alcohols in sodium dodecyl sulphate (SDS)

The procedure for the extraction of dodecyl alcohol is that of the Japanese Pharmacopeia XI, with some modifications [22]. Volumes of 3.0 ml of 10 mg/ml SDS (50% methanol) and 3.0 ml of 2.0 μg/ml stearyl alcohol (as an internal standard) were transferred to a screw-capped test-tube. This mixture was then extracted with 3.0 ml of light petroleum (b.p. 30–60°C, as an extraction solvent), centrifuged (1700 *g*, 5 min), and then the organic solvent layer collected. This process was repeated three times. The organic solvent layer was removed under reduced pressure and the residue dissolved with 6.0 ml of acetonitrile. This reaction solution was then used as a sample solution and derivatized with CDB.

RESULTS AND DISCUSSION

Pre-column derivatization

Derivatization solvent. Acetone, acetonitrile, benzene, chloroform, dichloromethane, dioxane, N,N-dimethylformamide, DMSO and pyridine were testred as reaction solvents for the pre-column derivatization of alcohols (Table I). The most intense detector response was obtained with acetonitrile, which was therefore selected as the reaction solvent.

Effect of CDB concentration. When CDB concentrations in the range 0.08–1.5% were used, the highest constant response was obtained; this concentration was therefore used in this procedure.

TABLE I

EFFECT OF REACTION SOLVENT ON THE DERIVATIZATION REACTION

Amount of cetyl alcohol taken, 1000 ng/ml. The derivatization reaction conditions were as follows: CDB 0.1% (w/v), 4-piperidinopyridine 5% (w/v), IDC 2% (w/v); reaction time, 20 min; temperature, 80°C. Average values were obtained from six runs. The detector response of the CDB derivative in acetonitrile was taken as 100.

Solvent	Detector response
Acetone	20
Acetonitrile	100
Benzene	25
Chloroform	75
Dichloromethane	90
Dioxane	10
N,N-Dimethylformamide	2
Dimethylsulphoxide	5
Pyridine	3

Effect of base. The derivatization of alcohols with CDB did not occur without a base catalyst. 4-Dimethylamionopyridine, 4-piperidinopyridine, 4-pyrrolidinopyridine, pyridine, triethylamine, tributylamine and 1,8-diazabicyclo[5,4,0]-7-undecene were tested (Table II). Pyridine derivatives substituted at the 4-position effectively gave CDB derivatives of alcohols. When 4-piperidinopyridine was used, the observed chromatographic interferences

TABLE II

EFFECT OF BASE ON THE DERIVATIZATION REACTION OF CDB AND ALCOHOL

Amount of base catalyst taken, 0.5 *M*; cetyl alcohol, 1000 ng/ml. Average values were obtained from six runs. The detector response of the CDB derivative using 0.5 *M* (*ca.* 8%, w/v) 4-piperidinopyridine was taken as 100. Other derivatization conditions as in Table I.

Base catalyst	Detector response
4-Dimethylaminopyridine	100
4-Piperidinopyridine	100
4-Pyrrolidinopyridine	100
Pyridine	1
Triethylamine	1
Tributylamine	1
1,8-Diazabicyclo[5,4,0]-7-undecene	15

TABLE III

EFFECT OF DCC DERIVATIVE ON THE DERIVATIZATION REACTION OF CDB AND ALCOHOL

Amount of DCC derivative taken, 0.1 *M*; cetyl alcohol, 1000 ng/ml. Average values were obtained from six runs. The detector response of the CDB derivative by 0.1 *M* (*ca.* 2.7%, w/v) IDC was taken as 100. The other derivatization conditions were as in Table I.

Condensing agent	Detector response
Dicyclohexylcarbodiimide (DCC)	3
1-Ethyl-3-(3-dimethylaminopropyl)carbodiimide hydrochloride	94
1-Cyclohexyl-3-(3-dimethylaminopropyl)carbodiimide perchlorate	100
1-Ethyl-3-(3-dimethylaminopropyl)carbodiimide perchlorate	100
1-Isopropyl-3-(3-dimethylaminopropyl)carbodiimide perchlorate (IDC)	100
1-Hydroxybenzotriazole	9
N-Ethyl-5-*m*-sulphophenylisoxazolium hydrochloride	–
2-Bromo-1-ethylpyridinium tetrafluoroborate	–

(*e.g.* unknown peaks from the reagent) were lower than with 4-dimethylamino- and 4-pyrrolidinopyridine. The highest constant response was obtained when 4-piperidinopyridine was used in the concentration range 2–10% (w/v); 5% (w/v) 4-piperidinopyridine was therefore selected.

Effect of dicyclohexylcarbodiimide. For the derivatization of alcohols with CDB, the following compounds were tested as condensing agents: dicyclohexylcarbodiimide (DCC), 1-ethyl-3-(3-dimethylaminopropyl)carbodiimide hydrochloride, 1-cyclohexyl-3-(3-dimethylaminopropyl)carbodiimide perchlorate, 1-ethyl-3-(3-dimethylaminopropyl)carbodiimide perchlorate, 1-isopropyl-3-(3-dimethylaminopropyl)carbodiimide perchlorate (IDC), 1-hydroxybenzotriazole, *N*-ethyl-5-*m*-sulphophenylisoxazolium hydrochloride and 2-bromo-1-ethylpyridinium tetrafluoroborate (Table III).

Good detector responses were obtained with water-soluble carbodiimides and, as a result of its solubility in acetonitrile, IDC was selected as the reagent. The highest constant response was obtained in ther ange 1–10% IDC solution; 2% IDC was therefore used in the procedure.

Reaction time and temperature

The reaction time was varied from 0 to 90 min and the temperature was varied from 25 to 90°C. The results are shown in Fig. 2. The highest detector response was obtained at 80 and 90°C within 20 min. However, the detection limits of the alcohols at 80°C were more sensitive than at 90°C and therefore heating at 80°C for 20 min was selected.

Extraction of CDB derivatives

To avoid interferences, CDB derivatives were extracted from the reaction solution. The extraction of CDB derivatives with the organic solvents dichloromethane, chloroform, ethyl acetate, benzene and hexane was examined under acidic, neutral and alkaline conditions. However, the CDB derivatives were not effectively extracted and it was decided to extract then with a short column. Sep-Pak silica, alumina (acidic, neutral and basic) and ODS cartridges were used with a water–organic mixture solvent. The CDB derivatives were effectively extracted by the Sep-Pak ODS cartridge with water–propan-2-ol and this solvent was selected for further work.

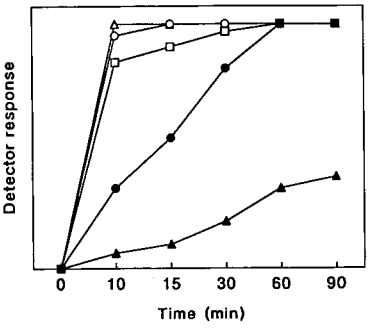

Fig. 2. Effect of reaction time and temperature on the derivatization reaction. Amount of cetyl alcohol used: 1000 ng/ml. ▲ = 25°C; ● = 50°C; □ = 70°C; ○ = 80°C; △ = 90°C; ■ = combination of 80 and 90°C.

Separation of CDB derivatives

The separation of mixtures of the fatty alcohols dodecyl alcohol, tetradecyl alcohol, cetyl alcohol, stearyl alcohol and eicosyl alcohol was studied. Methanol, acetonitrile and tetrahydrofuran were tested as mobile phases. And it was found that methanol–propan-2-ol was the most suitable for the separation. Optimum separation was achieved with a methanol/propan-2-ol ratio of 85:15 (v/v).

Determination of CDB derivatives

The excitation and emission spectra of cetyl alcohol in the HPLC eluent are shown in Fig. 3.

Secondary alcohols, for example, 2-tetradecyl alcohol (C_{14}), were examined in the same manner as the primary alcohols and it was found that the detector response for the secondary alcohol was less than one fiftieth of that of the primary alcohol. However, secondary alcohols in acyl glycerols (α,α'-dilaurin) and at the 3-position in cholesterols gave 50 and 70% reactor response of cetyl alcohol. Other secondary alcohols in steroids (*e.g.* prednisolone acetate and testosterone) did not react; tertiary alcohols also gave no reaction. The excitation maxima of the CDB derivatives from decyl alcohol (C_{10}) toeicosyl alcohol (C_{20}), cholesterols and acyl glycerols were about 338 nm, with emission maxima at about 428 nm. These excitation and emission wavelengths were therefore selected.

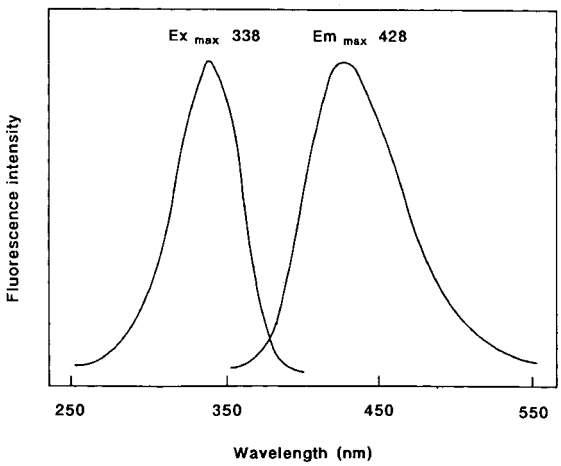

Fig. 3. Excitation and emission spectra of CDB derivative of cetyl alcohol in HPLC eluent. Amount of cetyl alcohol used: 1000 ng/ml.

Fig. 4 shows a chromatogram of five CDB derivatives (C_{12}–C_{20}) obtained by the proposed procedure. The detection limits of the five alcohols were 0.2–0.4 pg per 20 μl (signal-to-noise ratio of 3). The calibration graphs were linear up to 10 000–30 000 ng/ml. The relative standard deviations (n = 6) were 2.4 and 2.9% at 1000 and 10 ng/ml cetyl alcohol, respectively. The fluorescence of the CDB derivative from cetyl alcohol was stable for at least 5 days in daylight at room temperature. The efficiency of the conversion of cetyl alcohol to the CDB derivative was examined by comparing the detector response obtained under derivatizastion conditions with that given by the isolated reaction product (described under Experimental). The conversion rate was 52%. The proposed method is 5 to 800 times more sensitive than other chromatographic methods using fluorescence detection after derivatization [6–11].

Determination of alcohols in SDS

The proposed CDB method was applied to the determination of alcohol impurities in commercial

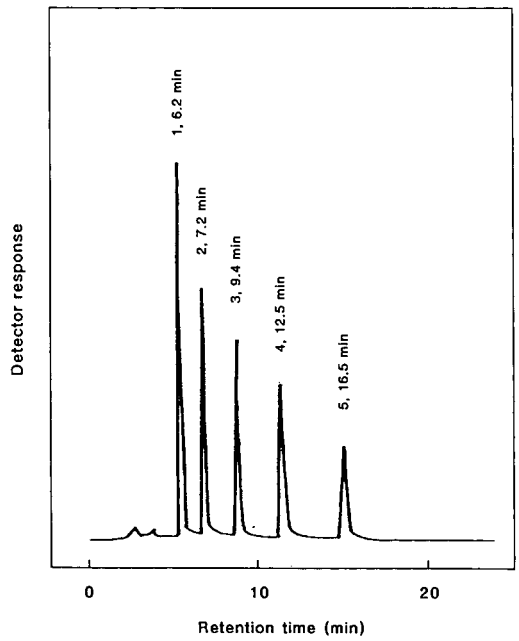

Fig. 4. Chromatogram of CDB derivatives. Amount of alcohol taken: 100 ng/ml. Peaks: 1 = dodecyl alcohol; 2 = tetradecyl alcohol; 3 = cetyl alcohol; 4 = stearyl alcohol; 5 = eicosyl alcohol.

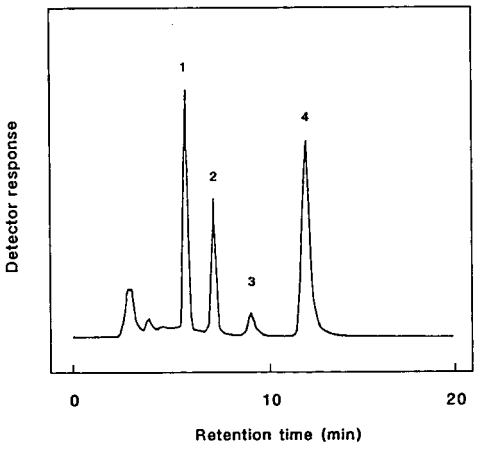

Fig. 5. Chromatogram of alcohols in SDS. Amount of SDS used: 0.1 mg/ml. Peaks: 1 = dodecyl alcohol; 2 = tetradecyl alcohol; 3 = cetyl alcohol; 4 = stearyl alcohol (internal standard).

SDS. SDS is a well known surface-active agent and is widely used as an emulusifier in medicines, cosmetics and as the reagent for SDS polyacrylamide gel electrophoresis. As SDS is made from dodecyl alcohol, trace amounts of alcohols are contained in it and these alcohols affect the formation of micelles [19]. The alcohol residue is defined in the Japanese Pharmacopeia XI [22]. Four commercial SDS samples were tested: A, an analytical standard for anion-type surface-active agent; B, for water analysis; C, for electrophoresis; and D, reagents for synthesis. These four commercial samples contained 0.63, 0.70, 0.81 and 75.10 μg of dodecyl alcohol per 10 mg, respectively. Sample D in particular contained tetradecyl alcohol and cetyl alcohol as other impurities (Fig. 5). The relative standards deviation (n = 6) for the analysis of the samples was about 7.0%.

CONCLUSIONS

The derivatization of alcohols with CDB can be performed at moderate temperatures and is superior to other pre-column derivatization HPLC methods with fluorimetric detection with respect to sensitivity and the stability of the reagent [6–11]. The application of this method to the determination of corticosteroids (*e.g.* cortisone, hydroxycortisone and aldosterone) and phenols (*p*-hydroxybenzoic acid esters) is in progress.

REFERENCES

1 R. J. Argauer, *Anal. Chem.*, 40 (1968) 122.
2 F. K. Kawahara, *Anal. Chem.*, 40 (1968) 1009.
3 J. F. Lawrence and R. W. Frei, *Chemical Derivatization in Liquid Chromatography*, Elsevier, Amsterdam, 1976, p. 151.
4 B. Björkqvist and H. Toivonen, *J. Chromatogr.*, 153 (1978) 265.
5 Y. Suzuki and K. Tani, *Bunseki Kagaku*, 28 (1979) 610.
6 J. Goto, N. Goto, F. Shamsa, M. Saito, S. Komatsu, K. Suzaki and T. Nambara, *Anal. Chim. Acta*, 147 (1983) 397.
7 C. Hamada, M. Iwasaki, N. Kuroda and Y. Ohkura, *J. Chromatogr.*, 341 (1985) 426.
8 A. Takadate, T. Tahara, H. Fujino and S. Goya, *Chem. Pharm. Bull.*, 30 (1982) 4120.
9 A. Takadate, M. Irikura, T. Suehiro, H. Fujino and S. Goya, *Chem. Pharm. Bull.*, 33 (1985) 1164.
10 T. Iwata, M. Yamaguchi, S. Hara, M. Nakamura and Y. Ohkura, *J. Chromatogr.*, 362 (1986) 209.
11 M. Yamaguchi, T. Iwata, M. Nakamura and Y. Ohkura, *Anal. Chim. Acta*, 193 (1987) 209.
12 M. Katayama, Y. Mukai and H. Taniguchi, *Anal. Sci.*, 3 (1987) 369.
13 M. Katayama, Y. Mukai and H. Taniguchi, *Anal. Sci.*, 3 (1987) 565.
14 M. Katayama, Y. Mukai and H. Taniguchi, *Analyst (London)*, 115 (1990) 9.
15 D. J. Harvey, J. M. Tiffany, J. M. Duerden, K. S. Pandher and L. S. Mengher, *J. Chromatogr.*, 414 (1987) 253.
16 D. J. Harvey, *J. Chromatogr.*, 494 (1989) 23.
17 M. Kito, H. Takamura, H. Narita and R. Urade, *J. Biochem. (Tokyo)*, 98 (1985) 327.
18 H. Takamura, H. Narita, R. Urade and M. Kito, *Lipids*, 21 (1986) 356.
19 M. J. Rosen, *J. Colloid Interface Sci.*, 79 (1981) 587.
20 G. Czichocki, H. Much and D. Vollhardt, *J. Chromatogr.*, 280 (1983) 109.
21 F. E. Ziegler and G. D. Berger, *Synt. Commun.*, 9 (1979) 539.
22 *The Japanese Pharmacopeia with Commentary*, Vol. XI, Pharmaceutical Society of Japan, Hirokawa Shoten, Tokyo, 1986, p. D-997.

Journal of Chromatography, 585 (1991) 225–231
Elsevier Science Publishers B.V., Amsterdam

CHROM. 23 550

Electrochemical and chromatographic properties of selected hydrazine and hydrazide derivatives of carbonyl compounds

Kyoji Ueno* and Tsuneji Umeda

Shionogi Research Laboratories, Shionogi & Co., Ltd., 5-12-4 Sagisu, Fukushima-ku, Osaka 553 (Japan)

(First received March 12th, 1991; revised manuscript received June 11th, 1991)

ABSTRACT

Electrochemical and chromatographic properties of selected hydrazine and hydrazide derivatives of carbonyl compounds were studied to find a new, highly sensitive and selective derivatization reagent for the determination of carbonyl compounds by high-performance liquid chromatography with electrochemical detection. Of the six hydrazines and five hydrazides investigated. 2,5-dihydroxybenzohydrazide was accepted as the most suitable reagent because (i) it and its hydrazones were stable and (ii) its hydrazones were sensitively detectable at a low oxidative potential. Seven ketosteroids derivatized with 2,5-dihydroxybenzohydrazide were satisfactorily separated on a reversed-phase column and detected at +0.20 V *vs.* Ag/AgCl. The detection limits were in the range of 60–500 fmol per injection.

INTRODUCTION

High-performance liquid chromatography (HPLC) with electrochemical detection (ED) has been widely used to determine trace amounts of electroactive compounds because of its high sensitivity and selectivity. Also, chemical derivatization approaches in HPLC–ED have become commonplace [1].

Some reports have appeared on the HPLC–ED derivatization reagents for the determination of carbonyl compounds: 4-nitrophenylhydrazine (4-NPH) for 17-ketosteroids [2,3] and 2,4-dinitrophenylhydrazine (2,4-DNPH) for aldehydes [4,5]. Recently, Bond *et al.* [6] discussed the analytical and mechanistic aspects of the electrochemical oxidation of 3- and 17-ketosteroids derivatized with 4-NPH, 2,4-DNPH and phenylhydrazine (PH). However, carbonyl compounds derivatized with these reagents were detected at relatively high oxidative potentials ($\geq$ +0.80 V *vs.* Ag/AgCl) or in the reductive mode. In reductive-mode HPLC–ED, excluding oxygen from both the mobile phase and the sample is somewhat troublesome. On the other hand, use of a high oxidative potential causes drift of the baseline, high noise level and faster deterioration of the electrode surface, and also lowers selectivity, which is one of the most important advantages of HPLC–ED. To overcome these problems, the derivatives resulting from HPLC–ED derivatization reagents should be detectable at lower oxidative potentials.

In the present study, the electrochemical and chromatographic properties of carbonyl compounds derivatized with selected reagents containing a hydrazine group were examined to find a new, highly sensitive and selective derivatization reagent for the determination of carbonyl compounds by HPLC–ED. This is the first paper reporting systematic studies on the potency of hydrazine reagents for HPLC–ED. The chromatographic separation with sensitive ED of seven ketosteroids derivatized with the most suitable reagent, 2,5-dihydroxybenzohydrazide (2,5-DHBH), is also described.

0021-9673/91/$03.50

EXPERIMENTAL

Apparatus

The HPLC system consisted of a Model L-5000 solvent delivery pump (Yanagimoto, Kyoto, Japan), a Model 7125 syringe-loading sample injector with a 100-μl sample loop (Rheodyne, Berkeley, CA, USA) and a Model LC-4B amperometric electrochemical detector (Bioanalytical Sytems, West Lafayette, IN, USA).

The electrochemical detector consisted of a Model TL-5 thin-layer detector cell with a glassy carbon working electrode and an Ag/AgCl reference electrode. The surface of the working electrode was polished to a mirror finish with alumina powder (0.05 μm) on a glass plate each day before use.

Peak area and peak height were calculated using a model C-R2AX integrator (Shimadzu, Kyoto, Japan).

All melting points are uncorrected. Mass spectra were obtained on a Model M-68 mass spectrometer (Hitachi, Tokyo, Japan). IR spectra were measured on a Model A-702 spectrometer (Nihon Bunko, Tokyo, Japan), and absorption data are given in cm^{-1}. ^1H NMR spectra were recorded with a Model XL-200 spectrometer (200.06 MHz, Varian, Sunnyvale, CA, USA) with the samples in hexadeuterodimethyl sulfoxide (DMSO-d_6) with tetramethylsilane as an internal standard.

Chemicals

The following chemicals were purchased: phenylhydrazine, 4-nitrophenylhydrazine, 2,4-dinitrophenylhydrazine, 2-hydrazinobenzothiazole, 3,4-dihydroxybenzoic acid, 2,5-dihydroxybenzoic acid, isoamyl nitrite, hydrazine monohydrate, androsterone (Wako, Osaka, Japan); 4-hydroxybenzohydrazide, 4-aminophenol hydrochloride, 2,4-dihydroxybenzoic acid, acetophenone, sodium 1-pentanesulfonate, pregnenolone, dehydroisoandrosterone (Nacarai Tesque, Kyoto, Japan); 4-methoxyphenylhydrazine, 3,4-dihydroxyphenylacetic acid, testosterone, ethisterone, norethisterone (Tokyo Kasei Kogyo, Tokyo, Japan); corticosterone (Sigma, St. Louis, MO, USA).

Methanol for HPLC was of HPLC grade (Kanto, Tokyo, Japan). Water was deionized and distilled before use. All other chemicals and solvents were of analytical grade.

Chromatographic conditions

Chromatography was performed at room temperature. Each mobile phase was filtered with a Type FR-40 membrane filter (0.4 μm, Fuji Photo Film, Tokyo, Japan) and degassed under reduced pressure before use. In this study, five chromatographic conditions were used: (1) column, Nucleosil C_{18} (10 μm, 250 mm × 4.6 mm I.D., home-packing, Macherey-Nagel, Düren, Germany); mobile phase, methanol–0.5% ammonium dihydrogenphosphate (pH 4.5) (80:20, v/v); flow-rate, 0.8 ml/min; (2) column, same as (1); mobile phase, methanol–0.5% ammonium dihydrogenphosphate (pH 4.5) (90:10, v/v); flow-rate, 1.0 ml/min; (3) column, μBondapak NH_2 (300 mm × 3.9 mm I.D., Waters Assoc., Milford, MA, USA); mobile phase, 0.1 *M* phosphate buffer (pH 6.8)–methanol (90:10, v/v); flow-rate, 1.0 ml/min; (4) column, μBondapak C_{18} (300 mm × 3.9 mm I.D., Waters Assoc.); mobile phase, 0.1 *M* sodium dihydrogenphosphate containing 0.01 *M* sodium 1-pentanesulfonate (pH 4.4)–methanol (75:25, v/v); flow-rate, 1.0 ml/min; (5) column, Chemcosorb 5-ODS-UH (150 mm × 4.6 mm I.D., Chemco, Osaka, Japan); mobile phase, 0.05 *M* phosphate buffer (pH 7.0)–acetonitrile (64:36, v/v); flow-rate, 1.0 ml/min; applied potential, +0.20 V *vs.* Ag/AgCl.

Registry No.

2,4-DNPH, 119-26-6; 4-NPH, 100-16-3; PH, 100-63-0; 4-MPH, 3471-32-7; 4-HPH · HCl, 54049-23-9; HBT, 615-21-4; 4-HBH, 5351-23-5; 2,4-DHBH, 13221-86-8; 3,4-DHBH, 39635-11-5; 2,5-DHBH, 15791-90-9; 3,4-DHPAH, 1132-47-4; AP-2,4-DNPH, 1677-87-8; AP-4-NPH, 2675-22-1; AP-PH, 583-11-9; AP-4-MPH, 89671-57-8; AP-HBT, 59972-88-2; AP-4-HBH, 100969-27-5; AP-2,5-DHBH, 77163-30-5; testosterone, 58-22-0; ethisterone, 434-03-7; norethisterone, 68-22-4; androsterone, 53-41-8; dehydroisoandrosterone, 53-43-0; pregnenolone, 145-13-1; corticosterone, 50-22-6.

Synthesis

4-Hydroxyphenylhydrazine hydrochloride (4-HPH · HCl). 4-HPH was prepared in a similar manner to that described in the literature [7,8].

2,4-Dihydroxybenzohydrazide (2,4-DHBH), 3,4-dihydroxybenzohydrazide (3,4-DHBH), 2,5-dihydroxybenzohydrazide (2,5-DHBH), 3,4-dihydroxy-

phenylacetohydrazide (3,4-DHPAH). 2,4-DHBH, 3,4-DHBH, 2,5-DHBH and 3,4-DHPAH were prepared in a similar manner to that described for 2,5-DHBH in the literature [9,10].

Acetophenone hydrazone of 2,5-DHBH (AP-2,5-DHBH). To 2,5-DHBH (100 mg, 0.59 mmol) in a 30-ml flask, methanol (5 ml), acetic acid (2 ml) and acetophenone (0.2 ml, 1.72 mmol) were added. The mixture was stirred for 3 h at room temperature, and then water (30 ml) was added. A precipitate was collected, washed with water and dried. Recrystallization from ethanol–water gave AP-2,5-DHBH as white needles (65 mg, 40%), m.p. 265°C (decomposition, ethanol–water). Analysis: Calculated for $C_{15}H_{14}N_2O_3$: C, 66.66; H, 5.22; N, 10.36. Found: C, 66.56; H, 5.32; N, 10.29.

Acetophenone hydrazone of 4-HBH, 3,4-DHBH, 2,4-DHBH, 3,4-DHPAH, 2,4-DNPH, 4-NPH, PH, 4-MPH, 4-HPH, BTH (AP-4-HBH, AP-3,4-DHBH, AP-2,4-DHBH, AP-3,4-DHPAH, AP-2,4-DNPH, AP-4-NPH, AP-PH, AP-4-MPH, AP-4-HPH, AP-HBT). AP-4-HBH, AP-3,4-DHBH, AP-2,4-DHBH, AP-3,4-DHPAH, AP-2,4-DNPH, AP-4-NPH, AP-PH, AP-4-MPH, AP-4-HPH and AP-HBT were prepared in a similar manner to that described above for AP-2,5-DHBH. The m.p. and elemental analysis data for new compounds which could not be found in literature are described below.

AP-3,4-DHBH: 31% yield, m.p. 246–248°C. Analysis: Calculated for $C_{15}H_{14}N_2O_3$: C, 66.66; H, 5.22; N, 10.36. Found: C, 66.85; H, 5.36; N, 10.36.

AP-2,4-DHBH: 68% yield, m.p. 230–232°C. Analysis: Calculated for $C_{15}H_{14}N_2O_3$: C, 66.66; H, 5.22; N, 10.36. Found: C, 66.56; H, 5.20; N, 10.20.

AP-3,4-DHPAH: 64% yield, m.p. 185–187°C. Analysis: Calculated for $C_{16}H_{16}N_2O_3$: C, 67.59; H, 5.67; N, 9.85. Found: C, 67.37; H, 5.82; N, 9.82.

AP-4-HPH: 13% yield, m.p. 136–137°C. Analysis: Calculated for $C_{14}H_{14}N_2O$: C, 74.31; H, 6.24; N, 12.38. Found: C, 74.18; H, 6.18; N, 12.23.

Androsterone hydrazone of 2,5-DHBH (A-2,5-DHBH). To a mixture of androsterone (140 mg, 0.48 mmol) and 2,5-DHBH (80 mg, 0.48 mmol) in a 30-ml flask, methanol (5 ml) and acetic acid (2 ml) were added. The reaction mixture was stirred for 1 h at room temperature, and then water (30 ml) was added. A precipitate was collected, washed with water and dried. Recrystallization from ethanol–water gave A-2,5-DHBH as white plates (168 mg, 80%), m.p. 290–291°C. Analysis. Calculated for $C_{26}H_{36}N_2O_4$ (molecular weight, 440.56): C, 70.88; H, 8.24; N, 6.36. Found: C, 70.78; H, 8.23; N, 6.44. Mass spectrometry (MS) *m/e*: 440 (M^+). IR (KBr) ν_{max} (cm^{-1}): 1655, 1645. ^1H NMR (DMSO-d_6) δ: 0.77 (3H, s), 0.86 (3H, s), 6.80 (2H, m), 7.34 (1H, m).

Corticosterone, dehydroisoandrosterone, testosterone, norethisterone, ethisterone, pregnenolone hydrazone of 2,5-DHBH (C-2,5-DHBH, D-2,5-DHBH, T-2,5-DHBH, N-2,5-DHBH, E-2,5-DHBH, P-2,5-DHBH). C-2,5-DHBH, D-2,5-DHBH, T-2,5-DHBH, N-2,5-DHBH, E-2,5-DHBH and P-2,5-DHBH were prepared in a similar manner to that described for A-2,5-DHBH.

C-2,5-DHBH: 70% yield, m.p. 181–183°C (methanol–water). Analysis. Calculated for $C_{28}H_{36}N_2O_6$ (molecular weight, 496.60): C, 67.72; H, 7.31; N, 5.64. Found: C, 67.61; H, 7.55; N, 5.31. MS *m/e*: 496 (M^+). IR (KBr) ν_{max} (cm^{-1}): 1705, 1645, 1615. ^1H NMR (DMSO-d_6) δ: 0.77 (3H, s), 1.24 (3H, s), 5.81 and 6.06 (1H, s and s), 6.81 (2H, m), 7.35 (1H, m).

D-2,5-DHBH: 64% yield, m.p. 295–297°C (methanol). Analysis. Calculated for $C_{26}H_{34}N_2O_4$ (molecular weight, 438.57): C, 71.21; H, 7.81; N, 6.39. Found: C, 71.23; H, 8.03; N, 6.62. MS *m/e*: 438 (M^+). IR (KBr) ν_{max} (cm^{-1}): 1635, 1615. ^1H NMR (DMSO-d_6) δ: 0.89 (3H, s), 0.99 (3H, s), 5.28 (1H, s), 6.80 (2H, m), 7.35 (1H, m).

T-2,5-DHBH: 29% yield, m.p. 294–296°C (acetone). Analysis. Calculated for $C_{26}H_{34}N_2O_4$ (molecular weight, 438.57): C, 71.21; H, 7.81; N, 6.39. Found: C, 71.03; H, 8.04; N, 6.52. MS *m/e*: 438 (M^+). IR (KBr) ν_{max} (cm^{-1}): 1620. ^1H NMR (DMSO-d_6) δ: 0.68 (3H, s), 1.06 (3H, s), 5.89 and 6.14 (1H, s and s), 6.80 (2H, m), 7.36 (1H, m).

N-2,5-DHBH: 45% yield, m.p. 196–198°C (acetone–hexane). Analysis. Calculated for $C_{27}H_{32}N_2O_4$ (molecular weight, 448.56): C, 72.30; H, 7.19; N, 6.25. Found: C, 72.10; H, 7.33; N, 6.36. MS *m/e*: 448 (M^+). IR (KBr) ν_{max} (cm^{-1}): 1635. ^1H NMR (DMSO-d_6) δ: 0.79 (3H, s), 5.98 and 6.24 (1H, s and s), 6.81 (2H, m), 7.36 (1H, m).

E-2,5-DHBH: 63% yield, m.p. 290–293°C (decomposition, ethanol–water). Analysis. Calculated for $C_{28}H_{34}N_2O_4$ (molecular weight, 462.59): C, 72.70; H, 7.41; N, 6.06. Found: C, 72.34; H, 7.55; N,

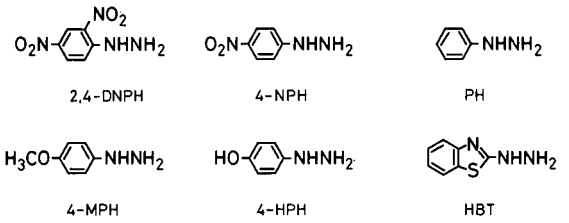

Fig. 1. Chemical structures of hydrazine reagents. 2,4-DNPH, 2,4-dinitrophenylhydrazine; 4-NPH, 4-nitrophenylhydrazine; PH, phenylhydrazine; 4-MPH, 4-methoxyphenylhydrazine; 4-HPH, 4-hydroxyphenylhydrazine; HBT, 2-hydrazinobenzothiazole.

5.91. MS *m/e*: 462 (M^+). IR (KBr) ν_{max} (cm^{-1}): 1645, 1620. ^1H NMR (DMSO-d_6) δ: 0.77 (3H, s), 1.06 (3H, s), 5.89 and 6.15 (1H, s and s), 6.80 (2H, m), 7.35 (1H, m).

P-2,5-DHBH: 5% yield, m.p. 294–296°C (ethanol). Analysis. Calculated for $C_{28}H_{38}N_2O_4$ (molecular weight, 466.62): C, 72.07; H, 8.21; N, 6.00. Found: C, 71.89; H, 8.25; N, 5.84. MS *m/e*: 466 (M^+). IR (KBr) ν_{max} (cm^{-1}): 1635, 1620. ^1H NMR (DMSO-d_6) δ: 0.56 (3H, s), 0.95 (3H, s), 1.90 (3H, s), 5.28 (1H, s), 6.80 (2H, m), 7.35 (1H, m).

RESULTS AND DISCUSSION

Figs. 1 and 2 show the chemical structures of the six hydrazine and five hydrazide reagents, respectively, used for this study.

Hydrazine reagents

First, six acetophenone hydrazones of the hydrazine reagents, AP-2,4-DNPH, AP-4-NPH, AP-PH, AP-4-MPH, AP-4-HPH and AP-HBT, were prepared to find the one most suitable for HPLC–ED

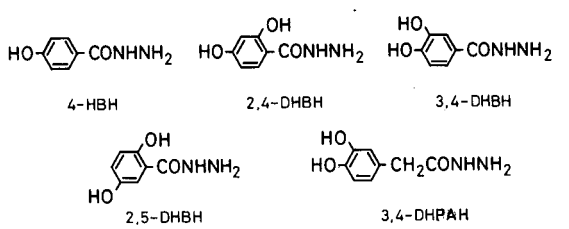

Fig. 2. Chemical structures of hydrazide reagents. 4-HBH, 4-hydroxybenzohydrazide; 2,4-DHBH, 2,4-dihydroxybenzohydrazide; 3,4-DHBH, 3,4-dihydroxybenzohydrazide; 2,5-DHBH, 2,5-dihydroxybenzohydrazide; 3,4-DHPAH, 3,4-dihydroxyphenylacetohydrazide.

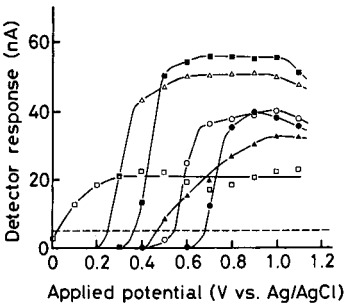

Fig. 3. Relationship between detector response and applied potential for 200 pmol of hydrazones. Symbols: ● = AP-2,4-DNPH; ○ = AP-4-NPH; ■ = AP-PH; △ = AP-4-MPH; □ = AP-4-HPH; ▲ = AP-HBT. HPLC conditions: column, Nucleosil C_{18} (10 μm, 250 mm × 4.6 mm I.D.); mobile phase and flow-rate, methanol–0.5% ammonium dihydrogenphosphate (pH 4.5) (80:20, v/v), 0.8 ml/min for AP-4-HPH; methanol–0.5% ammonium dihydrogenphosphate (pH 4.5) (90:10, v/v), 1.0 ml/min for the others.

derivatization. Electrochemical properties of the hydrazones were examined with their hydrodynamic voltammograms (Fig. 3). Fig. 3 indicates that the order of the potential at which each hydrazone shows a response of 5 nA per 200 pmol (dashed line) is AP-4-HPH < AP-4-MPH < AP-PH < AP-HBT < AP-4-NPH < AP-2,4-DNPH. AP-4-HPH responds even at about 0 V *vs.* Ag/AgCl. This order of the ease of electrochemical oxidation of those hydrazones agrees with the electron-donating ability of their substituent(s) (4-hydroxy > 4-methoxy > 4-hydrogen > 4-nitro > 2,4-dinitro), except for AP-HBT, which is not a phenylhydrazone derivative.

TABLE I

DETECTION LIMITS OF ACETOPHENONE HYDRAZONES OF AROMATIC HYDRAZINE DERIVATIVES

Signal-to-noise ratio = 2. HPLC conditions were the same as in Fig. 3.

Compound	Detection limit (fmol per injection)		
	+0.9 V	+0.5 V	+0.3 V
AP-2,4-DNPH	100	520 000	–
AP-4-NPH	50	500	–
AP-PH	40	30	4800
AP-4-MPH	60	50	60
AP-4-HPH	100	40	20
AP-HBT	100	240	45 000

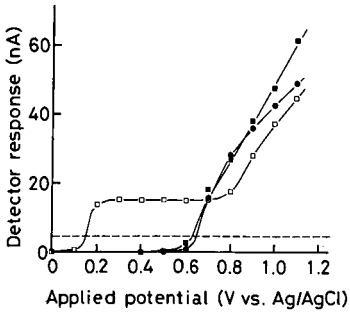

Fig. 4. Relationship between detector response and applied potential for 200 pmol of hydrazones. Symbols: ● = AP-4-HBH; ■ = AP-2,4-DHBH; □ = AP-2,5-DHBH. HPLC conditions: column, μBondapak NH_2 (300 mm × 3.9 mm I.D.); mobile phase, 0.1 *M* phosphate buffer (pH 6.8)–methanol (90:10, v/v); flow-rate, 1.0 ml/min.

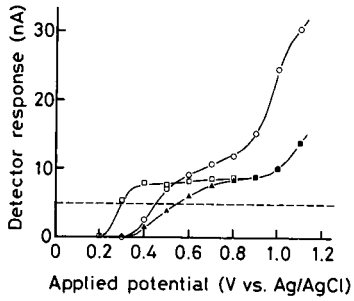

Fig. 5. Relationship between detector response and applied potential for 200 pmol of hydrazones. Symbols: ○ = AP-3,4-DHBH; □ = AP-2,5-DHBH; ▲ = AP-3,4-DHPAH. HPLC conditions: column, μBondapak C_{18} (300 mm × 3.9 mm I.D.); mobile phase, 0.1 *M* sodium dihydrogenphosphate containing 0.01 *M* sodium 1-pentanesulfonate (pH 4.4)–methanol (75:25, v/v); flow-rate, 1.0 ml/min.

Table I shows the detection limits of the hydrazones measured at the applied potentials of +0.9, +0.5 and +0.3 V *vs.* Ag/AgCl by HPLC–ED. Two hydrazones, AP-4-HPH and AP-4-MPH, have low detection limits even at +0.3 V *vs.* Ag/AgCl, but these two and also 4-HPH · HCl are unstable in air at room temperature.

Hydrazide reagents

Next, five hydrazide reagents were prepared. Each reagent was designed to have one or two carbon unit(s) between a hydrazine group as the chemical reaction part with carbonyl compounds, and a hydroxyphenyl group as the electrochemical reaction part for electrochemical detection in order to improve stability. All of these hydrazide reagents were stable in air at room temperature for six months. Five acetophenone hydrazones were synthesized with the hydrazide reagents (AP-4-HBH, AP-2,4-DHBH, AP-3,4-DHBH, AP-2,5-DHBH, AP-3,4-DHPAH), and all of these hydrazones were also stable in air at room temperature for six months.

As shown in Figs. 4 and 5, hydrodynamic voltammograms of the hydrazones were examined under the two HPLC conditions necessary to obtain appropriate retention and good peak shapes for all of them. For comparison of the data in Figs. 4 and 5, the hydrodynamic voltammograms of AP-2,5-DHBH were obtained under both conditions. The results indicate that the order of the potential at which each hydrazone shows a response of 5 nA per 200 pmol (dashed line) is AP-2,5-DHBH < AP-3,4-DHBH < AP-3,4-DHPAH < AP-2,4-DHBH ⩽ AP-4-HBH. This sequence is the same as that of the half-oxidative potentials for some of the hydroxy-substituted benzenes in acetonitrile containing 0.1 *M* lithium perchlorate with reference to a saturated calomel electrode [1,4-dihydroxybenzene (+0.75 V) < 1,2-dihydroxybenzene (+0.93 V) < 1,3-dihydroxybenzene (+1.13 V) < hydroxybenzene (+1.31 V)] [11,12].

Table II shows the detection limits of the hydrazones measured at the applied potentials of +0.9, +0.5 and +0.3 V *vs.* Ag/AgCl by HPLC–ED. AP-2,5-DHBH is the only hydrazone which has a low detection limit even at +0.3 V *vs.* Ag/AgCl.

From the above results, 2,5-DHBH is the most

TABLE II

DETECTION LIMITS OF ACETOPHENONE HYDRAZONES OF HYDRAZIDE DERIVATIVES

Signal-to-noise ratio = 2. HPLC conditions were the same as in Fig. 4 (AP-4-HBH, AP-2,4-DHBH and AP-2,5-DHBH) and Fig. 5 (AP-3,4-DHBH and AP-3,4-DHPAH).

Compound	Detection limit (fmol per injection)		
	+0.9 V	+0.5 V	+0.3 V
AP-4-HBH	100	2100	–
AP-2,4-DHBH	30	21 000	–
AP-3,4-DHBH	20	90	82 000
AP-2,5-DHBH	60	40	40
AP-3,4-DHPAH	60	400	5600

suitable derivatizing reagent of the hydrazines and the hydrazides investigated because (i) it and its hydrazone are stable in air at room temperature and they are easy to operate and (ii) its hydrazone is detectable at a lower oxidative potential which causes higher selectivity and a lower detection limit.

Properties of 2,5-DHBH derivatives of ketosteroids

The electrochemical and chromatographic properties of ketosteroids derivatized with 2,5-DHBH were also studied to prove its suitability. Seven ketosteroids were used: three 3-ketosteroids, testosterone (T), ethisterone (E), norethisterone (N); two 17-ketosteroids, androsterone (A), dehydroisoandrosterone (D); one 20-ketosteroid, pregnenolone (P); and one 3,20-diketosteroid, corticosterone (C). All ketosteroids were derivatized to hydrazones with 2,5-DHBH (T-2,5-DHBH, E-2,5-DHBH, N-2,5-DHBH, A-2,5-DHBH, D-2,5-DHBH, P-2,5-DHBH, C-2,5-DHBH). All hydrazone structures were verified by MS, IR, ^{1}H NMR and elemental analysis as described in the Experimental section: each carbonyl group of the monoketosteroids (T, E, N, A, D and P) was derivatized with 2,5-DHBH; only one carbonyl group was derivatized with 2,5-DHBH at the 3-position of the diketosteroid (C). The position presented for the derivatization of C seems to be reasonable because the 3-position of the steroid keto group has a higher reactivity than the 20-positon [13,14]. Several HPLC conditions were investigated and then 2,5-DHBH and all the hydrazones of ketosteroids were clearly separated on a reversed-phase column (Fig. 6). The hydrodynamic voltammograms of the hydrazones of ketosteroids were obtained under the conditions described in Fig. 6 (Fig. 7). Fig. 7 shows that: (i) all voltammograms have very similar shapes though they have slightly different responses caused by diverse retention times; (ii) all the hydrazones show responses even at about +0.1 V *vs.* Ag/AgCl; (iii) the responses show a plateau in the potential range from +0.2 to +0.7 V *vs.* Ag/AgCl; (iv) the responses increase with increasing potential in the range from +0.7 to +1.1 V *vs.* Ag/AgCl.

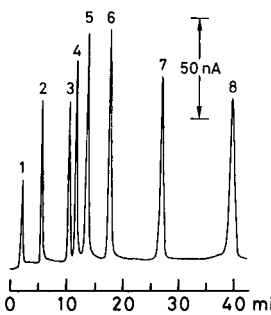

Fig. 6. Chromatogram of a synthetic mixture of 2,5-DHBH and its hydrazones of ketosteroids by HPLC–ED. Peaks (concentration injected): 1 = 2,5-DHBH (260 pmol); 2 = C-2,5-DHBH (650 pmol); 3 = D-2,5-DHBH (570 pmol); 4 = T-2,5-DHBH (830 pmol); 5 = N-2,5-DHBH (1330 pmol); 6 = E-2,5-DHBH (1280 pmol); 7 = A-2,5-DHBH (1260 pmol); 8 = P-2,5-DHBH (1710 pmol). HPLC conditions: column, Chemcosorb 5-ODS-UH (150 mm × 4.6 mm I.D.); mobile phase: 0.05 *M* phosphate buffer (pH 7.0)–acetonitrile (64:36, v/v), flow-rate: 1.0 ml/min, applied potential: +0.20 V *vs.* Ag/AgCl.

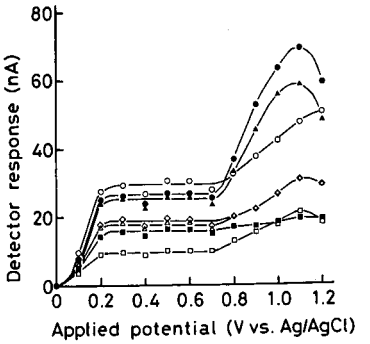

Fig. 7. Relationship between detector response and applied potential for 200 pmol of hydrazones. Symbols: ● = C-2,5-DHBH; ○ = D-2,5-DHBH; ▲ = T-2,5-DHBH; △ = N-2,5-DHBH; ◇ = E-2,5-DHBH; ■ = A-2,5-DHBH; □ = P-2,5-DHBH. HPLC conditions were the same as in Fig. 6.

TABLE III

DETECTION LIMITS OF 2,5-DHBH HYDRAZONES OF KETOSTEROIDS

Signal-to-noise ratio = 2. HPLC conditions were the same as in Fig. 6.

Compound	Detection limit (fmol per injection)				
	+0.8	+0.6	+0.5	+0.3	+0.2
C-2,5-DHBH	60	150	150	150	150
D-2,5-DHBH	100	200	150	150	150
T-2,5-DHBH	80	300	150	200	150
N-2,5-DHBH	200	400	250	300	300
E-2,5-DHBH	200	400	250	300	300
A-2,5-DHBH	200	400	400	300	500
P-2,5-DHBH	300	500	500	400	500

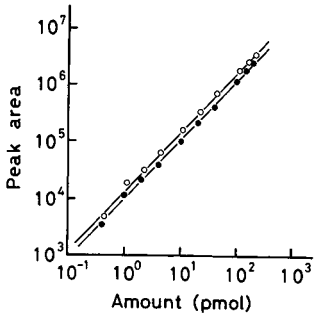

Fig. 8. Linearity of C-2,5-DHBH (●) and D-2,5-DHBH (○). Applied potential, +0.30 V *vs.* Ag/AgCl; other conditions were the same as in Fig. 6. C-2,5-DHBH: $b = 1.0138$, $t_b = 1.125 < t$ (9, 0.05) = 2.262, $r = 0.999$; D-2,5-DHBH: $b = 1.0148$, $t_b = 0.875 < t$ (9, 0.05) = 2.262, $r = 0.999$.

Table III shows detection limits of the ketosteroid hydrazones measured at the applied potentials of +0.8, +0.6, +0.5, +0.3 and +0.2 V *vs.* Ag/AgCl by HPLC–ED using authentic samples. The results shown in Tabnle III are as follows: (i) the detection limits are in the range of 60–500 fmol per injection; (ii) the detection limits of each hydrazone are not significantly different when the applied potentials are changed from +0.2 to +0.6 V *vs.* Ag/AgCl, as expected from the results of hydrodynamic voltammograms described above. As shown in Fig. 8, a good linear relationship was observed between the peak area and the concentration in the range of 0.4–200 pmol of C-2,5-DHBH and D-2,5-DHBH.

In conclusion, 2,5-DHBH is a suitable derivatization reagent for sensitive and selective HPLC–ED determination of carbonyl compounds because of its electrochemical properties, detection ability and stability. In order to demonstrate the usefulness of this reagent, further study to determine carbonyl compounds in biological fluids is in progress and will be reported elsewhere in the near future.

REFERENCES

1 I. S. Krull, C. M. Selavka, C. Duda and W. Jacobs, *J. Liq. Chromatogr.*, 8 (1985) 2845.
2 K. Shimada, M. Tanaka and T. Nambara, *Anal. Lett.*, 13 (1980) 1129.
3 K. Shimada, M. Tanaka and T. Nambara, *J. Chromatogr.*, 307 (1984) 23.
4 W. A. Jacobs and P. T. Kissinger, *J. Liq. Chromatogr.*, 5 (1982) 669.
5 G. Chiavari and C. Bergamini, *J. Chromatogr.*, 318 (1985) 427.
6 A. M. Bond, A. F. Hollenkamp, S. B. Thompson, A. R. Bourne, P. A. Huf and T. G. Watson, *Anal. Chem.*, 60 (1988) 1023.
7 J. Altschul, *J. Prakt. Chemie*, 57 (1898) 201.
8 W. Reid and K. Wagner, *Liebigs Ann. Chem.*, 724 (1969) 159.
9 M. Claesen, P. V. Duck and H. Vanderhaeghe, *J. Pharm. Pharmacol.*, 6 (1954) 127.
10 H. H. Fox and J. T. Gibas, *J. Org. Chem.*, 17 (1952) 1653.
11 N. V. Vasil'eve, V. F. Starichenko and V. A. Koptyug, *J. Org. Chem. (U.S.S.R.)*, 21 (1985) 729.
12 A. E. Lutskii, Y. I. Beilis and V. I. Fedorchenko, *Zh. Obsch. Khim.*, 43 (1973) 101.
13 H. Reich, K. F. Crane and S. J. Sanfilippo, *J. Org. Chem.*, 18 (1953) 822.
14 W. J. A. VandenHeuvel and E. C. Horning, *Biochim. Biophys. Acta*, 74 (1963) 560.

Journal of Chromatography, 585 (1991) 233–238
Elsevier Science Publishers B.V., Amsterdam

CHROM. 23 538

Estimation of the distributions of chain length of amylopectins by high-performance liquid chromatography with pulsed amperometric detection☆

Kyoko Koizumi* and Masako Fukuda

Faculty of Pharmaceutical Sciences, Mukogawa Women's University, 11-68 Koshien Kyuban-cho, Nishinomiya 663 (Japan)

Susumu Hizukuri

Department of Biochemical Sciences and Technology, Kagoshima University, 1-21-24, Kohrimoto, Kagoshima 890 (Japan)

(First received April 2nd, 1991; revised manuscript received June 3rd, 1991)

ABSTRACT

High-performance anion-exchange chromatography for a detailed estimation of the distribution of chain length of amylopectins was developed using a pulsed amperometric detector under alkaline conditions. As maltosaccharides having different degrees of polymerization, which were produced by debranching of amylopectin with isoamylase, exhibit different pulsed amperometric detector responses, the individual maltosaccharides (degree of polymerization 6–17) were isolated by high-performance liquid chromatography on an amino column and an octadecylsilane column to use as quantification standards. By the use of this high-performance anion-exchange chromatography the chain length distributions of some typical amylopectins were characterized in detail.

INTRODUCTION

The estimation of the chain length distribution is of primary importance for characterizing the molecular structure of amylopectin. Previously, Hizukuri [1] characterized the polymodal distribution of the chain length of the several kinds of amylopectin by size-exclusion chromatography using a differential refractometer and a small-angle laser light-scattering photometer. This technique is useful for this purpose but cannot separate individual members of the components of debranched amylopectins.

Recently, Koizumi *et al.* [2] showed that some homoglucan series could be well separated into the individual members [degree of polymerization (DP) up to over 50] by high-performance anion-exchange chromatography (HPAEC) with pulsed amperometric detection (PAD). However, it was impossible to determine the individual glucans directly by use of their peak areas in the chromatogram, as the responses of a pulsed amperometric detector to glucans having different DPs were different.

The purpose of this study was to develop a detailed method for quantitative analysis of maltosaccharides, the components of debranched amylopectin, and to characterize the chain length distributions of some typical amylopectins by HPAEC–PAD.

EXPERIMENTAL

Chromatography

HPAEC was performed with a Model 4000i Dionex BioLC system and a Model 2 PAD system

☆ Part of this work was presented at the *International Symposium on Cereal and Other Plant Carbohydrates, Kagoshima, August 7–9, 1990.*

0021-9673/91/$03.50

(Dionex, Sunnyvale, CA, USA). The pulse potentials and durations used were identical to those described in a previous paper [2]. The column used was a Dionex HPIC-AS6 (the same type of column is now called CarboPac PA-1) (250 × 4 mm I.D.) (10 μm) equipped with an AG6 guard column (50 × 4 mm I.D.). An 807 IT digital integrator (Jasco, Tokyo, Japan) was used to calculate peak areas.

High-performance liquid chromatography (HPLC) for isolation of individual maltosaccharides was conducted with a Jasco 880-PU pump, a U6K universal injector (Waters, Milford, MA, USA) and an SE-61 RI monitor (Showa Denko, Tokyo, Japan). The columns used were an Asahipak NH2P-50 (250 × 10 mm I.D.) (5 μm) (Asahi Kasei, Tokyo, Japan) and a YMC-Pack SH-343-5 AQ (250 × 20 mm I.D.) (5 μm) (YMC, Kyoto, Japan). For preparative chromatography at constant temperature a CO-1093C column oven (Uniflows, Tokyo, Japan) was used. Degassing of eluents on line was performed using Degasys DG-1200 (Uniflows).

Materials

Amylopectins tested were of wheat [3], rice (Sasanishiki [4] and Nihonbare, both Japonica), waxy rice (Hiyokumochi, Japonica) [5], corn [6], tapioca [5], edible canna, sweet potato (Minamiyutaka) [7], and potato [5]. Some of them were used in previous studies as cited. Edible canna and rice (Nihonbare) amylopectins were prepared from their corresponding starches by the same procedures as described elsewhere [4]. The individual maltosaccharides (DP 6–17) used as quantification standards were isolated from short-chain amylose EX-1 ($\overline{DP} \approx 17$) [a mixture of (1→4)-α-D-glucans] (Hayashibara, Okayama, Japan). All reagents were of analytical-reagent grade. The eluents for HPAEC were prepared in the same manner as those in a previous paper [2]. Reagent-grade organic solvents used for preparative chromatography were dried and freshly distilled before use. Water used in solvent preparations was distilled, deionized, redistilled and degassed by sonication.

Preparation of amylopectin isoamylolyzates

Amylopectin (100 mg) was dissolved in 25 m*M* acetate buffer, pH 4.5 (40 ml), and was debranched with isoamylase (30 I.U.) for 12 h at 45°C. The resulting linear chains were lyophilized after inactivating the enzyme by boiling. The lyophilized sample (2 mg) was dissolved in 1 ml of 150 m*M* sodium hydroxide solution and the aliquots of 20–30 μl were analyzed.

RESULTS AND DISCUSSION

Separation of individual members in the amylopectin isoamylolyzates

In order to achieve an effectice separation of individual members of a series of chains, several gradient programmes were examined. The gradient programme selected was as follows: 40% eluent B at 0 min, 50% at 2 min, 60% at 10 min and 80% at 40 min. All separations on a HPLC column were carried out at ambient temperature with a flow-rate of 1 ml/min. The HPAEC elution profile of the components of debranched wheat amylopectin is shown in Fig. 1 as an example. The number on each peak, indicating its DP, was confirmed by adding maltooligosaccharides of known DP. A baseline separation of chains up to DP ⩾ 55 was achieved as individual peaks. The smallest chain appears to be DP 6, which was common to amylopectins of other sources. The most abundant chain of the wheat amylopectin was apparently DP 11, with a shoulder at DP 18 and 19. Thus, the apparent distribution of

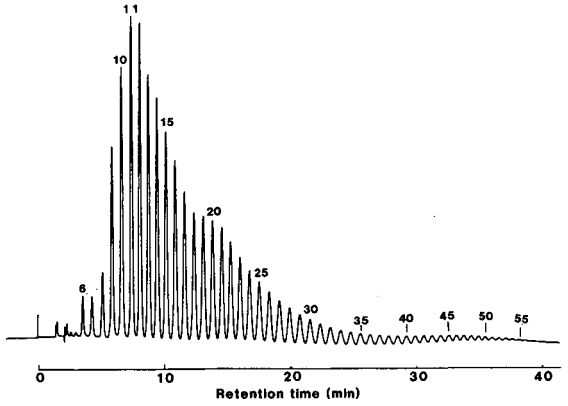

Fig. 1. HPAEC elution profile of the components of debranched wheat amylopectin. The number on each peak indicates its DP. Chromatographic conditions: column, HPIC-AS6 (250 × 4 mm I.D.); eluent A, 150 m*M* sodium hydroxide solution; eluent B, 150 m*M* sodium hydroxide solution containing 500 m*M* sodium acetate; gradient program, 40% eluent B at 0 min, 50% at 2 min, 60% at 10 min and 80% at 40 min; flow-rate, 1 ml/min; detector, PAD 2; meter scale, 10 000 nA; temperature, ambient.

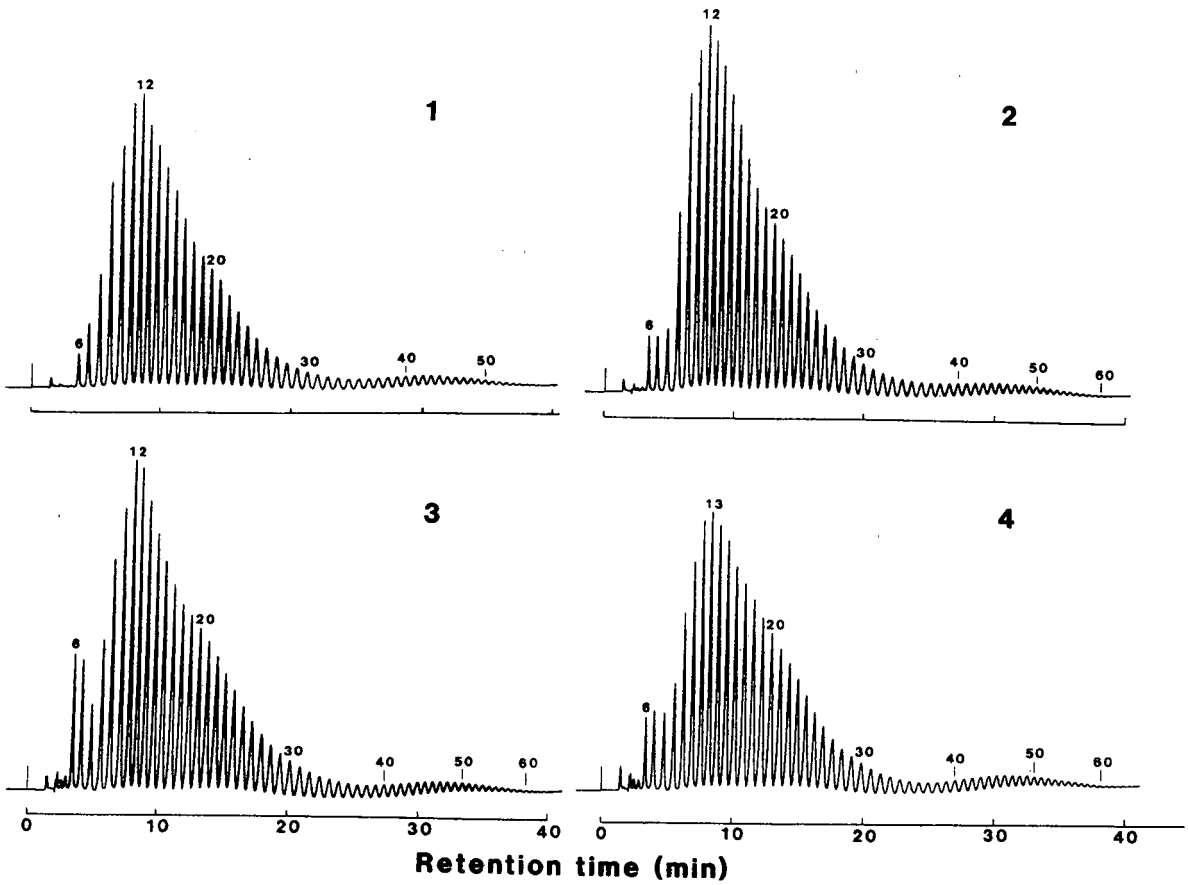

Fig. 2. Chromatograms of isoamylolyzates of some typical amylopectins. 1 = rice (Nihonbare); 2 = corn; 3 = sweet potato; 4 = edible canna. Chromatographic conditions as in Fig. 1.

chain length could be clearly characterized. Besides the peak top DPs, characteristic distributions by species were generally observed in the range DP 6–10 (Fig. 2).

Isolation of individual maltosaccharides (DP 6–17)

Previously we have found that PAD responses to a series of glucans increase with increasing DP [2]. Although this is favorable for detection of higher oligo- and polysaccharides, such differences in the PAD response to saccharides with different DPs require a quantification standard for each maltosaccharide in amylopectin isoamylolyzates to be determined. Therefore, isolation of the individual maltosaccharides was attempted.

Usually HPLC for the separation of oligosaccharides is conducted by using aminopropyl-bonded silica with acetonitrile–water as the eluent. However, amino columns have limited lifetimes, since the bonded phase is readily hydrolyzed. Recently, several attempts have been made to improve the packing stability. One of them, an Asahipak NH2P-50 column, packed with chemically polyamine-bonded vinyl alcohol copolymer gel (5 μm), was selected in this work for the isolation of each maltosaccharide.

Using a semipreparative-size column (250 × 10 mm I.D.) of Asahipak NH2P-50, a 3% aqueous solution of short-chain amylose EX-1 was first roughly separated into several fractions with acetonitrile–water (55:45, v/v) at a flow-rate 2 ml/min (Fig. 3), and then each fraction was purified by repeated rechromatography with gradually decreasing concentrations of acetonitrile (from 62 to 55%) with

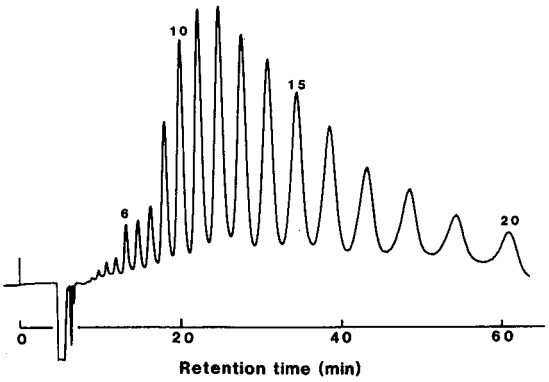

Fig. 3. Separation of maltosaccharides [short-chain amylose EX-1 ($\overline{DP} \approx 17$] on an Asahipak NH2P-50 (250 × 10 mm I.D.). Chromatographic conditions: eluent, acetonitrile–water (55:45, v/v); flow-rate, 2 ml/min; temperature, 33°C.

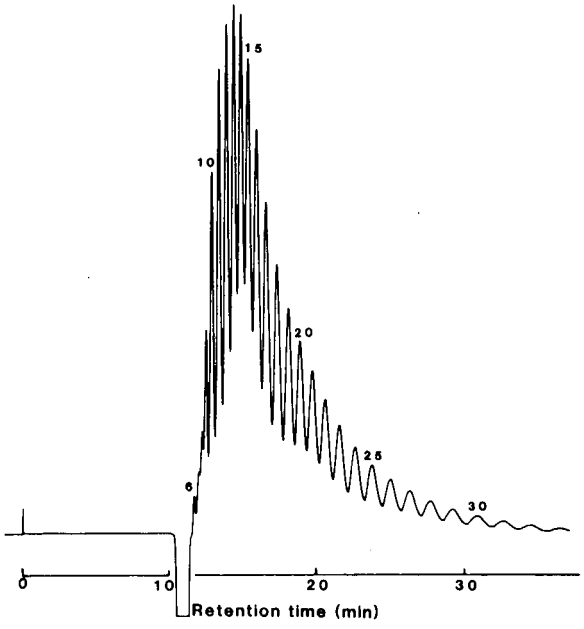

Fig. 4. Separation of maltosaccharides on a YMC-Pack SH-343-5 AQ (250 × 20 mm I.D.). Chromatographic conditions: eluent, 6.0% (v/v) methanol in water; flow-rate, 6 ml/min; temperature, 33°C.

increasing DP. However, the solubility of maltosaccharides, especially above DP 14, was not sufficient to allow chromatography on this column with acetonitrile–water, and, consequently, saccharides of higher DP frequently precipitated on the column. An advantage of this column is that a wider pH range (2–13) can be used, and hence polysaccharides precipitated on the column could be removed by washing with 50 m*M* sodium hydroxide solution, after which there was no change in column performance. The next attempt, in which polysaccharide samples were dissolved in 10% ethylenediamine solution (pH 12.7) and eluted with acetonitrile–water containing 10% ethylenediamine, did not give any satisfactory chromatograms, though precipitation of polysaccharides on the column could be prevented.

Fig. 4 shows the elution profile of short-chain amylose EX-1 on an octadecylsilane (ODS) column with 6.0% methanol at 33°C. In general, ODS columns are not used for the separation of oligosaccharides, because they lead to an undesirable resolution between the α- and β-anomers of the individual oligosaccharides in HPLC at room temperature and with pure water as the eluent. However, a chromatogram obtained under the conditions in Fig. 4 was similar to the elution profile of the same sample on an aminopropyl-bonded silica column obtained previously [8]. The loading capacity of this column (~60 mg) was much larger than that of the amino column described above (~2 mg) and, moreover, the eluent used for this HPLC, a few per cent methanol, was relatively favorable for dissolving higher saccharides.

Separation of maltosaccharides on this ODS column was performed as follows: fractions I (DP 6–13) and II (DP 14–20) were collected under the conditions in Fig. 4, fraction I was rechromatographed with 2.0% methanol (the methanol concentrations of the eluents were accurately adjusted using whole pipettes and a volumetric flask to obtain the best separation of a pair of α- and β-anomers from other pairs) (Fig. 5) to isolate individual maltosaccharides of DP 6–13, and each saccharide was purified by HPLC on the same column with a suitable concentration of methanol (1.0% for DP 6 and 7, 1.2% for DP 8, 1.4% for DP 9, 1.6% for DP 10, 1.8% for DP 11, and 2.0% for DP 12 and 13). As shown in Fig. 5, the α- and β-anomers of all maltosaccharides are resolved by using 2.0% methanol as the eluent. To ensure that two adjacent peaks arose from the same saccharide, the two peaks were separately collected and analyzed on an Asahipak NH2P-50 column and an HPIC-AS6 column. These two fractions

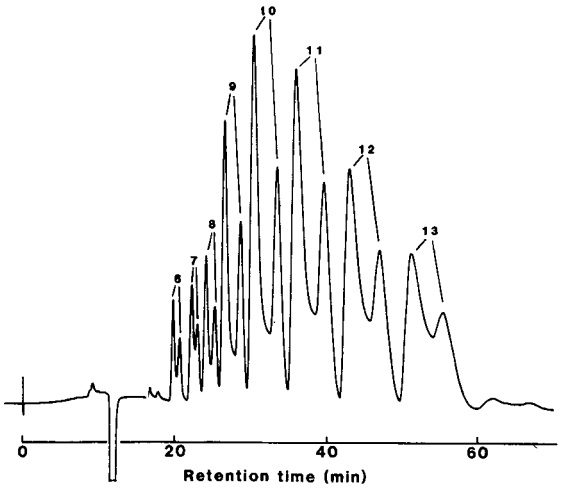

Fig. 5. Separation of maltosaccharides (DP 6–13) on a YMC-Pack SH-343-5 AQ. Chromatographic conditions: eluent, 2.0% (v/v) methanol in water; other conditions as in Fig. 4.

each gave a single peak with the same retention time on an Asahipak NH2P-50, whereas on an HPIC-AS6 the former fraction showed a single peak but the latter fraction showed another small peak immediately in front of the main peak having the same retention time as that of the former fraction. The small peak may correspond to a glucan having the same DP as that of the main peak and containing one (1→6)-α-linkage, since the (1→6)-α-D-glucan moves more slowly on the ODS column [9] and faster on the HPIC-AS6 column [2] than the (1→4)-α-D-glucan. A comparison of the chromatographic behavior of maltohexaose and 6^3-O-α-maltotriosyl-maltotriose, which is a hydrolyzate of pullulan with DP 6, substantiated this prediction. This result revealed that short-chain amylose EX-1 does not consist of homogeneous (1→4)-α-D-glucans, but contains a small amount of (1→4)-α-D-glucans containing (1→6)-α-linkages, and the latter can be separated from the former on the ODS column but not on an Asahipak NH2P-50 column. Although individual maltosaccharides of DP 14–17 were also isolated from fraction II on the ODS column with 2.3% methanol, those of DP over 18 could not be purified, as their solubilities are too small to allow solutions to be made, even in pure water.

Relative detector responses of maltooligosaccharides and maltopolysaccharides

Relative detector responses (RDRs) of individual isolated maltosaccharides are summarized in Table I. The RDRs of maltosaccharides of DP 8–13 increase approximately in proportion to the number of hydroxyl groups in the molecule, and the responses per hydroxyl group in maltosaccharides of over DP 14 decrease little by little, whereas those of DP 6 and 7 are slightly higher. These facts may suggest that undetectable hydroxyl groups increase with increasing molecular weight, owing to the formation of random coil.

The individual peak area obtained from chromatograms of amylopectin isoamylolyzates such as in Figs. 1 and 2 was corrected by dividing by the relative detector response. Using the corrected peak area, the exact distributions of chain length (DP 6–17) of some typical amylopectins were compared (Fig. 6). These chain length distributions were characterized by sources and could be regarded as fingerprints. Wheat amylopectin exhibited a somewhat sharp peak with three chains (DP 10, 11 and 12), which was maximal at DP 10 and decreased gradually above DP 13. Tapioca amylopectin gave a similar pattern but peaked at DP 11. These characteristics agreed well with those found by gel-exclusion HPLC [1,3]. Three rice amylopectins (Sasanishiki, Nihonbare and Hiyokumochi) showed similar pat-

TABLE I

RELATIVE PAD RESPONSES OF MALTOSACCHARIDES

Chromatographic conditions as in Fig. 1. The amounts of maltosaccharides used were 1.5 nmol each. RDR = relative PAD response on molar basis.

DP	No. of HCOH	RDR	RDR per HCOH unit
6	20	0.74	1.08
7	23	0.82	1.03
8	26	0.89	0.99
9	29	1.00	1.00
10	32	1.10	1.00
11	35	1.20	1.00
12	38	1.31	1.00
13	41	1.38	0.99
14	44	1.46	0.97
15	47	1.55	0.96
16	50	1.59	0.92
17	53	1.65	0.90

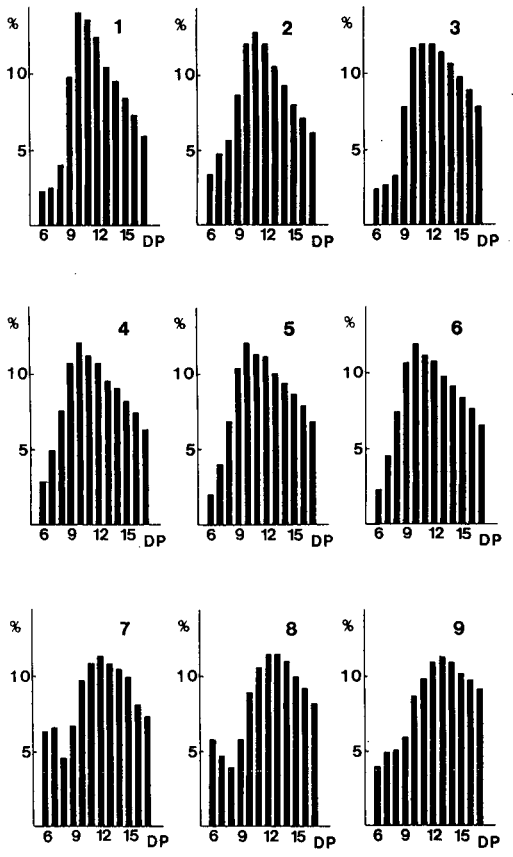

Fig. 6. Comparison of exact distributions of chain length (DP 6–17) of some typical amylopectins. 1 = wheat; 2 = tapioca; 3 = corn; 4 = rice (Sasanishiki); 5 = rice (Nihonbare); 6 = waxy rice (Hiyokumochi); 7 = sweet potato; 8 = potato; 9 = edible canna.

terns, with a slightly broader peak (maximum at DP 10) and gradually decreasing at chains longer than DP 10. Corn amylopectin consisted of only tiny amounts of DP 6–8 chains and showed a dull peak with chains of DP 9–12 (maximum at 10 and 11). Sweet potato and potato amylopectins gave characteristic patterns in the range of DP 6–9, having a hollow at DP 8 and peaks at DP 12, and 12 and 13, respectively. Small amounts of phosphorylated chains at C-6 or C-3 [10,11] in these specimens were not detectable under the experimental conditions and were left for future studies. Edible canna amylopectin exhibited a gradual increase and decrease to and from the peak at DP 13. These minute chain length distributions between DP 6 and 17, although a very limited range, are informative for characterization of amylopectin by sources. We are attempting to expand the range for better elucidation and characterization of the amylopectin structure.

REFERENCES

1 S. Hizukuri, *Carbohydr. Res.*, 147 (1986) 342–347.
2 K. Koizumi, Y. Kubota, T. Tanimoto and Y. Okada, *J. Chromatogr.*, 464 (1989) 365–373.
3 S. Hizukuri and Y. Maehara, *Carbohydr. Res.*, 206 (1990) 145–159.
4 Y. Takeda, S. Hizukuri and B. O. Juliano, *Carbohydr. Res.*, 168 (1987) 79–88.
5 S. Hizukuri, *Carbohydr. Res.*, 141 (1985) 295–306.
6 Y. Takeda, T. Shitaozono and S. Hizukuri, *Starch/Stärke*, 40 (1988) 51–54.
7 Y. Takeda, N. Tokunaga, C. Takeda and S. Hizukuri, *Starch/Stärke*, 38 (1986) 345–350.
8 K. Koizumi, T. Utamura and Y. Okada, *J. Chromatogr.*, 321 (1985) 145–157.
9 K. Koizumi and T. Utamura, *J. Chromatogr.*, 436 (1988) 328–333.
10 S. Tabata and S. Hizukuri, *Stärke*, 23 (1971) 267–272.
11 Y. Takeda and S. Hizukuri, *Carbohydr. Res.*, 102 (1982) 321–327.

Journal of Chromatography, 585 (1991) 239–246
Elsevier Science Publishers B.V., Amsterdam

CHROM. 23 475

Determination of phosphatidylcholine, phosphatidylglycerol and their lyso forms from liposome dispersions by high-performance liquid chromatography using high-sensitivity refractive index detection

Mustafa Grit* and Daan J. A. Crommelin

Department of Pharmaceutics, Faculty of Pharmacy, University of Utrecht, Sorbonnelaan 16, P.O. Box 80 082, 3508 TB Utrecht (Netherlands)

Johanna Lang

Liposome Technology Inc., 1050 Hamilton Court, Menlo Park, CA 94025 (USA)

(First received February 5th, 1991; revised manuscript received May 7th, 1991)

ABSTRACT

An assay for quantitative analysis of phosphatidylcholine and phosphatidylglycerol, and their corresponding hydrolysis products lysophosphatidylcholine and lysophosphatidylglycerol using high-performance liquid chromatography with high-sensitivity refractive index detection was developed. The separation of the phospholipids of interest was achieved on a Zorbax NH_2 column (25 cm × 4.6 mm I.D.) with a mobile phase consisting of acetonitrile–methanol–10 m*M* ammonium dihydrogenphosphate solution pH 4.8 (64:28:8, v/v/v) at a flow-rate of 1.5 ml/min. The response of the refractive index detector to different types of phosphatidylcholine with varying degrees of unsaturation was constant, while the ultraviolet detector response was strongly dependent on the degree of unsaturation. This makes refractive index detection suitable for the determination of natural phospholipids which show a wide variety of fatty acid composition. The method was validated for the determination of phosphatidylcholine, phosphatidylglycerol, lysophosphatidylcholine and lysophosphatidylglycerol in a model liposome dispersion. Synthetic phospholipids of high purity served as external standards and quantitation was based on peak areas. Calibration curves were linear over two orders of magnitude, and detection limits of phosphatidylcholine, phosphatidylglycerol, lysophosphatidylcholine and lysophosphatidylglycerol were 22, 29, 30 and 50 μg/ml, respectively. The method precision for a standard phospholipid mixture and for a phosphatidylcholine–phosphatidylglycerol containing liposome dispersion was in the range of 0.6–4.5% relative standard deviation.

INTRODUCTION

Liposomes, (phospho)lipid vesicles which form spontaneously in an aqueous environment, can be used as pharmaceutical drug carriers [1]. As a part of pharmaceutical formulation process, the long-term stability of liposomes has become an important issue. In an aqueous phospholipid liposome dispersion, the liposomal phospholipids can hydrolyse to free fatty acids and lysophospholipids [2], a process which destabilizes the liposome dispersions and limits the shelf life of liposome-based pharmaceuticals.

Traditionally, thin-layer chromatography (TLC) followed by phosphorus analysis has been the preferred technique for quantitative phospholipid analysis. The different TLC procedures used have been reviewed extensively [3]. TLC, however, is time-consuming, shows high variability and cannot be easily applied to the routine analysis of a large

0021-9673/91/$03.50

number of samples. High-performance liquid chromatographic (HPLC) methods have been used to overcome these limitations.

Phospolipid analysis using HPLC can be divided into two groups: separation of phopholipid classes (*i.e.* by the nature of the head group) and separation of the molecular species within a phospholipid classes (*i.e.* by the nature of the fatty aids). Separation of the phospholipid classes has been achieved on silica gel [4–10], cyano phase [11], diol phase [11,12], amino phase [12,13] and ion-exchange columns [14], while reversed-phase columns separate phospholipids primarily by the molecular species within a given phospholipid class [15–21]. Most of the available methods deal with the determination of phospholipids from biological sources and require solvent or flow gradients to elute the phospholipid classes with good peak shapes and reasonable retention times. Most commonly phospholipids are monitored by low-wavelength UV detection, which is compatible with most solvent systems. The UV response is highly dependent on the nature of the fatty acid residues and varies with the degree of unsaturation. The highly unsaturated phospholipids yield a good response, while the sensitivity for the fully saturated species is poor. This makes UV detection unsuitable for the quantitation of phospholipids with undefined or varying phospholipid composition such as natural phospholipids (phospholipids isolated from natual sources). Usually liposomes consist of more than one phospholipid class and are often made of natural phospholipid raw materials with a wide range of molecular species with varying degrees of unsaturation.

In this study, the usefulness of high-sensitivity refractive index (RI) detection as a mass-sensitive HPLC detector was investigated for the quantitative analysis of phosphatidylchloline (PC) and phosphatidylglycerol (PG), and the corresponding lysophospholipids, lysophosphatidylchloline (LPC) and lysophosphatidylglycerol (LPG), in a model liposome formulation. The column separation was developed from a previously described HPLC procedure [13]. Mobile phase composition was optimized for the separation of the phospholipids of interest. The HPLC–RI assay was validated for the quantiative determination of PC, PG, LPC and LPG.

EXPERIMENTAL

Materials

Dimyristoylphosphatidylcholine (DMPC), monomyristoylphosphatidylcholine (MPC, lysophosphatidylcholine), dimyristoylphosphatidylglycerol (DMPG) and monomyristoylphosphatidylglycerol (MPG, lysophosphatidylglycerol) were purchased from Avanti (Pelham, AL, USA). Dipalmitoylphosphatidylcholine (DPPC), distearoylphosphatidylcholine (DSPC), dipalmitoylphosphatidylglycerol (DPPG) and distearoylphosphatidylglycerol (DSPG) were purchased from KSV (Helsinki, Finland). Dioleylphosphatidylcholine (DOPC) and dilinoleylphosphatidylcholine (DLPC) were purchased from Sigma (St. Louis, MO, USA). Natural egg phosphatidylcholine (EPC, iodine value 65) and partially hydrogenated egg phosphatidylcholines with iodine values of 40, 30, 20, 10 and 1 were purchased from Asahi (Tokyo, Japan) through Austin (Rosemont, IL, USA). Natural egg phosphatidylglycerol (EPG) and Phospholin 100H were products of Nattermann (Cologne, Germany). Other chemicals used were of analytical grade.

HPLC system

The HPLC system consisted of a solvent delivery system (Autochrom M 500, Knauer, Berlin, Germany), a Rheodyne injection unit (loop volume 5 or 20 μl), a variable-wavelength detector (Model SF 773, Kratos, Ramsey, NJ, USA), a differential refractometer (Waters 410 RI detector, Waters Assoc., Milford, MA, USA) and a Turbochrom 2700 (PE-Nelson, Cupertino, CA, USA) data acquisition and processing system. In some experiments a Hewlett-Packard Type 3390A integrator (Avondale, PA, USA) was used. The separation of the phospholipids was carried out on a Zorbax amino phase column (25 cm × 4.6 mm I.D., 5 μm particle size, Du Pont, Wilmington, DE, USA) at ambient temperature at a flow-rate of 1.5 ml/min, unless otherwise stated. Detection was carried out both with an RI detector and with a UV detector at 206 nm. The detectors were set up in series with the column effluent first passing through the UV detector.

Preparation of the mobile phase

The mobile phase used in this study consisted of acetonitrile, methanol and a 10 m*M* ammonium dihydrogenphosphate solution pH 4.8 (64:28:8, v/v/v). The 10 m*M* ammonium dihydrogenphosphate solution, pH 4.8, was prepared by adjusting the pH of a 10 m*M* phosphoric acid solution to pH 4.8 with a dilute ammonium hydroxide solution. To prepare the mobile phase, acetonitrile and methanol were mixed first and finally the ammonium dihydrogenphosphate solution was added. Direct mixing of acetonitrile and the ammonium dihydrogenphosphate solution caused precipitation of the salt.

Preparation of (standard) phospholipid solutions

All solid phospholipid materials were dissolved in chloroform–methanol (6:4, v/v). This solvent mixture proved to be an acceptable solvent for all phospholipids tested and exhibited minimal interference of the solvent front with the relevant phospholipid peaks in the chromatogram. Pure chloroform was a superior solvent but resulted in a large broad solvent peak.

Preparation of samples from aqueous liposome dispersions

A model liposome dispersion consisting of EPC (iodine value 40) and EPG was prepared by the "film" method [22]. After formation of the phospholipid film in a round-bottom flask from a solution of phospholipids in chloroform in a rotary evaporator at ~50°C, the film was left overnight under reduced pressure. It was hydrated at ~50°C with 0.05 *M* acetate buffer (pH 4.0) containing 0.8% sodium chloride. The initial EPC and EPG concentrations were 24 and 8 mg/ml, respectively. The liposome dispersion was filled into 1-ml ampoules and stored at 70°C for up to 53 h.

The samples were prepared for HPLC analysis by ten-fold dilution of the liposome dispersion with the chloroform–methanol (6:4, v/v). In the diluted samples the salts and the buffer components of the liposome formulation formed a precipitate. These samples were made particle-free by centrifugation at 2700 *g* for 15 min and injected directly into the HPLC system.

RESULTS AND DISCUSSION

Optimization of mobile phase composition for the separation of the PC, PG, LPC and LPG

As RI detectors are sensitive to changes in flow and mobile phase composition, they require isocratic constant-flow conditions for the column separation. Of the numerous HPLC separations reported in the literature, only few can achieve a satisfactory separation of phospholipid classes under isocratic conditions and without flow gradients. HPLC conditions as described by Shimbo [13] for the analysis of rat liver phospholipids proved to be suitable for the isocratic separation of typical liposomal phospholipids PC and PG and their lyso products. Fig. 1 shows the separation of a mixture of synthetic phospholipid standards, DMPC, DMPG, MPC and MPG, under the conditions described by Shimbo. When the flow-rate increased to 1.2 and 1.5 ml/min, the peak shapes improved and the retention times were shorter without loss of resolution. A chromatogram representing the separation of a mixture of the phospholipids carried out at a flow-rate of 1.5 ml/min is presented in Fig. 2A.

Lysophospholipid standards, MPC and MPG, consistently eluted as two peaks. This is consistent

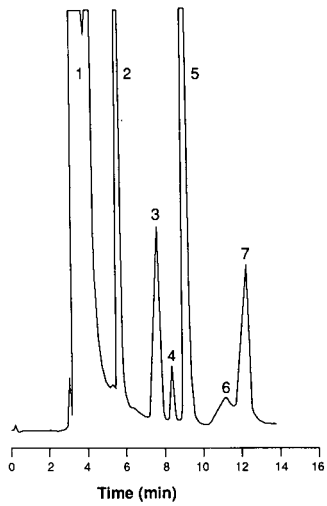

Fig. 1. HPLC profile of phospholipids. Peaks: 1 = solvent front; 2 = phosphatidylcholine (PC); 3 = phosphatidylglycerol (PG); 4 = 2-acyl lysophosphatidylcholine (LPC); 5 = 1-acyl LPC; 6 = 2-acyl lysophosphatidylglycerol (LPG); 7 = 1-acyl LPG. HPLC conditions: mobile phase, acetonitrile–methanol–10 m*M* ammonium dihydrogenphosphate solution pH 4.8 (61:29:10, v/v/v); flow-rate, 1.0 ml/min; detection, RI.

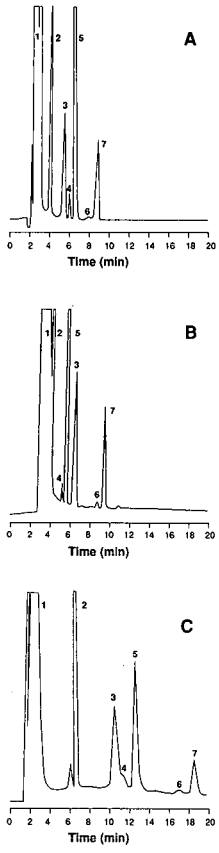

Fig. 2. HPLC profiles of phospholipids. Numbers refer to the same components as in Fig. 1. (A) Mobile phase, acetonitrile–methanol–10 m*M* ammonium dihydrogenphosphate solution pH 4.8 (61:29:10, v/v/v); flow rate, 1.5 ml/min. (B) Mobile phase, acetonitrile–methanol–10 m*M* ammonium dihydrogenphosphate solution pH 4.8 (50:40:10, v/v/v); flow rate, 1.5 ml/min. (C) Mobile phase, acetonitrile–methanol–10 m*M* ammonium dihydrogenphosphate solution pH 4.8 (64:31:5, v/v/v); flow-rate, 1.5 ml/min. Other conditions as in Fig. 1.

with a separation of the lysophospholipids into the two positional isomers which form via acyl migration during the formation of lysophospholipids by the action of phospholipase A_2 and upon subsequent storage; the equilibrium mixture contains approximately 10% of the 2-acyl isomer [23]. Presumably, the peaks eluting before the major lysophospholipids were the 2-acyl isomers of MPC and MPG.

The effect of the mobile phase composition on the separation of the phospholipids was studied by determination of the retention times of the phospholipids with different mobile phase compositions. Either the acetonitrile/methanol ratio (volume fraction of the ammonium dihydrogenphosphate solution kept constant) or the ammonium dihydrogenphosphate solution volume fraction (acetonitrile/methanol ratio kept constant) was varied. Typical examples of chromatograms are presented in Fig. 2B and C. Increasing the concentration of methanol and conversely decreasing the concentration of acetonitrile in the mobile phase resulted in changes in the elution order: from PC, PG, LPC and LPG to PC, LPC, PG and LPG (Fig. 2A and B), while a decrease in the volume fraction of the ammonium dihydrogenphosphate solution in the mobile phase caused longer retention times for all phospholipids (Fig. 2A and C).

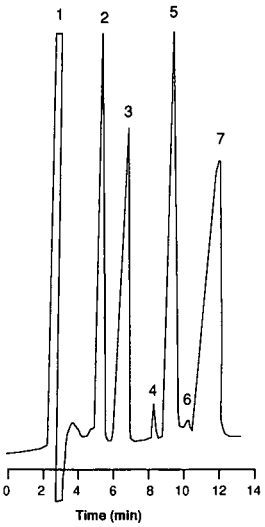

Fig. 3. HPLC profile of phospholipids. Numbers refer to the same components as in Fig. 1. HPLC conditions: mobile phase, acetonitrile–methanol–10 m*M* ammonium dihydrogenphosphate solution pH 4.8 (64:28:8, v/v/v); flow-rate, 1.5 ml/min; detection, RI.

On the basis of these chromatograms, the optimal mobile phase composition was modelled on the Drylab I [24] solvent optimization program. Maximal resolution for all phospholipids of interest in the shortest overall run time was obtained with a mobile phase composition of acetonitrile–methanol–10 m*M* ammonium dihydrogenphosphate solution pH 4.8 (64:28:8, v/v/v). Fig. 3 shows a typical chromatogram of the phospholipid standard mixture under these optimized conditions.

Separation of the other phospholipid classes such as phosphatidylethanolamine (PE), phosphatidic acid (PA), phosphatidylserine (PS), phosphatidylinositol (PI) and sphingomyelin (SPH) was investigated by the analysis of spiked mixtures. Except SPH, all other phospholipids were well separated from PC, PG, LPC and LPG and eluted after the LPG peak (results not shown). SPH, however, was eluted together with PG. The separation of α-tocopherol and cholesterol, which are often used in liposomal preparations, as well as fatty acids, which are hydrolysis products of phospholipids, was also investigated. Standard solutions of α-tocopherol, cholesterol or palmitic acid did not show peaks within a 20-min run time. α-Tocopherol and cholesterol were found in the solvent front when the collected solvent front fraction was analysed on another HPLC system [25].

RI and UV detector response to phospholipids

For both the RI and UV detectors the detection limit for the phospholipid of interest was defined as the concentration which resulted in a signal-to-noise ratio of 2. Detection limits obtained were $3 \cdot 10^{-5}$, $4 \cdot 10^{-5}$, $6 \cdot 10^{-5}$ and $1 \cdot 10^{-4}$ *M* by RI detection and $9 \cdot 10^{-5}$, $1 \cdot 10^{-4}$, $2 \cdot 10^{4}$ and $4 \cdot 10^{-4}$ *M* by UV detection for DMPC, DMPG, MPC (lyso) and MPG (lyso), respectively. The values were determined at an attenuation of 16× for the RI detector and 0.01 a.u.f.s. for the UV detector. It is clear that for saturated phospholipids the detection limit for RI detection is lower than that achievable by UV detection. The difference is slightly more pronounced for the determination of the lysophospholipid.

The RI and UV detector response to different types of phosphatidylcholine species was investigated by determination of the molar response of phosphatidylcholine with varying iodine value, varying chain length and varying number of unsaturated bonds. The iodine values for the synthetic phosphatidylcholine carrying unsaturated bonds, namely DOPC and DLPC, were calculated on the basis of the iodine values reported for oleic acid and linoleic acid. The results show that the UV detector response is strongly dependent on the degree of saturation, while the RI detector response is not significantly affected by the degree of saturation of phosphatidylcholine (Fig. 4). Neither of the two detectors showed a chain length-dependent response (results not shown).

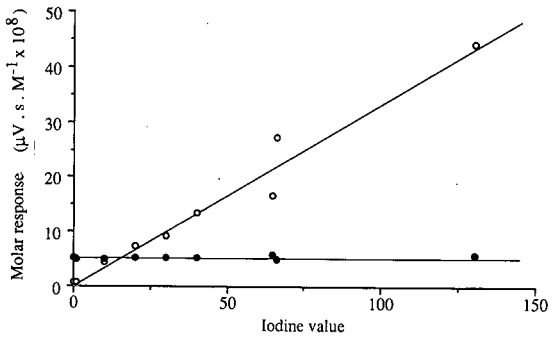

Fig. 4. Relationship between the molar response of different species of phosphatidylcholine with varying degrees of saturation with the RI (●) and UV (○) detectors.

Linearity of response

Fig. 5 shows the relationship between peak area and concentration for DMPC, DMPG, MPC and MPG. In all cases the RI detector response was linear with concentration (Fig. 5). Quantitation by peak area was chosen over peak heights because PG and LPG peaks were not symmetrical and the relationship between peak height and concentration was not linear.

Precision

The precision of the determination was tested by repetitive injection a mixture of phospholipids at different concentrations. The results indicated relative standard deviations (R.S.D.) between 0.6 and

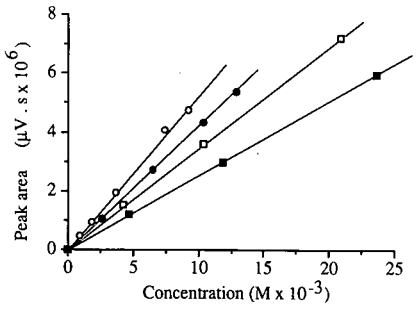

Fig. 5. Standard calibration curves of the phospholipids of interest: ○ = DMPC, ● = DMPG; □ = MPC; ■ = MPG. Lines were calculated by linear regression analysis. Each data point is the average of two determinations.

TABLE I

PRECISION OF THE DETERMINATION

HPLC conditions were the same as in Fig. 3. Injection volume, 20 μl; $n = 8$; C.V., coefficient of variation.

Phospholipid	Concentration (M)	Area (mean ± S.D.) (mV s)	C.V. (%)
Phospholipon 100H	$2.7 \cdot 10^{-4}$	710 ± 30	3.7
	$2.2 \cdot 10^{-3}$	5880 ± 40	0.7
Egg PG	$2.4 \cdot 10^{-4}$	560 ± 20	4.2
	$2.7 \cdot 10^{-3}$	5650 ± 140	2.6
MPC	$4.3 \cdot 10^{-4}$	700 ± 20	2.6
	$3.6 \cdot 10^{-3}$	5810 ± 40	0.6
MPG	$4.9 \cdot 10^{-4}$	720 ± 20	2.8
	$5.5 \cdot 10^{-3}$	8390 ± 140	1.6

4.2% (Table I). The precision of the analysis of a liposome sample was in the range of 1.7–4.5% R.S.D. (Table II).

Analysis of phospholipids in aqueous liposome dispersions

The liposome dispersion was analysed shortly after preparation and again after 30 and 53 h of storage at 70°C for its content of PC, PG and the hydrolysis products LPC and LPG. Representative chromatograms are presented in Fig. 6A–C for fresh samples and liposomes aged for 30 and 53 h at 70°C, respectively. A quantitative analysis of the composition of the dispersion on storage is presented in Table II. The recovery of the phospholipids from the aqueous liposome dispersion was complete for the fresh liposome samples. For aged samples a substantial drop in PC and PG content was observed. Lower total lipid recovery of the aged samples is due to the further hydrolysis of lysophospholipids to glycerophospho compounds [26,27].

TABLE II

RESULTS OF THE ANALYSIS OF EPC–EPG-CONTAINING LIPOSOME DISPERSION

Composition: 24 mg/ml EPC and 8 mg/ml EPG; samples were diluted ten times and 20 μl were injected ($n = 8$). Other conditions are the same as in Fig. 3.

Compound	Concentration (mean ± S.D.) (mg/ml)	C.V. (%)	Recovery (mean ± S.D.) (%)
t = 0			
EPC	24.1 ± 0.44	1.9	100.4 ± 1.9
EPG	7.9 ± 0.17	2.2	98.8 ± 2.1
t = 30 h			
EPC	12.4 ± 0.21	1.7	
EPG	2.8 ± 0.08	3.0	
LPC	3.7 ± 0.07	1.9	
LPG	1.4 ± 0.06	4.5	
t = 53 h			
EPC	8.1 ± 0.24	3.0	
EPG	1.3 ± 0.05	3.9	
LPC	4.1 ± 0.06	1.5	
LPG	1.6 ± 0.07	4.0	

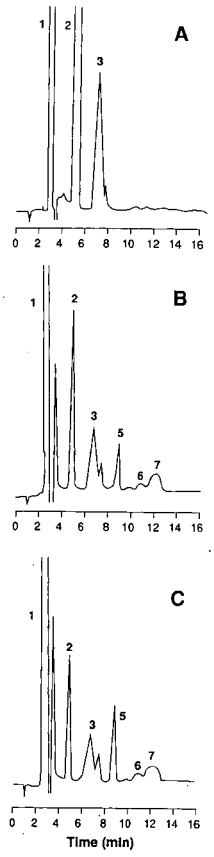

Fig. 6. HPLC profiles of egg phosphatidylcholine (EPC)–egg phosphatidylglycerol (EPG)-containing liposome samples. Numbers refer to the same components as in Fig. 1. HPLC conditions same as in Fig. 3. Composition of liposome dispersion: 24 mg/ml EPC and 8 mg/ml EPG dispersed in pH 4.0 acetate buffer (0.05 *M*); samples were diluted ten times and 20 μl of this solution injected into the HPLC system. (A) Fresh liposome dispersion, (B) 30 h aged at 70°C, (C) 53 h aged at 70°C.

CONCLUSIONS

The analysis of phospholipids by HPLC has advantages over TLC, *.e.g* improved sensitivity, precision and resolution and the possibility of automation. Most of the methods for phospholipid analysis by HPLC available in the literature require either a solvent or a flow gradient to elute the phospholipids with a reasonable retention time, acceptable resolution and a good peak shape. Gradient elution, however, is not compatible with RI detection. Therefore, an isocratic method is essential for the analysis of phospholipids by RI detection.

In this study low-wavelength UV and RI detection systems were compared in terms of sensitivity and changes in the molar response of the phospholipids as a function of phospholipid type, degree of unsaturation and chain length of fatty acid components. As shown in Fig. 4, the UV response is mainly dependent on the degree of unsaturation. The highly unsaturated phospholipids yield a good response while the sensitivity for fully saturated species is poor. The RI detector response, however, is not affected by the degree of unsaturation. This is an advantage of the RI detection over UV detection in the quantitative analysis of phospholipids. Also, RI detection is more sensitive than UV detection for fully saturated phospholipids. PC can be detected at a concentration as low as $3 \cdot 10^{-5}$ *M*. Upon hydrolysis of natural phospholipids, lysophospholipids with a variety of saturated and unsaturated fatty acids are produced. The molar extinction coefficients of these lysophospholipids depends on their fatty acid composition. These lipids cannot be accurately quantified by UV detection. This study shows that within a phospholipid class, the molar response on the RI detector is not significantly affected by either the degree of saturation or the length of the fatty acyl chain; thus, a response factor can be determined once for all molecular species of a phospholipid class using a well defined (synthetic) model lipid as a reference standard. Such a reference standard was used for quantitative analysis of a phospholipid sample with a qualitatively known composition. We found highly purified DMPC, DMPG, MPC and MPG to be good external standards to quantitate PC, PG, LPC and LPG from liposome dispersions.

REFERENCES

1 U. K. Nassander, G. Storm, P. A. M. Peeters and D. J. A. Crommelin, in M.Chasin and R. Langer (Editors), *Biodegradable Polymers as Drug Delivery Systems*, Marcel Dekker, New York, 1990.
2 M. Grit, J. H. de Smidt, A. Struijke and D. J. A. Crommelin, *Int. J. Pharm.*, 50 (1989) 1.
3 W. W. Christie, *Lipid Analysis*, Pergamon Press, Oxford, 2nd ed. 1982.
4 F. C. Phillips, W. L. Erothal and O. S. Privett, *Lipids*, 17 (1982) 992.
5 W. W. Christie, *J. Lipid Res.*, 26 (1985) 507.
6 S. Shi-hua Chen and A. Y. Kou, *J. Chromatogr.*, 307 (1984) 261.

7 O. Hasaka, T. Hori, K. Sasahara, Y. Wakafayashi, F. Takahashi and H. Rhee, *J. Biochem.*, 95 (1984) 1671.
8 K. Aitzetmuller and D. Handt, *Fette Seifen Anstrichm.*, 8 (1984) 322.
9 J. G. Hamilton and K. Comai, *Lipids*, 23 (1988) 1150.
10 T. L. Kaduce, K. C. Norton and A. A. Spector, *J. Lipid Res.*, 24 (1983) 1398.
11 A. G. Andrews, *J. Chromatogr.*, 336 (1984) 139.
12 R. M. Sheely, W. J. Hurst, D. M. Sheely and R. A. Martin, *J. Liq. Chromatogr.*, 10 (1987) 3173.
13 K. Shimbo, *Agric. Biol. Chem.*, 50 (1986) 2643.
14 R. W. Gross and B. E. Sobel, *J. Chromatogr.*, 197 (1980) 79.
15 A. W. Nicholas, L. G. Klisuri, J. C. Ellington and N. A. Porter, *Lipids*, 18 (1983) 434.
16 M. H. Creer and R. W. Gross, *Lipids*, 20 (1985) 922.
17 S. J. Robins and G. M. Palton, *J. Lipid Res.*, 27 (1986) 131.
18 N. Sotirhos, C. Thörngren and B. Herslöf, *J. Chromatogr.*, 331 (1985) 313.
19 L. A. Smith, H. A. Norman, S. Ho Cho and G. A. Thompson, *J. Chromatogr.*, 346 (1985) 291.
20 M. L. Blank, M. Robinson, V. Fitzgerald and F. Snyder, *J. Chromatogr.*, 298 (1984) 473.
21 M. Kito, H. Takamura, H. Narita and R. Urade, *J. Biochem.*, 98 (1985) 327.
22 F. Szoka and D. Papahadjopoulos, *Annu. Rev. Biophys. Bioeng.*, 9 (1980) 467.
23 A. Plückthun and E. A. Dennis, *Biochemistry*, 21 (1982) 1743.
24 *Drylab I*, LC Resources, Lafayette, CA.
25 J. K. Lang, *J. Chromatogr.*, 507 (1990) 157.
26 M. Grit and D. J. A. Crommelin, *J. Pharm. Sci.*, submitted for publication.
27 C. R. Kensil and E. A. Dennis, *Biochemistry*, 20 (1981) 6079.

Journal of Chromatography, 585 (1991) 247–254
Elsevier Science Publishers B.V., Amsterdam

CHROM. 23 551

Identification of aromatic moieties and mycosamine in antifungal heptaenes with high-performance liquid chromatography, high-performance liquid chromatography–mass spectrometry and gas chromatography–mass spectrometry

Olavi Raatikainen*

Department of Pharmaceutical Chemistry and Department of Pharmacology and Toxicology, University of Kuopio, P.O. Box 1627, SF-70211 Kuopio (Finland)*

Seppo Auriola

Department of Pharmaceutical Chemistry, University of Kuopio, P.O. Box 1627, SF-70211 (Finland)

Jouko Tuomisto

National Public Health Institute, Department of Environmental Hygiene and Toxicology, Kuopio (Finland)

(First received April 3rd, 1991; revised manuscript received June 11th, 1991)

ABSTRACT

A high-performance liquid chromatographic (HPLC) method for the determination of the aromaticity of heptaene polyene antibiotics has been developed. The released aromatic moiety of the heptaene polyenes aureofungin, candicidin, candimycin, hamycin and trichomycin was assayed after alkaline hydrolysis. The presence of *p*-aminoacetophenone (PAAP) and N-methyl-*p*-aminoacetophenone (N-methyl-PAAP) in the hydrolysates was determined by HPLC, HPLC–mass spectrometry (HPLC–MS) and gas chromatography–MS (GC–MS). Candicidin and hamycin contained only the PAAP residue; aureofungin contained both PAAP and N-methyl-PAAP. Trichomycin contained PAAP and also some unknown component of molecular weight 179. The aromatic nature of the individual components of the heptaene complex was demonstrated using radioactivity flow detection for the determination of the incorporation of [^{14}C]-*p*-aminobenzoic acid to individual candicidin components. Ammonia chemical ionization MS was successfully used for the GC–MS identification of the acetylated mycosamine moiety of heptaenes.

INTRODUCTION

The antifungal heptaene antibiotics belong to the group of polyenes and are produced dominantly in various *Streptomyces* strains. The heptaenes are divided into two subgroups on the basis of their aromaticity: aromatic and non-aromatic heptaenes. Heptaenes and other polyenes usually contain mycosamine as a sugar moiety [1]. The complete structure has been identified for only a few individual heptaenes such as amphotericin B, candicidin D (levorin A) and partricins A and D [1]. Most heptaene complexes, such as aureofungin (Fig. 1), are only partially characterized based on their UV spectra and the presence and structure of their aromatic and sugar moieties.

Aromatic heptaenes usually contain the *p*-aminoacetophenone (PAAP) moiety but some hep-

0021-9673/91/$03.50

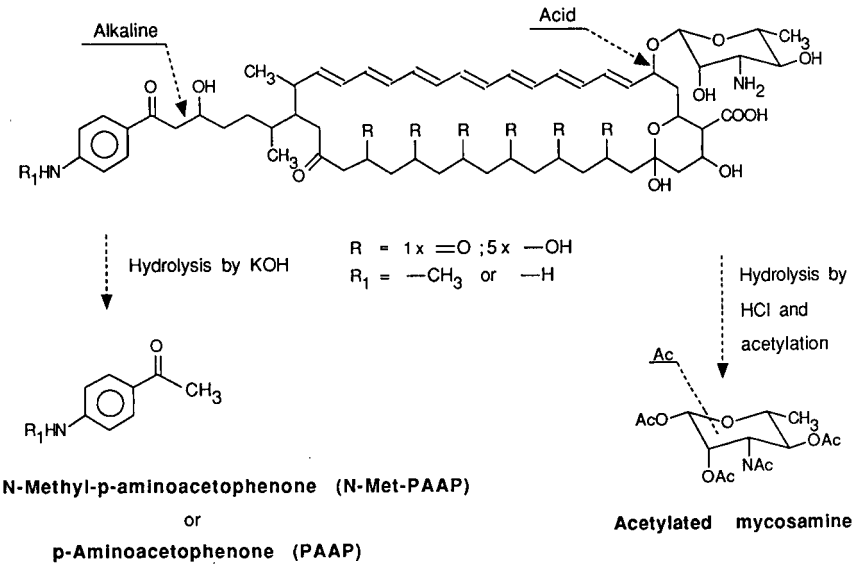

Fig. 1. Structures of the aromatic moieties (PAAP and N-methyl-PAAP) and acetylated sugar moiety mycosamin found in aureofungin. The structure of the aureofungin molecule is according to ref. 1.

taenes also contain N-methyl-*p*-aminoacetophenone (N-methyl-PAAP) moiety [1,2]. The aromatic moiety apparently originates from *p*-aminobenzoic acid (PABA), which has been postulated to be the starter unit for the biosynthesis of aromatic heptaenes [2]. Aromatic heptaenes are always produced as a complex of several individual heptaenic components [3,4]. The aromatic nature of heptaenes can be determined by hydrolysing the molecule with alkaline solution and identifying the released aromatic group by thin-layer chromatography (TLC) or gas chromatography–mass spectrometry (GC–MS) [5,6]. There are no previous data on the aromatic nature of the individual components in the heptaene complex. On the basis of the postulation that PABA is needed as a starter unit for the biosynthesis of the macrolide ring in candicidin [2] it is plausible, however, that all the components in candicidin and probably in other heptaene complexes are aromatic.

The aminosugar mycosamine (3-amino-3,6-dideoxy-D-mannose) is found in most glycosylated polyene macrolide antibiotics but its isomer perosamine (4-amino-4,6-dideoxy-D-mannose) has been found only in perimycin [1]. These aminosugars are attached to the macrolide ring with a β-glycosidic linkage which can be hydrolysed by treatment with acid [5,6]. The released mycosamine has been separated by TLC and identified using GC–MS [5,6]. The technique of ammonia chemical ionization within GC–MS has been successfully used for the determination of O-acetyl [7] and O-trimethylsilyl [8] derivatives of various carbohydrates, but not used for the determination of aminosugars of various polyenes.

In this work chromatographic methods for the determination of the aromaticity and mycosamine contents of some heptaenes were developed. The aromatic group in some heptaenes was determined by high-performance liquid chromatography (HPLC), HPLC–MS and GC–MS. The aromatic character of individual components of the candicidin complex was verified by determining the [^{14}C]PABA incorporation into the candicidin complex. The analysis of acetylated mycosamine was performed by GC–MS. The methods presented here are applicable to the characterization of new heptaenes. These methods are also useful for biosynthetic studies and for the development of analysis techniques for polyene residues in biological samples.

EXPERIMENTAL

Reagents

Heptaene antibiotics were supplied from several sources (Table I)) and they were dissolved in dimethylsulphoxide before use at a concentration of 1 mg/ml. For the [^{14}C]PABA incorporation experiments candicidin was synthesized in *Streptomyces griseus* (ATCC strain 11746).

Ammonium acetate (Merck, Darmstadt, Germany), PAAP (98%, Aldrich-Chemie, Steinheim, Germany), potassium hydroxide (Merck), methyl-α-D-mannoside (Sigma, St. Louis, MO, USA), radioactive [^{14}C]-*p*-aminobenzoic acid (2.04 GBq/mmol, Amersham, UK), acetonitrile (HPLC grade, Rathburn, Walkerburn, UK) and chloroform (Merck) were the main reagents and solvents. Water was purified using the Milli Q system (Millipore, Molsheim, France) and was sonicated before use. N-methyl-PAAP was synthesized from PAAP by methylation using methyliodide under basic conditions. Briefly, alkaline PAAP was shaken with chloroform containing methyl iodide. The synthesized *N*-methyl-PAAP was identified in the organic layer by GC–MS and used as a reference standard.

Assay of aromatic groups in heptaene

A small amount (1.5–8 mg) of heptaene and 300 μl of potassium hydroxide (10%, w/v) per milligram of polyene was boiled for 30 min in a water-bath (90 ± 5°C). After cooling the mixture was diluted about five fold with water, saturated with sodium chloride and extracted three times with about equal amounts of acetonitrile to achieve more than 99% recovery. As acetonitrile is miscible with water, sodium chloride was used to salt out the acetonitrile layer [9]. Before analysis the acetonitrile-containing phase was evaporated to dryness, redissolved in 200 μl of dichloromethane and filtered.

An aliquot (5–20 μl) of filtrates was analysed in an isocratic HPLC system (LC pump T 414, Kontron, Zürich, Switzerland) equipped with an UV detector (Uvicon 735 LC, Kontron) and an integrator (Enica 21, Delsi Instruments, Suresnes, France). The aromatic moieties were separated at ambient room temperature on a column (125 × 4 mm) filled with ODS Hypersil 5-μm reversed-phase (Bischoff Chromatography, Leonberg, Germany) using 0.05 *M* ammonium acetate buffer (pH 3.8)–acetonitrile (30:70, v/v) as the mobile phase. The flow-rate was 1.0 ml/min and the eluate was monitored at 314 nm. The determination of PAAP was calibrated by using PAAP instead of the antibiotic in the hydrolysis process.

A quadrupole VG Trio 2 mass spectrometer (VG Analytical, Manchester, UK) with the VG thermospray–plasmaspray probe was used to analyse the acetonitrile extracts of the hydrolysates. The samples (20 μl containing 2–10 μg of aromatic moieties) were pumped with a Kontron 420 dual-piston pump to the thermospray probe at a flow-rate of 1 ml/min using 0.10 *M* ammonium acetate buffer (pH 3.5)–acetonitrile (75:25) as the mobile phase and a 125 × 4 mm column filled with ODS Hypersil 5-μm phase (at ambient room temperature). The temperatures of the thermospray probe (210°C) and ion source (200°C) were adjusted so that a maximum solvent ion signal was achieved. The protonated

TABLE I

CLASSIFICATION OF HEPTAENES ANALYSED

Classification data are from ref. 1.

Heptaene	Aromatic moiety	Sugar moiety	Supplier
Amphotericin B	None	Mycosamine	Dumex, Copenhagen, Denmark
Aureofungin	PAAP	Mycosamine	Hindustan Antibiotics, Pimpri, India
Hamycin	PAAP	Mycosamine	Hindustan Antibiotics, Pimpri, India
Candicidin	PAAP	Mycosamine	Dumex, Copenhagen, Denmark
Thricomycin	PAAP	Mycosamine	Fujisawa Pharmaceutical, Osaka, Japan
Candimycin	None	No information	Takeda Chemical Industries, Osaka, Japan

molecular ions $(M+H)^+$ of PAAP (*m/z* 136) and N-methyl-PAAP (*m/z* 150) were monitored and their mass spectra recorded.

The presence of PAAP and N-methyl-PAAP in the acetonitrile extracts was also verified by GC–MS using electron ionization (EI). The mass fragmentation of PAAP and N-methyl-PAAP was performed with a JEOL JMS-D 300 (Jeol, Tokyo, Japan) mass spectrometer equipped with a JMA 2000 mass data analysis system. The samples were separated on a Hewlett-Packard gas chromatograph fitted with a 25 m × 0.2 mm I.D. fused-silica capillary column (0.1-μm NB-1 phase, HNU-Nordion, Helsinki, Finland). The EI fragmentation at 70 eV was investigated for all components possessing the fragment ions at *m/z* 135 (PAAP) or at *m/z* 149 (N-methyl-PAAP) and for other possible prominent ions which were found with HPLC–MS system.

Biosynthesis and HPLC of ^{14}C-labelled candicidin

The original candicidin-producing strain, *Streptomyces griseus* ATCC 11746, was grown on yeast–malt–glucose (YMG; 1, 2.5 and 1 g/l, respectively) agar (1%, w/v) plates. The primary culture was shaken in liquid YMG medium for 15–18 h. Studies of the [^{14}C]PABA incorporation in candicidin were made in YMG medium containing 750 000 dpm/ml [14C]PABA in labelling experiments. The medium (2 ml) was inoculated with 100–150 mg (wet weight) of primary culture shaken in glass tubes at a rate of 250 rev/min rpm at 28°C for 50 h. The cells were centrifuged at 1000 *g* and extracted with acetonitrile–water (300 μl per 100 mg wet cell mass).

The components of candicidin complex were separated with the same HPLC system as used for the aromatic groups and a 0.05 *M* ammonium acetate buffer (pH 3.8)–acetonitrile solution (38:62) was used as the mobile phase at a flow-rate of 1 ml/min (ambient room temperature). The components were monitored by UV absorption at 380 nm. A radioactivity flow detector (Radiomatic FlowOne/β CR, Radiomatic Instruments, Tampa, FL, USA) was used for ^{14}C-activity monitoring. Homogeneous detection in 2.5-ml flow cell was performed by mixing the 1 ml/min eluate with a 4 ml/min scintillant (Ecoscint, National Diagnostics, Manville, NJ, USA). Counts (print-out of average counts every 6 s) between energies of 5 and 100 keV were accepted and the integrated background was subtracted manually. The counting was about 68% effective, as determined by the injection of different amounts of pure [^{14}C]PABA into the counting cell.

Assay of mycosamine residue in heptaenes

To achieve the release of aminosugar from the polyene molecule, small amounts (10 mg) of candicidin or amphotericin B were incubated in 2 *M* hydrochloric acid at room temperature for 2 h [5]. Hydrolysis was confirmed with TLC on silica gel TLC plates (Kieselgel 60 F254, Merck) using a chloroform–methanol (1:1) solvent system. The sugars were identified by spraying the plates with a 1:1 mixture of 1% (v/v) ninhydrin and 3% iodoplatinate solution. The carbohydrates in the hydrolysates were acetylated after reduction [10] and the acetylated aminosugar (Fig. 1) was identified by ammonia chemical ionization MS after separation by GC in an OV-1 capillary column.

RESULTS

Aromatic groups

The chromatogram of aureofungin hydrolysate shows the separation of PAAP and N-methyl-PAAP (Fig. 2) on ODS Hypersil with UV detection at 315 nm. The recovery of the PAAP moiety in the extraction was more than 99% after three repeated extractions. Owing to the lack of aromatic groups, amphotericin B was assayed as a non-aromatic heptaene control. No interfering substances were seen in the hydrolysate of amphotericin B monitored at 315 nm.

The HPLC–MS profile of the hydrolysate of au-

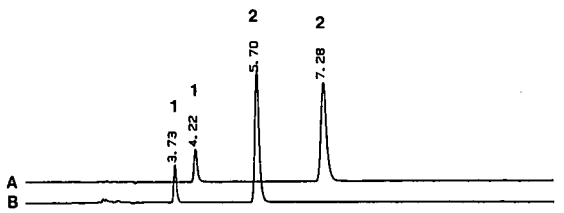

Fig. 2. HPLC separation of the aromatic components (about 4 μg total) (1) PAAP and (2) N-methyl-PAAP on ODS Hypersil C_{18} phase with acetonitrile–0.05 *M* ammonium acetate, pH 3.8. UV detection at 314 nm. The components were released from aureofungin by alkaline hydrolysis. The percentage of acetonitrile in mobile phase was (A) 25% or (B) 30%.

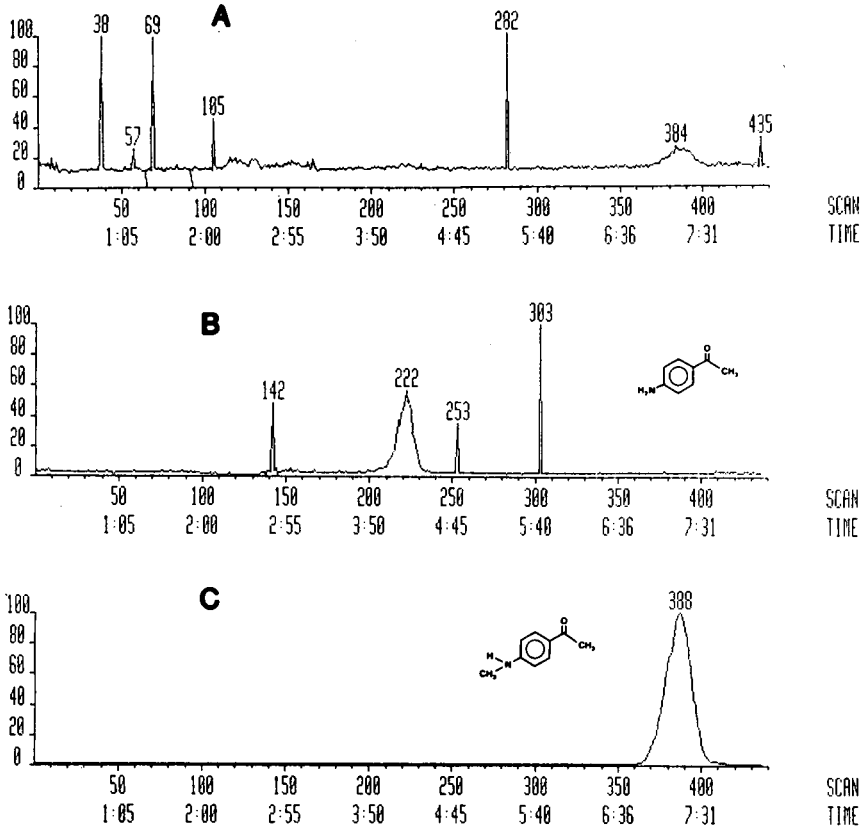

Fig. 3. HPLC–MS total ion current chromatogram (A), and HPLC–MS selected ion current profiles of *m/z* 136 (B) and *m/z* 150 (C) of aureofungin hydrolysate. The sharp peaks are due to the lack of background subtraction.

reofungin shows the separation of the peaks which were seen with HPLC at 315 nm (Fig. 3). Notice the noise peaks, which lowered the relative intensity of PAAP and N-methyl-PAAP (Figs. 3A and B). The peak had *m/z* value (M + 1) 136 for PAAP in aureofungin (Fig. 4A). Candicidin, hamycin and trichomycin also contained the PAAP signal (chromatograms not shown). In aureofungin the main peak was *m/z* 150 (Fig. 4B), indicating the presence of the N-methyl-PAAP moiety which was identified from the fragmentation data (Fig. 4B, inset). In trichomycin there was one minor peak in HPLC with an *m/z* value of 180 in the HPLC–MS system (data not shown). No fragmentation of PAAP and N-methyl-PAAP occurred in the HPLC–MS analysis but several ions originating from the solvent were found (Fig. 4A and B).

The peaks separated by HPLC were also verified by GC–MS. The most prominent ions of PAAP were the fragments *m/z* 92 and 120 (base peak), accompanied by the molecular ion *m/z* 135 (Fig. 4A, inset). The respective ions of N-methyl-PAAP were *m/z* 106, *m/z* 134 (base peak) and molecular ion *m/z* 149 (Fig. 4B, inset). The fragmentation of the ions *m/z* 135 and *m/z* 149 were similar to the PAAP and N-methyl-PAAP standards (spectra not shown).

According to the HPLC profiles, candicidin and hamycin contain only PAAP. Aureofungin and candimycin were identical, each containing about 30% PAAP and 70% N-methyl-PAAP. The trichomycin sample contained about 85% PAAP and 15% of some unknown component of molecular weight 179 which absorbed at 314 nm. The structure of this compound was not identified on the mass spectrum. The relative amounts of the peaks were calculated from the integrated areas.

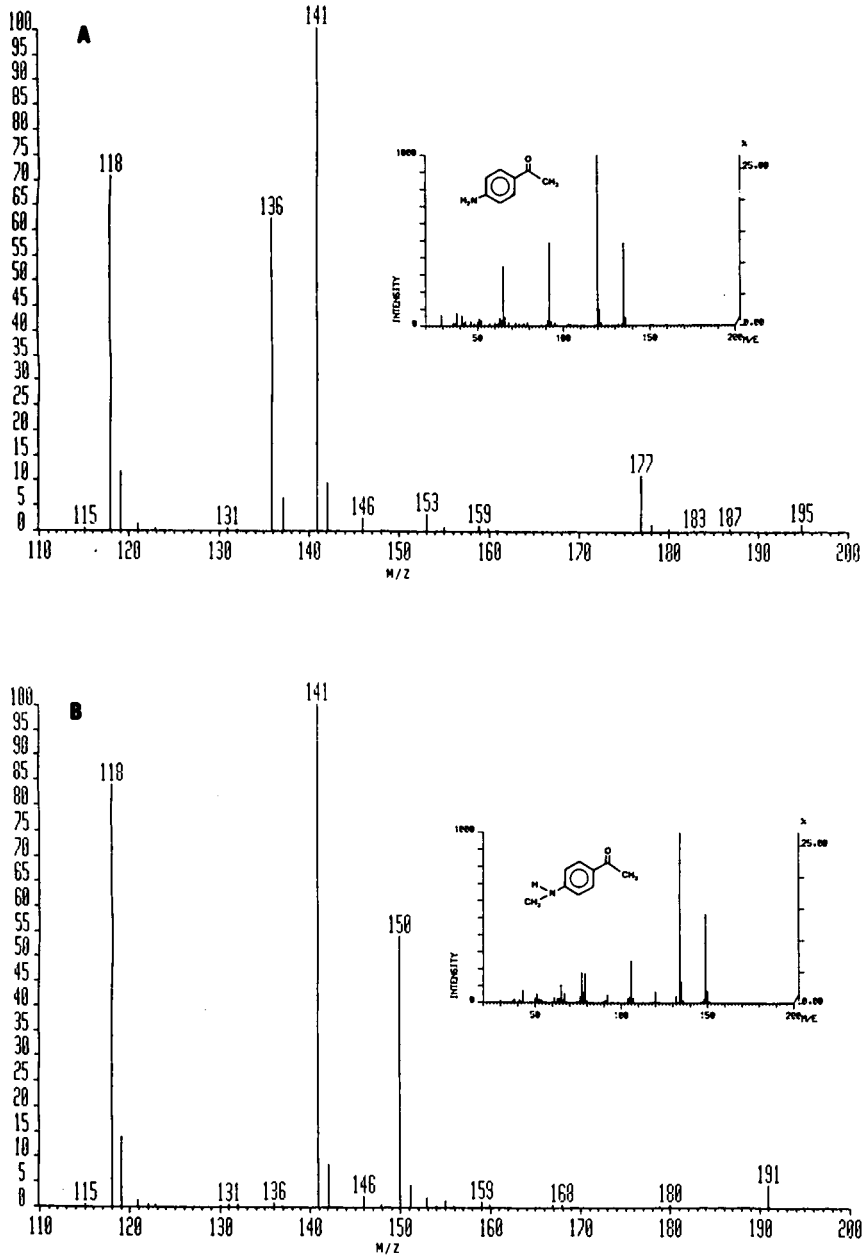

Fig. 4. Mass spectrum of PAAP (A; *m/z* 136) and N-methyl-PAAP (B; *m/z* 150) after HPLC separation. Ions 118, 141 and 177 originated from the eluent. The EI fragmentation spectrum (inset) of the aromatic components of aureofungin indicating the presence of PAAP (A) and N-methyl-PAAP (B) are shown also.

[^{14}C]PABA incorporation

The UV chromatogram of candicidin shows that synthesized heptaene includes three to four main and several other minor components (Fig. 5A). The presence of seven double bonds of the heptaene chromophore was investigated from the UV spectrum of the complex. Absorption maxima found at about 360, 380 and 404 nm are typical for heptaene

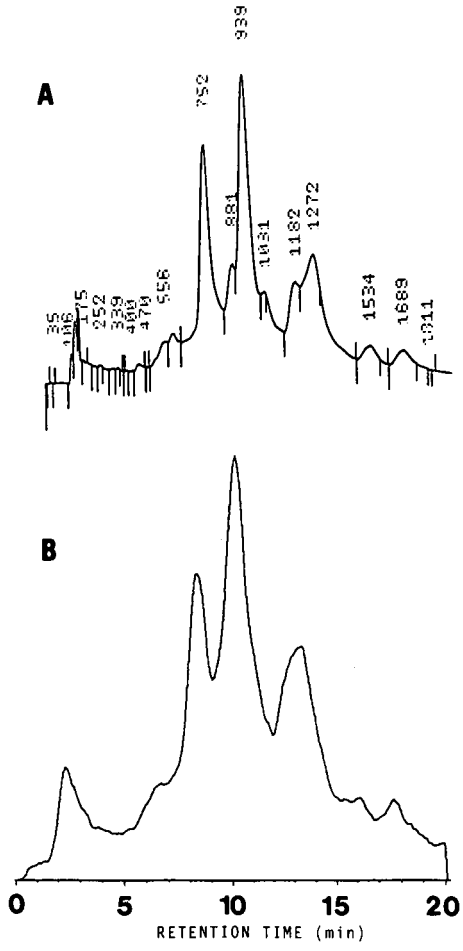

Fig. 5. HPLC separation of candicidin produced in *Streptomyces griseus* ATCC 11746. The UV-absorbance at 314 nm (A) or ^{14}C radioactivity (B) of candicidin was monitored.

polyenes [1]. The ^{14}C chromatogram shows the ^{14}C radioactivity of the candicidin complex (Fig. 5B). The first minor peak before the candicidin peaks probably comes from unused [^{14}C]PABA and may also include small amounts of labelled phenylalanine, tryptophan and tyrosine, which are known by products and suppressors of candicidin biosynthesis [2]. A comparison of the chromatograms presenting UV absorption and ^{14}C activity shows that the individual candicidin components are labelled, suggesting the incorporation of [^{14}C]PABA into the molecule. About 40% of the total activity added was incorporated into candicidin.

Mycosamine

The separation of the acetylated derivatives of mycosamine and α-methylmannoside was good using these GC conditions used (Fig. 6A). The retention time of the acetylated saccharide from the hydrolysate of candicidin (Fig. 6) was identical to the acetylated derivative of mycosamine found in the amphotericin B hydrolysate. The fragmentation was also similar in both candicidin and amphotericin. The ammonia chemical ionization mass spectrum of the acetylated mycosamine of candicidin exhibits strong proton-capture ($[M+H]^+$, m/z 376) and ammonium adduct ($[M+NH_4{}^+]^+$, m/z 393) ions (Fig. 6B). With these ions the molecular weight of the acetylated derivatives of the saccharide from polyene hydrolysates can be easily determined. The spectrum also exhibits a strong $[M+H]^+$–acetic acid ion (m/z 316). This ion was the base peak in the

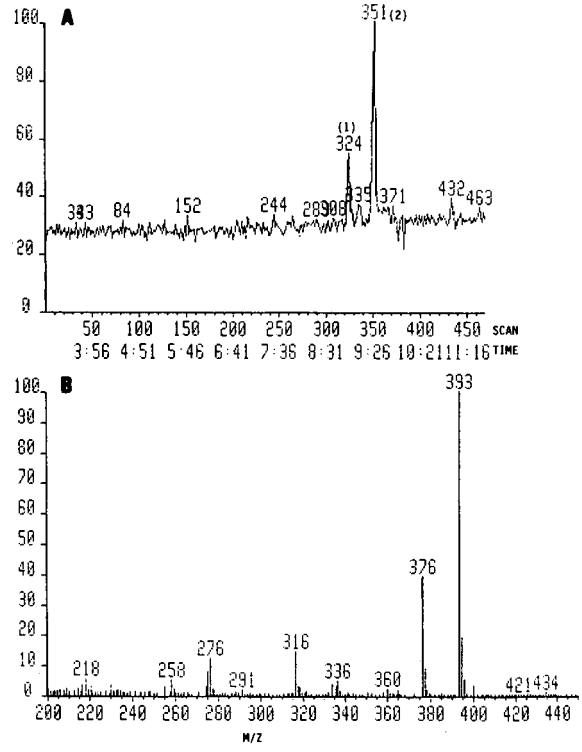

Fig. 6. Separation of internal standard α-methylmannoside (1) and mycosamine (2) with GC–MS using ammonia chemical ionization (A): total ion chromatogram of the acetyl derivatives from the hydrolysate of candicidin (A) and fragmentation of mycosamine from candicidin (B).

methane chemical ionization spectrum, whereas the molecular ion M + H and adduct ion $[M + C_2H_5]^+$ (*m/z* 404) were of much lower abundance. Ammonia was used for the ionization because of the total fragmentation of the molecular ion with methane ionization. The ammonia chemical ionization mass spectra of the internal standard α-methylmannoside derivative showed abundant $[M + H]^+$ ions with less fragmentation (data not shown).

DISCUSSION

The results indicate that this sample of aureofungin contained PAAP and N-methyl-PAAP (Fig. 1). It has been reported that aureofungin contains N-methyl-PAAP, but the PAAP moiety has not been mentioned [1]. Candicidin and hamycin contained only the PAAP residue, and candimycin contained PAAP and N-methyl-PAAP. The trichomycin extract contained PAAP and some unknown component of molecular weight 179 which was not characterized. [^{14}C]PABA incorporated into all the heptaene components found in the candicidin complex (Fig. 5.) and the percentage of incorporation was the same as described previously [2]. These results support the notion that all of the candicidin components contain an aromatic group, and generally all the individual components in aromatic heptaene complexes probably contain aromatic groups. This is in accordance with previous data that *p*-aminobenzoic acid (released as PAAP when hydrolysed with alkaline) is needed as the starter unit for the biosynthesis of the aglycone of aromatic heptaenes [2].

The methyl group in N-methyl-PAAP may originate from L-methionine as has been proposed previously for the biosynthesis of fungimycin [11]. Thus it is possible that the presence of both PAAP and N-methyl-PAAP in aureofungin could be due to limited methylation of PAAP during the biosynthesis of the antibiotic.

The identification of PAAP was confirmed by comparing the UV-spectra of the eluted peak and PAAP standard (data not shown). The UV spectra of the HPLC effluent at the PAAP peak seemed to be identical with the standard, supporting the similarity of the eluate and PAAP. Chlorination of PAAP occurred during extraction if chloroform was used (data not shown); this chlorination was not seen in the UV spectrum. To avoid false results from unwanted chlorinated aromatic groups, acetonitrile was used for the extraction of the released aromatic groups instead of chloroform.

The results of the mycosamine analysis show that the acetylation of mycosamine and subsequent GC–MS analysis with ammonia chemical ionization is the method of choice for the assay of the sugar moieties of all kind of polyene antibiotics.

Only a few milligrams of a heptaene were needed for the determination of the aromatic moiety and mycosamine. These methods are very convenient for the characterization and classification of new polyene antibiotics. The incorporation of radioactivity into the individual polyene components can be determined after HPLC separation with a radioactive flow detector and may be useful in studies of polyene biosynthesis.

ACKNOWLEDGEMENTS

We thank Dr. J. Gynther Ph.D. for the synthesis of N-methyl-*p*-aminoacetophenone and Dr. M. Tammi, M-D., for acetylation of the sugars. The skillful technical assistance of Mr. J. Knuutinen and Mrs. A. Kinnunen is acknowledged.

REFERENCES

1 S. Ōmura and H. Tanaka, in S. Ōmura (Editor), *Macrolide Antibiotics, Chemistry, Biology, and Practice,* Academic Press, New York and London, 1984, p. 351.
2 J. F. Martin, in S. Ōmura (Editor), *Macrolide Antibiotics, Chemistry, Biology, and Practice*, Academic Press, New York and London, 1984, p. 405.
3 A. Thomas and P. Newland, *J. Chromatogr.*, 354 (1986) 317.
4 A. H. Thomas, *Analyst (London)*, 101 (1976) 321.
5 C. M. Liu, L. E. McDaniel and C. P. Schaffner, *J. Antibiot.*, 25 (1972) 116.
6 R. C. Tweit, R. C. Pandey and K. L. Rinehart, Jr., *J. Antibiot.*, 35 (1982) 97.
7 D. Horton and J. Wander, *Carbohydr. Res.*, 36 (1974) 75.
8 T. Murata and S. Takahashi, *Carbohydr. Res.*, 62 (1978) 1.
9 U. Nousiainen and O. Raatikainen, *J. Chromatogr.*, 308 (1984) 376.
10 A.-M. Säämänen and M. Tammi, *Glycoconjugate J.*, 5 (1988) 235.
11 C. M. Liu, L. E. McDaniel and C. P. Schaffner, *J.Antibiot.*, 25 (1972) 187.

Journal of Chromatography, 585 (1991) 255–258
Elsevier Science Publishers B.V., Amsterdam

CHROM. 23 559

Determination of sennoside A and B in the pharmaceutical preparation Otsuji-to using ion-pair high-performance liquid chromatography with column switching

Toshiyuki Oshima, Fusayoshi Hirayama*, Mitsuhiro Masuda, Tadao Maruta, Kazuhiko Sagara and Taku Mizutani

Research Center, Taisho Pharmaceutical, 1-403, Yoshino-cho, Ohmiya-shi, Saitama 330 (Japan)

Li-Yi He, Yu-Yi Tong and Yu-Heng Chen

Institute of Materia Medica, Chinese Academy of Medical Sciences, 1 Xian Nong Tan Street, Beijing (China)

Hideji Itokawa

Tokyo College of Pharmacy, 1432-1, Horinouchi, Hachioji-shi, Tokyo 192-03 (Japan)

(First received February 27th, 1991; revised manuscript received June 7th, 1991)

ABSTRACT

Ion-pair high-performance liquid chromatography with column switching was used to determine sennoside A and B in the oriental pharmaceutical preparation Otsuji-to. The fraction containing sennoside A and B eluted immediately from the pretreatment column and was transferred to the analysis column where it was separated by the ion-pair mobile phase. Sennoside A and B in Otsuji-to were determined with recoveries of 100%.

INTRODUCTION

The oriental pharmaceutical preparation Otsuji-to [1], which is used for the treatment of haemorrhoids, is prepared from six crude drugs: *Angelicae radix* (Japanese angelica root), *Bupleuri radix* (bupleurum root), *Scutellariae radix* (scutellaria root), *Glycyrrhizae radix* (glycyrrhiza), *Cimicifugae rhizoma* (cimicifuga rhizome) and *Rhei rhizoma* (rhubarb) [2]. The sennosides in *Rhei rhizoma* are well known as laxatives and the main components are sennoside A and B (Fig. 1).

In work using high-performance liquid chromatography (HPLC) for the determination of natural

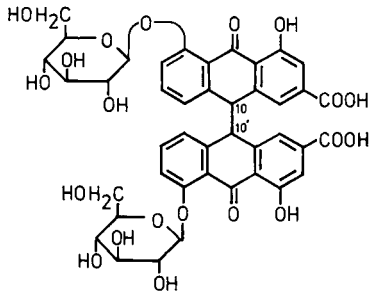

Fig. 1. Structures of sennoside A and B. Sennoside A, 10–10′ = *threo*: sennoside B, 10–10′ = *erythro*.

0021-9673/91/$03.50

products in crude drugs, sennoside A and B were determined in *Rhei rhizoma* by an ion-pair technique using tetra-*n*-heptylammonium bromide as the counter ion [3]. However, this method was not applicable to the determination of sennoside A and B in Otsuji-to because of the low concentration of *Rhei rhizoma* and interferences from the other drugs present.

However, the combination of ion-pair HPLC and column switching allowed the determination of tropane alkaloids in complex preparations without complicated pretreatment [4].

In this work, ion-pair HPLC and column switching were used for the determination of sennoside A and B in Otsuji-to.

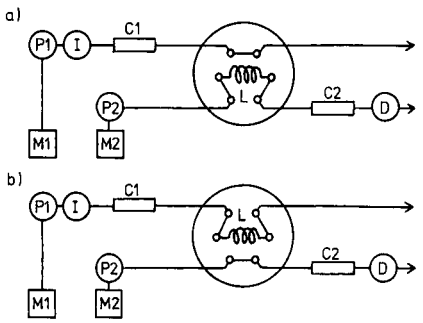

Fig. 2. Column switching system. (a) Waiting and analysis mode; (b) trapping mode. P1, P2 = pumps; C1 = pretreatment column; C2 = analysis column; D = detector; L = loop; M1 = primary mobile phase; M2 = secondary mobile phase; I = injector.

EXPERIMENTAL

Reagents

Sennoside A was purchased from Wako Pure Chemical (Osaka, Japan), sennoside B from Alps Pharmaceutical (Gifu, Japan) and tetra-*n*-heptylammonium bromide from Aldrich (Milwaukee, WI, USA). Acetonitrile of chromatographic grade was used; deionized water was further purified using a Millipore filter.

Apparatus

The Shimadzu LC-6AD system consisted of: a SIC chromatocoder 12 computing integrater; two Shimadzu LC-6AD pumps; a Shimadzu SCL-6B system controller; a Shimadzu SIL-6B autoinjector; a Shimadzu CTO-6A column oven; a sample loop switching valve; Rheodyne 7027 Shimadzu FCV-2AH; and a Shimadzu SPD-6A UV detector. The pretreatment (50 × 4 mm I.D.) and analysis (250 × 4 mm I.D.) columns were packed with chemically bonded ODS silica gel (TSKgel ODS-120A, 5 μm, Tosoh, Tokyo, Japan) by slurry-packing. The loop volume was 1 ml. This switching system is shown in Fig. 2.

HPLC conditions

A mixture of water, acetonitrile and acetic acid (680:320:1) was used as the primary mobile phase for the pretreatment column, and a mixture of pH 5.0 acetate buffer (0.1 *M*) and acetonitrile (680:320) containing 15 m*M* tetra-*n*-heptylammonium bromide was used as the secondary mobile phase for the analysis column. The column temperature were maintained at 50°C and the flow-rates of the mobile phases were 1.0 ml/min. The eluted substances were detected by UV absorption at 340 nm.

Sample preparation

Otsuji-to was prepared in this laboratory from a mixture of six crude drugs: *Angelicae radix* (5 g), *Bupleuri radix* (4 g), *Scutellariae radix* (3 g), *Glycyrrhizae radix* (3 g), *Cimicifugae rhizoma* (1.5 g) and *Rhei rhizoma* (1 g). About 340 ml of water were added to the mixture and reduced by boiling to about 170 ml. The supernatant is Otsuji-to. A blank was prepared in the same manner but without *Rhei rhizoma.*

Assay procedure

A 10-μl portion of the sample solution filtered through a membrane filter (0.45 μm) was injected into the pretreatment column of the HPLC system. The eluate fraction from 0.35 to 0.85 min was trapped in the loop and transferred to the analysis column. The sennoside A and B concentrations were calculated from the relevant peak areas.

Calibration graphs and detection limits

The calibration graphs for sennoside A and B using column switching were obtained for the concentration ranges 5.36–53.60 and 2.35–23.45 μg/ml, respectively. The corresponding regression equations were: $y = 6000x - 1200$ ($r = 0.999$) and $y = 5564x + 1531$ ($r = 0.999$).

The detection limits for sennoside A and B were 1.2 and 1.0 ng, respectively, at a signal-to-noise ratio of 3 for the peak height.

RESULTS AND DISCUSSION

Ion-pair HPLC methods have been applied to the determination of several natural ionic products in crude drugs [5–9]. Ion-pair HPLC has several advantages for such determinations, including the fact that the counter ion only affects the ionic compounds and it is possible to control the retention time by changing the counter ion and its concentration. The pH of the mobile phase also influences the peak retention time.

A simple and rapid ion-pair HPLC method [3] was developed for the determination of sennoside A and B in *Rhei rhizoma*. This method is applicable to some simple oriental pharmaceutical preparations. However, this method is not applicable to the determination of these compounds in the complex oriental pharmaceutical preparation Otsuji-to, because the concentration of *Rhei rhizoma* is low and there are interferences from other components, mainly *Scutellariae radix*. *Scutellariae radix* contains a large amount of acidic components, including baicalin and other flavone glucuronides. Sennoside A is not separated from these compounds (Fig. 3). Several HPLC methods have been studied to determine sennoside A and B in *Rhei rhizoma* [10–14]; however, except for this method, none has been reported for the determination of sennoside A and B in Otsuji-to. Column switching has frequently been used for on-line sample clean-up, the analysis of complex preparations and the determination of trace amounts of biological materials [15]. This technique is applicable to the determination of natural products in crude drugs or pharmaceutical preparations.

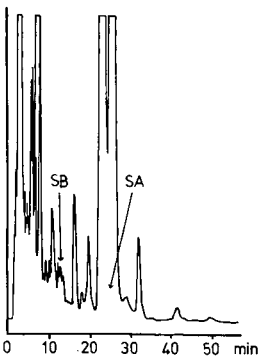

Fig. 3. Chromatogram of Otsuji-to by direct analysis. Mobile phase, pH 5.0 acetate buffer (0.1 *M*)–acetonitrile (680:320) containing 5 m*M* tetra-*n*-heptylammonium bromide; column, TSKgel ODS-120A, 5 μm, 250 × 4 mm I.D. Peaks: SA = sennoside A; SB = sennoside B.

Combinations of these two techniques have allowed the on-line determination of tropane alkaloids in complex preparations without complicated pretreatment [4]. The tropane alkaloid fraction immediately eluted with the primary mobile phase, without the counter ion, from a pretreatment column and was then transferred to an analysis column and separated by the ion-pair mobile phase. This strategy was applied to the determination of sennoside A and B, which are acidic compounds, in Otsuji-to.

HPLC conditions

At first, a mixture of pH 5.0 acetate buffer (0.1 *M*) and acetonitrile (680:320) was used as the primary mobile phase for the 50 mm long pretreatment column, and the primary mobile phase containing 5 m*M* tetra-*n*-heptylammonium bromide was used as the secondary mobile phase for the 250 mm long analysis column. Under these conditions, in the standard solution, the sennoside A and B fraction immediately eluted with the primary mobile phase and was transferred to the analysis column where it was separated by the ion-pair mobile phase. However, in the sample solution, a large amount of acidic compounds, especially baicalin and other flavone glucuronides from *Scutellariae radix*, showed a similar behaviour to that of sennoside A and B in the pretreatment column and the sennosides could not be separated from these compounds.

Ion suppression was tried for the pretreatment column. A water–acetonitrile–phosphoric acid system and a water–acetonitrile–acetic acid system were tested for use as the primary mobile phase. When water–acetonitrile–acetic acid (680:320:1) was used, sennoside A and B were eluted immediately and most of the other acidic compounds were suppressed and retained in the pretreatment column.

Under the original analysis conditions, the sennoside A and B peaks were slightly broader and sennoside B was not clearly separated from the other components after column switching with the initial

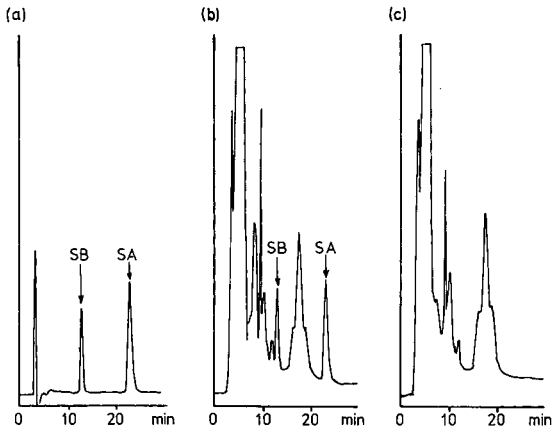

Fig. 4. Chromatograms of (a) standards, (b) Otsuji-to and (c) the blank preparation by column switching. Peaks: SA = sennoside A; SB sennoside B.

primary mobile phase. The concentration of the counter ion for the secondary mobile phase was varied to find the optimum conditions. The final concentration for the secondary mobile phase was selected as 15 m*M*.

When the fraction eluted from 0.35 to 0.85 min after injection into the pretreatment column was transferred to the analysis column, the recoveries of the sennoside A and B standards from the pretreatment column were 100.1% [$n = 5$, coefficient of variation (C.V.) = 1.1%] and 100.3% ($n = 5$, C.V. = 1.1%), respectively.

Analysis of Otsuji-to

Fig. 4 shows the chromatograms of standards, Otsuji-to and the blank preparation. The blank preparation which had no *Rhei rhizoma* present, was prepared to check the interferences at the positions of sennoside A and B on the chromatogram. Most interferences from the other crude drugs were removed by this column switching technique, and no peak appeared at the sennoside A and B positions. The concentrations of sennoside A and B in Otsuji-to prepared in this work were 20.83 μg/ml ($n = 5$, C.V. = 1.2%) and 8.36 μg/ml ($n = 5$, C.V. = 1.1%), respectively. The recoveries of sennoside A and B added to the blank preparation were 99.8% ($n = 5$, C.V. = 1.0%) and 99.5% ($n = 5$, C.V. = 1.0%), respectively.

CONCLUSIONS

The determination of sennoside A and B in Otsuji-to was achieved by a combination of ion-pair HPLC and the column switching technique without complicated pretreatment. This system seems to be applicable to the on-line determination of other ionic components in complex preparations.

REFERENCES

1 Ministry of Health and Welfare, Japan, *Ippanyokampo-shohonotebiki*, Yakugyojiho, Tokyo, 1986, p. 30.
2 Jiangsu New Medical College, *Zhong Yao Da Ci Dian (Dictionary of Chinese Materia Medica)*, Shanghai Scientific and Technological Publisher, Shanghai, 1977, p. 102.
3 K. Sagara, T. Oshima and T. Yoshida, *J. Chromatogr.*, 403 (1987) 253.
4 T. Oshima, K. Sagara, F. Hirayama, T. Mizutani, L. Y. He, Y. Y. Tong, Y. H. Chen and H. Itokawa, *J. Chromatogr.*, 547 (1991) 175.
5 T. Misaki, K. Sagara, M. Ojima, S. Kakizawa, T. Oshima and H. Yoshizawa, *Chem. Pharm. Bull.*, 30 (1982) 354.
6 K. Sagara, T. Oshima and T. Misaki, *Chem. Pharm. Bull.*, 31 (1983) 2359.
7 K. Sagara, Y. Ito, T. Oshima and T. Misaki, *Chem. Pharm. Bull.*, 33 (1985) 5364.
8 K. Sagara, Y. Ito, T. Oshima, T. Misaki, H. Murayama and H. Itokawa, *J. Chromatogr.*, 328 (1985) 289.
9 T. Oshima, K. Sagara, Y. Y. Tong, G. D. Zhang and Y. H. Chen, *Chem. Pharm. Bull.*, 37 (1989) 2456.
10 Y. Ohshima and K. Takahashi, *J. Chromatogr.*, 258 (1983) 292.
11 T. Imao, M. Ohmiya, K. Morisaki, A. Yoshida and N. Hayashi, *11th Shoyakubunsekitoronkai, Kobe, August 1982*, Abstracts of Papers, p. 34.
12 T. Seto, Y. Iwasaki, I. Yasuda, T. Hamano and K. Akiyama, *11th Shoyakubunsekitoronkai, Kobe, August 1982*, Abstracts of Papers, p. 37.
13 H. Oshio and N. Nakamura, *Shoyakugaku Zasshi*, 39 (1985) 131.
14 Y. Ohshima, Y. Ohno, K. Kajiyama and K. Takahashi, *J. Chromatogr.*, 360 (1986) 303.
15 K. A. Ramsteiner, *J. Chromatogr.*, 456 (1988) 3.

Journal of Chromatography, 585 (1991) 259–266
Elsevier Science Publishers B.V., Amsterdam

CHROM. 23 522

Determination of chlorophylls and carotenoids by high-performance liquid chromatography during olive lactic fermentation

M. Isabel Mínguez-Mosquera*, Beatriz Gandul-Rojas, Alfredo Montaño-Asquerino and Juan Garrido-Fernández

Unidad Estructural de Biotecnología de Alimentos, Instituto de la Grasa y sus Derivados (CSIC), Avenida Padre García Tejero 4, 41012 Seville (Spain)

(First received August 3rd, 1990; revised manuscript received May 14th, 1991)

ABSTRACT

Eighteen pigments, including chlorophylls, carotenoids and their degradation products, were separated by reversed-phase ion-pair high-performance liquid chromatography during the lactic fermentation and later preservation phase of green table olives. The method consists of an elution gradient using two solvents: water–ion-pair reagent–methanol (1:1:8, v/v/v) and methanol–acetone (1:1, v/v). Absorbance detection of all the pigments is carried out spectrophotometrically at 430 nm. Pigment concentrations are calculated from an extension of Beer's law. This procedure is compared with the external standard method. The analysis of variance showed no significant differences between the results given by the two methods.

INTRODUCTION

The use of olive fruit as table olives dates back to the first century A.D. or earlier [1]. In 1930 Cruess was the first to do some research in their elaboration [2] and his work was continued by Vaughn (1943) [1]. In 1947, De la Borbolla *et al.* [2] began research into the fermentation of green olives, succeeding in 1956 in converting the olive elaboration into a truly technological process, subject to physico-chemical and microbiological control standards.

The traditional process of preparation for this type of olives involves treatment with 2% sodium hydroxide solution for 6 h, washing with water for 8 h, and subsequent conditioning of the fruit in brine (10% sodium chloride solution). The sugars, vitamins and amino acids of the fruit pass to the brine by osmotic process, converting it gradually into a suitable medium for microorganism growth, where the fruits undergo a total lactic fermentation. The complete process of fermentation and curing lasts *ca.* 6–7 months, at the end of which period the fruit should have certain organoleptic characteristics [1]. Recent innovations in the traditional process of elaboration of green table olives, to minimize the volume of waste water, have affected the physico-chemical and organoleptic characteristics of the finished product, although this has still not been fully studied [3]. One of the more seriously affected characteristics is that of the colour of the fruit. As colour is an important attribute of quality, special attention has been given for some years to research into the components responsible by means of the qualitative and quantitative evaluation of chlorophylls and carotenoids during the traditional fermentation process of the olive, with the aim of establishing which variables take part in pigment transformation, and attempting to direct their action without giving up the necessary modifications of the process.

Analysis of pigments in olives has proved more

0021-9673/91/$03.50

TABLE I

CHROMATOGRAPHIC AND SPECTROSCOPIC CHARACTERISTICS OF STANDARDS

The pigments were purified by TLC on silica gel 60 GF_{254} using the following eluents: A = ligh petroleum (b.p. 40–60°C); B = dichloromethane–ethyl acetate (4:1) [28]; C = benzene–ethanol (22:1) [25]; D = benzene–acetone (4:1) [28]; E = light petroleum (b.p. 65–95°C)–acetone–diethylamine (10:4:1) [6]; F = light petroleum (65–95°C)–acetone–pyridine (10:4:2.5) [22]; G = hexane–pyridine–diethylamine (10:1:0.5). Peak ratio is % III/II for carotenoids [27] and Soret band absorbance divided by the maximum absorbance in the red region for chlorophylls and derivatives [8].

Pigment	Purification by TLC		Spectral data								IR		Epoxide test (HCl treatment)	
	Eluent	R_F values	Light petroleum				Chloroform				OH	C=O	Colour on TLC	Hypsochromic shift (C_2H_5OH) (nm)
			Maxima (nm)			Peak ratio	Maxima (nm)			Peak ratio				
			I	II	III		I	II	III					
Carotenoids														
β-Carotene	A	0.24	(426)	444	470	30	(434)	458	482	7	–	–	Yellow	0
Phytofluene	A	0.12	330	348	367	81					–	–	Yellow	0
ζ-Carotene	A	0.01	378	400	422	80	384	405	430		–	–	Yellow	0
Lutein	B	0.35	418	442	470	79	430	452	482	71	+	–	Brown and green	0
Lutein isomer	B	0.32	416	438	466	58		452	480		+	–	Brown and green	0
Mutatoxanthin	B	0.25	(402)	424	448	31	410	434	460	10	+	–	Blue green	0
Auroxanthin	B	0.12	(378)	400	424	109	388	410	436	103	+	–	Blue	0
Luteoxanthin	C	0.05	402	426	448	107	404	428	456	101	+	–	Blue	20
Violaxanthin	D	0.31	414	436	466	96	422	446	476	93	+	–	Blue	40
Neochrome	D	0.18	399	418	446	76	402	426	454	65	+	–	Blue green	0
Neoxanthin	D	0.13	412	436	466	86	420	444	474	82	+	–	Blue green	14
			Acetone										Colour on TLC (white light)	
			Maxima (nm)			Peak ratio								
			I	II	III									
Chlorophylls and derivatives														
Chlorophyll *a*	E	0.51	428	616	662	1.4							Blue-green	
Chlorophyll *b*	E	0.44	454	596	644	3.0							Yellow-green	
Pheophytin *a*	E	0.57	410	468	668	2.4							Grey	
Pheophytin *b*	E	0.53	432	522	656	5.1							Brown	
Chlorophyllide *a*	E	0.00	428	616	652	1.5							Blue-green	
Chlorophyllide *b*	E	0.00	454	596	644	3.1							Yellow-green	
Pheophorbide *a*	F	0.45	410	468	668	3.1							Grey	
Pheophorbide *b*	F	0.34	432	522	656	8.0							Brown	
Pyropheophytin *a*	G	0.45	410	468	668	2.4							Grey	
Pyropheophytin *b*	G	0.23	432	522	656	5.5							Brown	

difficult than for other fruits or vegetables. The high lipid content of the olive (15–30%) [4] was a serious obstacle in isolating these liposoluble pigments even by thin-layer chromatography (TLC) and prior attainment of a fat-free pigment extract was necessary [5]. Mínguez-Mosquera *et al.* [6] found that the process of lactic fermentation in olives involves only the transformation of pigments, without their loss or destruction. Recently, they also found that the total quantification of carotenoids, chlorophylls and chlorophyll derivatives from the absorption spectrum of the crude extracts of pigments was correlated with a subjective classification of the fruit by colour, the classification decreasing as the pigment concentration increases [7]. However, for monitoring the individual pigments changes during the fermentation process, the use of high-performance liquid chromatography (HPLC) might be more appropriate, offering significant advantages over TLC, including speed, automatic detection and lower detection limits [8]. Since 1975, numerous studies have been made on the application of HPLC to the determination of chlorophyllic and carotenoid pigments in vegetable tissues. It seems that reversed-phase columns, mainly C_{18} [8–14], offer more advantages than normal-phase columns [15–17]. Thus, pigment degradation and long conditioning times are two drawbacks which have been cited when using silica as HPLC packing material [8,13].

In previous work, using the fat-free pigment extract, reversed-phase HPLC was used successfully for the separation of chlorophylls and carotenoids although only in fresh green olives [18]. In this work, reversed-phase ion-pair HPLC was used for the qualitative and quantitative control of the individual pigment changes throughout the fermentative process and later conservation of green table olives, Spanish style, achieving a satisfactory separation even for the acidic pigment (chlorophyllides and pheophorbides).

EXPERIMENTAL

Samples

The study was carried out on olives of the Hojiblanca variety, *Olea europaea arolensis*. The fruits were picked from the tree when green-yellowish, and processed using the traditional method of Spanish-style fermentation in brine [1]. The pigments were monitored at the following stages: (a) fresh fruit, (b) at the beginning of fermentation phase, (c) at the end of fermentation phase and (d) in the subsequent brine conservation of the fruit prior to packing.

Preparation of extract free of fatty material

Samples were made from a triturate homogenized from 100 de-stoned fruits, (*ca.* 500 g), by accurately weighing 5–15-g duplicates for each analysis according to the number of days of fermentation. The pigment extraction was made with N,N-dimethylformamide. The filtrates were next treated with hexane in a decantation funnel in order to extract and separate the characteristic fatty olive matter from the previous solution. The hexane phase in turn carried over the carotene fraction, while that corresponding to N,N-dimethylformamide retained chlorophylls, chlorophyll derivatives and the remaining carotenoids. The extraction processes have been described previously [5].

Standards

The reference samples of chlorophyll *a* and *b* were supplied by Sigma (St. Louis, MO, USA). Pheophytin *a* and *b* were obtained by acidification with 13% (v/v) hydrochloric acid of the respective chlorophyll solutions [19]. Chlorophyllide *a* and *b* were prepared by enzymic de-esterification of the respective chlorophylls following the method proposed by Jones *et al.* [20]. Pheophorbides *a* and *b* were then obtained from their respective chlorophyllides by acidification [21]. Pyropheophytins *a* and *b* were prepared by refluxing pheophytins in collidine [10]. Chlorophyll and pheophytin C-10 epimers were prepared by treatment with chloroform according to Watanabe *et al.* [21]. All standards were purified by thin-layer rechromatography on silica gel GF_{254} (20 × 20 cm plates, thickness 0.7 mm) (Merck, Darmstadt, Germany) using different eluents (Table I).

The carotenoid standards were obtained from fresh and elaborated olives whose pigment composition has been studied in detail and identified previously [5,22–24]. The starting point was a pigment extract in acetone obtained by the traditional method of Smith and Benítez [26]. This extract was saponified with methanolic potassium hydroxide solution (20%) for 1 h at room temperature to purify

it of lipids and chlorophylls [24]. Although some carotenoid are sensitive to alkaline media [27], none has been identified in the olive. Hence saponification is a sound method for carotenoid purification. The reference samples were accumulated from separations by TLC as described above. The first separation was carried out using light petroleum (b.p. 65–95°C)–acetone–diethylamine (10:4:1) as eluent. Once a sufficient amount of each of the carotenoids has been obtained it was purified by TLC, using different eluents (specified in Table I). To confirm the identification of all the pigments, the absorption spectra in acetone for the chlorophyllic pigments and in light petroleum and chloroform for the carotenoids were compared with those published in the literature [26–28]. The colour in TLC after spraying with hydrochloric acid and the hypsochromic change in the absorption spectrum in ethanol after acidifying with hydrochloric acid were used to identify the 5,6-epoxycarotenoids [29]. The presence of hydroxyl groups was confirmed by rechromatography after acetylation [30] and by the IR spectrum [28].

Column liquid chromatography

The pigment extract (20 μl), previously filtered through a nylon membrane of 0.45 μm (Micron Separations, Westboro, MA, USA) was injected into a liquid chromatograph (Perkin-Elmer, Series 4) equipped with a Rheodyne Model 7125 injector valve. Separations were carried out on a 25 cm × 4 mm I.D. column filled with Spherisorb ODS-2, 5-μm particle size (Supelco, Bellefonte, PA, USA). A short column (5 cm × 4 mm I.D.) of Pelliguard LC-18, 40 μm (Supelco), was placed immediately before the main column.

The solvents used as the mobile phase were proposed by Mantoura and Llewellyn [13], but in this work their proportions and the type of gradient were modified to obtain an adequate detection (sharper peaks) of pyropheophytins and to improve the separation between carotenoids and pheophorbides. The eluents used were the following: eluent A, water–solution P–methanol (1:1:8, v/v/v) and eluent B, acetone–methanol (1:1, v/v). Solution P (ion-pair reagent) is tetrabutylammonium acetate (0.05 *M*)–ammonium acetate (1 *M*) in water. To avoid any deterioration of silica particles by the ion-pair reagent [13], the column was stored in methanol–water (1:1, v/v).

The pigments were eluted using the gradient scheme outline in Table II, at a flow-rate of 2 ml/min, and detected using an absorbance detector (Perkin-Elmer LC-85B) set at 430 nm. A recording integrator (Hewlet-Packard Model 3396A) was used. Identification was made by comparing the retention times with those of authentic standards. In addition, a programmable photodiode-array detector (Waters Assoc., Model 994) allowed pigment spectra to be obtained without the need to stop the solvent flow. The absorption spectra were measured between 350 and 700 nm and recorded on a Waters Assoc. Model 5200 printer–plotter.

Quantification

The weight (W, μg) of pigments were calculated from an extension of Beer's law [13]:

$$W = \frac{aF}{A^{1\%}_{430\ nm}}$$

where a is the area of the peak expressed as counts supplied by the integrator, $A^{1\%}_{430\ nm}$ the absorptivity of the pigment at 430 nm and F a calibration factor to transform the units of the integrator into units of absorption. To calculate this factor, for the carotenoid group different solutions of β-carotene (Sigma) of known concentration under the chromatographic conditions used were analysed for an atten-

TABLE II

GRADIENT SCHEME USED FOR THE SEPARATION OF PIGMENTS

Flow-rate = 2 ml/min. The numbers in parentheses correspond to the curve type included in the programmer of a Perkin-Elmer Series 4 chromatograph.

Time (min)	Mobile phase		Curve
	A (%)	B (%)	
Initial	75	25	
8	25	75	Linear (1)
10	25	75	Isocratic
18	10	90	Convex (0.3)
23	0	100	Concave (5)
30	75	25	Concave (5)

uation of the detector of 0.04 a.u.f.s. For chlorophyllic derivatives group the same procedure was applied with chlorphyll *a* (Sigma). The values obtained for F were $1.70 \cdot 10^4$ for β-carotene and $2.19 \cdot 10^4$ for chlorophyll *a*. The values of $A^{1\%}_{430\ nm}$ were calculated from the absorption spectrum obtained with the photodiode-array detector of each pigment and from the values of $A^{1\%}_{\lambda max}$ given in the literature [7,27]. For routine determinations, it was necessary to analyse standard samples of β-carotene and chlorophyll *a* periodically, and those factors calculated to take into account the variations in instrumental sensitivity.

The calibration lines for each pigment were calculated from plots of the peak areas against concentration of pure pigment. The approximate detection limit was calculated from the calibration lines as a function of the peak height, taking as the lower limit the peak height equal to twice the noise signal.

Reagents

All reagents were of analytical-reagent grade, except acetone and methanol, which were of HPLC grade. The water was deionized and filtered through a 0.45-μm nylon membrane (Supelco, Bellefonte, PA, USA).

RESULTS AND DISCUSSION

Separation and identification of the pigments

Fig. 1 shows the HPLC, using an absorbance detector, of pigment extracts of olives in distinct phases of the fermentation process (Spanish or Sevillian style): (a) fresh fruit, (b) at the beginning of the fermentation phase, (c) at the end of the fermentation phase and (d) in the conservation phase. Table III shows all the pigments identified, with their chromatographic and spectroscopic characteristics. The proposed technique allowed the detection and identification of carotenoids not previously detected in this product by TLC [6]. HPLC of the pigment extract from fresh fruit using the absorption detector (Fig. 1a) showed the following pigments in order of elution: neoxanthin, violaxanthin, luteoxanthin, antheraxanthin, lutein, chlorophyll *b*, chlorophyll *a* and β-carotene. Neoxanthin was shown by HPLC to consist of two isomers (peaks 3 and 3′). The same occurred for anteraxanthin (peaks 8 and 8′). Lutein (peak 10) was accompanied by two isomers (10′ and 10″). The epimers of chlorophylls on C-10 were also separated (peaks 13′ and 14′).

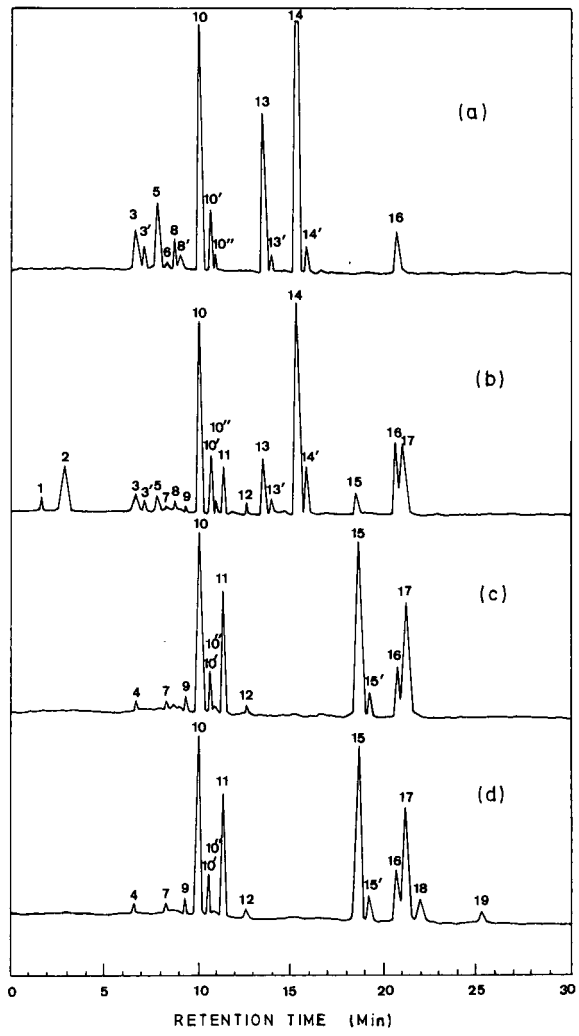

Fig. 1. HPLC using absorbance detector (430 nm) of pigment extracts of olives: (a) fresh fruit; (b) at the beginning of the fermentation phase; (c) at the end of the fermentation phase; (d) in the preservation phase. Peaks: 1 = chlorophyllide *b*; 2 = chlorophyllide *a*; 3 = neoxanthin; 3′ = neoxanthin isomer; 4 = neochrome; 5 = violaxanthin; 6 = luteoxanthin; 7 = auroxanthin; 8 = anteraxanthin; 8′ = anteraxanthin isomer, 9 = mutatoxanthin; 10 = lutein; 10′ = lutein isomer; 10″ = lutein isomer; 11 = pheophorbide *b*; 12 = pheophorbide *a*; 13 = chlorophyll *b*; 13′ = chlorophyll *b*′; 14 = chlorophyll *a*; 14′ = chlorophyll *a*′; 15 = pheophytin *b*; 15′ = pheophytin *b*′; 16 = β-carotene; 17′ = pheophytin *a*; 17 = pheophytin *a*; 18 = pyropheophytin *b*; 19 = pyropheophytin *a*.

The chromatogram from a pigment extract of

TABLE III

PIGMENTS SEPARATED BY HPLC: IDENTITIES, CAPACITY FACTORS AND SPECTRA DATA

$K'_c = (t_r - t_m)/t_m$, where t_r = retention time of the pigment peak and t_m = retention time of an unretained component. Published spectral data are in diethyl ether for chlorophylls and derivatives and in ethanol for carotenoids.

Peak No.	K'_c	Pigment	Spectral data in the eluent				Published data				
			Maxima (nm)			Peak ratio	Maxima (nm)			Peak ratio	Ref.
			I	II	III		I	II	III		
1	0.17	Chlorophyllide *b*	466	600	650	3.3					
2	0.96	Chlorophyllide *a*	432	616	664	1.3	428		662		8
3	3.28	Neoxanthin	414	438	466	90	416	440	468	89	8
3′	3.60	Neoxanthin isomer	414	438	466	90					
4	3.69	Neochrome	398	422	448	78	401	424	451		
5	4.11	Violaxanthin	416	440	470	94	417	440	470	93	8
6	4.46	Luteoxanthin	400	424	450	107	396	420	446		31
7	4.56	Auroxanthin	380	400	424	103	380	402	428	103	8
8	4.75	Anteraxanthin	(420)	444	474	22	422	444	472	54	8
8′	4.96	Anteraxanthin isomer	(420)	444	474	22					
9	5.22	Mutatoxanthin	(404)	426	452	39		427	457		
10	5.52	Lutein	424	446	474	60	422	445	474	62	8
10′	6.05	Lutein isomer	418	440	468	42					
10″	6.26	Lutein isomer	416	438	466	27					
11	6.42	Pheophorbide *b*	426		650	8.3	433	525	655	4.56	32
12	7.29	Pheophorbide *a*	400	504	662	3.3	408	504	667	2.07	32
13	7.96	Chlorophyll *b*	466	600	650	3.3	453	593	642	2.89	33
13′	8.24	Chlorophyll *b′*	466	600	650	2.8	453	592	642	2.86	34
14	9.18	Chlorophyll *a*	432	616	664	1.3	430	615	661	1.32	33
14′	9.57	Chlorophyll *a′*	432	616	664	1.1	428	614	661	1.24	34
15	11.21	Pheophytin *b*	436	599	654	5.1	433	599	654	4.81	33
15′	11.91	Pheophytin *b′*	436	598	654	5.1					
16	12.84	β-Carotene		452	478	23		450	477	20	8
17	13.22	Pheophytin *a*	410	506	666	1.8	408	503	667	2.14	33
18	13.79	Pyropheophytin *b*	436	524	654	5.4	436		655		35
19	16.05	Pyropheophytin *a*	410	506	666	2.4	409		666		35

fruits at the beginning of the fermentation phase (Fig. 1b) shows new peaks, which were identified as degradation products of the pigments present in the fresh fruit. With respect to the chlorophyllic fraction, chlorophyllide *a* and *b*, pheophorbide *a* and *b* and pheophytin *a* and *b* were detected. As shown in previous work [6], the chlorophyllides appear in the few first days of fermentation, when the olives still have an alkaline pH from the sodium hydroxide treatment, which favours the action of the enzyme chlorophyllase, present in most green tissues. The presence of pheophytins and pheophorbides is due to the acidic pH of the medium caused by the products of the lactic fermentation [6]. Because of this, in the carotenoid fraction, the 5,8-epoxides carotenoids neochrome, auroxanthin and mutatoxanthin were also detected.

In the totally fermented fruit (Fig. 1c) the chlorophylls and chlorophyllides have disappeared, being transformed into pheophytins and pheophorbides. In the carotenoid fraction, neoxanthin, violaxanthin and anteraxanthin have been totally transformed into their corresponding furanoid derivatives neochrome, auroxanthin and mutatoxanthin, respectively. Lutein and β-carotene remain the main pigments in this fraction. Finally, in the brine conservation phase, additional degradation reactions may take place. Thus, pyropheophytin *a* and *b* are detected, formed from the corresponding pheophytins by the loss of the C-10 carbomethoxy

group. The last pigment to elute is pyropheophytin *a*, which has a retention time of about 25 min (Fig. 1d). The absorbance chromatograms discussed previously show that during fermentation and subsequent preservation of the fruits it is the chlorophyllic fraction of pigments which undergoes the greatest transformation. The main carotenoids, lutein and β-carotene, remain virtually unaltered.

Quantification of the pigments

The slow and labour-consuming operation to obtain carotenoids and chlorophyllic derivatives, and the difficult conservation of the standard mixtures due to the sensibility of these pigments to high temperature, etc., limit the possibilities of using the traditional methods with internal or external standards. These problems extend substantially the time required for the analysis and makes it inappropriate for the control of the pigment changes during the lactic fermentation of olives (6–7 months).

To compare the external standard method with the proposed method, four analyses of two pigment extracts from fresh and elaborated olives were carried out. All the pigment concentrations were calculated from the calibration lines and from the empirical factor for carotenoids and chlorophyllic derivatives. Table IV shows the average values obtained by both procedures and the corresponding absorptivities at 430 nm. Anteraxanthin and mutatoxanthin were not included because insufficient amounts to estimate the calibration line were obtained. The errors of the concentration calculated from the empirical factors and the $A^{1\%}_{430\ nm}$ values ranges from

TABLE IV

QUANTIFICATION BY HPLC OF PIGMENTS USING THE EXTERNAL STANDARD METHOD (METHOD 1) AND BEER'S LAW (METHOD 2)

Means of four injections from fresh and fermented olive extracts (mg/kg). Values of $A^{1\%}_{430\ nm}$ calculated from the absorption spectrum obtained with the photodiode array detector and from the values of $A^{1\%}_{\lambda max}$. Error of the concentrations calculated from method 2.

Pigment	Method 1	Method 2	$A^{1\%}_{430\ nm}$	Error (%)
Neoxanthin	1.0275	1.0175	1353	1.0
Neochrome	0.5125	0.5000	1751	2.4
Violaxanthin	0.5750	0.5650	1909	1.7
Auroxanthin	0.7725	0.7625	1709	1.0
Lutein	3.3825	3.3625	1777	0.6
Pheophorbide *b*	2.0650	2.0550	1545	0.5
Pheophorbide *a*	0.7750	0.7680	268	0.2
Chlorophyll *b*	11.6800	11.6100	356	0.6
Chlorophyll *a*	21.1275	21.1050	840	0.0
Pheophytin *b*	6.2650	6.2350	1545	0.5
β-Carotene	2.3250	2.3350	1844	0.0
Pheophytin *a*	23.9725	23.9225	268	0.2

TABLE V

QUANTIFICATION BY HPLC OF PIGMENTS IN PICKLED GREEN OLIVES FROM BEER'S LAW AND ESTIMATION OF PRECISION OF HPLC METHOD AND THE DETECTION LIMITS

Mean ± S.D. of triplicate injections from pitted fresh olive extract.

Pigment	Extract 1		Extract 2		Detection limit (ng)
	mg/kg	R.S.D. (%)	mg/kg	R.S.D. (%)	
Neochrome	0.320 ± 0.014	4.37	0.340 ± 0.014	4.12	5.9
Auroxanthin	0.465 ± 0.021	4.52	0.530 ± 0.028	5.28	3.2
Mutatoxanthin	0.285 ± 0.010	0.35	0.340 ± 0.014	4.12	–
Lutein	2.995 ± 0.021	0.70	3.205 ± 0.064	2.00	2.5
Lutein isomer	0.500 ± 0.014	2.80	0.560 ± 0.014	2.50	2.5
Pheophorbide *b*	1.745 ± 0.064	3.67	1.890 ± 0.042	2.22	8.0
Pheophorbide *a*	0.845 ± 0.049	5.80	1.155 ± 0.035	3.03	44.0
Pheophytin *b*	2.220 ± 0.042	1.90	2.735 ± 0.035	1.28	8.0
β-Carotene	1.195 ± 0.010	0.08	1.175 ± 0.021	1.79	19.0
Pheophytin *a*	14.980 ± 0.028	0.19	16.175 ± 0.431	2.66	44.0
Pheophytin *a'*	5.040 ± 0.085	1.69	5.475 ± 0.120	2.19	44.0
Pyropheophytin *a*	3.475 ± 0.035	1.01	3.615 ± 0.078	2.16	44.0

0.2 to 2.4%. The analysis of variance of such data showed insignificant differences between the results given by the two methods. Table V gives the precision of the method (0.1–5.8%) and the detection limits, which varied between 44 ng for pheophytin *a* and 2.5 ng for lutein.

CONCLUSION

The method developed in this study for rapid control of qualitative and quantitative assessments of individual pigments is of great interest for establishing the presence of appropriate pigments during each fermentation phase. This information permits the correction during the fermentation process of any deviation from the normal pattern that could affect the parameters that influence the pigments. Also, a correlation between the subjective colour and the type and amount of each pigment could be obtained. In general, the proposed method could also be used with other products that contain chlorophylls and carotenoids, if the sum of the pigments is high and the preparation of standards might be too tedious owing to the instability of these compounds.

ACKNOWLEDGEMENTS

The authors express their sincere gratitude to CICYT for supporting this research project. Thanks are also due to M. Bodineau Bada for technical assistance.

REFERENCES

1 M. J. Fernández, R. de Castro, A. Garrido, F. G. Cancho, F. G. Pellissó, M. Nosti, A. Heredia, M. I. Mínguez, L. Rejano, M. C. Durán, F. Sánchez, P. García and A. de Castro, in *Biotecnología de la Aceituna de Mesa, Madrid 1985*, CSIC, Madrid, 1985, Ch. 1, p. 5 and Ch. 4, p. 51.
2 J. M. R. de la Borbolla, C. Gómez, F. G. Cancho, M. J. Fernández-Díez, R. Gutiérrez, A. Izquierdo, F. G. Pellissó, R. Vázquez and R. Guzmán, *El Aderezo de Aceitunas Verdes*, CSIC, Madrid, 1956, Ch. 6, p. 105.
3 A. Garrido-Fernández, L. Rejano-Navarro, F. Sánchez-Roldán, A. de Castro-Gómez, P. García-García, A. H. Sánchez-Gómez and M. Brenes-Balbuena, in *First Conference on Food Science and Technology for Mediterranean Countries*, Egyptian Society of Food Science and Technology, Cairo, 1986, p. 88.
4 A. Vázquez-Roncero, *Grasas Aceites*, 14 (1963) 262.
5 M. I. Mínguez-Mosquera and J. Garrido-Fernández, *J. Agric. Food Chem.*, 37 (1989) 1.
6 M. I. Mínguez-Mosquera, J. Garrido-Fernández and B. Gandul-Rojas, *J. Agric. Food Chem.*, 37 (1989) 8.
7 M. I. Mínguez-Mosquera, J. Garrido-Fernández and B. Gandul-Rojas, *J. Agric. Food Chem.*, 38 (1990) 38.
8 S. W. Wright and J. D. Shearer, *J. Chromatogr.*, 294 (1984) 281.
9 T. Brauman and L. H. Crimme, *J. Chromatogr.*, 170 (1979) 264.
10 S. J. Schwartz, S. L. Woc and J. H. Von Elbe, *J. Agric. Food Chem.*, 29 (1981) 533.
11 J. F. Fisher and R. L. Rouseff, *J. Agric. Food Chem.*, 34 (1986) 985.
12 F. Khachik, G. R. Beecher and N. F. Whittaker, *J. Agric. Food Chem.*, 34 (1986) 603.
13 R. F. C. Mantoura and C. A. Llewellyn, *Anal. Chim. Acta*, 151 (1983) 297.
14 C. Fisher and J. A. Kocis, *J. Agric. Food Chem.*, 35 (1987) 55.
15 K. Iriyama, M. Yoshiura and M. Shiraki, *J. Chromatogr.*, 154 (1978) 302.
16 J. K. Abaychi and J. P. Riley, *Anal. Chim. Acta*, 107 (1979) 1.
17 M. Rahmani and A. S. Csallany, *Rev. Fr. Corps Gras*, 32 (1985) 257.
18 M. I. Mínguez-Mosquera, A. Montaño-Asquerino, J. Garrido-Fernández and B. Gandul-Rojas, *Grasas Aceites*, 39 (1988) 363.
19 G. Sievers and P. H. Hynninen, *J. Chromatogr.*, 134 (1977) 359.
20 I. D. Jones, L. S. Butler, E. Gibbs and R. C. White, *J. Chromatogr.*, 70 (1972) 87.
21 T. Watanabe, A. Hongu, K. Hond, M. Nakazato, M. Konno and S. Saitoh, *Anal. Chem.*, 56 (1984) 251.
22 M. I. Mínguez-Mosquera, B. Gandul-Rojas and J. Garrido-Fernández, *Grasas Aceites*, 40 (1989) 114.
23 M. I. Mínguez-Mosquera and J. Garrido-Fernández, *Grasas Aceites*, 36 (1985) 376.
24 M. I. Mínguez-Mosquera, J. Garrido-Fernández and J. Pereda-Marín, *Grasas Aceites*, 37 (1986) 272.
25 M. I. Mínguez-Mosquera, J. Garrido-Fernández and J. Pereda-Marin, *Grasas Aceites*, 37 (1986) 320.
26 J. H. C. Smith and A. Benítez, in K. Paech and M. V. Tracey (Editors), *Modern Methods of Plant Analysis*, Vol. 1. Springer, Berlin, Göttingen, Heidelberg, 1955, p. 142.
27 B. H. Davies, in T. W. Goodwin (Editor), *Chemistry and Biochemistry of Plant Pigments*, Vol. 2, Academic Press, London, 1975, p. 38.
28 F. H. Foppen, *Chromatogr. Rev.*, 14 (1971) 133.
29 D. F. Hildebrang and T. Hymowitz, *J. Agric. Food Chem.*, 30 (1982) 705.
30 D. B. Rodríguez, P. L. Simpson and C. O. Chichester, *Int. J. Biochem.*, 4 (1973) 213.
31 B. H. Davies and H. P. Köst, in H. P. Köst (Editor), *Handbook of Chromatography*, Vol. 1, CRC Press, Boca Raton, FL, 1988, p. 3.
32 P. H. Hynninen, *Acta Chem. Scand.*, 27 (1973) 1771.
33 P. H. Hynninen and N. Ellfolk, *Acta Chem. Scand.*, 27 (1973) 1463.
34 P. H. Hynninen, *Acta Chem. Scand.*, 27 (1973) 1487.
35 M. S. Fraser and G. Fankl, *J. Am. Oil Chem. Soc.*, 62 (1985) 113.

Journal of Chromatography, 585 (1991) 267–271
Elsevier Science Publishers B.V., Amsterdam

CHROM. 23 516

Determination of polyphosphates in intermediate materials for detergent manufacture by ion high-performance liquid chromatography with post-column derivatization

P. Linares, M. D. Luque de Castro* and M. Valcárcel

Department of Analytical Chemistry, Faculty of Sciences, University of Córdoba, 14004 Córdoba (Spain)

(Received April 3rd, 1991)

ABSTRACT

A method for the determination of polyphosphates [ortho- (P_1), pyro- (P_2), tripoly- (P_3), and trimeta- (P_4) phosphate] based on the use of ion chromatography and gradient elution is proposed. The method was optimized for application to intermediate products in detergent manufacture, which feature rather different concentrations of the analytes (90–95% P_3 and 10–5% for the sum of the other three). The proposed method was applied to real samples with good results and throughput of four samples per hour.

INTRODUCTION

The individual determination of the different phosphorus oxoacids has been addressed by using both batch and continuous methods, most of which rely on the formation of a heteropolyacid with molybdenum as derivatizing reagent, which follows prior to hydrolysis when the analyte is a condensed orthophosphate form. In this way, phosphorous species have been determined in various matrices (soils, plants [1–9]) without special problems, while mixtures of condensed phosphates have been determined globally by segmented flow analysis following hydrolysis at 95°C [10]. Problems in this respect are posed by the individual determinations of these analytes in mixed samples; such is the case with products used by the detergent industry, which require very frequent monitoring and control of the ratio between the four components that make the intermediate manufactured product, namely ortho- (P_1), pyro- (P_2), tripoly- (P_3) and trimeta-(P_4) phosphate. The prior separation of the analytes required can be accomplished by ion chromatography using 0.23 *M* potassium chloride as eluent, but takes as long as 48 min per analysis [11] with samples containing similar concentrations of the analytes ($1 \cdot 10^{-4}$ *M*). The gradient elution technique and ion-exchange chromatography, used in conjunction with a Technicon Autoanalyzer, allow resolution of phosphate mixtures in detergents, but are rather time-consuming (90 min per analysis) [12].

Post-column derivatization by formation of heteropolyacids has been performed on different mixtures by using flow systems with continuous mixing of the reagent and chromatographic eluate. Thus, orthophosphonate and polyphosphate were determined after chromatographic separation, hydrolysis at 140°C and derivatization, which resulted in an analysis time of 15 min, but only for similar amounts of the analytes. Enzymatic hydrolysis allowed development of an easier yet more expensive procedure that was applied to the determination of ortho-, pyro- and tripolyphosphate by isocratic elution with 0.2 *M* potassium chloride in 20 min [13].

In this work we developed a method based on the use of ion-exchange chromatography, gradient elu-

0021-9673/91/$03.50

tion, hydrolysis and derivatization under optimal conditions for the resolution of polyphosphate mixtures in ratios typical of intermediate materials used in detergent manufacture, which requires the intermediate step to be performed with a P_3 content as high as possible and the content of the minor components (P_1, P_2, P_4) to be known in order to control the process. Therefore, both P_3 and the other components must be determined precisely.

EXPERIMENTAL

Reagents and solutions

The eluent consisted of 0.1 or 0.2 *M* potassium chloride containing 1 m*M* Na_4EDTA and adjusted to pH 9.0 with sodium hydroxide. A hydrolysis solution composed of 3 *M* sulphuric acid, 5% (w/v) sodium molybdate in 3 *M* sodium hydroxide and 2% (w/v) ascorbic acid was used. The standard sample contained 1% orthophosphate, 5% pyrophosphate, 92% tripolyphosphate and 2% trimetaphosphate, referred to 100% polyphosphate, plus 1.6% sodium sulphate, 250 ppm sodium fluoride and 1.2% sodium chloride as impurities.

Instruments and apparatus

The chromatographic system was made up of a Hewlett-Packard 1050 high-pressure pump with quaternary gradient, a Rheodyne 7125 injection valve, an Ion-120 ion chromatographic column (120 × 4.6 mm I.D., 100 μequiv./g equivalent capacity) and an Ion-Guard GA-100 anion-exchange pre-column. The post-column system consisted of a Gilson Minipuls-2 peristaltic pump, a UV–visible spectrophotometer equipped with a Hellma 178.12QS flow cell (inner volume 18 μl), three connectors and PTFE tubing of 0.5 mm I.D. A Selecta thermostat filled with Vaseline oil and another furnished with a laboratory-made thermostating chamber were also used.

Sample preparation and procedure

The weighed sample was dissolved in 0.1 *M* potassium chloride. Aliquots of the resulting solution were injected into the system (Fig. 1) and driven to the pre-column for removal of interferences that might reduce the effectiveness of the chromatographic column; the eluent was merged with a 3 *M* sulphuric acid stream at point a, after which the mixture was heated at 90°C in a thermostatic bath filled with Vaseline oil. As the derivatizing reaction developed optimally at room temperature, a cooling recirculating system was used to heat the stream at a suitable temperature for development of this reaction in L_2 after merging with the derivatizing reagents (an on-line mixture of ascorbic acid and sodium molybdate in a basic medium for partial neutralization of the eluent). The reaction product was monitored photometrically at 820 nm. The pressure inside reactor L_3 avoided the formation of bubbles in the system owing to the high temperature achieved by circulating the sample through L_1.

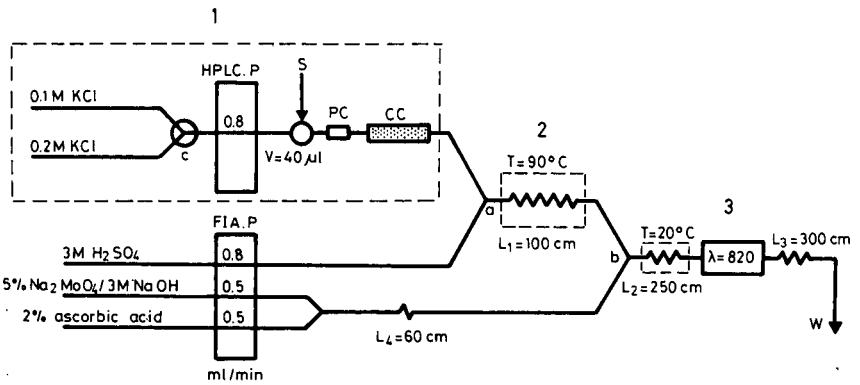

Fig. 1. Configuration for the determination of polyphosphates in intermediate products for detergent manufacture. 1 = clean-up and separation steps; 2 = hydrolysis; 3 = derivatization; c = gradient unit; P = pump; S = sample; PC = pre-column; CC = chromatographic column; a and b = confluence points; W = waste.

RESULTS AND DISCUSSION

Inasmuch as the aim of this work was to develop a method for analysis of intermediate materials used in detergent manufacture, real samples of this type were used to optimize the working conditions and to adapt them to the rather different concentrations at which the analytes are present in them. Both chromatographic variables and those typical of the post-column system were optimized by the univariate method.

Optimization of the chromatographic system

Various eluents (acetic acid–sodium acetate, sodium chloride, potassium chloride) were checked in a preliminary study. The best for our purpose (well defined peaks and short elution times) was found to be potassium chloride. The influence of the eluent flow-rate was studied between 0.6 and 1.2 ml/min. Acceptable resolution was achieved at 0.8 ml/min. Higher flow-rates gave rise to peak overlap, while lower values lengthened the analysis time unduly. Concentrations of potassium chloride ranging from 0.1 to 0.4 *M* were assayed. Increasing salt concentrations resulted in decreasing retention times and hence in growing peak overlap. Under isocratic conditions, the best resolution was achieved with 0.1 *M* potassium chloride, but the resulting analysis time was 30 min; the elution sequence was P_1, P_2, P_3 and P_4. The chromatogram obtained under isocratic conditions with 0.1 *M* potassium chloride reflects adequate separation between P_1, P_2 and P_3, but rather a lengthy separation between P_3 and P_4, which makes the overall analysis time too long. The long elution time required by P_4 results in a high dispersion. This, together with the low concentration of this analyte, gave rise to a wide, low peak. The most suitable gradient was found to be that created by changing the eluent concentration from 0.1 to 0.2 *M* 5 min after injection, followed by another change from 0.2 to 0.1 *M* potassium chloride 9 min after injection. The elution time of the chromatogram obtained under these conditions was shortened from 30 to 15 min. The peaks heights changed linearly ($5 \cdot 10^{-3}$ a.u./μl) with the injected volume over the range 20–180 μl. We chose an injected volume of 40 μl, which ensured adequate sensitivity for the analyte concentrations in the samples. However, the sensitivity can be augmented at will by using larger injected volumes. The effect of the eluent pH was investigated between 7 and 10. The maximum peak resolution and height were obtained at pH 9.0.

Optimization of the post-column system

The hydrolysis step implemented to convert the polyphosphates into orthophosphates was enacted with hot sulphuric acid. By merging the eluate with 3 *M* sulphuric acid (flow-rate 0.8 ml/min) at point a and keeping reactor L_1 at 90°C, the hydrolysis yield achieved was 30% for P_3 and P_4 and 65% for P_2, *i.e.* more than adequate for the sample studied. The optimal length of L_1 was 10 m. Shorter lengths resulted in inadequate hydrolysis, whereas longer lengths resulted in increased hydrolysis efficiency but also in dramatically increased eluate dispersion.

The derivatization reaction involved formation of a heteropolyacid with molybdate and reduction of complexed molybdenum (VI) to molybdenum (V) by ascorbic acid. The optimum temperature for this reaction was between 15 and 30°C, which required the stream emerging from L_1 to be cooled. This was accomplished by using a device that was designed and constructed in our laboratory where the cooled water entered a chamber through a cylinder around which reactor L_2 was coiled; thus, the fluid held in the length of L_2 in contact with the cylinder was first cooled and then used to fill the remainder of the chamber, which was left through the top. The optimum concentration of complexing agent (sodium molybdate) and reducing agent (ascorbic acid) was 5 and 2%, respectively; they were included in separate solutions that were mixed prior to merging with the main stream. As the optimum pH for development of the derivatizing reaction was 0.9, the sodium molybdate solution was prepared in 3 *M* sodium hydroxide: such pH was accomplished by mixing along reactor L_2, the optimum length of which was 250 cm. The effect of the overall flow-rate of the continuous post-column manifold was studied by changing it between 1.0 and 2.5 ml/min while keeping the flow-rate ratio between the three channels as follows: 3/4 q(sulphuric acid) = q(sodium molybdate) + q(ascorbic acid), the last two being equal. The best overall flow-rate was found to be 1.5 ml/min.

Under the above optimal working conditions, bubbles wer formed along the system that yielded

TABLE I

CONCENTRATION OF THE ANALYTES IN THE STANDARDS

Sample	Concentration (g/l)			
	P_1	P_2	P_3	P_4
1	0.005	0.025	0.460	0.010
2	0.010	0.050	0.920	0.020
3	0.025	0.125	2.300	0.050
4	0.050	0.250	4.600	0.100
5	0.100	0.500	–[a]	0.200
6	0.200	1.000	–[a]	0.400
7	0.400	2.000	–[a]	0.800

[a] Beyond the capacity of the detector.

parasitic signals on arrival at the flow cell. A suitable length of tubing after the flow cell created an overpressure in the continuous manifold that prevented the bubbles from circulating freely and thus reaching the detector. A length of 300 cm was sufficient for this purpose.

Calibration curves

Calibration curves were obtained by running different standard mixed solutions made by direct weighing and diluting them with the mobile phase. The weight of standard for each solution (expressed as weight/volume percentage) and the concentration of each analyte in the samples are listed in Table I. The concentration of tripolyphosphate in standard samples 5–7 was beyond the capacity of the photometric detector. Peak-height data were used to establish equations relating this parameter to the concentration of the corresponding analyte.

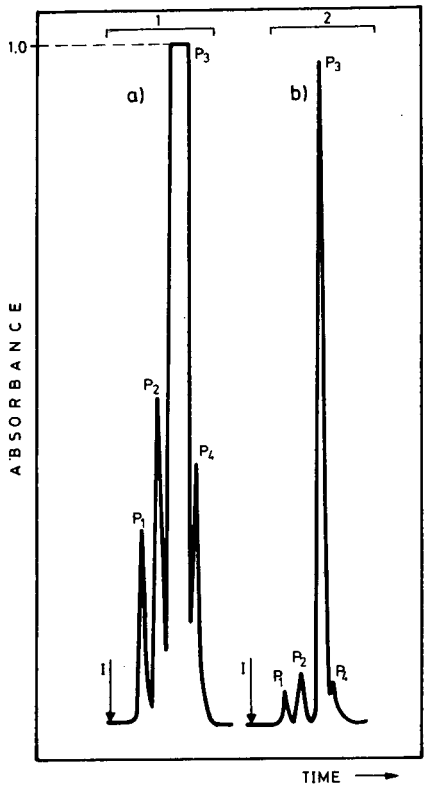

Fig. 2. Chromatograms obtained by gradient elution. 1 = 2% (w/v) dilution; 2 = 0.2% (w/v) dilution.

Such equations, their regression coefficients and relative standard deviations (R.S.D.) each analyte are listed in Table II.

Application of the method to real samples

The differences in concentrations of the analytes in the samples required two dilutions to be made in

TABLE II

FEATURES OF THE CALIBRATION CURVES

Analyte	Equation[a]	Regression coefficient	R.S.D. (%)
Orthophosphate	$A = 0.0082 + 1.0505\,[P_1]$	0.9967	2.5
Pyrophosphate	$A = 0.0136 + 0.3377\,[P_2]$	0.9985	3.2
Tripolyphosphate	$A = 0.1331 + 0.3079\,[P_3]$	0.9958	1.9
Trimetaphosphate	$A = 0.0168 + 0.6621\,[P_4]$	0.9963	3.0

[a] A = absorbance units; concentration in g/l.

order to be able to determine the four phosphates precisely. A 2% (w/v) solution for the determination of minor components and a 0.2% (w/v) solution for the major components were used. The recordings shown in Fig. 2 were obtained by injecting sequentially the two samples into the overall configuration (Fig. 1). Three different samples supplied by a national industry that manufactures the intermediate products were analysed; the results obtained are consistent with those of the analysis made at the factory laboratory (chromatographic separation in a flow-pressure column followed by derivatization with sodium molybdate–ascorbic acid in a segmented-flow analyser).

CONCLUSIONS

The use of ion chromatography and gradient elution in addition to an optimized post-column manifold and chemical variables involved in the post-column steps allowed us to develop an efficient method for the determination of the four most common phosphates present in intermediate material used for detergent manufacture with clear advantages over previous methods such shorter analysis times, a simpler post-column system [13], milder hydrolysis conditions [14] and lower analytical costs [15]. The optimization of the proposed method for the presence and concentration ratios of these four analytes is also a novelty that makes it directly implementable by industries devoted to detergent or intermediate product manufacture.

REFERENCES

1 J. Ruzicka and J. W. B. Steward, *Anal. Chim. Acta*, 79 (1975) 79.
2 W. D. Basson, J. F. van Staden and P. M. Cattin, *Z. Anal. Chem.*, 307 (1981) 373.
3 H. Bergamin, E. A. G. Zagatto, F. J. Krug and B. Reis, *Anal. Chim. Acta*, 101 (1978) 17.
4 B. Reis, E. A. G. Zagatto, A. O. Jacintho, F. J. Krug and H. Bergamin, *Anal. Chim. Acta*, 119 (1980) 305.
5 L. Sun, Z. Gao, C. Yu and Z. Fang, *Fenxi Huaxue*, 9 (1981) 586.
6 Z. Fang, L. Sun, Z. Gao, X. Wang and N. L. Li, *Turang Tongbao*, 4 (1982) 40.
7 J. W. B. Steward and J. Ruzicka, *Anal. Chim. Acta*, 82 (1976) 137.
8 O. Royset, *Anal. Chim. Acta*, 178 (1985) 217.
9 N. Yoza, Y. Kurokawa, Y. Hirai and S. Ohashi, *Anal. Chim. Acta*, 121 (1980) 281.
10 D. P. Lundgren and N. P. Loeb, *Anal. Chem.*, 33 (1961) 366.
11 D. P. Lundgren, *Anal. Chem.*, 32 (1960) 824.
12 H. Schwab, W. Rieman and P. A. S. Vaughan, *Anal. Chem.*, 29 (1957) 471.
13 Y. Baba, N. Yoza and S. Ohashi, *J. Chromatogr.*, 295 (1984) 153.
14 N. Yoza, H. Hirano, Y. Baba and S. Ohashi, *J. Chromatogr.*, 325 (1985) 385.
15 B. Y. Spivakov, T. A. Maryutina, L. K. Shpigun, V. M. Shkinev, Y.A. Zolotov, E. Ruseva and I. Havezov, *Talanta*, 9 (1990)889.

Journal of Chromatography, 585 (1991) 273–280
Elsevier Science Publishers B.V., Amsterdam

CHROM. 23 531

Gas chromatographic separation and automatic identification of complex mixtures of organic solvents in industrial wastes

Gianrico Castello and Sonia Vezzani

Istituto di Chimica Industriale, Universitá di Genova, Corso Europa 30, I-16132 Genoa (Italy)

Tomaso C. Gerbino

Castalia, Soc. Italiana per l'Ambiente SpA, Via dei Pescatori 35, I-16129 Genoa (Italy)

(First received March 5th, 1991; revised manuscript received June 4th, 1991)

ABSTRACT

The analysis of complex mixtures of industrial solvents in chemical wastes was carried out by the simultaneous use of non-polar and polar wide-bore capillary or packed columns. The co-eluting peaks on one of the two phases were resolved on the other phase, and the identification and quantitative analysis of mixtures containing up to 32 compounds was possible. Some integrators and data collectors were tested to allow the automatic identification of the compounds by comparing the chromatograms obtained from a 50:50 split of the sample into two parallel columns connected to identical flame ionization detectors.

INTRODUCTION

The disposal of toxic industrial wastes through landfill, incineration or other procedures is a controversial subject, as toxic chemicals or their decomposition products may contaminate water courses or escape into the atmosphere during the production, conservation and treatment of the wastes. The lack of adequate regulation and official treatment and disposal plants in many countries has led to the illegal collection, transportation and dumping of wastes that, after the introduction of legislation designed to control the problem, must be recovered, identified and properly disposed of.

A significant part of the problem is the analysis of the complex mixtures of industrial solvents that, being in liquid form and often stored in metallic drums which are subject to corrosion, may contaminate the landfill sites and be leached by running water, or escape into the atmosphere as a result of their appreciable vapour pressures. The various analytical procedures for such samples have been tested and certified by official test methods [1–7]. The characterization of the components of these mixtures is also necessary to determine the most convenient and safe disposal or destruction procedure. This characterization may be very difficult owing to the lack of information on the origin of the waste and any prior treatment. This difficulty was recently illustrated by the phenomenon of the so-called "poison ships", *i.e.* freighters which, loaded with industrial waste destined for dumping sites overseas, had to search for unloading ports after changes in local rules forbade the discharge at the original destination.

An example of this situation is the Syrian vessel MV *Zanoobia*, the third of a series of cargo-ships (*Linx*, *Makiri* and *Zanoobia*) which were involved in a complex sequence of loading, transfer and unloading of poisons. *Linx* was originally chartered

0021-9673/91/$03.50

for the carriage of 2100 tons of industrial waste to a dumping site at Djbouti (East Africa). The load was not accepted for discharge at Djbouti, and the cargo was then carried to Puerto Cabello (Venezuela) and transferred from *Linx* to *Makiri* and then to *Zanoobia*, which attempted to call at other Asiatic and European ports (Tartous, Salonika, Cagliari, Carrara) and was eventually moored, unloaded and decontaminated in Genoa harbour. During this long journey, the identification tags on the barrels were cancelled, freight documents were lost, spilt or damaged containers were replaced and their contents mixed together, and the resulting composition of the cargo (10 800 barrels) was completely unknown [8]. Similar problems were found in the decontamination of other freighters (*Jolly Rosso, Karin B, Deep Sea Carrier*) and of many dumping sites and waste repositories.

The routine analysis of this type of sample requires the identification of the components of the mixture and their determination at concentrations ranging from a tenth of a part per million to percentage values. This peculiar application influences the choice of instrumentation suitable for screening these samples: gas chromatography (GC) with flame ionization detection (FID) has to be used, as this technique offers the required sensitivity and linearity over a wide concentration range. The use of narrow-bore capillary columns should be avoided for the preliminary screening of unknown samples owing to their reduced sample capacity and shortened life in the presence of samples contaminated with high-boiling-point compounds (such as oils, polymers, additives, organometallics and surfactants). For the same reason, the use of gas chromatography–mass spectrometry (GC–MS) should be restricted to the final confirmation of some components and cannot be used for a general screening due to the enormous number of samples.

The analysis of complex mixtures on packed or wide-bore capillary columns offers the efficiency and selectivity required for identification purposes when stationary phases of different polarities are used and the retention times or index values of the components are compared with those of previously known standard samples. Simultaneous analysis on different columns is necessary to reduce the analysis time.

Polar and non-polar stationary phases were therefore used for the analysis of samples containing the 32 compounds most frequently found as components of industrial solvents or waste mixtures. The performance of packed and wide-pore capillary columns was evaluated, and the possibility of using commercial integration systems to automatically identify the components of the mixtures was investigated.

EXPERIMENTAL

The analyses were carried out using a Varian (Palo Alto, CA, USA) Model 3400 gas chromatograph equipped with dual flame ionization detector, packed columns, capillary split–splitless injectors and an integration system.

The following columns were used (Supelco, Bellefonte, PA, USA). (a) Two wide-bore glass capillary columns (60 m × 0.75 mm I.D.), *i.e.* a non-polar dimethylpolysiloxane (SPB-1) column and a polar polyethylene glycol column (Supelcowax-10). Both were operated at a flow-rate (nitrogen) of 7 cm^3/min. (b) Two packed columns (3 m × 2.1 mm I.D.), *i.e.* a non-polar column with 10% SP-2100 methylsilicone and a polar column with 10% SP-1000 (polyglycol substituted terephthalic acid) both on 80–100 mesh Supelcoport and operated at a flow-rate (nitrogen) of 30 cm^3/min.

The analyses used for measuring the absolute and relative retentions of the compounds were carried out under isothermal temperature conditions (60°C). The practical use of the method for routine analyses allowed a decrease of the total run time by proper temperature programming up to 150–180°C. The injector and detector temperatures were 200 and 250°C, respectively. The packed columns were installed on the two injectors and connected to the two flame ionization detectors to allow simultaneous injections onto the polar and non-polar phases. The wide-bore capillary columns were installed alone for the initial calibration and then connected in parallel to the split–splitless injectors by a microsplitting Y-shaped glass connector (press-fit fittings, Varian, Sunnyvale, CA, USA) that allowed the injected samples to be divided between the two columns leading to identical detectors. Splitless injections were made to avoid sample partition due to the different boiling points.

The outputs of the detectors were monitored with

dual-channel integrators or data systems (Varian 4400, Spectra Physics Chromjet, Varian Vista 420, Varian DS 650), the performances of which were evaluated to determine the possibility of achieving automatic identification of the mixture components.

The retention times of individual compounds were measured by injecting samples diluted in carbon disulphide with concentrations between 0.1 and 1 g/l, taking into account the different sensitivity of FID to various compounds, to give peaks with similar areas. Partial or complete mixtures of the components were also injected to check the effective capacity of the columns to separate closely eluting peaks.

RESULTS AND DISCUSSION

Table I lists the components of the mixture used in the order of elution on the non-polar column and their adjusted retention times, retention indices and retention relative to toluene on wide-bore non-polar and polar columns. Toluene was chosen as the reference compound because, as shown in Table III,

TABLE I

RETENTION VALUES ON NON-POLAR AND POLAR WIDE-BORE CAPILLARY COLUMNS

Adjusted retention times (t'_R), retention index with respect to *n*-alkanes (I) and retention relative to toluene (r) are shown. Column temperature, 60°C; carrier gas, nitrogen; flow-rate, 7 cm^3/min.

Compound	SPB-1			Supelcowax-10		
	t'_R (min)	I	r	t'_R (min)	I	r
(1) Ethanol	0.26	388	0.06	3.03	944	0.44
(2) Acetone	0.38	405	0.08	1.40	832	0.20
(3) Propan-2-ol	0.39	412	0.09	2.85	935	0.41
(4) Propan-1-ol	0.52	428	0.11	6.34	1046	0.92
(5) Dichloromethane	0.61	439	0.13	3.09	946	0.45
(6) Butan-2-one	1.01	482	0.22	2.55	919	0.37
(7) Ethyl acetate	1.21	496	0.26	2.26	902	0.33
(8) Trichloromethane	1.27	501	0.28	5.82	1034	0.85
(9) Butan-2-ol	1.38	520	0.30	9.18	1095	1.33
(10) 2-Methoxyethanol	1.46	533	0.32	17.14	1184	2.49
(11) 1,2-Dichloroethane	1.60	552	0.35	8.22	1080	1.19
(12) Isopropyl acetate	1.85	584	0.41	2.41	911	0.35
(13) Butan-1-ol	1.85	584	0.41	13.09	1146	1.90
(14) Benzene	1.97	598	0.44	3.50	964	0.51
(15) 2-Nitropropane	2.23	631	0.49	11.63	1129	1.69
(16) 1,2-Dichloropropane	2.47	658	0.54	6.94	1058	1.01
(17) Trichloroethylene	2.63	675	0.58	4.87	1010	0.71
(18) 2-Ethoxyethanol	2.75	687	0.61	23.22	1231	3.38
(19) Toluene	4.57	757	1.00	6.88	1057	1.00
(20) Isobutyl acetate	4.59	757	1.01	5.45	1025	0.79
(21) *n*-Butyl acetate	6.29	796	1.38	8.32	1082	1.21
(22) Tetrachloroethylene	6. 53	801	1.43	5.97	1038	0.87
(23) 4-Hydroxymethylpentan-2-one	7.20	813	1.58	59.59	1374	8.66
(24) 5-Methylhexan-2-one	8.69	836	1.90	13.53	1150	1.97
(25) Ethylbenzene	9.56	848	2.10	12.37	1138	1.80
(26) *p*-Xylene	10.23	856	2.25	13.00	1145	1.89
(27) *m*-Xylene	10.23	856	2.25	13.62	1151	1.98
(28) Cyclohexanone	10.60	861	2.35	35.97	1301	5.23
(29) Isoamylacetate	10.65	862	2.37	11.79	1131	1.71
(30) *o*-Xylene	12.16	878	2.67	18.24	1193	2.65
(31) 2-Ethoxyethyl acetate	12.64	882	2.80	40.53	1319	5.89
(32) 2-Butoxyethanol	13.18	888	2.93	79.52	1416	11.56

it is present in most of the samples. Table II shows the retention times and relative retention measured on packed columns. The choice of the mixture compounds was made on the basis of available data on the typical composition of industrial solvents, MS identification of the components of various wastes and statistical evaluation of the probability of finding some compounds in different kinds of process by-products. As an example, Table III shows the distribution of the main components in the cargo of MV *Zanoobia*. The percentage value of samples (barrels) containing the listed compounds as main components or at a concentration greater than 0.5% is given. Other compounds listed in Tables I and II but not in Table III were also found in some samples in various concentrations.

Table IV shows the compounds listed in order of elution on the non-polar and polar wide-bore capillary columns, and the compounds that are not resolved on each column are bracketed. The elution order on the packed non-polar and polar columns (SP-2100 and SP-1000) was similar to that observed on the corresponding wide-bore capillary column. A greater number of interfering groups was observed, as shown in Table V.

The different polarities of the stationary phases

TABLE II

RETENTION VALUES ON NON-POLAR AND POLAR PACKED COLUMNS

Adjusted retention times (t'_R) and retention relative to toluene (r) are shown. Column temperature, 60°C; carrier gas, nitrogen; flow-rate, 30 cm^3/min.

Compound	SP-2100		SP-1000	
	t'_R (min)	r	t'_R (min)	r
(1) Ethanol	0.20	0.04	6.12	0.48
(2) Acetone	0.51	0.10	2.71	0.21
(3) Propan-2-ol	0.51	0.10	5.55	0.44
(4) Propan-1-ol	0.66	0.13	12.17	0.96
(5) Dichloromethane	0.66	0.13	5.61	0.44
(6) Butan-2-one	1.20	0.24	4.94	0.39
(7) Ethyl acetate	1.41	0.28	4.34	0.34
(8) Trichloromethane	1.41	0.28	10.65	0.84
(9) Butan-2-ol	1.55	0.31	17.39	1.38
(10) 2-Methoxyethanol	1.76	0.35	34.41	2.72
(11) 1,2-Dichloroethane	1.76	0.35	15.11	1.20
(12) Isopropryl acetate	2.15	0.42	4.56	0.36
(13) Butan-1-ol	2.15	0.42	25.93	2.05
(14) Benzene	2.15	0.42	6.41	0.51
(15) 2-Nitropropane	2.48	0.49	21.77	1.72
(16) 1,2-Dichloropropane	2.71	0.54	12.86	1.02
(17) Trichloroethylene	2.88	0.57	8.91	0.71
(18) 2-Ethoxyethanol	3.50	0.69	45.77	3.62
(19) Toluene	5.06	1.00	12.63	1.00
(20) Isobutyl acetate	5.06	1.00	10.44	0.83
(21) *n*-Butyl acetate	7.14	1.41	15.95	1.26
(22) Tetrachloroethylene	7.14	1.41	11.08	0.88
(23) 4-Hydroxymethylpentan-2-one	8.22	1.62	112.87	8.94
(24) 5-Methylhexan-2-one	9.77	1.93	25.77	2.04
(25) Ethylbenzene	10.49	2.07	22.89	1.81
(26) *p*-Xylene	11.25	2.22	23.43	1.86
(27) *m*-Xylene	11.25	2.22	25.10	1.99
(28) Cyclohexanone	11.84	2.34	68.23	5.40
(29) Isoamyl acetate	11.84	2.34	22.44	1.78
(30) *o*-Xylene	13.34	2.64	33.61	2.66
(31) 2-Ethoxyethyl acetate	14.44	2.85	77.29	6.12
(32) 2-Butoxyethanol	16.68	3.30	153.32	12.14

TABLE III

RELATIVE ABUNDANCE OF SAMPLES CONTAINING VARIOUS SOLVENTS IN THE CARGO OF THE MV *ZANOOBIA*

Compound	Percentage of samples containing compound
Toluene	54
Xylene	53
Benzene	23
Tetrachloroethylene	21
Trichloroethylene	19
Trichloromethane	18
Dichloromethane	12
Acetone	11
Ethyl acetate	7
Butan-2-one	7
1,2-Dichloroethane	6
2-Butoxyethanol	3
1,2-Dichloropropane	3
2-Ethoxyethylacetate	1
2-Methoxyethanol	1
Ethanol	1

result in a very different distribution of peaks in the chromatograms and therefore no couple of compounds shows the same interference on both columns. Capillary columns are much more efficient than packed columns and therefore less interfering peaks are observed.

The data in Table I and II refer to isothermal analysis to allow a correct determination of the retention index values and the relative retention. These values can also be applied to programmed temperature analysis by correction factors or by using interpolation programmes.

For routine analysis, the total time needed for the complete elution of all of the listed compounds can be reduced by temperature programming, without an appreciable reduction in the resolution; the peaks separated during isothermal runs show the same behaviour during programmed analysis. In some instances, the separation of partially co-eluted peaks (see Tables IV and V) slightly increases in programmed runs, probably due to a different slope of the vapour pressure *versus* temperature plot.

Programming the temperature from the initial 60°C at a rate of 5°C/min decreased the retention time of the last eluting peaks on polar columns by about 50%. By decreasing the initial temperature at about 35°C and by programming the temperature of non-polar columns, the resolution of the fast eluting peaks increased and the total run length decreased by about 20%.

Quantitative determination of co-eluted peaks

When two or more compounds are co-eluted on a column, the confirmation of the identity and the quantitation have to be carried out using the chromatogram obtained on the other column. Table IV shows that on the Supelcowax-10 five couples and a triplet of compounds are co-eluted, whereas eight couples show interference on SPB-1. Some of the couples observed on the Supelcowax-10 column are formed by a chlorinated compound and an alcohol (peaks 1 and 5), an aromatic (peaks 20 and 16) and an acetate (peaks 11 and 21), interferences which are not common in real samples. It is therefore convenient to use the polar column for the analysis and the non-polar column for confirmation.

If all the listed compounds are simultaneously contained in the mixture, as a result of the mixing of industrial by-products and wastes of various origins, the complete identification and quantitation are carried out by taking into account both columns. Some typical examples of the procedure, which can also be used as a track for the compilation of computer programs for automatic identification, are given below.

1. Compounds co-eluted on the Supelcowax-10 column are separated on the SPB-1 column (peaks 11 and 21); quantitative analysis is made by using the results obtained on the non-polar column.

2. Compounds co-eluted on the Supelcowax-10 column (couples 1 and 5, 8 and 22, 20 and 16, 15 and 29) are well separated on the SPB-1 column (peaks 1, 15, 16, 22), whereas other peaks show interference with other substances. Comparison of the corrected peak areas allow their amounts to be calculated. As an example, if ethanol is the only component of the couple 1 and 5 to be present, it can be identified on the SPB-1 column and the amounts of compound on both columns is equal. If only dichloromethane is present in the sample, no peak will be observed on the SPB-1 column at the ethanol retention time, and the amount of dichloromethane is calculated from the area of the peak on the polar column. If both compounds are present, the amount of ethanol is measured on the SPB-1

column and dichloromethane by the difference between the two columns. The single peak of propan-1-ol on the Supelcowax-10 column can assist in confirming the composition of the couple 4 and 5 and the SPB-1 column.

3. When a triplet of compounds is co-eluted (peaks 13, 24 and 27) a similar procedure can be followed. If only 5-methyl-2-hexanone (compound 24) is present in the sample, the amount on the SPB-1 column should be equal to the amount on the Supelcowax column. On the SPB-1 column butan-1-ol is co-eluted with isopropyl acetate. The latter compound shows no interference on the Supelcowax-10 column and can therefore be quantitated on this column and used to calculated the amount of butan-1-ol by difference on the SPB-1 column. The same procedure can be followed for the third component of the triplet (*m*-xylene), which is co-eluted on the SPB-1 column with *p*-xylene, but as this compound shows no interference on the Supelcowax-10 column, quantitation by difference is possible.

Data integration and automatic identification

The performance of different integrators and data systems for the automatic identification of the

TABLE IV

ELUTION ORDER OF ANALYSED COMPOUNDS

Non-polar (SPB-1) and polar (Supelcowax-10) wide-bore capillary columns were used at 60°C. Compounds not resolved are bracketed. Numbers as in Tables I and II.

SPB-1	Supelcowax-10
(1) Ethanol	(2) Acetone
[(2) Acetone	(7) Ethyl acetate
(3) Propan-2-ol	(12) Isopropyl acetate
[(4) Propan-1-ol	(6) Butan-2-one
(5) Dichloromethane	(3) Propan-2-ol
[(6) 2-Butan-2-one	[(1) Ethanol
(7) Ethyl acetate	(5) Dichloromethane
(8) Trichloromethane	(14) Benzene
[(9) Butan-2-ol	(17) Trichloroethylene
(10) 2-Methoxyethanol	(20) Isobutyl acetate
(11) 1,2-Dichloroethane	[(8) Trichloromethane
[(12) Isopropyl acetate	(22) Tetrachloroethylene
(13) Butan-1-ol	(4) Propan-1-ol
(14) Benzene	[(19) Toluene
(15) 2-Nitropropane	(16) 1,2-Dichloropropane
(16) 1,2-Dichloropropane	[(11) 1,2-Dichloroethane
(17) Trichloroethylene	(21) *n*-Butyl acetate
(18) 2-Ethoxyethanol	(9) Butan-2-ol
[(19) Toluene	[(15) 2-Nitropropane
(20) Isobutyl acetate	(29) Isoamyl acetate
(21) *n*-Butyl acetate	(25) Ethylbenzene
(22) Tetrachloroethylene	(26) *p*-Xylene
(23) 4-Hydroxymethylpentan-2-one	⌐ (13) Butan-1-ol
(24) 5-Methylhexan-2-one	| (24) 5-Methyl-hexan-2-one
(25) Ethylbenzene	⌊ (27) *m*-Xylene
[(26) *p*-Xylene	(10) 2-Methoxyethanol
(27) *m*-Xylene	(30) *o*-Xylene
[(28) Cyclohexanone	(18) 2-Ethoxyethanol
(29) Isoamyl acetate	(28) Cyclohexanone
(30) *o*-Xylene	(31) 2-Ethoxyethyl acetate
(31) 2-Ethoxyethyl acetate	(23) 4-Hydroxymethyl-pentan-2-one
(32) 2-Butoxy ethanol	(32) 2-Butoxyethanol

separated compounds was evaluated. The following three commercially available devices were tested: Varian 4400 with memory module and replot option (equivalent to Spectra Physics Chromjet), Varian Vista 420 and Varian DS 650, all equipped with dual-channel input.

The aim was to investigate if the standard features of the integrators were suitable for identification of the compounds without the need for special programming.

Fig. 1 shows a flow-chart for the procedure in which the integrators compare the results of two chromatographic runs on the basis of the identified peaks, independent of their retention on the two columns (Varian data systems).

The outputs of the two flame ionization detectors are integrated by the data systems and names are attributed to the peaks on the basis of the retention times within a fixed tolerance and the retention times of individual peaks corrected by linear interpolariton between the retention times of "reference peaks" (generally the largest peaks in a given portion of the chromatogram), identified with variable tolerance of the retention times (window).

After the identification, correction factors are applied and the quantitative report for each column is

TABLE V

ELUTION ORDER OF ANALYSED COMPOUNDS

Non-polar (SP-2100) and polar (SP-1000) packed columns were used at 60°C. Compounds not resolved are bracketed. Numbers as in Tables I and II.

SPB-2100	SP-1000
(1) Ethanol	(2) Acetone
[(2)Acetone	(7) Ethyl acetate
[(3) Propan-2-ol	(12) Isopropyl acetate
(4) Propan-1-ol	(6) Butan-2-one
[(5) Dichloromethane	[(3) Propan-2-ol
(6) Butan-2-one	[(5) Dichloromethane
[(7) Ethyl acetate	(1) Ethanol
[(8) Trichloromethane	(14) Benzene
(9) Butan-2-ol	(17) Trichloroethylene
[(10) 2-Methoxyethanol	[(20) Isobutyl acetate
[(11) 1,2-Dichloroethane	[(8) Trichloromethane
[(12) Isopropyl acetate	[(22) Tetrachloroethylene
[(13) Butan-1-ol	[(4) Propan-1-ol
[(14) Benzene	[(19) Toluene
(15) 2-Nitropropane	[(16) 1,2-Dichloropropane
(16) 1,2-Dichloropropane	(11) 1,2-Dichloroethane
(17) Trichloroethylene	(21) *n*-Butyl acetate
(18) 2-Ethoxyethanol	(9) Butan-2-ol
[(19) Toluene	[(15) 2-Nitropropane
[(20) Isobutyl acetate	[(29) Isoamyl acetate
[(21) *n*-Butyl acetate	[(25) Ethylbenzene
[(22) Tetrachloroethylene	(26) *p*-Xylene
(23) 4-Hydroxymethylpentan-2-one	[(27) *m*-Xylene
(24) 5-Methylhexan-2-one	[(24) 5-Methyl-hexan-2-one
(25) Ethylbenzene	[(13) Butan-1-ol
[(26) *p*-Xylene	[(30) *o*-Xylene
[(27) *m*-Xylene	[(10) 2-Methoxyethanol
[(28) Cyclohexanone	(18) 2-Ethoxyethanol
[(29) Isoamyl acetate	(28) Cyclohexanone
(30) *o*-Xylene	(31) 2-Ethoxyethyl acetate
(31) 2-Ethoxyethyl acetate	(23) 4-Hydroxymethyl-pentan-2-one
(32) 2-Butoxy ethanol	(32) 2-Butoxyethanol

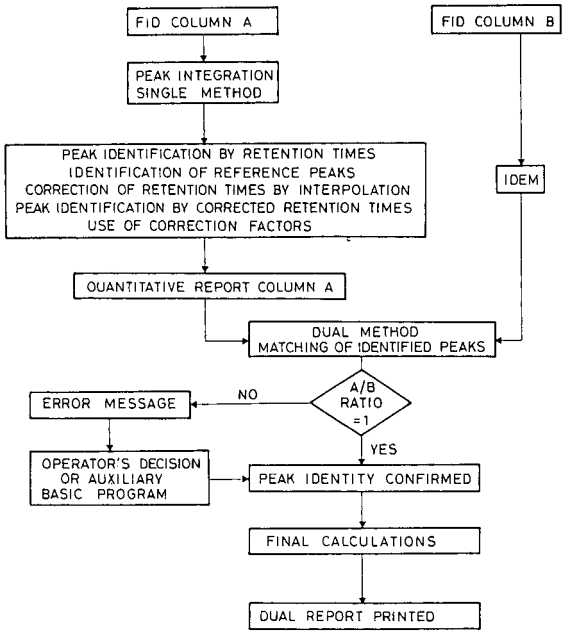

Fig. 1. Flow-chart of the program used by the integrators or data system to identify peaks by simultaneous analysis on columns of various polarities.

printed. By further elaboration, the ratio between the areas or the corrected amounts of the peaks identified on the two columns can be determined automatically. If the ratio for a given compound is equal or nearly equal to unity, this peak can be considered as free of interferences on both columns and, as a result of the different polarities of the stationary phases, its identity is confirmed. If the ratio is not unity, an error message appears and the chromatogram should be interpreted by the operator as described earlier to determine what kind of interference is present and to identify the peaks correctly.

A BASIC program can also be written for the Varian 4400 or Spectra Physics integrators equipped with this option, or for the standard Varian DS 650 data system, which, by using simple IF/AND/OR statements and comparing the calculated corrected peak areas, can determine whether (a) peaks mixed on column A are fully separated on column B and (b) peaks mixed on column A show interference with other peaks on column B.

The first situation, identical to example (1) of the preceding section, is relatively easy to solve because the total amount calculated on column A should correspond to the sum of amounts calculated for the two peaks on column B (after the application of correction factors), whereas complex consideration, and sophisticated programming may be necessary for solving situation (b). The logical flow-sheet of the program can follow the procedure outlined in examples (2) and (3) of the preceding section. Complex programs can identify all the compounds listed in Tables I and II automatically. Relatively simple programs are often sufficient, because the occurrence of situation (b) is infrequent in real samples as waste from different industries has a typical composition, is generally composed of only few substances and never contains all the compounds in this text mixture.

For quantitative analysis, it should be taken into account that sample distribution between the two columns connected in parallel, the different elution order on polar and non-polar columns and the changing peak shapes (due to the polarity of the compounds or to column overloading by highly concentrated samples) may lead to appreciable differences between the correction factors for the same compound on the two detectors. These must therefore be experimentally measured and checked periodically by injecting known samples.

REFERENCES

1 *Organic Solvents in Air*, NIOSH Manual of Analytical Methods, Part I, DHEW (NIOSH) Publication No. 77-157-A, National Institute for Occupational Safety and Health, Cincinatti, OH, 1987.
2 *Direct Injection of Solvent-based Paints in a Gas Chromatograph for Solvent Analysis*, ASTM D3271/76, ASTM Standards on Gas Chromatography, Philadelphia, PA, 1981.
3 *Measuring Volatile Organic Matter in Water by Aqueous Injection Gas Chromatography*, ASTM-D-2908, ASTM Standards on Chromatography, Philadelphia, PA, 1981.
4 *Methods for Organic Chemical Analysis of Municipal and Industrial Waste Water*, U.S. Environmental Protection Agency, Washington, DC, Publication No. 605/4-82-057, 1982.
5 *Analysis of Organic Compound Vapors Collected by the Activated Charcoal Adsorption Method*, ASTM-D-3687, ASTM Standards on Chromatography, Philadelphia, PA, 1981.
6 N. Kishen, B. Thomson and E. Almasi, *Varian Instruments at Work*, Varian Instrument Group, Walnut Creek, CA, 96 (1987) 1–19.
7 *Test Methods for Evaluating Solid Waste (Physical/Chemical Methods)*, U.S. Environmental Protection Agency, Washington, DC, Publication No. SW-846, 1B, 1986.
8 S. Arazzini, G. M. Baruchello and G. Lupoi, presented at the *5th International Conference on Solid Waste, Sludge and Residual Material, Rome, April 26–29, 1989.*

Journal of Chromatography, 585 (1991) 281–288
Elsevier Science Publishers B.V., Amsterdam

CHROM. 23 523

Studies on steroids

CCLIII[☆]. Capillary gas chromatographic behaviour of diethylhydrogensilyl–diethylsilylene derivatives of stereoisomeric bile acids

Junichi Goto*, Yukari Teraya and Toshio Nambara

Pharmaceutical Institute, Tohoku University, Aobayama, Sendai 980 (Japan)

Takashi Iida

College of Engineering, Nihon University, Koriyama 963 (Japan)

(First received March 15th, 1991; revised manuscript received May 30th, 1991)

ABSTRACT

The capillary gas chromatographic behaviour of diethylhydrogensilyl (DEHS) ethers and/or diethylsilylene (DES) derivatives of fifty bile acids including 4- and 6-hydroxylated compounds is described. The methylene unit (MU) values of methyl and pentafluorobenzyl esters of bile acids were determined as their trimethylsilyl (TMS), dimethylethylsilyl (DMES) ethers and DEHS–DES derivatives. The differences in methylene unit values between the corresponding TMS ethers and DMES ethers or DEHS–DES derivatives were used for estimating the number and stereochemistry of hydroxyl groups on the steroid nucleus. On treatment with the silylating agent N,O-bis (diethylhydrogensilyl)trifluoroacetamide, bile acids possessing isolated hydroxyl in addition to diaxial *trans*-glycol groups were easily converted into the DEHS ehters, whereas those having a vicinal glycol group except for the diaxial group were converted into cyclic DES derivatives. The mass spectrometric properties obtained with negative-ion chemical ionization detection are discussed.

INTRODUCTION

Bile acids are the major biotransformation products from cholesterol and assist the lipolysis and absorption of fats by the formation of mixed micelles in the intestinal lumen. Unusual bile acids having a vicinal glycol structure at C-3,4 or C-6,7 have recently been found in patients with liver diseases and in newborn infants and foetuses [1–3]. Accordingly, the development of a reliable method for the determination of these unusual bile acids in biological materials in connection with the diagnosis of hepatobiliary diseases is urgently required.

Gas chromatography (GC) is a powerful tool for the profile analysis of bile acids in biological specimens. The trimethylsilyl (TMS) [4,5] and dimethylethylsilyl (DMES) ethers [6–8] have been extensively used as derivatives suitable for the GC determination of bile acids. However, no satisfactory derivatization of bile acids including unusual ones is at present available for their complete separation. Also, diacetoxydimethylsilane has been shown to be suitable for the derivatization of biological substances with a vicinal glycol moiety [9]. Unfortu-

[☆] For Part CCLII, see J. Goto, Y. Saisho and T. Nambara, *J. Chromatogr.*, 567 (1991) 343.

0021-9673/91/$03.50

nately, this derivatizatization procedure has a disadvantage regarding the stability of the resulting dimethylsiliconide [10]. Although alkyl boronic acids are commonly used for the formation of stable cyclic boronates from the 1,2- and 1,3-glycols, this method requires successive derivatization of isolated hydroxyl groups [11].

In order to overcome these problems, a new silylating agent, N,O-bis(diethylhydrogensilyl)trifluoroacetamide (DEHS-BSTFA), has recently been developed and applied to the separation and determination of steroids and prostaglandins in biological fluids [12–14]. This novel reagent reacts readily with an isolated hydroxyl group to form the diethylhydrogensilyl (DEHS) ether and with a vicinal glycol to form the cyclic diethylsilylene (DES) derivative simultaneously. This paper deals with the capillary GC behaviour of DEHS ether and/or DES derivatives of bile acids having hydroxyl group(s) at C-3, -4, -6, -7 and/or -12.

EXPERIMENTAL

Gas chromatography

A Model GC-15A gas chromatograph (Shimadzu, Kyoto, Japan) equipped with a flame ionization detector and a Van den Berg solventless injector was employed. A cross-linked methylsilicone fused-silica capillary column (25 m × 0.3 mm I.D.) (Hewlett-Packard, Avondale, PA, USA) was used. The temperature of the column oven was maintained at 240–290°C and those of the injection heating block and detector were kept at 280°C and 290°C, respectively. The carrier gas was nitrogen at a linear velocity of 40 cm/s.

Gas chromatography–mass spectrometry (GC–MS)

Capillary GC–MS was carried out using a Model MM12030 quadrupole mass spectrometer (VG Analytical, Manchester, UK) interfaced to an HP 5790A gas chromatograph (Hewlett-Packard) with a Van den Berg solventless injector. Isobutane was used as a reagent gas. A cross-linked 5% phenylmethylsilicone fused-silica capillary column (20 m × 0.3 mm I.D.) (J &W Scientific, Folsom, CA, USA) was inserted into the ion source through the direct inlet. The carrier gas was helium at a linear velocity of 65 cm/s. The injection port, column oven and ion source were kept at 280, 260–290 and 270°C, respectively. The ionization energy was 70 eV and the emission current was 400 μA.

Materials

Cholic, chenodeoxycholic, deoxycholic and lithocholic acids were purchased from Sigma (St. Louis, MO, USA) and ursodeoxycholic acid was kindly donated by Tokyo Tanabe (Tokyo, Japan). Other stereoisomeric bile acids were prepared in these laboratories by methods reported previously [15–17]. Dimethylethylsilylimidazole was supplied by Tokyo Kasei Kogyo (Tokyo, Japan) and DEHS-BSTFA, supplied by Tokyo Kasei Kogyo, was synthesized by a known method [12]. All chemicals employed were of analytical-reagent grade and purified by distillation prior to use.

Derivatization of bile acids

The pentafluorobenzyl (PFB) esters were prepared by treating bile acids with 5% (v/v) PFB bromide in acetonitrile (60 μl) and diisopropylethylamine (10 μl) at 37°C for 45 min. The reaction mixture was treated on a Sep-Pak C_{18} cartrdige (Waters–Millipore, Milford, MA, USA) and the PFB esters were eluted with ethanol–acetonitrile (1:1) [18]. The methyl esters of bile acids were prepared by treatment with hydrochloric acid–methanol or diazomethane–diethyl ether–methanol in the usual manner [4].

The bile acid esters thus obtained were derivatized to the corresponding TMS, DMES and DEHS–DES derivatives with hexamethyldisilazane–trimethylchlorosilane in pyridine at 60°C for 90 min, DMES-imidazole in 1% pyridine in hexane at 60°C for 60 min and DEHS-BSTFA in pyridine for 60 min at room temperature, respectively. The reaction product exhibited a single peak of the theoretical shape.

RESULTS AND DISCUSSION

Gas chromatographic behaviour of bile acids with hydroxyl groups at C-3, -7 and -12

Fifty bile acids were used for investigating the GC behaviour of DEHS ether and/or DES derivatives as well as dimethylethylsilyl (DMES) ethers, which have been widely utilized in the GC analysis of biologically active compounds [6–8].

Initially, methylene unit (MU) values of DMES

and DEHS ethers of bile acids with isolated hydroxyl group(s) at C-3, -7 and -12 were determined and the results obtained are given in Table I. The $\Delta[Um]_{DMES}$ and $\Delta[Um]_{DEHS}$ values [19], which are defined as the differences in MU values between TMS ethers and DMES or DEHS ethers, are also listed. All bile acids were readily converted into TMS, DMES and DEHS ethers under the mild condition and the resulting derivatives exhibited a single peak of the theoretical shape. The DEHS ethers gave larger MU values than the corresponding DMES ethers. The $\Delta[Um]_{DEHS}$ values of methyl esters were 1.80 ± 0.26 for six monohydroxylated, 3.32 ± 0.24 for twelve dihydroxylated and 4.84 ± 0.25 for eight trihydroxylated bile acids, whereas those of PFB esters were 1.69 ± 0.32, 3.30 ± 0.25 and 4.74 ± 0.22, respectively.

The relationships between hydroxyl group number and Δ[Um] values of DMES and DEHS ethers are shown in Fig. 1. When $\Delta[Um]_{DEHS}$ values of the methyl and PFB esters were plotted against hydroxyl group number, good linearities, defined as $y = 1.514x + 0.294$ ($r = 0.979$) and $y = 1.517x + 0.217$ ($r = 0.976$), were observed. The data indicate that the presence of one hydroxyl group exerts consistently an increment of 1.5 units in the $\Delta[Um]_{DEHS}$ value. Regression lines expressed as $y = 0.940x + 0.347$ ($r = 0.979$) and $y = 0.985x + 0.187$ ($r = 0.977$) were obtained for DMES ether-methyl ester and -PFB ester derivatives, respectively. These results are in good agreement with earlier findings on hydroxysteroids [6], implying that the number of hydroxyl groups on the steroid nucleus of bile acids may possibly be deduced from the regression equation.

Gas chromatographic behaviour of bile acids with a vicinal glycol

The MU and Δ[Um] values of 4- and 6-hydroxylated bile acids were then determined (Table II). The Δ[Um] values of DMES ethers obtained from the data were 2.42 ± 0.24 (methyl ester) and 2.27 ± 0.15 (PFB ester) for seven dihydroxylated, 3.08 ± 0.18 (methyl ester) and 3.00 ± 0.18 (PFB ester) for thirteen trihydroxylated and 3.98 ± 0.21 (methyl esters) and 3.89 ± 0.20 (PFB ester) for four tetrahydroxylated bile acids, being in good agreement with those of bile acids listed in Table I [dihydroxylated, 2.23 ± 0.12 (methyl ester), 2.20 ± 0.14 (PFB ester); trihydroxylated, 3.16 ± 0.20 (methyl ester), 3.11 ± 0.16 (PFB ester)].

On the other hand, bile acid derivatives obtained with DEHS-BSTFA exhibited different chromatographic behaviour. Bile acids possessing isolated hydroxyl groups and/or a diaxial *trans*-glycol group at C-3,4 or C-6,7 provided almost identical Δ[Um] values with those of bile acids described above. These results indicate that all hydroxyl groups on the steroid nucleus would be derivatized into DEHS ethers. The correlation of MU values between DMES ethers of bile acids and corresponding DEHS ethers is expressed as the regression line A ($y = 1.072x - 1.412$, $r = 0.993$, $n = 68$) in Fig. 2. The Δ[Um] values obtained from bile acids possess-

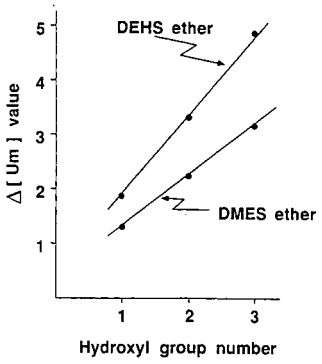

Fig. 1. Correlations between hydroxyl group number and Δ[Um] values of DMES or DEHS ethers for bile acid methyl esters with isolated hydroxyl group(s).

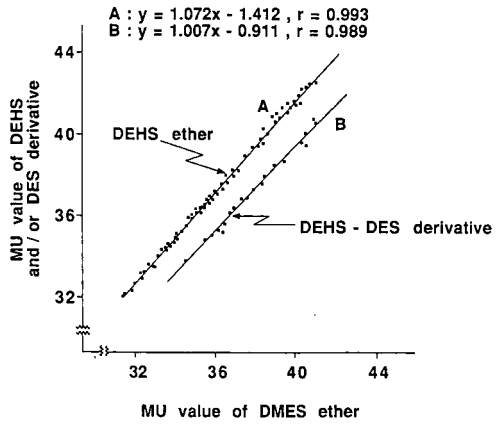

Fig. 2. Correlations in MU values between the corresponding DMES ethers and DEHS ethers or DEHS–DES derivatives.

TABLE I

METHYLENE UNIT AND Δ[Um] VALUES OF BILE ACIDS WITH ISOLATED HYDROXYL GROUP(S)

5β-Cholanoic acid	TMS MU	DMES		DEHS	
		MU	Δ[Um][a]	MU	Δ[Um][a]
Methyl ester					
3α	30.95	32.39	1.44	32.98	2.03
3β	30.88	32.31	1.43	32.97	2.09
7α	29.46	30.74	1.28	31.12	1.66
7β	30.32	31.43	1.11	32.17	1.85
12α	29.29	30.44	1.15	30.68	1.39
12β	29.10	30.38	1.28	30.90	1.80
3α,7α	31.88	34.23	2.35	35.27	3.39
3α,7β	32.43	34.65	2.22	35.86	3.43
3β, 7α	31.49	33.76	2.27	34.93	3.44
3β,7β	32.41	34.76	2.35	36.06	3.63
3α,12α	31.59	33.78	2.19	34.82	3.23
3α,12β	31.50	33.62	2.12	34.88	3.38
3β,12α	31.58	33.74	2.16	34.73	3.15
3β,12β	31.65	33.94	2.29	35.32	3.67
7α,12α	30.09	32.51	2.42	33.05	2.96
7α,12β	30.02	32.29	2.27	33.30	3.28
7β,12α	31.04	33.02	1.98	33.90	2.86
7β,12β	31.20	33.39	2.19	34.59	3.39
3α,7α,12α	32.00	35.39	3.39	36.94	4.94
3α,7α,12β	32.18	35.08	2.90	36.78	4.60
3α,7β,12α	32.67	35.62	2.95	37.20	4.53
3α,7β,12β	32.79	35.86	3.07	37.63	4.84
3β,7α,12α	31.76	35.14	3.38	36.76	5.00
3β,7α,12β	31.92	35.14	3.22	36.81	4.89
3β,7β,12α	32.67	35.70	3.03	37.30	4.63
3β,7β,12β	33.01	36.38	3.37	38.29	5.28
PFB ester					
3α	36.32	37.51	1.19	38.19	1.87
3β	36.36	37.66	1.30	38.38	2.02
7α	34.73	35.76	1.03	36.38	1.65
7β	35.35	36.70	1.35	37.25	1.90
12α	34.58	35.45	0.87	35.72	1.14
12β	34.25	35.24	0.99	35.82	1.57
3α,7α	36.93	39.14	2.21	40.26	3.33
3α,7β	37.39	39.48	2.09	40.84	3.45
3β,7α	36.56	38.91	2.35	39.90	3.34
3β,7β	37.40	39.85	2.45	41.16	3.76
3α,12α	36.71	38.80	2.09	39.72	3.01
3α,12β	36.36	38.46	2.10	39.74	3.38
3β,12α	36.70	38.91	2.21	39.86	3.16
3β,12β	36.60	39.01	2.41	40.13	3.53
7α,12α	35.19	37.52	2.33	38.49	3.30
7α,12β	35.03	37.12	2.09	37.98	2.95
7β,12α	35.86	37.88	2.02	38.79	2.93
7β,12β	35.86	38.02	2.16	39.23	3.37
3α,7α,12α	36.98	40.40	3.42	41.80	4.82
3α,7α,12β	36.72	39.80	3.08	41.36	4.64
3α,7β,12α	37.50	40.40	2.90	41.88	4.38
3α,7β,12β	37.27	40.30	3.03	42.08	4.81
3β,7α,12α	36.67	39.88	3.21	41.52	4.85
3β,7α,12β	36.65	39.73	3.08	41.42	4.77
3β,7β,12α	37.47	40.44	2.97	41.98	4.51
3β,7β,12β	37.69	40.84	3.15	42.80	5.11

[a] Differences in MU values between the corresponding TMS ethers and DMES or DEHS ethers.

TABLE II

METHYLENE UNIT AND Δ[Um] VALUES OF 4- AND 6-HYDROXYLATED BILE ACIDS

5β-Cholanoic acid	TMS MU	DMES		DEHS and/or DES	
		MU	Δ[Um][a]	MU	Δ[Um][a]
Methyl ester					
3α,4β	33.17	35.34	2.17	34.85	1.68
3β,4α	31.22	33.57	2.35	34.97	3.75
3β,4β	32.66	34.97	2.31	34.51	1.85
3α,4β,7α	33.60	36.72	3.12	35.96	2.36
3α,4β,12α	33.74	37.01	3.27	35.43	1.69
3β,4β,7α	33.92	36.76	2.84	35.65	1.73
3β,4α,12α	32.49	35.67	3.18	36.86	4.37
3β,4β,12α	32.88	36.00	3.12	36.02	3.14
3α,4β,7α,12α	34.48	38.45	3.97	37.62	3.14
3β,4β,7α,12α	34.24	38.00	3.76	37.35	3.11
3α,6α	32.17	34.49	2.32	35.86	3.69
3α,6β	31.98	34.38	2.40	35.80	3.82
3β,6α	32.28	34.76	2.48	36.14	3.86
3β,6β	31.51	34.42	2.91	35.80	4.29
3α,6α,7α	32.94	36.02	3.08	37.31	4.37
3α,6α,7β	34.21	37.00	2.79	36.62	2.41
3α,6β,7α	32.08	35.21	3.13	36.82	4.74
3α,6β,7β	33.11	36.16	3.05	37.14	4.03
3β,6α,7α	32.81	35.92	3.11	36.54	3.73
3β,6α,7β	34.44	37.20	2.76	36.35	1.91
3β,6β,7α	31.70	34.94	3.24	36.54	4.84
3β,6β,7β	33.17	36.47	3.30	37.14	3.97
3α,6α,7α,12α	32.92	37.18	4.26	38.64	5.72
3α,6β,7β,12α	32.79	36.70	3.91	38.54	5.75
PFB ester					
3α,4β	38.42	40.56	2.14	40.10	1.68
3β,4α	36.47	38.65	2.18	40.48	4.01
3β,4β	38.14	40.28	2.14	39.76	1.62
3α,4β,7α	38.70	41.64	2.94	41.12	2.42
3α,4β,12α	38.91	41.98	3.02	40.42	1.51
3β,4β,7α	38.96	41.66	2.70	40.76	1.80
3β,4α,12α	37.45	40.66	3.21	41.96	4.51
3β,4β,12α	37.86	41.00	3.14	41.16	3.30
3α,4β,7α,12α	39.39	43.18	3.79	42.66	3.27
3β,4β,7α,12α	38.98	42.66	3.68	42.30	3.32
3α,6α	37.24	39.46	2.22	40.94	3.70
3α,6β	37.08	39.32	2.24	40.86	3.78
3β,6α	37.45	39.98	2.53	41.40	3.95
3β,6β	37.02	39.46	2.44	41.02	4.00
3α,6α,7α	37.82	40.88	3.06	42.38	4.56
3α,6α,7β	39.10	41.96	2.86	41.54	2.44
3α,6β,7α	36.91	39.96	3.05	41.66	4.75
3α,6β,7β	38.20	41.02	2.82	42.08	3.88
3β,6α,7α	37.74	40.92	3.18	41.68	3.94
3β,6α,7β	39.35	42.06	2.71	41.40	2.05
3β,6β,7α	36.63	39.72	3.09	41.38	4.75
3β,6β,7β	38.16	41.40	3.24	42.26	4.10
3α,6α,7α,12α	37.74	41.88	4.14	43.42	5.68
3α,6β,7β,12α	37.34	41.30	3.96	43.32	5.98

[a] Differences in MU values between the corresponding TMS ethers and DMES ethers or DEHS–DES derivatives.

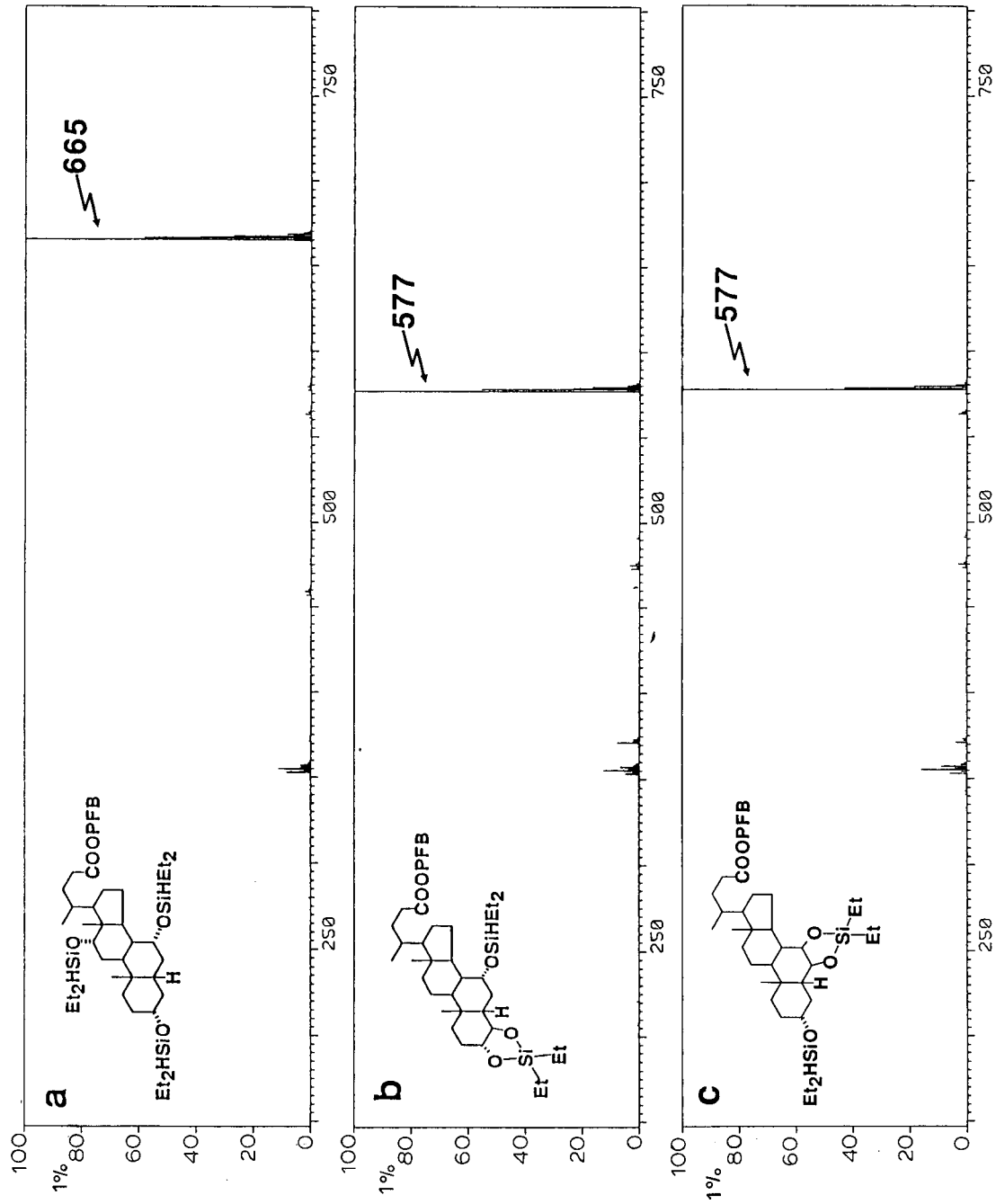

Fig. 3. Isobutane NICI mass spectra of trihydroxylated bile acids. (a) DMES ether of 3α, 7α, 12α-trihydroxy-5β-cholanoic acid (cholic acid) (b) DEHS–DES derivative of 3α,4β,7α-trihydroxy-5β-cholanoic acid; (c) DEHS–DES derivative of 3α,6β,7β-trihydroxy-5β-cholanoic acid. Et = Ethyl.

ing a diequatorial *trans*-glycol or axial–equatorial *cis*-glycol structure at C-3,4 and a diequatorial *trans*-glycol structure at C-6,7 were much smaller than those of DEHS ethers obtained from bile acids with isolated hydroxyl groups. Moreover, the MU values of these bile acid derivatives were smaller than those of the corresponding DMES ethers, as shown in the regression line B ($y = 1.007x - 0.911$, $r = 0.989$, $n = 20$), indicating the formation of cyclic DES derivatives. It is of interest that the Δ[Um] values of 6-hydroxylated bile acids having a *cis*-glycol of axial–equatorial nature (or *vice versa*), which are easily transformed into cyclic boronates with alkylboronic acids [20], were much larger than those of DES derivatives of bile acids mentioned above, but smaller than those of DEHS derivatives of bile acids having isolated hydroxyl groups.

It has been demonstrated that the introduction of a PFB group into the carboxyl function would be most favourable for the formation of a characteristic carboxylate anion, $[M-PFB]^-$, in the negative-ion chemical ionization (NICI) mode [6,18]. Therefore, GC–MS with NICI detection was utilized for the structural characterization of these derivatives. As illustrated in Fig. 3a, DEHS derivatives exhibited carboxylate anions at appropriate mass number (*m/z*: monohydroxylated, 461; dihydroxylated, 563; trihydroxylated, 665; tetrahydroxylated, 767), reflecting the persilylated structure. On the other hand, the DES derivatives gave intense negative ions, $[M-PFB]^-$, with a decrement of 88 mass units from those of the corresponding DEHS derivatives (Fig. 3b). As illustrated in Fig. 3c, the mass spectrum of the reaction product from 3α, 6β, 7β-trihydroxylated bile acid with DEHS-BSTFA indicates the formation of the DES derivative. The stereoisomeric 6-hydroxylated bile acids with a *cis*-glycol exhibited the same mass spectrometric properties, indicating the formation of the C-6,7 DES derivatives.

CONCLUSIONS

Isolated hydroxyl groups of bile acids were readily converted into DEHS ethers, while vicinal glycols except for that of diaxial nature were transformed into cyclic DES derivatives. The use of DEHS ether and/or DES derivatives in combination with the corresponding TMS or alkyldimethylsilyl ethers may provide valuable information for establishing the number and nature of hydroxyl groups on the steroid nucleus of bile acids. In addition, as the DES derivative has a much lower molecular weight than the corresponding DEHS ether, the combined use of the PFB–DEHS–DES derivative and capillary GC–MS with NICI detection would be more favourable for the trace analysis of unusual bile acids with a vicinal glycol group. Applications of the present derivatization method to the determination of 4- and 6-hydroxylated bile acids in biological fluids are being studied and the results will be reported elsewhere.

ACKNOWLEDGEMENTS

The authors express their sincere thanks to Dr. M. Ishibashi, Research Laboratories of the Pharmaceuticals Group, Nippon Kayaku, for valuable suggestions. This work was supported in part by grants from the Tokyo Biochemical Research Foundation and the Ministry of Education, Science and Culture of Japan.

REFERENCES

1 W. H. Elliot, in H. Danielsson and J. Sjövall (Editors), *Sterols and Bile Acids*, Elsevier, Amsterdam, 1985, p. 303.
2 R. Dumaswala, K. D. R. Setchell, L. Zimmer-Nechemias, T. Iida, J. Goto and T. Nambara, *J. Lipid Res.*, 30 (1989) 847.
3 M. Nakagawa and K. D. R. Setchell, *J. Lipid Res.*, 31 (1990) 1089.
4 P. Eneroth and J. Sjövall, in P. P. Nair and D. Kritchevsky (Editors), *The Bile Acids*, Vol. 1, Plenum Press, New York, 1971, p. 121.
5 J. M. Street and K. D. R. Setchell, *Biomed. Chromatogr.*, 2 (1988) 229.
6 H. Miyazaki, M. Ishibashi, M. Itoh and T. Nambara, *Biomed. Mass Spectrom.*, 4 (1977) 23.
7 J. Yanagisawa, M. Itoh, M. Ishibashi, H. Miyazaki and F. Nakayama, *Anal. Biochem.*, 104 (1980) 75.
8 J. Goto, K. Watanabe, H. Miura, T. Nambara and T. Iida, *J. Chromatogr.*, 388 (1987) 379.
9 T. A. Baillie, C. J. W. Brooks and B. S. Middleditch, *Anal. Chem.*, 44 (1972) 30.
10 R. W. Kelly, *J. Chromatogr.*, 43 (1969) 229.
11 C. J. W. Brooks and D. J. Harvey, *J. Chromatogr.*, 54 (1971) 193.
12 H. Miyazaki, M. Ishibashi, M. Itoh and K. Yamashita, *Biomed. Mass Spectrom.*, 11 (1984) 377.
13 M. Ishibashi, T. Irie and H. Miyazaki, *J. Chromatogr.*, 399 (1987) 197.
14 K. Yamashita, K. Watanabe, M. Ishibashi, M. Katori and H. Miyazaki, *J. Chromatogr.*, 424 (1988) 1.

15 T. Iida, T. Momose, T. Tamura, T. Matsumoto, F. C. Chang, J. Goto and T. Nambara, *J. Lipid Res.*, 30 (1989) 1267.
16 T. Iida, T. Momose, F. C. Chang, J. Goto and T. Nambara, *Chem. Pharm. Bull.*, 37 (1989) 3323.
17 T. Iida, I. Komatsubara, S. Yoda, J. Goto, T. Nambara and F. C. Chang, *Steroids*, 55 (1990) 530.
18 J. Goto, H. Miura, M. Inada, T. Nambara, T. Nagakura and H. Suzuki, *J. Chromatogr.*, 452 (1988) 119.
19 H. Miyazaki, M. Ishibashi, K. Yamashita and M. Katori, *Biomed. Mass Spectrom.*, 8 (1981) 521.
20 T. Iida, I. Komatsubara, F. C. Chang, J. Goto and T. Nambara, *J. Chromatogr.*, 537 (1991) 345.

Journal of Chromatography, 585 (1991) 289–295
Elsevier Science Publishers B.V., Amsterdam

CHROM. 23 541

Determination of trace amounts of fluoride in raw materials for pharmaceuticals by gas–liquid chromatography

A. M. Bouygues-de Ferran

Service de Toxicologie et Pharmacie, Hôpital Necker-Enfants Malades, 149 Rue de Sèvres, 75015 Paris (France)

C. Pham-Huy*

Laboratoire de Toxicologie (Pr. J.R. Claude), Faculté de Pharmacie, 4 Avenue de l'Observatoire, 75006 Paris (France) and Service de Toxicologie et Pharmacie, Hôpital Necker-Enfants Malades, 149 Rue de Sèvres, 75015 Paris (France)

M. Postaire

Service de Toxicologie et Pharmacie, Hôpital Necker-Enfants Malades, 149 Rue de Sèvres, 75015 Paris (France)

M. Hamon

Service de Toxicologie et Pharmacie, Hôpital Necker-Enfants Malades, 149 Rue de Sèvres, 75015 Paris (France) and Laboratoire de Chimie Analytique, Faculté de Pharmacie de Paris XI, Rue Jean Baptiste Clément, 92290 Chatenay Malabry (France)

(First received February 6th, 1991; revised manuscript received June 3rd, 1991)

ABSTRACT

Trace amounts of inorganic fluoride present in raw materials for pharmaceuticals are converted into an organic compound by trimethylchlorosilane at acidic pH. The trimethylfluorosilane formed is determined by gas–liquid chromatography with flame ionization detection using isopentane as an internal standard. Seventeen pharmaceutical raw materials were analysed by this method. The fluoride levels found varied from 0.10 ppm in potassium chloride to 162 ppm in a sample of tribasic calcium phosphate. Coefficients of variation were 0.6–0.8% and the sensitivity was 0.01 ppm. This method is suitable for the determination of trace amounts of fluoride in raw materials for pharmaceuticals because of its simplicity, its accuracy and sensitivity.

INTRODUCTION

The presence of fluoride impurities in some inorganic raw materials for pharmaceuticals such as alkaline earth salts is well known. These impurities result from contamination by minerals such as fluorapatite $[Ca_{10}F_2(PO_4)_6]$ or francolite $[Ca_{10}F_2(PO_4)_6, xCaCO_3]$ found in the ores of these raw materials.

Fluoride is considered as an essential trace element necessary for bone formation and the prevention of dental caries. However, an excess of fluoride is toxic and can induce diverse bone diseases such as fluorosis, osteoporosis and skeletal fragility [1–4]. The cytotoxicity of fluoride has also been reported [5–8]. For these reasons, different pharmacopoeia give a maximum concentration of fluoride in certain raw materials. Two methods of determination are

used in the main pharmacopoeia. A spectrophotometric method after a distillation procedure is described in the European [9], French [10] and British Pharmacopoeia [11]. This technique is tedious, time-consuming and insensitive. A potentiometric method with a specific fluoride electrode is described in the United States Pharmacopoeia (USP) [12]. However, this technique is not linear at less than 50 μg/l fluoride and can give errors as a result of interference from OH^- [13]. The lengthy equilibration period of the electrodes at low concentrations is also inconvenient [13]. Fluoride has also been determined by ion chromatography in water and various other materials [14,15]. This technique is more specific than the spectrophotometric and potentiometric methods. However, the direct determination of fluoride by suppressed conductivity ion chromatography does have problems and the detection is limited to the ppm level [15].

This paper reports a precise, sensitive and simple method for the determination of trace amounts of fluoride in raw materials for pharmaceuticals using gas–liquid chromatography (GLC). This procedure is a modified technique described elsewhere [16–21] for the determination of fluoride in biological fluids. In this chromatographic method, the fluoride ion is converted into an organic derivative by trimethylchlorosilane (TMCS) at acidic pH. The organofluoro derivative is extracted with toluene and determined by GLC with flame ionization detection using isopentane as an internal standard (I.S.). The conversion reactions are as follows [18]:

$$(CH_3)_3\ SiCl + H_2O \rightarrow (CH_3)_3\ Si\ OH + HCl$$

$$(CH_3)_3\ SiOH + HF \rightarrow (CH_3)_3\ Si\ F + H_2O$$

The TMCS is first hydrolysed by water into the corresponding silanol which then reacts with the fluoride ion at acidic pH to form the trimethylfluorosilane (TMFS).

EXPERIMENTAL

Apparatus and materials

A Delsi Model 330 gas chromatograph equipped with a flame ionization detector was used in conjunction with a Servotrace 1-mV recorder. The chromatographic separation was performed using a 2.5 m × 3 mm (1/8 in.) stainless-steel column packed with 20% DC 200 (methyl silicone fluid) on Chromosorb P-AW, 80–100 mesh (Chrompack). The column was maintained at 100°C and the injection port and detector were operated at 120 and 200°C, respectively. Nitrogen was used as the carrier gas at a flow-rate of 30 ml/min, which developed a head column pressure of about 2.2 bars. The hydrogen and air flow-rates were 40 and 350 ml/min, respectively. The chart speed of the recorder was 5 mm/min. A Maximix Model Vortex (Bioblock) was used for tube agitation. Polyethylene tubes (10 ml) with polyethylene stoppers (Polylabo), resistant to organic solvents, were used for the extraction.

Reagents

TMCS was purchased from Sigma. Isopentane (2-methylbutane) (purissim for gas chromatography), purchased from Fluka and used as the I.S., was diluted 1:2000 (v/v) in TMCS. The I.S. solution was stored at about −20°C in 5-ml vials with PTFE septa and screw caps and was stable for about two weeks. Toluene and concentrated hydrochloric acid were of analytical-reagent grade (Merck) and were stored at about −20 and +4°C, respectively.

The stock solution of 100 ppm fluoride was prepared by the dissolution of 221.4 mg of accurately weighed Pharmacopoeia sodium fluoride in distilled water in a 1-l calibrated flask. The standard solution of 10 ppm fluoride was obtained by transferring 10.0 ml of the stock solution to a 100-ml calibrated flask and diluting to volume with water. The fluoride stock and standard solutions were stored in plastic bottles.

Standard calibration

Into six 10-ml polyethylene tubes, 0.05, 0.1, 0.2, 0.5, 1 and 2 ml of 10 ppm fluoride standard solution were added plus a sufficient amount of water to give a final volume of 2 ml corresponding to 0.5, 1, 2, 5, 10 and 20 ppm fluoride. A 100-μl volume of I.S. in TMCS (−20°C), 1 ml of toluene (−20°C) and 2 ml of concentrated HCl (+4°C) were then added. A blank reagent with 2 ml of water and the same reagents was prepared. All reagents were added rapidly and in the specified order. The tubes were stoppered and vortexed for 1 min and then centrifuged for 4 min at 2500 *g*. A 0.5-ml volume of the organic extract (upper layer) of each standard was immedi-

ately transferred into each of the 3-ml stoppered vials and stored at about −20°C before use. A 5-µl volume of each standard extract was injected into the chromatograph. The standard extracts were stable for about one week if stored at about −20°C in tightly stoppered vials.

Sample preparation

About 100 ± 0.1 mg of the raw material under test was transferred to a 10-ml polyethylene tube and 2 ml of distilled water, 100 µl of I.S. in TMCS (−20°C), 1 ml of toluene (−20°C) and 2 ml of concentrated HCl (+4°C) were added in order. The same procedure was then followed as for the standard calibration. The sample weights vary between 100 and 500 mg depending on the concentration of fluoride in the raw materials.

Calculation

The determination of the fluoride ion in the sample was based on the peak-height ratio of TMFS to the I.S. This is given by a standard curve obtained by dividing the TMFS peak height by the I.S. peak height for each standard. The concentration of the fluoride ion expressed in ppm in the raw material was calculated by the relationship $(C_1 \times 1000)/M$, where C_1 is the concentration of the fluoride ion in the sample, taken from a calibration graph and M is the mass in milligrams of sample taken. The concentration can also be calculated by comparing the TMFS/I.S. peak-height ratio of the sample to that of a single standard containing a known amount of fluoride ion: $C_2\ (R_1/R_2)\ (1000/M)$. In this relationship C_2 is the concentration of the fluoride ion in ppm in a single standard, R_1 and R_2 are the TMFS/I.S. peak-height ratios of the sample and standard, respectively, and M is mass of sample taken in milligrams.

RESULTS

Chromatographic analysis

Typical chromatograms of a sample and a blank reagent are shown in Figs. 1 and 2. The TMFS peak appears first with a retention time about 1.5 min, followed by the I.S. peak (isopentane) with a retention time of about 2 min. The other peaks (trimethylsilanol, TMCS, toluene and all the impurities of these solvents) appeared after TMFS and the I.S. To obtain the complete elimination of all the parasite peaks, the chromatographic time was about 20 min. No interfering peak was observed with the blank reagent at the retention time of TMFS (Fig. 2).

Analytical variables

Linearity. The standard calibration graphs gave a good linearity for fluoride ions in the range of concentrations tested with a correlation coefficient $r = 1.0002$ and a regression line $y = 0.281x + 0.027$, in which y is the TMFS/I.S. peak-height ratio and x is the concentration of fluoride standards in ppm.

Sensitivity. The detection limit for the assay was 0.01 ppm of fluoride ion in the raw material. As the TMFS peak appears on the chromatogram before the solvent peaks, an adequate sensitivity was obtained by varying the attenuation or the volume of sample injected.

Accuracy. The coefficients of variation (C.V.) determined from replicate analysis ($n = 6$) of two standards (1 and 2 ppm) were 0.6 and 0.7%, respectively. The intra-day C.V. for a sample of raw material (tribasic calcium phosphate) with $n = 6$ was 0.8%.

Recovery. The recovery was studied by a second extraction of about 3.6 ml of the same aqueous phase by 1 ml of toluene plus 100 µl of TMCS without the I.S. No peaks of TMFS or I.S. were observed in the chromatogram after the second extraction of a 2-ppm standard and of a tribasic calcium phosphate sample. The recovery was about 100% for TMFS and the I.S.

Interferences. No peaks of the solvents or their impurities were observed with the reagent blank (Fig. 2) at the retention time of the TMFS peak. It is recommended to wait about 20 min after injection for the complete elimination of all solvent peaks to avoid further interferences.

Interferences were also studied with ions such as Al^{3+}, B^{3+}, Fe^{3+}, Ca^{2+} and Mg^{2+}, for which fluoride has a great affinity. The interference assay was performed as follows: 100 mg of each raw material [aluminium hydroxide, $Al(OH)_3$; sodium borate, $Na_2B_40_7 \cdot l0H_2O$; boric acid, H_3B0_3; tribasic calcium phosphate, $Ca_3(PO_4)_2$; yellow iron(III) oxide, Fe_2O_3; or magnesium hypophosphite, $Mg(H_2P0_2)_2 \cdot 6H_2O$] were analysed as described earlier. Another 100-mg sample spiked with 20 ppm of fluoride was

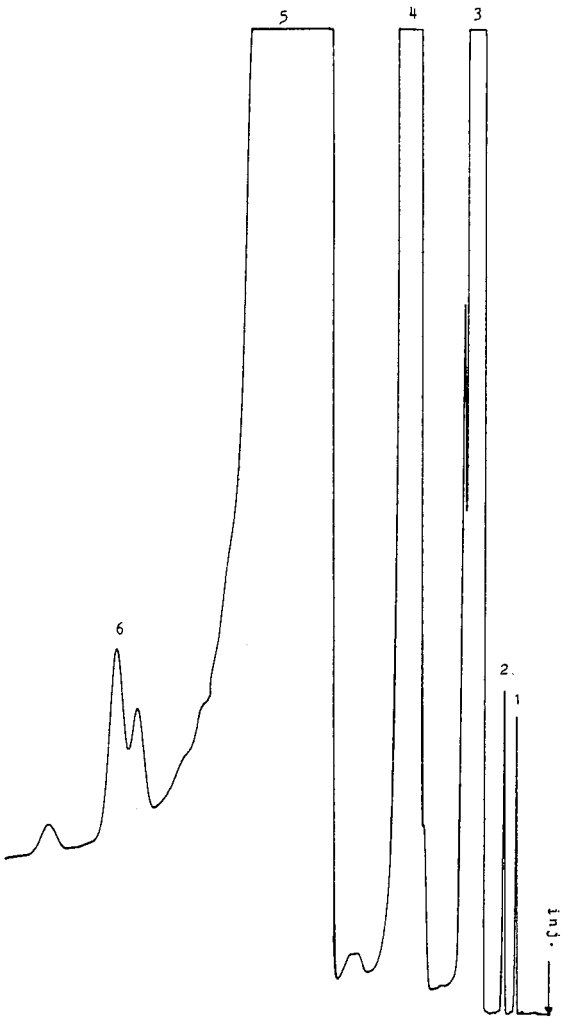

Fig. 1. Chromatogram of a sample tribasic calcium phosphate (pharmaceutical grade). The fluoride level found was 42 ppm. Peaks: 1 = trimethylfluorosilane; 2 = isopentane (I.S.); 3 = trimethylsilanol; 4 = trimethylchlorosilane; 5 = toluene; 6 = solvent impurities.

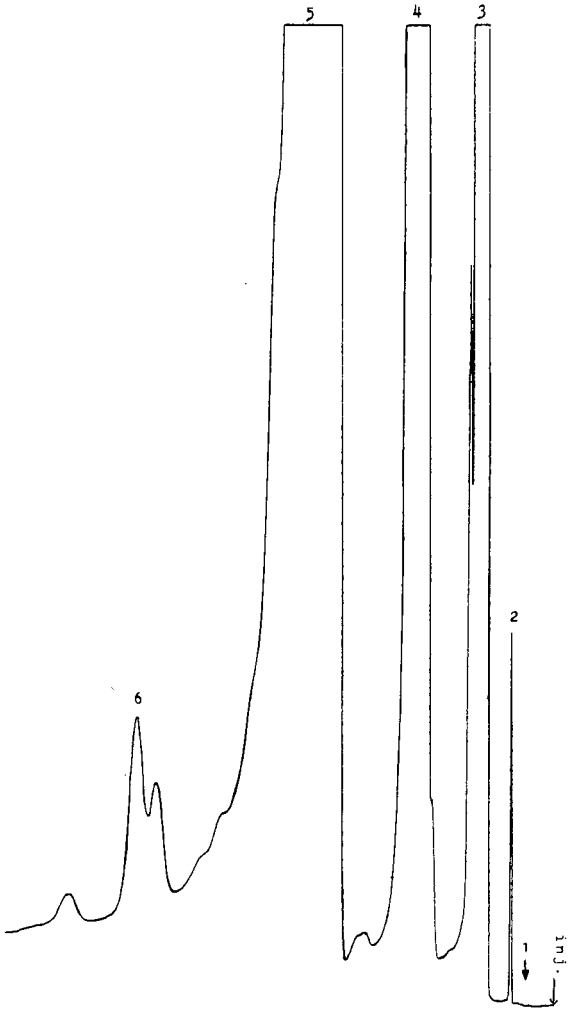

Fig. 2. Chromatogram of blank reagent. Peaks as in Fig. 1.

analysed in parallel. The difference of the TMFS/I.S. peak-height ratios between the second and the first assay was compared with the peak-height ratio of a 20-ppm standard. The results of this assay are presented in Table I and show no important interference of fluoride with these ions. This means that fluoride has a greater affinity for TMCS than for Al^{3+}, B^{3+}, Fe^{3+}, Ca^{2+} or Mg^{2+} ions.

Raw material studies

Seventeen raw materials used in the pharmaceutical industry, most of which were calcium salts, were analysed by this method. The fluoride concentrations found in these compounds are presented in Table II. In addition, an inorganic fluoride compound, a sodium monofluorophosphate [$FPO(ONa)_2$] used as raw material in toothpaste, was also determined after dilution of the sample in water (1:10 000). The amount of fluoride found was 13.1%. All previous compounds tested were of pharmaceutical grade, except for one sample of tribasic calcium phosphate which was of technical grade and had a fluoride concentration exceeding the normal values required by the three pharmacopoeia.

TABLE I

INTERFERENCE OF VARIOUS IONS WITH DETERMINATION OF FLUORIDE

Raw material tested	TMFS/I.S. peak-height ratio (mean ± S.D., n = 6)			Recovery of 20-ppm F^- standard (%)[a]
	First assay (100-mg sample)	Second assay (100-mg sample + 20 ppm F^-)	20-ppm F^- standard	
Aluminium hydroxide	0.74 ± 0.015	5.10 ± 0.12	4.50 ± 0.05	97
Sodium borate	0.34 ± 0.005	4.94 ± 0.14	4.50 ± 0.05	102
Boric acid	0.32 ± 0.005	4.87 ± 0.12	4.50 ± 0.05	101
Calcium phosphate, tribasic	0.94 ± 0.008	5.41 ± 0.10	4.50 ± 0.05	99.5
Iron(III) oxide	0.04 ± 0.002	4.60 ± 0.15	4.50 ± 0.05	101
Magnesium hypophosphite	0.25 ± 0.004	4.66 ± 0.08	4.50 ± 0.05	98

[a] Results are (second assay − first assay)/20-ppm standard.

DISCUSSION

Technical studies

Owing to the high volatility of the TMFS formed and of isopentane used as the I.S. (boiling points 16.4 and 28°C, respectively) [19,21], it is necessary to freeze toluene and the I.S. solution in TMCS at about −20°C before use to avoid the loss of these two compounds during vortex extraction. It is also recommended to store the extracts at about −20°C

TABLE II

CONCENTRATIONS OF FLUORIDE IONS IN RAW MATERIALS USED FOR PHARMACEUTICALS

Raw material tested	Fluoride level (ppm)[a]	Limit values of F ions[b]			
		USP (1990) (%)	European Pharmacopoeia (2nd ed.) (ppm)	British Pharmacopoeia (1988) (ppm)	French Pharmacopoeia (10th ed.) (ppm)
Aluminium hydroxide	32 ± 0.65	ND	ND	ND	ND
Sodium borate	15 ± 0.23	ND	ND	ND	ND
Boric acid	14 ± 0.23	ND	ND	ND	ND
Calcium acetate	18 ± 0.42	0.005	NA	ND	NA
Calcium bromide	25 ± 0.52	NA	NA	NA	NA
Calcium carbonate	38 ± 1.05	0.005	ND	ND	ND
Calcium citrate	6.7 ± 0.21	0.003	NA	NA	NA
Calcium glycerophosphate	10.4 ± 0.35	NA	NA	NA	ND
Calcium phosphate, monobasic	2.6 ± 0.05	NA	NA	NA	NA
Calciumphosphate, dibasic	98 ± 1.10	0.005	100	100	100
Calcium phosphate, tribasic (PG)[c]	42 ± 0.33	0.0075	ND	50	100
Calcium phosphate, tribasic (TG)[c]	162 ± 2.65	0.0075	ND	50	100
Iron(III) oxide	1.7 ± 0.08	ND	NA	NA	ND
Magnesium hypophosphite	11 ± 0.18	NA	NA	NA	NA
Magnesium lactate	5 ± 0.10	NA	NA	NA	NA
Potassium chloride	0.1 ± 0.004	ND	ND	ND	ND
Sodium chloride	0.5 ± 0.01	ND	ND	ND	ND

[a] Results given as mean ± standard deviation; n = 6.
[b] ND = Not determined; NA = not available.
[c] PG = pharmaceutical grade; TG = technical grade.

in stoppered vials for the same reasons. The solvents remain as liquid at this temperature and can be used immediately for preparing the sample or for injection into the chromatograph. Yamamoto *et al.* [21] have recommended working in a cold room to prevent evaporation of the solvents. However, this is not always possible in every laboratory and cooling the solvents in a freezer is simpler to achieve. The I.S. can be stored in TMCS for about two weeks instead of being prepared each time as recommended elsewhere [21]. An assay was carried out with all the reagents stored at room temperature or at +6°C; the linearity and reproducibility were less satisfactory than at −20°C (r = 0.922 and 0.965, C.V.$_S$ = 10.8 and 8.4% for reagents stored at room temperature and +6°C, respectively).

Triethylchorosilane (TECS) and tributylchlorosilane (TBCS) were also used for fluoride derivatization. The triethylfluorosilane (TEFS) and tributylfluorosilane (TBFS) formed are less volatile than TMFS and the sample preparation can be performed at room temperature. However, according to Yamamoto *et al.* [21], the reaction time for these derivatization procedures is 90 min instead of 1 min by this technique and many other peaks can appear in the same range as the fluoride derivatization peak. Using the chromatographic conditions described here, TEFS appeared at the same time as the toluene peak (20 min) and TECS at about 40 min; consequently, the chromatographic time using TECS was twice as long as that using TMCS. If TBCS was used under these conditions, TBFS and TBCS were not eluted at 100°C, but at 200°C. Using hexane as the extraction solvent and setting the column temperature to 200°C, many solvent peaks and their impurities appeared before and in the same range as the fluoride derivatization peak using the TECS of TBCS derivatization procedure. These interfering peaks make the fluoride determination difficult and could involve large errors. In contrast, with derivatization by TMCS, no peak was observed before or at the same time as the TMFS and I.S. peaks, as TMFS and I.S. are more volatile than the solvents used in the reaction. Moreover, the slow reaction of TECS or TBCS with fluoride could lead to interferences from Al^{3+}, B^{3+}, Fe^{3+}, Ca^{2+} or Mg^{2+} ions.

As a result of the high reactivity of hydrofluoric acid and fluoride ions on glass to form silicon tetrafluoride, the use of polyethylene tubes resistant to organic solvents is necessary for the extraction and storage of the fluoride standards. After about 30 injections, it is recommended that the detector is cleaned and the column heated at 200°C overnight to eliminate silyl deposits.

Analytical variables

This chromatographic method has a good accuracy (C.V. about 0.7%), a high sensitivity (0.01 ppm) and good linearity (r = 1.0002). It is more rapid, simple and sensitive than the spectrophotometric method used by some European pharmacopoeia. It is also more simple, specific and reproducible than the potentiometric method, described in the USP. In this method, the presence of some metal ions (Al^{3+}, Fe^{3+}), and especially OH^- ions, can interfere with the electrode measurements [22]. In the proposed chromatographic method it was established that Al^{3+}, Fe^{3+}, B^{3+}, Ca^{2+} and Mg^{2+} ions do not interfere because fluoride has a greater affinity towards TMCS than towards these ions (Table I). In addition, the lengthy adjustment period of the electrodes in the low concentration ranges is also a major inconvenience. Some electrodes can cause errors due to excessive drift [13].

Raw material analysis

Table II shows the presence of fluoride ions in all seventeen raw materials tested with a concentration varying between 0.1 and 162 ppm. This variation of fluoride concentrations is due to the presence or absence of this ion in the original minerals and to the manufacture of the raw material. Calcium salts, especially phosphate and carbonate, are the most contaminated by the fluoride ion because most were prepared from ores containing it. The higher fluoride level in tribasic calcium phosphate, technical grade (162 ppm), than in its pharmaceutical grade (42 ppm) has proven the important presence of fluoride in this salt and the necessity for its purification and control in pharmaceutical use. However, the low fluoride level (2.6 ppm) in monobasic calcium phosphate [$Ca(PO_4H_2)_2) \cdot H_20$] is due to its preparation which consists in heating dibasic calcium phosphate with a strong acid; the fluoride is transformed to hydrofluoric acid which is then eliminated by evaporation.

Some other organic calcium salts such as calcium

citrate (6.7 ppm), calcium glycerophosphate (10.4 ppm) and calcium acetate (18 ppm) contain less fluoride than inorganic calcium salts such as phosphates or carbonates because these synthetic compounds are generally obtained by the condensation of inorganic calcium salts with their organic acid; the fluoride present in the inorganic raw materials could be partially eliminated either by purification of the synthetic organic compound formed or by the evaporation of the hydrofluoric acid if the synthesis reaction is sufficiently acid. The lower fluoride concentrations in magnesium lactate (5 ppm) than in magnesium hypophosphite (11 ppm) could be explained by these reasons.

The traces of fluoride in potassium chloride (0.1 ppm) are explained by the purity of this ore. Sodium chloride contains more fluoride (0.5 ppm) because it is generally obtained from sea water containing about 1 ppm fluoride [2]. The presence of large amounts of fluoride (32 ppm) in aluminium hydroxide is explained by the use of calcium fluoride as a flux in aluminium metallurgy. No limit value for the concentration of fluoride in aluminium hydroxide is given in any pharmacopoeia. In the USP, many descriptions of calcium salts (Table II) require a limit of fluoride ions, contrary to the European pharmacopoeia in which an assay is required for only two compounds of calcium phosphate. In this work, 38 ppm of fluoride were found in calcium carbonate.

The proposed chromatographic method determines total inorganic fluorides, including water-soluble and insoluble forms, as do the two techniques cited previously. Most fluorides in calcium salts are in the form of calcium fluoride. This may be less soluble in the gastrointestinal tract than sodium fluoride and consequently less toxic. According to Whitford [23], the gastrointestinal absorption of calcium fluoride in food is about 63%, compared with 90% for sodium fluoride. Ericsson [24] reported that certain studies show the formation of various complex ions such as $(CaF)^+$ or $(MgF)^+$ which are more soluble and are susceptible to metabolism in humans. Calcium fluoride can be as toxic as sodium fluoride if the amount ingested is large [2]. This explains the endemic fluorosis observed in the Darmous population (Morocco) who absorbed calcium fluoride present in food, air and water.

The determination of the fluoride ion in inorganic raw materials for pharmaceuticals is necessary because of the easy contamination of these compounds during manufacture and the potential toxicity of the fluoride ion. The simple, rapid and accurate gas chromatographic method proposed should be developed in the pharmaceutical industry for the routine control of trace amounts of fluoride.

REFERENCES

1 G. Boivin, P. Chavassieux, M. C. Chapuy, C. A. Baud and P. Meunier, *Pathol. Biol.*, 34 (1986) 33.
2 G. Le Moan, *Ann. Falsif. Expert. Chim.*, 77 (1984) 115.
3 B. L. Riggs, S. F. Hodgson, W. M. O. Fallon, E. Y. S. Chao, H. W. Wahner, J. M. Muhs, S. L. Cedel and L. J. Melton, *N. Engl. J. Med.*, 322 (1990) 802.
4 K. W. Stephan, W. J. N. Collin, D. R. McCall and T. R. Watkins, *Dental Health*, 2 (1982) 317.
5 P. Grandjean, K. Juel and O. M. Jensen, *Am. J. Epidemiol.*, 121 (1985) 57.
6 R. I. Holland, *Acta Odontol. Scand.*, 38 (1980) 69.
7 O. Strubelt, *Dtsch. Med. Wochenschr.*, 110 (1985) 730.
8 P. R. N. Sutton, *Med. Hyg.*, 23 (1987) 335.
9 *Pharmacopée Européenne*, Maisonneuve, Nancy, 2nd ed., 1980, p. V.3.2.5.
10 *Pharmacopée Française*, ONP, Paris, 10th ed., 1983, p. V.3.2.5.
11 *British Pharmacopoeia*, HMSO, London, 1988, p. A110.
12 *United States Pharmacopoeia*, USPC, Rockville, MD, 22nd ed., 1990, p. 218.
13 C. Fuchs, D. Dorn, C. A. Fuchs, H. V. Henning, C. McIntosh and F. Scheler, *Clin. Chim. Acta*, 60 (1975) 157.
14 J. J. Potter, A. E. Hilliker and G. J. Breen, *J. Chromatogr.*, 367 (1986) 423.
15 R. T. Talasek, *J. Chromatogr.*, 465 (1989) 1.
16 A. Sahui Gnassi, C. Pham Huy, G. Dumortier, S. Raspaud, P. L. Nguyen and M. Hamon, *Ann. Falsif. Expert. Chim.*, 80 (1987) 203.
17 C. Pham Huy, N. Sadeg, L. Massias, A. Sahui Gnassi, P. L. Nguyen and M. Hamon, *Ann. Falsif. Expert. Chim.*, 80 (1987) 405.
18 R. Bock and H. J.Z. Semmler, *Zh. Anal. Khim.*, 230 (1967) 161.
19 J. A. Freesen, F. H. Cox and M. J. Witter, *Pharm. Weekbl.*, 103 (1968) 909.
20 R. I. Henishi, T. Kitagaria, M. Nishuidi, K. Takehara, H. Nakagaiva, M. Sawai and T. Yamashita, *Chem. Pharm. Bull.*, 36 (1988) 662.
21 G. Yamamoto, K. Yoshitake, T. Kimura and T. Ando, *Anal. Chim. Acta*, 222 (1989) 121.
22 W. Freuzel and P. Bratter, *Anal. Chim. Acta*, 187 (1986) 1.
23 G. M. Whitford, in H. T. Myers (Editor), *Monographs in Oral Sciences, No. 13*, Karger, Basle, 1989, p. 14.
24 Y. Ericsson, *Fluor et Santé, Series No. 59*, World Health Organization, Geneva, 1972, p. 15.

Journal of Chromatography, 585 (1991) 297–308
Elsevier Science Publishers B.V., Amsterdam

CHROM. 23 553

Isotachophoretic separation of minor components from a matrix component in the case of strong electrolytes☆

Takeshi Hirokawa*, Akihiro Omori, Yasuro Yokota☆☆, Jian-Ying Hu and Yoshiyuki Kiso

Applied Physics and Chemistry, Faculty of Engineering, Hiroshima University, Kagamiyama 1, Higashi-Hiroshima 724 (Japan)

(First received April 25th, 1991; revised manuscript received June 13th, 1991)

ABSTRACT

In order to clarify the cause of underestimation in the isotachophoretic analysis of minor components, the effect of the ratio of sample components on the separation efficiency was studied on the basis of computer simulation and the observation of the transient state of separation. It was confirmed for binary mixtures of strong electrolytes that the separation efficiency was almost unaffected by this ratio. On the other hand, when the number of sample components was more than two, the resolution time was no longer independent of the component ratio. However, if the total molar amount was kept constant, the dependence was not so serious and the resolution time was about double that for the equimolar mixture. The most important point in the analysis of the isotachopherogram of minor components was to avoid overloading of the sample solution, as the formation of a mixed zone of the matrix and a minor component is difficult to detect.

INTRODUCTION

One of the practical problems encountered in isotachophoretic analysis is the underestimation of minor components in a matrix component. The essential reason is sample overloading, *i.e.*, when the amount of electricity is insufficient for the separation of a sample, the sample zones would reach the detector before complete separation [1,2]. If the number of sample components is known and they are nearly equimolar, the unresolved zone is easily distinguished. However, in minor component analysis, a serious point is that the mixed zone between the minor component and the matrix is frequently overlooked, as the detector signals of the mixed zone resemble those of the steady-state zone of the matrix component, whatever detector is used. As a result, the separation tube tends to be overloaded to increase the zone length of the minor components. Therefore, it is natural that the minor components are sometimes underestimated. To avoid such underestimation, the zone length of the steps in isotachopherograms should be carefully checked by varying the amount of the sample injected.

In a previous paper [3], we clarified the cause of the delay in the resolution time of a two-component mixed zone by the addition of a third component (the composition effect on the separation efficiency). It was due to the change in the potential gradient of the binary mixed zone and the extent of the delay depended on both the molar amount and the mobility of the co-existing sample components. The present problem with minor component analysis is closely related to the composition effect.

In order to clarify how the separation efficiency of minor components is affected by the matrix com-

☆ Presented at the *7th International Symposium on Capillary Electrophoresis and Isotachophoresis, Tatranská Lomnica, October 2–4, 1990*. The majority of the papers presented at this symposium have been published in *J. Chromatogr.*, Vol. 545, No. 2 (1991).

☆☆ Present address: Mitsubishi Paper Mills Ltd., Tsukuba Research Laboratories, Tsukuba, Ibaraki, Japan.

0021-9673/91/$03.50

ponent, the separation process of six components was simulated by varying the ratio of the molar amounts. The separation processes of several actual samples were observed by the use of a 32-channel UV photometric array detector and an ultraviolet (UV) scanning detector [4]. The observed resolution time was compared with the simulated time to confirm the validity of the simulation. Practical aspects concerning the quantitative determination of minor components using zone lengths are also discussed.

THEORETICAL

Two-component mixture

Assume two monovalent strong ions, A and B. The absolute mobility of ion A (m_A) is larger than that of ion B (m_B). In the separation process, the two-component mixed zone AB is formed from the solution injected. The resolution time of the zone AB can be expressed as follows [5,6]:

$$t_{res,AB} = \frac{l_A}{E_A\overline{m}_A - E_{AB}\overline{m}_{B,AB}} \quad (1)$$

where l_A is the zone length of component A in a separation tube after the AB mixed zone is resolved (the steady state), E_A the potential gradient of zone A at the steady state, $\overline{m}_A$ the effective mobility of ion A in zone A, E_{AB} the potential gradient of the mixed zone AB and $\overline{m}_{B,AB}$ the effective mobility of ion B in the mixed zone.

A different expression for $t_{res,AB}$ is obtained on the assumption that the separation process follows the diagram reported by Brouwer and Postema [7]:

$$t_{res,AB} = \frac{l_B}{E_{AB}\overline{m}_{A,AB} - E_B\overline{m}_B} \quad (2)$$

where l_B is the zone length of component B at the steady state, $\overline{m}_{A,AB}$ the effective mobility of ion A in the mixed zone, E_B the potential gradient of zone B and $\overline{m}_B$ the effective mobility of ion B.

In a previous paper [3], we showed that the resolution time of a binary mixture, $t_{res,AB}(2)$, can be expressed by a simple equation reduced from eqn. 1, when the components are equimolar strong electrolytes. If the components are not equimolar, one can derive the following equation on the basis of similar assumption:

$$t_{res,AB}(2) = \frac{Fn_t}{i(N_R+1)}(1 + m_Q/m_A)\frac{\overline{m}_A + N_R\overline{m}_B}{\overline{m}_A - \overline{m}_B} \quad (3)$$

$$N_R = n_B/n_A \quad (4)$$

$$n_t = n_A + n_B \quad (5)$$

where N_R is the ratio of the molar amount of components A and B (n_A and n_B), n_t the total amount, F the Faraday constant, i the migration current and m_Q the absolute mobility of counter ion as the pH buffer. The potential gradient of E_{AB} was expressed using E_A as follows:

$$E_{AB} = \frac{(1 + N_R)\overline{m}_A}{\overline{m}_A + N_R\overline{m}_B} \cdot E_A \quad (6)$$

With the ultimate conditions $n_A \gg n_B$ and $n_A \ll n_B$, the following expressions are obtained.

Case $n_A \gg n_B$. In this case N_R is very small and component A can be regarded as the matrix component, and eqn. 1 suggests that the resolution time reaches to a limiting value defined as follows:

$$t_{res,AB}(2) = \frac{Fn_t}{i}(1 + m_Q/m_A)\frac{\overline{m}_A}{\overline{m}_A - \overline{m}_B} \quad (7)$$

It is apparent from eqn. 6 that E_{AB} approaches the potential gradient of the matrix component A at the steady state:

$$E_{AB} \approx E_A \quad (8)$$

Case $n_A \ll n_B$. By reducing eqn. 2, one can obtain a different expression for $t_{res,AB}(2)$ as follows:

$$t_{res,AB}(2) = \frac{Fn_t}{i(1/N_R+1)}(1 + m_Q/m_B)\frac{\overline{m}_A/N_R + \overline{m}_B}{\overline{m}_A - \overline{m}_B} \quad (9)$$

where t_B is the time-based zone length of zone A at the steady state. When N_R is larger than 1 and component B can be regarded as the matrix component, the limiting resolution time at $N_R = \infty$ can be expressed as follows:

$$t_{res,AB}(2) = \frac{Fn_t}{i}(1 + m_Q/m_B)\frac{\overline{m}_B}{\overline{m}_A - \overline{m}_B} \quad (10)$$

E_{AB} can be correlated with E_B as follows:

$$E_{AB} = \frac{\overline{m}_B(1 + N_R)}{\overline{m}_A + N_R\overline{m}_B} \cdot E_B \quad (11)$$

It is apparent from eqn. 11 that E_{AB} approaches the potential gradient of the matrix component B at the steady state when N_R is very large:

$$E_{AB} \approx E_B \quad (12)$$

It should be noted that the values of the resolution time under the extreme conditions $n_A \gg n_B$ and $n_A \ll n_B$ are almost equal when the total amount of the sample components is constant:

$$\frac{t_{res,AB}(2)_{N_R=\infty}}{t_{res,AB}(2)_{N_R=0}} = \frac{m_B + m_Q}{m_A + m_Q} \approx 1 \quad (13)$$

The resolution time of a binary mixture is almost insensitive to the sampling ratio, when the mobility difference is small and the components are monovalent ions. If one of the components is multivalent, there will be a distinct difference as its time-based zone length differs significantly from that of the monovalent ion. An example for actual samples will be shown later.

The potential gradient of the mixed zone is always between the two extreme values of E_A and E_B:

$$E_A < E_{AB} < E_B \quad (14)$$

The validity of these equations will be discussed later in comparison with the separation process of actual samples.

Multi-component mixture

In this instance, the separation efficiency of the binary mixed zone of interest will be affected by the existence of the other components, as discussed for the equimolar mixture in a previous paper [3]. As the extent of the delay of the resolution time depends on the amount and the mobility of the coexisting ions, the resolution time of the mixed zone is no longer independent of the component ratio. However, provided that the total molar amount of the sample is kept constant, the change in the resolution time is not so serious, as shown later.

To confirm the above conclusion for the minor components, first the separation process of a binary mixture was studied in detail, varying the ratio of the component amounts. Then the effect of the component ratio on the resolution time of a four-component mixture was studied.

EXPERIMENTAL

The samples used were 4,5-dihydroxy-3-(*p*-sulphophenylazo)-2,7-naphthalenedisulphonic acid (SPADNS), monochloroacetic acid (MCA) and picric acid (PA). Except for MCA, these samples absorb visible and UV light. The sodium salt of SPADNS was purchased from Dojin (Kumamoto, Japan) in the purest form. The other chemicals were guaranteed-grade reagents obtained from Tokyo Kasei (Tokyo, Japan). Stock sample solutions were prepared by dissolving them in distilled water without further purification.

Mixtures of SPADNS and MCA (SM) and of MCA and PA (MP) were used for the observation of the characteristics of binary mixtures. The pairs were selected so as to contain UV-transparent MCA. This is very important in transient state analysis using a UV detector, as will be apparent in the observed isotachopherogram. The ratio of the sample components was varied in the range 100:1 to 1:100. The total amount of the mixture injected was 50 nmol for SM and 35 nmol for MP. The pH of these solutions was adjusted to 3.6 by adding β-alanine.

An array detection system constructed in our laboratory [8] was used to observe the separation process of these two-component mixtures. The array detector had 32 equidistant UV detectors along a 16-cm separation tube. A single cycle to acquire the UV signals, namely time resolution of the system, was 243.2 ms. Usually 5000–7000 data were acquired in a single run. In order to determine the boundary-detected time and the boundary velocity, the observed UV signals were differentiated with respect to time, and the positive and negative peaks of the differentiated signals were searched for. Linear equations describing the progression of the boundaries can be evaluated by the least-squares method on the basis of these numerical data. The resolution time can be obtained by solving simultaneous equations for the different boundaries.

A potential gradient profile for the binary mix-

ture MP was also measured by the use of a Shimadzu (Kyoto, Japan) IP-2A isotachophoretic analyser. The ratio of sample amounts was MCA:PA = 10:1.

The four-component mixture used was a solution of SPADNS, MCA, PA and 2,3-dihydroxybenzoic acid (DBA), the SPADNS:MCA:PA:DBA ratio being varied from 1:1:1:1 to 10:1:1:1. The total amount of the sample injected was 100 nmol and the volume injected was 10 μl. A scanning UV photometric detector was used for the observation of the separation process. For scanning a linear head equipped with a UV lamp and a detector was driven by a computer-controlled stepping motor. The separation tube used was a fused-silica capillary (32 cm × 0.53 mm I.D. × 0.7 mm O.D.). The UV radiation from a deuterium lamp was passed through a UV glass filter (Toshiba Glass, Tokyo, Japan; Model D33S, λ_{max} = 330 nm). A single cycle to scan the 32-cm tube was 7.025 s and the number of data in a single scan was 5333. The resolution was 0.06 mm per data point, which was sufficient to trace the separation process accurately. For data acquisition, an NEC (Tokyo, Japan) PC9801VX microcomputer was used (CPU = 80286, coprocessor = 80287, clock 10 MHz). All experiments were carried out at 25°C.

The concentration of the leading electrolyte (hydrochloric acid) was 5 m*M*. The pH was adjusted to 3.6 by adding β-alanine. A 5 m*M* leading electrolyte was used in order to avoid the saturation of the UV detector owing to the high concentration of the sample in each zone. The migration current applied was 50 μA. The terminator was 10 m*M* caproic acid. Hydroxypropylcellulose (HPC, 0.2%) was added to the leading and terminating electrolytes to suppress electroendosmosis. The viscosity of a 2% aqueous solution is 1000–4000 cP at 20°C according to the specification. The sample solution was injected into the terminating electrolyte near the boundary between the leading and terminating electrolytes. The pH of the terminating electrolyte was also adjusted to 3.6 by adding β-alanine to ensure that the pH of the sample solution at the initial stage of migration was equal to the prepared value. The pH measurements were carried using a Horiba (Tokyo, Japan) Model F7ss expanded pH meter.

In the simulations of the transient state, the microcomputer used was an NEC PC-9801RA2 (CPU = 80386, coprocessor = 80387, clock 16 MHz). The physico-chemical constants used in the simulations are summarized in Table I. In our simulation program SIPSR [3,9,10], the effect of the ionic strength on the mobility and dissociation constants were corrected. However, in the correction the viscosity of pure water was used as that of electrolyte solution in the separation tube, although the electrolyte contained HPC and other chemicals. This may cause small errors in simulation.

RESULTS AND DISCUSSION

Two-component mixture

Table II shows the resolution time of the binary mixtures exactly simulated for several model anions using our computer program SIPSR [3,9,10]. Table II also summarizes the approximate values obtained by the use of eqn. 3. The mobility of ion A was $60 \cdot 10^{-5}$ or $30 \cdot 10^{-5}$ cm^2 V^{-1} s^{-1} and the mobility difference between ions A and B was in the range $1 \cdot 10^{-5}$–$10 \cdot 10^{-5}$ cm^2 V^{-1} s^{-1}. The total sample amount was 100 nmol and the sampling ratios (N_R) were 0.0204 (98:2), 1 (50:50) and 49 (2:98). The leading ion was chloride and the mobility was $79.08 \cdot 10^{-5}$ cm^2 V^{-1} s^{-1}. The concentration of the leading ion was 10 m*M* and the migration current was 100 μA, which might be practical for a separation tube with I.D. = 0.5 mm. The pH of the leading electrolyte was 6 and the pH buffer was histidine ($m_Q = 29.6 \cdot 10^{-5}$ cm^2 V^{-1} s^{-1}). Apparently from Table II, the agreement between the exactly

TABLE I

PSYSICO-CHEMICAL CONSTANTS USED IN SIMULATION (25°C)

m_0 = Absolute mobility (10^{-5} cm^2 V^{-1} s^{-1}); pK_a = thermodynamic acid dissociation constants, assumed values being used for Cl^-, $(SPADNS)^-$ and $(SPADNS)^{2-}$.

Ion	m_0	pK_a
Cl^-	79.08	−2
$(\beta$-Alanine$)^+$	36.7	3.552
$(Histidine)^+$	29.7	6.04
$(SPADNS)^-$	21.0	−3
$(SPADNS)^{2-}$	42.0	−2
$(SPADNS)^{3-}$	63.0	3.55
$(Monochloroacetate)^-$	41.1	2.865
$(Picrate)^-$	31.5	0.708
$(2,4\text{-Dihydroxybenzoate})^-$	32.0	3.395

TABLE II

EXACTLY SIMULATED RESOLUTION TIME (EXAC) AND APPROXIMATE RESOLUTION TIME (APPR) OF TWO-COMPONENT SYSTEM

n_A, n_B in nmol; m_A, m_B = absolute mobilities of components A and B (10^{-5} cm^2 V^{-1} s^{-1}); current = 100 μA; leading electrolyte, is 10 mM HCl–histidine (pH 6); approximate resolution time was evaluated using eqn. 3.

		Resolution time(s)								
		$n_A=2$, $n_B=98$			$n_A=50$, $n_B=50$			$n_A=98$, $n_B=2$		
m_A	m_B	EXAC	APPR	Difference (%)	EXAC	APPR	Difference (%)	EXAC	APPR	Difference (%)
60	59	8065	8551	6.0	8075	8573	6.2	8120	8642	6.4
60	58	3969	4229	6.6	4014	4250	5.9	4059	4320	6.4
60	57	2607	2788	6.9	2660	2810	5.6	2705	2879	6.4
60	56	1935	2068	6.9	1983	2089	5.3	2029	2158	6.4
60	55	1533	1635	6.7	1577	1657	5.1	1625	1726	6.2
60	50	719	771	7.2	765	792	3.5	810	862	6.4
30	29	5232	5658	8.1	5247	5655	7.8	5293	5747	8.6
30	28	2543	2783	9.4	2600	2779	6.9	2646	2871	8.5
30	27	1671	1824	9.2	1717	1821	6.1	1763	1913	8.5
30	26	1231	1345	9.3	1276	1342	5.2	1322	1434	8.5
30	25	964	1058	9.8	1011	1054	4.3	1057	1146	8.4
30	20	433	483	11.5	481	479	−0.4	528	571	8.1

evaluated and the approximated values is very good. It can be seen in Table II that the resolution time of the binary mixture was almost independent of the sampling ratio when the total sample amount was kept constant.

Table III shows the simulated potential gradient of the mixed zones (E_{AB}) for the same model mixtures as used in Table II. It is apparent that E_{AB} depends strongly on the sampling ratio. From this it is easily estimated that the mixed zone may be overlooked when a potential gradient or a conductivity detector is used. As shown for the actual samples in the next section, the situation is the same with UV detection.

Figs. 1 and 2 show the transient isotachopherograms of monochloroacetic acid and picric acid observed with the use of the array detector [8]. The ratios of the sample amounts (M:P) were 100:1, 20:1, 10:1, 5:1 and 2:1 in Fig. 1 and 1:1, 1:2, 1:5, 1:10 and 1:20 in Fig. 2. The total amount of the mixture injected was kept constant at 35 nmol. The boundaries between the leading and the MCA zones were rearranged at the same abscissa position. The small peak at the boundary was due to the small amount of SPADNS added to the sample solution as a position marker. The zone distributions at the transient and steady states are apparent from Figs. 1 and 2. The mixed zone was distinguishable from both a UV-transparent monochloroacetic acid zone and a UV-absorbing picric acid zone, because the concentration of picric acid in the mixed zone was smaller than the separated steady-state zone when the concentration of picric acid in the sample is small. When the amount was increased, it became difficult to distinguish the mixed zone from the steady-state zone because the concentration of picric acid in the mixed zone was similar to that of the steady-state zone. The time-based zone lengths of the whole sample zones were almost constant during detection.

Fig. 3 summarizes the dependence of the resolution time on the ratio of the sample components. It is apparent that the resolution time of this mixture was almost constant and was independent of the ratio of sample components, although under the ultimate conditions the resolution of the mixed zone could not be observed clearly, as shown in Figs. 1 and 2.

TABLE III

SIMULATED POTENTIAL GRADIENT OF STEADY ZONES AND MIXED ZONES OF MODEL ANIONS

n_A, n_B in nmol; E_A, E_B and E_{AB} = potential gradients of steady zones A and B and that of the mixed zone AB, respectively; m_A, m_B = absolute mobilities of components A and B (10^{-5} cm^2 V^{-1} s^{-1}).

		Potential gradient (V cm^{-1})				
m_A	m_B	E_A	E_B	E_{AB}		
				$n_A=2$, $n_B=98$	$n_A=50$, $n_B=50$	$n_A=98$, $n_B=2$
60	59	69.5	70.8	70.8	70.2	69.6
60	58	69.5	72.0	72.0	70.8	69.6
60	57	69.5	73.4	73.3	71.4	69.6
60	56	69.5	74.7	74.6	72.1	69.7
60	55	69.5	76.1	76.0	72.7	69.7
60	50	69.5	84.1	83.8	76.4	69.8
30	29	143.8	149.1	149.0	146.5	144.0
30	28	143.8	154.8	154.6	149.2	144.1
30	27	143.8	160.9	160.5	152.1	144.2
30	26	143.8	167.5	167.0	155.2	144.3
30	25	143.8	174.6	174.0	158.5	144.4
30	20	143.8	221.9	220.0	179.0	145.1

On the other hand, the resolution time varies significantly when the charge of the sample component varies. This was investigated using a mixture of SPADNS and MCA. Fig. 4 shows the transient isotachopherogram observed for SPADNS and MCA. The ratio of the sample amounts (S:M) was 5:1, 2:1, 1:1, 1:2 and 1:5 and the total amount of the mixture injected was 50 nmol. The small peak at the boundary of the MCA and terminating zones was due to the small amount of picric acid used as a position marker.

Fig. 5 summarizes the dependence of the resolu-

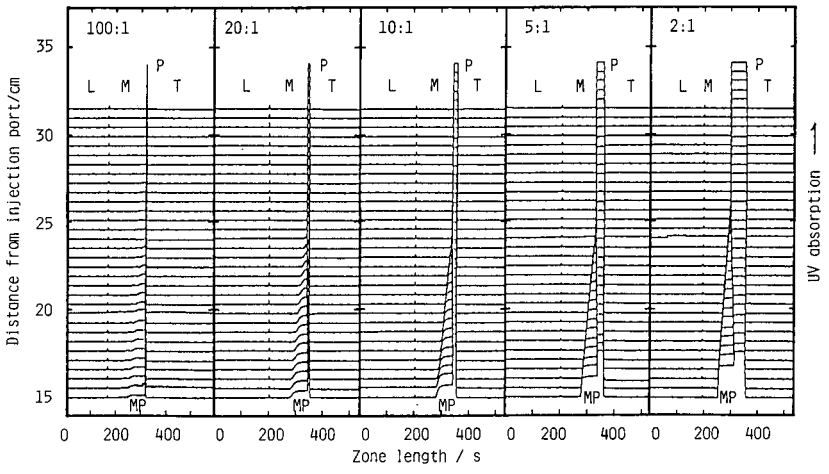

Fig. 1. Transient isotachopherogram observed for monochloroacetic acid and picric acid by the use of a 32-channel UV array detector. The ratio of the sample amounts (M:P) was 100:1, 20:1, 10:1, 5:1 and 2:1. Total amount of the mixture injected, 35 nmol; pH of leading electrolyte, 3.6 (β-alanine buffer); migration current, 50 μA.

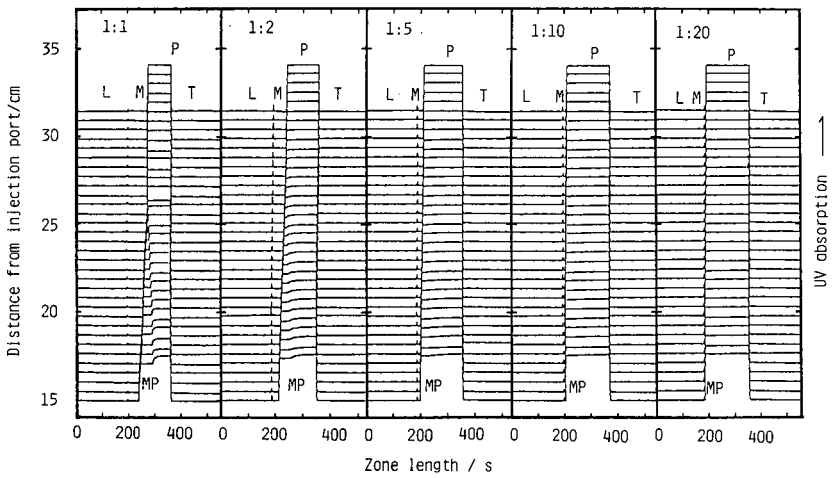

Fig. 2. Transient isotachopherogram observed for monochloroacetic acid and picric acid by the use of a 32-channel UV array detector. The ratio of the sample amounts (M:P) was 1:1, 1:2, 1:5, 1:10 and 1:20. Other conditions as in Fig. 1.

tion time on the ratio of the sample component. It is apparent that the resolution time of this system varies with the ratio of the sample components. As the zone length of SPADNS was about twice that for the same amount of MCA, the resolution time varied by a factor of two. As can be seen in Figs. 1, 2 and 4, it became difficult to distinguish the existence of the unresolved mixed zone only from an isotachopherogram if the sample had an extreme component ratio. The situation must be the same with potential gradient detection (PGD).

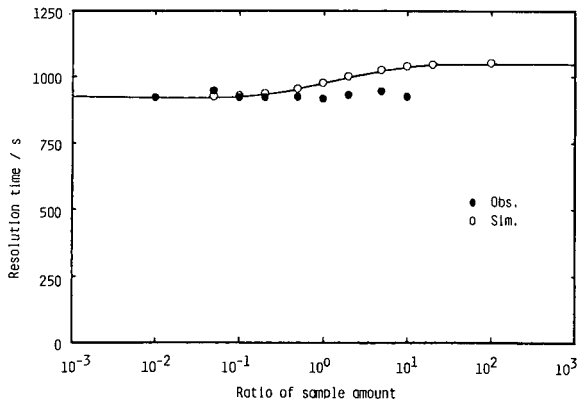

Fig. 3. Dependence of the resolution time on the ratio of the sample components. Samples, monochloroacetic acid and picric acid; total amount of the mixture injected, 35 nmol. Other conditions as in Fig. 1.

Fig. 6 shows the simulated isotachopherograms for equimolar and 10:1 MP. The total sample amount was 35 nmol and the migration current was 50μA. Apparently from Fig. 6, the mixed zone of MP is distinguishable from the steady-state zones if the mixture is equimolar. However, the potential gradient of the mixed zone of the 10:1 mixture had a value very close to that of monochloroacetic acid.

Fig. 7 shows the actual isotachopherograms of MP (M:P = 10:1) obtained with PGD. The total sample amount injected was varied from 10 to 120 nmol. In Fig. 7, the two steps between picric acid and the terminator zones are due to the unknown impurities present in the electrolytes used. Apparently there was no mixed zone between monochloroacetic acid and picric acid, but in fact this was not so because, although the overall zone length increased linearly with the sample amount, as seen in Fig. 7, the increase in the minor component picric acid was not proportional to the increase in the total zone.

The observed zone length of monochloroacetic acid and picric acid is shown in Fig. 8. Apparently from Fig. 8, the relationship between the zone length of picric acid and the total sample amount injected had a bend at *ca.* 50 nmol, suggesting that the maximum sample load of the separation tube used was 50 nmol. When a total amount greater than 50 nmol was injected, the mixed zone of MP could not be resolved, although the mixed zone

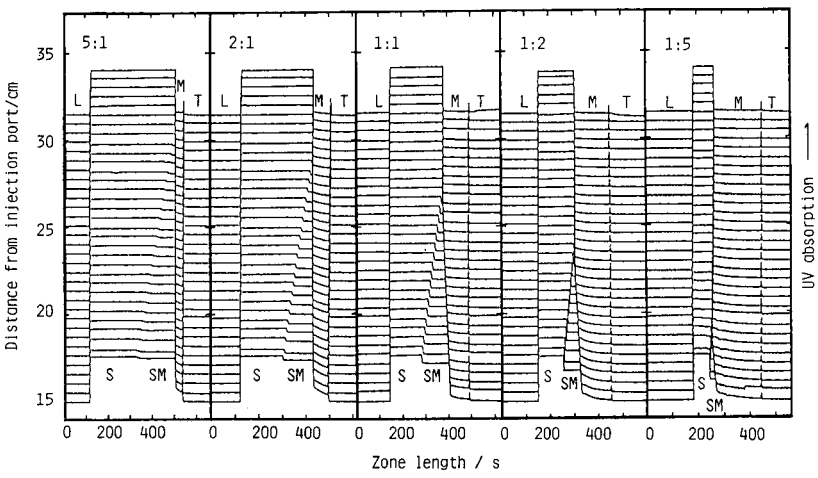

Fig. 4. Transient isotachopherogram observed for SPADNS and MCA. The ratio of the sample amounts (S:M) was 5:1, 2:1, 1:1, 1:2 and 1:5. Total amount of the mixture injected, 50 nmol; pH of leading electrolyte, 3.6 (β-alanine buffer); migration current, 50 μA.

could not be identified in Fig. 7 because the potential gradient of the mixed zone was almost the same as that of the monochloroacetic acid zone. Therefore, if one does not take account of such a bend, it is apparent that the minor component may be underestimated. The degree of underestimation depends, of course, on the amount of sample injected. If a larger amount is injected, a poorer accuracy will be obtained. In such a case, it is very important to measure zone lengths with varying sample amounts injected not only for the standard but also for the actual sample. As discussed above, the overload can be easily found from the irregular behaviour of the zone length. Table IV summarizes the simulated concentrations, potential gradients and resolution times for the transient zone MP.

Multi-component mixture

The dependence of resolution time on the ratio of the sample amounts was simulated for a six-component system of model anions. The mobilities of model anions of A–F were $60 \cdot 10^{-5}$, $55 \cdot 10^{-5}$, $50 \cdot$

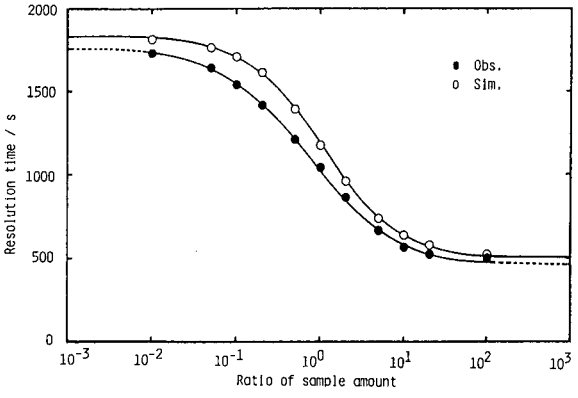

Fig. 5. Dependence of the resolution time on the ratio of the sample components. Samples, SPADNS and monochloroacetic acid. Total amount, 50 nmol. Other conditions as in Fig. 4.

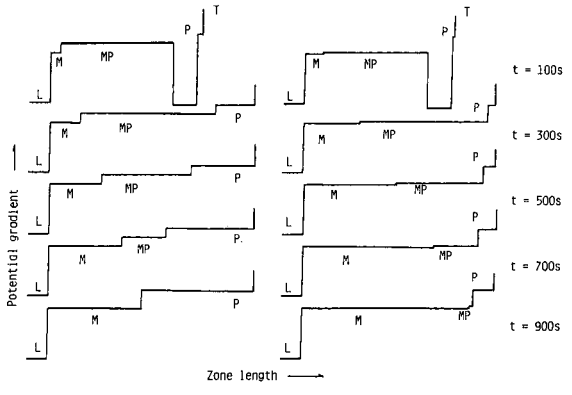

Fig. 6. Simulated isotachopherograms of equimolar and 10:1 mixtures of monochloroacetic acid and picric acid. Total sample amount, 35 nmol.

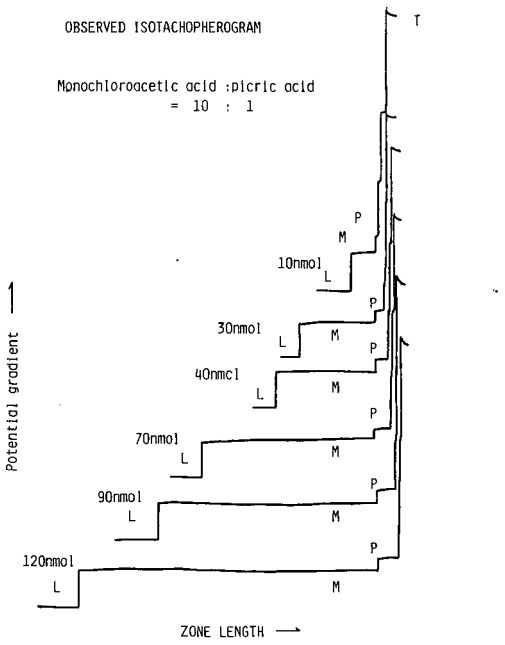

Fig. 7. Observed isotachopherograms of monochloroacetic acid (M)–picric (P) acid mixture (10:1) with the use of a potential gradient detector. Leading electrolyte (L), 5 m*M* HCl–β-alanine (pH 3.6); terminating electrolyte (T), 10 m*M* caproic acid; migration current, 50 μA.

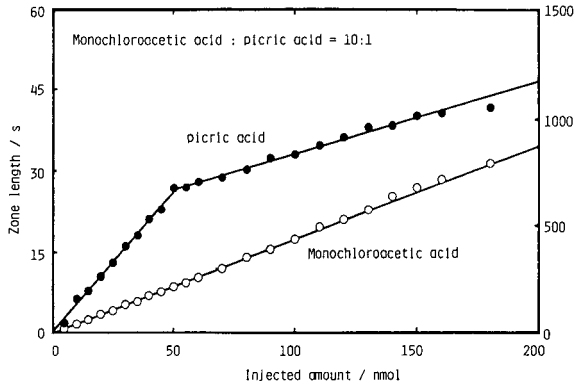

Fig. 8. Observed time-based zone length of monochloroacetic–picric acid mixture (10:1) *vs.* total molar amount. Conditions as in Fig. 7.

10^{-5}, $45 \cdot 10^{-5}$, $40 \cdot 10^{-5}$ and $35 \cdot 10^{-5}$ $cm^2 V^{-1} s^{-1}$. The pK_a values are assumed to be -1. The total amount of the components was kept constant at 100 nmol and the amount of component A was increased and the others were decreased.

Fig. 9 shows the separation diagram for the six model anions for equimolar, 4:1:1:1:1:1 and 8:1:1:1:1:1 mixtures. The leading ion was 10 m*M* chloride and the pH of the leading electrolyte was 6 (histidine buffer). The migration current was 100

TABLE IV

SIMULATED CONCENTRATIONS, POTENTIAL GRADIENTS AND RESOLUTION TIMES FOR THE TRANSIENT ZONES OF MONOCHLOROACETIC ACID AND PICRIC ACID

Total sample amount, 35 nmol; leading electrolyte, 5 m*M* HCl–β-alanine (pH 3.6); migration current, 50 μA. $C_{t,M,MP}$ and $C_{t,P,MP}$ = total concentration (m*M*) of monochloroacetic acid and picric acid in the transient mixed zone; E_{MP} = potential gradient (V cm^{-1}) of the mixed zone. Steady state: $C_{t,M}$ = 3.67 m*M*, $C_{t,P}$ = 3.10 m*M*, E_M = 86.8 V cm^{-1} and E_P = 103.8 V cm^{-1}.

	Monochloroacetic acid (M) : picric acid (P)								
	100:1	10:1	5:1	2:1	1:1	1:2	1:5	1:10	1:100
t_A	151.1	138.7	127.2	101.7	76.30	50.86	25.43	13.87	1.511
t_B	1.790	16.44	30.14	60.27	90.41	120.5	150.7	164.4	179.0
pH_M	3.820	3.822	3.824	3.827	3.831	3.834	3.837	3.838	3.840
$C_{t,M,MP}$	3.621	3.234	2.890	2.185	1.549	0.976	0.462	0.245	0.026
$C_{t,P,MP}$	0.041	0.366	0.657	1.252	1.788	2.272	2.706	2.889	3.074
E_{MP}	87.03	88.53	89.92	92.91	95.81	98.61	101.3	102.5	103.7
$v_{M/MP}$	2.559	2.604	2.645	2.735	2.821	2.905	2.984	3.019	3.056
m_M	35.24	35.26	35.28	35.32	35.35	35.39	35.42	35.43	35.45
m_P	29.41	29.41	29.42	29.43	29.45	29.46	29.47	29.47	29.47
$t_{res,MP}$	923.0	930.5	938.1	956.3	977.0	1000	1026	1039	1054

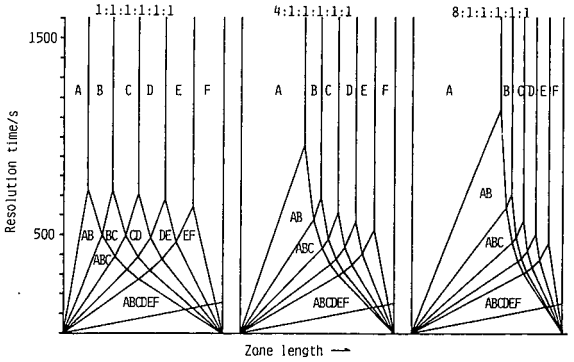

Fig. 9. Separation diagrams simulated for an equimolar six-component mixture of model anions (A–F). The mobilities of A–F were $60 \cdot 10^{-5}$, $55 \cdot 10^{-5}$, $50 \cdot 10^{-5}$, $45 \cdot 10^{-5}$, $40 \cdot 10^{-5}$ and $35 \cdot 10^{-5}$ cm^2 V^{-1} s^{-1}, respectively. The pK_a values were assumed to be -1. The total amount of separands was 100 nmol. For the equimolar mixture, the amount of A–F was 16.67 nmol, for the 4:1:1:1:1:1 mixture the amount of A was 44.44 nmol and that of B–F was 11.11 nmol and for the 8:1:1:1:1:1 mixture, the amount of A was 61.54 and that of B–F was 7.69 nmol.

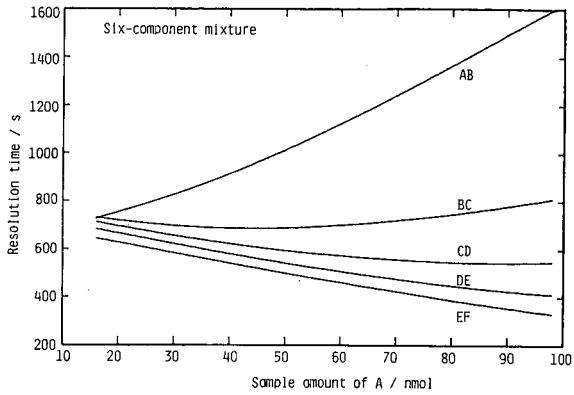

Fig. 10. Amount of component A *vs.* resolution time of the mixed zones AB, BC, CD, DE and EF for a six-component model mixture (total amount = 100 nmol). Simulation conditions as in Fig. 9. The migration current was 100 μA.

μA. The amount of B–F in the equimolar mixture is twice that in the 8:1:1:1:1:1 mixture. If the components E and F are separated independently as a binary mixture, the resolution time of equivalent amounts of E and F in these cases should differ by a factor of two. However, as seen in Fig. 9, the resolution time of E and F for the 8:1:1:1:1:1 mixture slightly smaller than that for the equimolar mixture. This can be explained by the effect of the coexisting components being more significant with the 8:1:1:1:1:1 mixture than with the equimolar mixture.

Fig. 10 shows the simulated dependence on the ratio of the components of the resolution time for five binary mixed zones of a six-component mixture. Apparently, $t_{res,AB}$ increased with increase in the total amount of A and B. The resolution time of the other mixed zones (BC, CD, DE and EF) decreased gradually with increase in the amount of A. The $t_{res,AB}$ value for the six-component equimolar mixture [$t_{res,AB}(6)$] was 733.5 s [16.67 nmol each, separation number [5,6] (S) = 0.22] and that of the binary mixture [$t_{res,AB}(2)$] was 526.0 s (S = 0.031). The difference was caused by the effect of the coexisting components on the potential gradient of the mixed zone AB. With the 15:1:1:1:1:1 mixture, $t_{res,AB}(6)$ was 1303.3 s and $t_{res,AB}(2)$ was 1294.7 s. The amount of A was 75 nmol and S was 0.056. In this instance the difference in $t_{res,AB}$ was very small because of the coexisting components of A and B,

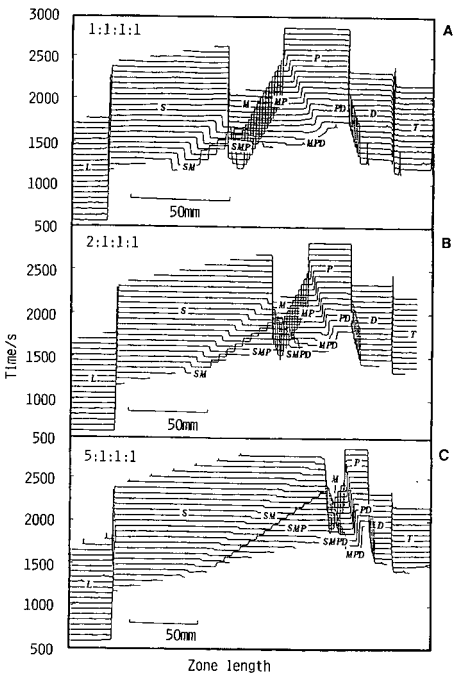

Fig. 11. Observed separation process for a mixture of SPADNS, monochloroacetic acid, picric acid and 2,4-dihydroxybenzoic acid with the use of a scanning UV detector. The ratio of the component amounts was (A) 1:1:1:1, (B) 2:1:1:1 and (C) 5:1:1:1. Leading electrolyte, 5 mM HCl–β-alanine (pH 3.6); terminating electrolyte, 10 mM caproic acid; migration current, 50 μA.

i.e., the amount of C–F is smaller than for the equimolar mixture. On the other hand, for example, $t_{res,EF}(6)$ was 642.3 s for the six-component equimolar mixture and $t_{res,EF}(2)$ was 400.3 s (S = 0.0250 and 0.04018, respectively). With the 15:1:1:1:1:1 mixture, the amount of B–F was 5 nmol. The $t_{res,EF}$ (6) value was 404.5 s and $t_{res,EF}(2)$ was 120.2 s (S = 0.012 and 0.040, respectively). The significant delay was due to the large amount of the coexisting ions A–D (total amount = 90 nmol). From this simulation it is concluded that the resolution time of a sample present in a very small amount in a matrix is affected by the coexistence of the other components. If the total amount of the mixture is kept constant, it depends on the ratio of the sample amount, although the dependence is not very strong.

This effect was observed for the mixture of SPADNS, monochloroacetic acid, picric acid and 2,4-dihydroxybenzoic acid. The total amount was 100 nmol and the ratio was varied as 1:1:1:1, 2:1:1:1, 5:1:1:1 and 10:1:1:1. The leading electrolyte was 5.00 m*M* hydrochloric acid–*β*-alanine (pH 3.6) and the migration current was 50 *μ*A. Fig. 11 shows the transient isotachopherograms obtained with the use of the scanning UV detector [4] except for the 10:1:1:1 case. Table V and Fig. 12 summarize the observed resolution times of the mixed zones. Good agreement was obtained, confirming our theoretical estimates.

From Fig. 11 and Table V, it is apparent that the resolution time of the mixed zone of SPADNS and monochloroacetic acid (SM) increased with increase in SPADNS concentration, the values being 1199, 1526, 2118 and 2472 s, respectively. On the other hand, the resolution time of picric acid and

TABLE V

RESOLUTION TIME OF MIXED ZONE IN THE SEPARATION PROCESS OF SPADNS, MONOCHLOROACETIC ACID, PICRIC ACID AND 2,4-DIHYDROXYBENZOIC ACID

Total amount = 100 nmol; leading electrolyte, 5 m*M* HCl–*β*-alanine (pH = 3.6); migration current, 50 *μ*A. S:M:P:D = SPADNS : monochloroacetic acid : picric acid : 2.4-dihydroxybenzoic acid.

S:M:P:D	Mixed zones	Resolution time(s)		
		Observed	Simulated	Difference (%)
1:1:1:1	SM	1199	1306	8.9
	MP	1896	1915	1.0
	PD	1469	1514	3.1
	SMP	1014	1075	6.0
	MPD	1110	1154	4.0
	SMPD	–	823	–
2:1:1:1	SM	1526	1737	13.8
	MP	1908	1968	3.1
	PD	1548	1547	−0.1
	SMP	1279	1387	8.4
	MPD	1220	1251	2.5
	SMPD	–	1034	–
5:1:1:1	SM	2118	2445	15.4
	MP	2049	2171	6.0
	PD	1614	1648	2.1
	SMP	1715	1870	9.0
	MPD	1401	1459	4.1
	SMPD	1275	1353	6.1
10:1:1:1	SM	2472	2919	18.1
	MP	2150	2352	9.4
	PD	–	1730	–
	SMP	1955	2183	11.7
	MPD	–	1614	–
	SMPD	1420	1556	9.6

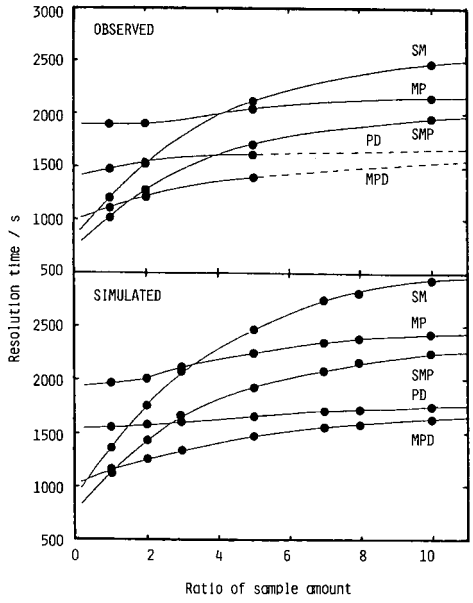

Fig. 12. Observed and simulated resolution times of four-component mixture of SPADNS (S), monochloroacetic acid (M), picric acid (P) and 2,4-dihydroxybenzoic acid (D). The abscissa scale corresponds to S:M:P:D = 1:1:1:1 to 10:1:1:1. Conditions as in Fig. 11.

2,4-dihydroxybenzoic acid (PD) increased slightly (1469, 1548 and 1614 s). This increase was not simulated for the model strong electrolytes. The cause of the difference between the simulation for strong electrolytes and the observation for the present sample was due to the fact that 2,4-dihydroxybenzoic acid is a weak electrolyte and the difference in the pH of the mixed zones affected the resolution time. Although we emphasized resolution time under a constant migration current from a practical viewpoint, it should be noted that the essential factor is the amount of electricity applied during the migration process [1,2].

In conclusion, the present simulation and experiments confirmed that isotachophoresis has very high separation efficiency even for the separation of minor components in a matrix. If a highly sensitive detection method could be applied, the utility of isotachophoresis would be increased. We are currently trying to use particle-induced X-ray emission (PIXE) for the targets fractionated off-line.

ACKNOWLEDGEMENT

T.H. expresses his thanks to the Ministry of Education, Science and Culture of Japan for support of part of this work under a Grant-in-Aid for Scientific Research (No. 1540482).

REFERENCES

1 P. Bocek, M. Deml, B. Kaplanova and J. Janak, *J. Chromatogr.*, 160 (1978) 1.
2 P. Gebauer and P. Bocek, *J. Chromatogr.*, 320 (1985) 49.
3 T. Hirokawa, Y. Yokota and Y. Kiso, *J. Chromatogr.*, 545 (1991) 267.
4 T. Hirokawa, Y. Yokota and Y. Kiso, *J. Chromatogr.*, 538 (1991) 403.
5 F. E. P. Mikkers, F. M. Everaerts and J. A. F. Peek, *J. Chromatogr.*, 168 (1979) 293.
6 F. E. P. Mikkers, F. M. Everaerts and J. A. F. Peek, *J. Chromatogr.*, 168 (1979) 317.
7 G. Brouwer and G. A. Postema, *J. Electrochem. Soc.*, 117 (1970) 874.
8 T. Hirokawa, K. Nakahara and Y. Kiso, *J. Chromatogr.*, 463 (1989) 39.
9 T. Hirokawa, K. Nakahara and Y. Kiso, *J. Chromatogr.*, 463 (1989) 51.
10 T. Hirokawa, K. Nakahara and Y. Kiso, *J. Chromatogr.*, 470 (1989) 21.

Journal of Chromatography, 585 (1991) 309–314
Elsevier Science Publishers B.V., Amsterdam

CHROM. 23 567

Short Communication

Ligand-exchange chromatography of alkenes on stationary phases containing palladium(II) complexes

Enantiomeric separation of *trans*-1,2-divinylcyclohexane

Christina Moberg*, Torbjörn Norin*, László Rákos and Kristina Sjödin

Department of Organic Chemistry, Royal Institute of Technology, S-100 44 Stockholm (Sweden)

(First received November 20th, 1990; revised manuscript received June 11th, 1991)

ABSTRACT

Alkenes can be separated from alkanes and alkenes with terminal double bonds from other alkenes using palladium(II) complexes of chelating N,O-ligands supported on polystyrene–divinylbenzene. A palladium complex containing a polymer-bound chiral aminoalcohol has been shown to separate the enantiomers of *trans*-1,2-divinylcyclohexane with a separation factor of 1.3. The resolution is, however, still not satisfactory.

INTRODUCTION

The present high demand for chiral compounds has stimulated the development of chromatographic techniques for the separation of enantiomeric compounds on both analytical and preparative scales [1,2]. Of the various techniques developed, ligand-exchange chromatography, using the complexing properties of grafted metal complexes, has proven particularly useful for the separation of amino acids and their derivatives and for other molecules containing polar functional groups, most commonly on copper(II)-containing resins [3,4]. Considerably less attention has been paid to the separation of enantiomeric alkenes. The separation of such compounds is important in organic chemistry as many biologically active compounds, such as terpenoids and pheromones, contain alkene groups as the only functionality.

A number of examples of enantiomeric separations of simple alkenes by gas chromatography have been reported [5–8], but this technique is often unsatisfactory as a result of the decomposition of compounds that may occur at the higher temperatures required. Therefore the development of liquid chromatographic methods is desirable. To the authors' knowledge, the only examples of the direct separation of the enantiomers of chiral alkenes use acetylated microcrystalline cellulose [9,10] and chiral polyacrylate [11]. Other reported methods rely on the separation of preformed diastereomeric metal complexes, which require subsequent decomplexation [12–16]. Separation on a preparative scale is often required, which is usually more convenient using liquid chromatography. It has now been found that palladium complexes of chiral chelating ligands supported on cross-linked polystyrene can be used for the enantioseparation of alkenes.

0021-9673/91/$03.50

EXPERIMENTAL

The structures of the numbered compounds discussed are given in Fig. 1.

Resin **1** [17] and polystyrene functionalized with chiral non-racemic epoxy groups [18] were prepared as described previously using Bonopore (a macroporous styrene–divinylbenzene polymer) beads with an average particle size of 100 μm. Reaction mixtures containing this polymer were shaken to minimize particle breakdown. After each reaction step the polymers were dried under vacuum at ambient temperature for at least 15 h. Tetrahydrofuran (THF) was freshly distilled from benzophenone ketyl radical. IR spectra (KBr) were recorded on a Perkin-Elmer 1710 FT spectrophotometer.

Preparation of stationary phases

Preparation of ***3***. Polystyrene–divinylbenzene substituted with α-methoxy-β-tosyloxyethyl groups[a] (1.76 g), containing approximately 0.4 mmol of tosyl groups per gram of polymer, was treated with 2-cyano-8-hydroxyquinoline (340 mg) and anhydrous potassium carbonate (312 mg) in N,N-dimethyl formamide (DMF) at 85°C under nitrogen for 48 h. The polymer was filtered off, washed [methanol, water, methanol–water (1:1), acetone, dichloromethane, methanol] and dried. This procedure gave 1.80 g of a polymer (IR 2237 cm^{-1}, weak, CN) of which 1.76 g was treated with a mixture of sulphuric acid (1.2 ml), acetic acid (13 ml) and water (1.2 ml) at 80°C for 24 h and then washed [water, methanol–water (1:1), methanol] and dried to give 1.72 g of quinaldic acid containing polymer **3** (IR 1735 cm^{-1}), COOH).

Preparation of ***5***. A polymer containing approximately 2 mmol/g (*R*)-styrene oxide groups [18] (3.83 g) was reacted with (*S*)-α-phenethylamine (3.57 g) in refluxing methanol for five days, washed (methanol, methanol–water, dichloromethane, methanol) and dried, resulting in 4.20 g of a polymer containing amino alcohol units. To a suspension of this polymer (1.5 g) and sodium hydride (54 mg) in THF was added a solution ot *tert*-butanol (133 mg) in THF. This mixture was left to react for 4.5 h at ambient temperature under an atmosphere of nitrogen. Methyl iodide (1.7 g) was added and the mixture left for a further 17 h. The polymer was filtered off, washed (methanol, water, methanol, dichloromethane, methanol) and dried to give 1.50 g of polymer **5**.

Preparations of polymer-supported palladium complexes. General procedure. The functionalized polymers were treated with a slight excess of Pd $(OAc)_2$ in THF under nitrogen for 20, 6.5 and 72 h for polymers **2**, **4** and **6**, respectively, then washed (THF) under nitrogen and dried. All operations were performed in a Schlenck apparatus to avoid the presence of air. The amount of palladium was determined by elemental analyses to be 0.39 and 0.58 mmol/g for resins **2** and **6**, respectively, whereas that of resin **4** was estimated to be about 0.1 mmol/g by the increase in weight during the preparation of the complex.

Chromatographic instrumentation

An Omni glass chromatography column (150 mm × 6.6 mm) was used, together with an FMI RPG-400 pump. The sample was injected directly into the PTFE tubing leading to the column and eluted with *n*-hexane–methylene chloride (4:1). No detector was used; the collected fractions were analysed by gas chromatography using a DB-wax column (30 m × 0.25 mm I.D., J&W Scientific). The enantiomeric composition of *trans*-1,2-divinylcyclohexane was determined using a fused-silica capillary Cyclodex-B column (permethylated β-cyclodextrin–DB-1701, 30 m × 0.25 mm I.D., J&W Scientific, column temperature 90°C, carrier gas 120 kPa helium, internal standard *n*-nonane).

The polymeric palladium complex **2** (1.5 g) was allowed to swell in methylene chloride and the slurry was then packed onto the column; complexes **4** and **6** (1.2 and 1.4 g, 10.5 cm, respectively) were dry-packed onto the column.

Liquid chromatographic separation of n-dodecane, trans-5-decene and 1-decene

Complex ***2***. A solution (0.4 ml) of *trans*-5-decene and 1-decene (1 μl of each compound in 1 ml of solvent) was injected. Fractions of 60 drops were

[a] Obtained by opening of polymer-supported (*R*)-styrene oxide (90% enantiomeric excess) with methanol under the influence of boron trifluoride etherate and subsequent treatment with *p*-toluenesulphonyl chloride. This reaction sequence is under further study and will be described in more detail elsewhere.

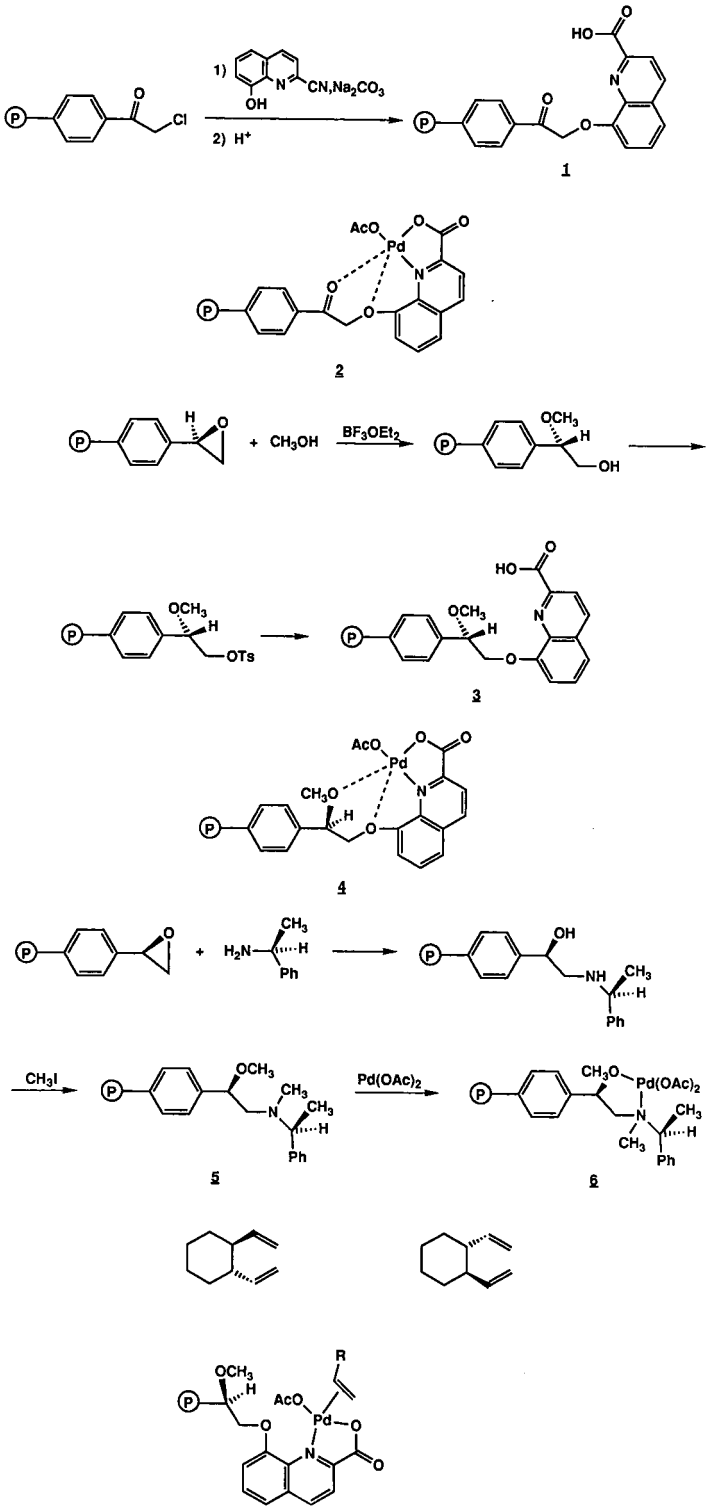

Fig. 1. Structures of compounds **1–6**. Ac = Acetyl; Et = ethyl.

collected at a flow-rate of 0.2 ml/min. The retention volumes were: V (*trans*-5-decene), about 700 drops; V (1-decene), about 800 drops; V (dodecane, obtained independently), about 300 drops.

Complex ***4***. A solution (0.4 ml) of *n*-dodecane, *trans*-5-decene and 1-decene (0.5 μl of each compound in 1.6 ml of solvent) was injected. Fractions of 20 drops were collected at a flow-rate of 0.4 ml/min. V (dodecane), 170 drops; V (*trans*-5-decene), 210 drops; V (1-decene), 350 drops.

Complex ***6***. A solution (0.4 ml) of *n*-dodecane, *trans*-5-decene and 1-decene (0.5 μl of each compound in 0.8 ml of solvent) was injected. Fractions of 20 drops were collected at a flow-rate of 0.3 ml/min. V (dodecane), 180 drops; V (*trans*-5-decene), 190 drops; V (1-decene), 270 drops.

Liquid chromatographic separation of trans-1,2-divinylcyclohexane

Complex ***4***. A solution (0.4 ml) of *trans*-divinylcyclohexane and *n*-dodecane (0.5 μl of each compound in 1.6 ml of solvent) was injected. Fractions of 60 drops were collected at a flow-rate of 0.4 ml/min. V (dodecane), 185 drops, V (divinylcyclohexane), 500 drops.

Complex ***6***. A solution (0.1 ml) of *trans*-divinylcyclohexane and *n*-dodecane (2 μl of each compound in 1.6 ml of solvent) was injected. Fractions of 0.1 ml (5 drops) were collected at a flow-rate of 0.4 ml/min. V (dodecane), 178 drops; V (1), 228 drops; V (2), 243 drops, yielding an α-value of 1.3 [V_o = V(dodecane)].

RESULTS AND DISCUSSION

Macroporous polystyrene–divinylbenzene with pendant chloroacetyl groups was reacted with 2-cyano-8-hydroxyquinoline and hydrolysed according to a previously described procedure to yield the polymeric ligand **1** [17]. Treatment of this polymeric ligand with palladium(II) acetate gave a palladium complex, which probably has a square planar structure (**2**) in which the carboxylate oxygen, the quinoline nitrogen, one of the two remaining oxygen atoms of the ligand and one acetate group take part in the co-ordination to the metal ion. When this polymer was used as a stationary phase for column liquid chromatography, 1-decene was eluted after 5-decene, which in turn was eluted after *n*-dodecane, demonstrating the ability of complex **2** to co-ordinate alkenes, thus offering a method complementary to argentation chromatography [19,20].

A chiral analogue of **2** was then considered in an investigation of the separation of enantiomeric alkenes. For this purpose, polymer-supported (*R*)-styrene oxide, prepared via the asymmetric reduction of chloroacetylated polystyrene–divinylbenzene [18], was reacted with methanol in the presence of BF_3OEt_2 to yield a hydroxyether which was tosylated, and the resulting polymer was reacted with 2-cyano-8-hydroxyquinoline and then hydrolysed to yield stationary phase **3**. A palladium complex of this ligand (**4**), with a chiral centre next to the phenyl ring of the polymer backbone, was also found to retain alkenes, the retention times being similar to those of complex **2**, taking into account the different concentration of palladium on the two resins. However, no, or little chiral recognition was achieved on the attempted separation of (*R,R*)- and (*S,S*)-1,2-divinylcyclohexane using this polymeric complex.

A second ligand (**5**), containing two asymmetric centres, was prepared by the reaction of polymer-supported (*R*)-styrene oxide with (*S*)-α-phenethylamine followed by O- and N-methylation. Subsequent treatment with palladium acetate yielded complex **6**. Shorter retention times were observed with this phase compared with the quinoline-substituted resins **2** and **4**. It was possible to separate *n*-dodecane, *trans*-5-decene and 1-decene with this material, and also to observe enantioselective interactions with the divinylcyclohexanes. The chromatographic system has not been optimized. Although a separation factor (α) of 1.3 was obtained, the chromatographic separation of the enantiomers was far from complete due to the low efficiency of the column (Fig. 2).

The polymer could be used repeatedly without any noticeable change in properties. The amount of palladium complexed to the polymer was determined and was unchanged, even after repeated use.

The co-ordination of an alkene to the polymeric four-co-ordinate palladium complexes probably results in ligand exchange involving the decomplexation of one (or two if two alkenes are co-ordinated) of the initially co-ordinated groups rather than in the formation of five co-ordinate complexes. The hard neutral oxygen donor is probably exchanged.

This proposed mechanism for the co-ordination of alkenes explains why enantiomeric separation is achieved only with complex **6**, in spite of the strong complexing properties of complex **4**, as on complexation of the alkene, the only chiral centre in complex **4** is a long way from the metal atom.

The functional yields in the reaction sequences leading to polymers **4** and **6** are less than quantitative and all the reactions are probably non-selective, thus giving rise to by-products bound to the polymer. Such by-products may take part in the complexation of palladium and thus disturb the interactions with the molecules being separated. Furthermore, the optical purity of resins **4** and **6** is lower than 100%, as polymeric epoxide with an enantiomeric excess of about 90% was used and the boron trifluoride-catalysed opening of the epoxy ring is known to cause some further racemization [21]. Although enantioselective separation can be achieved even on stationary phases which are not monochiral, optimization of the reaction conditions leading to the present stationary phases is expected to result in polymers with superior properties.

In this study, overlapping of the peaks due to low column efficiency and tailing was observed. Whether these effects are due to the support material or to slow kinetics in the exchange process is not known, but polymers better suited for this purpose will be investigated in future work. The performance of the chromatographic system also needs to be improved. Furthermore, ligands with chirality in close proximity to the metal atom are presently being prepared and their chromatographic properties will be studied.

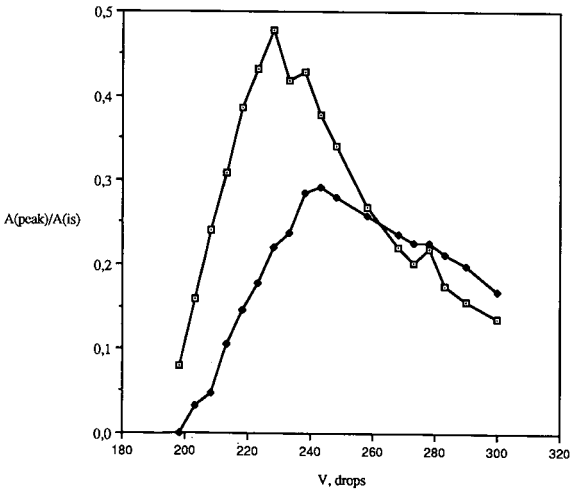

Fig. 2. Efficiency of the chromatographic separation determined from gas chromatographic data of the collected fractions. A = Integrated area; is = internal standard; V = retention volume. □ = Peak 1; ◆ = peak 2.

ACKNOWLEDGEMENTS

This work was supported by the Swedish Board for Technical Development and by the Swedish Natural Science Research Council. Valuable discussions with Dr. Johan Roeraade are gratefully acknowledged. The Polymer Bonopore was a generous gift from Nobel Chemicals AB.

REFERENCES

1 S. G. Allenmark, *Chromatographic Enantioseparation, Methods and Applications*, Ellis Horwood, Chichester, 1988.
2 W. H. Pirkle and T. C. Pochapsky, *Chem. Rev.*, 89 (1989) 347.
3 J. Porath, J. Carlsson, I. Olsson and G. Belfrage, *Nature (London)*, 258 (1975) 598.
4 V. A. Davankov, J. D. Navratil and H. F. Walton, *Ligand Exchange Chromatography*, CRC Press, Boca Raton, FL, 1988.
5 V. Schurig, *Angew. Chem. Int. Ed. Engl.*, 16 (1977) 110.
6 W. A. König, R. Krebber, P. Evers and G. Bruhn, *J. High Resolut. Chromatogr.*, 13 (1990) 328.
7 G. Takeoka, R. A. Flath, T. R. Mon, R. G. Buttery, R. Teranishi, M. Güntert, R. Lautamo and J. Szejtli, *J. High Resolut. Chromatogr.*, 13 (1990) 202, and references cited therein.
8 V. Schurig and H.-P. Nowotny, *Angew. Chem. Int. Ed. Engl.*, 29 (1990) 939.
9 G. Hesse and R. Hagel, *Liebigs Ann. Chem.*, (1976) 996.
10 R. Isaksson, J. Roschester, J. Sandström and L.-G. Wistrand, *J. Am. Chem. Soc.*, 107 (1985) 4074.
11 H. Yuki, Y. Okamoto and I. Okamoto, *J. Am. Chem. Soc.*, 102 (1980) 6356.
12 J. Köhler and G. Schomburg, *Chromatographia*, 14 (1981) 559.
13 M. Goldman, Z. Kustanovich, S. Weinstein, A. Tishbee and E. Gil-Av, *J. Am. Chem. Soc.*, 104 (1982) 1093.
14 J. Köhler and G. Schomburg, *J. Chromatogr.*, 255 (1983) 311.
15 J. Köhler, A. Degee and G. Schomburg, *Chromatographia*, 18 (1984) 119.
16 D. Schmidt and E. Gil-Av, *J. Organomet. Chem.*, 307 (1986) 377.
17 C. Moberg, M. Muhammed, A. C. Nilsson and M. Weber, *React. Polym.*, 12 (1990) 31.
18 T. Antonsson, U. Jacobsson, C. Moberg and L. Rákos, *J. Org. Chem.*, 54 (1989) 1191.

19 O. K. Guha and J. Janák, *J. Chromatogr.*, 68 (1972) 325.
20 M. Lienne, P. Gareil, R. Rosset, J. F. Husson, M. Emmelin and B. Neff, *J. Chromatogr.*, 395 (1987) 255; and references cited therein.
21 C. Moberg, L. Rákos and L. Tottie, in preparation.

Journal of Chromatography, 585 (1991) 315–317
Elsevier Science Publishers B.V., Amsterdam

CHROM. 23 595

Short Communication

Ligand-exchange ion chromatographic determination of malic acid enantiomers in apple juice with photometric detection

Atsushi Yamamoto*, Akinobu Matsunaga and Eiichi Mizukami

Toyama Institute of Health, 17-1, Nakataikoyama, Kosugi-machi, Toyama 939-03 (Japan)

Kazuichi Hayakawa and Motoichi Miyazaki

Faculty of Pharmaceutical Sciences, Kanazawa University, 13-1, Takara-machi, Kanazawa 920 (Japan)

(First received April 26th, 1991; revised manuscript received June 26th, 1991)

ABSTRACT

An ion chromatographic separation with photometric detection using a chiral copper(II) complex as the eluent has been developed for the resolution of enantiomers of malic acid in commercially available apple juices. The results obtained by this method were in good agreement with those by an enzymatic method with separation by high-performance liquid chromatography.

INTRODUCTION

Chiral organic compounds usually exist in nature in only one enantiomeric form. For example, malic acid in pure apple juices is wholly in the L-form [1,2]. In Japan, a synthetic racemic mixture of malic acid may be used as a food additive to reduce production costs, although concentrations of the respective enantiomers in the commercial product have rarely been reported.

A time-consuming enzymatic method with separation by high-performance liquid chromatography (HPLC) has been used for the determination of malic acid enantiomers [1,2]. Direct HPLC separation of these enantiomers has been also attempted [3–7]. However, complicated post-column reaction requirements still prevent this method from being applied to real samples. Direct detection after chromatographic separation has been reported [8], but the system could not simultaneously determine the enantiomers in actual samples as a result of the presence of interfering peaks.

A simple, selective system has been reported [9] for the direct separation and detection of malic acid enantiomers by ligand-exchange photometric ion chromatography (PIC). This paper reports the application of this system to the determination of these enantiomers in commercially available apple juices and sour drinks.

EXPERIMENTAL

The PIC apparatus and reagents were as described previously [9]. The enantiomeric separation

0021-9673/91/$03.50

was performed with a 5 cm × 4.6 mm I.D. anion-exchange column (TSK gel IC-Anion-PW, Tosoh, Tokyo, Japan) maintained at 40°C. An eluent containing 1.5 m*M* copper(II) hydroxide and 3 m*M* L-tartaric acid (adjusted to pH 4.8 with sodium hydroxide solution) was delivered at a flow-rate of 0.8 ml/min. The detection wavelength was 283 nm.

Eleven commercially available apple juices and five sour drinks were analysed. The only pretreatment of the sample was dilution with the eluent, followed by ultrafiltration through a Tosoh Ultracent-10 disposable cartridge. A 30-μl volume of the ultrafiltrate was injected into the PIC system.

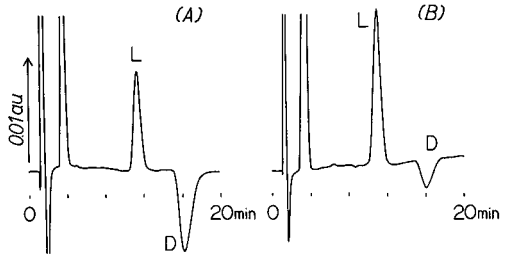

Fig. 1. Photometric ion chromatograms of (A) standard L- and D-malic acid (30 nmol each) and (B) a commercially available apple juice (No. 4 in Table I) diluted twenty-fold with eluent. Peaks: L = L-malic acid; D = D-malic acid.

RESULTS AND DISCUSSION

Previous studies [9] of the separation and resolution of malic acid enantiomers had shown that an increase for copper(II) hydroxide and L-tartaric acid in the eluent led to a reduction in the time required for the analysis, although the sensitivity was lower. An increase in the molar ratio of copper to tartrate or in the pH value of the eluent led to an improvement in the separation of the enantiomers, although the elution of the analyte was delayed. Consequently, an aqueous solution containing 1.5 m*M* copper hydroxide and 3 m*M* L-tartaric acid was chosen as the eluent. Under these conditions, L-malic acid eluted before the D-isomer and the D-isomer gave a negative peak at all pH values, although the L-isomer showed an inversion of the peak direction as the pH increased. When the pH of the eluent was 4.8, both the peak height of L-malic acid and the peak depth of D-malic acid were approximately equal and linear calibration graphs were obtained for a plot of the peak areas *versus* the amount injected in the range 3–100 nmol. Fig. 1A shows a typical chromatogram of a standard solution. The standard deviation for repeated injections of this mixture was less than 2% for each enantiomer. Care must be taken when performing successive injections as the system peak appears at about 50 min. However, this peak can be removed from the chromatogram by a column-switching procedure [10], in which the pretreatment column is joined to the anion-exchange column by a switching valve.

In this system, peaks are only obtained with a compound such as malic acid which has a complex formation constant with copper similar to that of tartrate. This PIC method, highly specific for malic

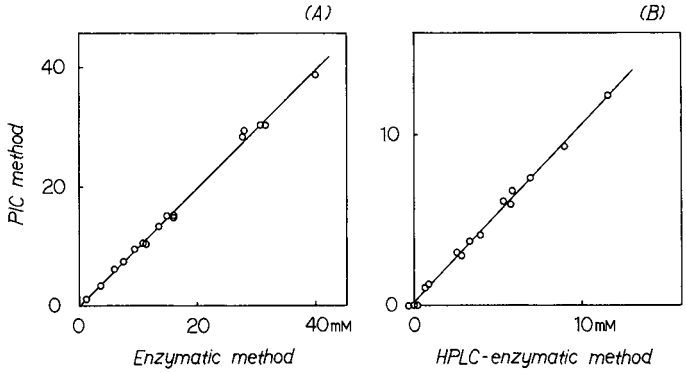

Fig. 2. Comparison of the results obtained for malate enantiomers by the proposed PIC and enzymatic methods. (A) L-malic acid, r = 0.998, n = 16; (B) D-malic acid, r = 0.997, n = 15.

TABLE I

CONCENTRATION OF MALIC ACID ENANTIOMERS IN COMMERCIAL FRUIT JUICES

Sample description	Sample No.	Malic acid concentration (g/100 g)			D-isomer (%)
		Total	L-isomer	D-isomer	
Fruit juice (juice = 100%)	1	0.460	0.405	0.055	11.9
	2	0.431	0.393	0.038	8.9
	3	0.517	0.517	nd	0
	4	0.495	0.404	0.091	18.3
	5	0.238	0.197	0.041	17.4
Fruit juice drink (50 ⩽ juice < 100%)	6	0.201	0.201	nd	0
	7	0.478	0.378	0.100	21.0
Fruit soft drink (10 ⩽ juice < 50%)	8	0.260	0.179	0.081	31.3
	9	0.098	0.098	nd	0
	10	0.142	0.128	0.014	9.8
	11	0.266	0.141	0.125	47.0
	12	0.138	0.138	nd	0
Soft drink (0 < juice < 10%)	13	0.366	0.201	0.165	45.1
Sour drink (juice = 0%)	14	0.031	0.015	0.016	51.7
	15	0.096	0.046	0.050	52.2
	16	0.162	0.083	0.079	48.9

acid, does not require any sample pretreatment other than dilution and ultrafiltration. Even with only this simple treatment, no interfering peaks are present, as shown in Fig. 1B.

The proportions of malic acid in commercially available apple juices and sour drinks were determined by both this method and the enzymatic method with HPLC separation. Fig. 2A compares the results for L-malic acid obtained by the PIC and enzymatic methods. Fig. 2B compares the results for the D-isomer obtained by the PIC method and results calculated from the difference between the analytical values obtained using HPLC and the enzymatic method. The results from the proposed PIC method agreed well with those obtained by other methods with correlation coefficients $\geqslant 0.997$.

Sixteen real samples were divided into five groups according to their content of pure fruit juice and the concentrations of malic acid enantiomers were determined (Table I). D-malic acid was detected in twelve samples. Four of the five fruit juices, in which pure apple juice alone was indicated, contained D-malic acid. Approximately the same amounts of malic acid enantiomers were observed in the sour drinks, which contain no fruit juice. Using the proposed method, it was possible to detect synthetic DL-malic acid in adulterated fruit juice at concentrations as low as 10%. The PIC method described here is simple and can be used for the routine detection of apple juice adulteration.

REFERENCES

1 L. R. Mattick and J. C. Moyer, *J. Assoc. Off. Anal. Chem.*, 66 (1983) 1251.
2 R. H. Evans, A. W. Soestberger and K. A. Ristow, *J. Assoc. Off. Anal. Chem.*, 66 (1983) 1517.
3 W. A. König and S. Sievers, *J. Chromatogr.*, 200 (1980) 189.
4 W. A. König, I. Benecke and S. Sievers, *J. Chromatogr.*, 217 (1981) 71.
5 I. Benecke, *J. Chromatogr.*, 291 (1984) 155.
6 R. Horikawa, H. Sakamoto and T. Tanimura, *J. Liq. Chromatogr.*, 9 (1986) 537.
7 L. W. Doner and P. J. Cavender, *J. Food Sci.*, 53 (1988) 1898.
8 T. A. Eisele and J. R. Heuser, *J. Food Sci.*, 55 (1990) 1614.
9 A. Yamamoto, K. Hayakawa, A. Matsunaga, E. Mizukami and M. Miyazaki, *Anal. Sci.*, 7 (1991) 149.
10 I. Yoshida, K. Hayakawa and M. Miyazaki, *Nippon Kagaku Kaishi*, (1986) 1046.

Journal of Chromatography, 585 (1991) 318–321
Elsevier Science Publishers B.V., Amsterdam

CHROM. 23 583

Short Communication

High-performance liquid chromatographic separation of *p*-hydroxyphenylpyruvic acid

Satoshi Kawai*, Kazuhiko Hanai, Katsuhiko Ito and Satoshi Kitahara

Gifu Pharmaceutical University, 6-1, Mitahora-higashi 5 chome, Gifu 502 (Japan)

Akio Kuwae

College of General Education, Nagoya City University, Mizuho-ku, Nagoya 467 (Japan)

(First received December 5th, 1990; revised manuscript received June 19th, 1991)

ABSTRACT

This paper reports the development of a reliable method for the separation and determination of *p*-hydroxyphenylpyruvic acid by high-performance liquid chromatography. An aqueous solution of *p*-hydroxyphenylpyruvic acid was injected into a Cosmosil C_{18}-5 column with a mobile phase consisting of acetonitrile–acetic acid–water (18:1:81, v/v/v) with detection at 283 nm. Three peaks were observed on the chromatogram, and were identified as the keto–enol tautomers and the decomposition product *p*-hydroxybenzaldehyde. The enol form and *p*-hydroxybenzaldehyde were determined without derivatization and the keto form as its oxime from their peak heights by comparison with those of known amounts of the enol form, *p*-hydroxybenzaldehyde and the oxime standard of the keto form.

INTRODUCTION

p-Hydroxyphenylpyruvic acid (HPPA) is formed from tyrosine by tyrosine aminotransferase [1], and a large amount of HPPA is excreted in the urine of patients with tyrosinosis [2] or tyrosinaemia [3,4]. It is well known that HPPA in aqueous solution undergoes tautomeric changes [5] and also decomposes to *p*-hydroxybenzaldehyde (HBA) [6,8]. The observation which led us to the present study was that HPPA is quite unstable. Several methods have been reported for the high-performance liquid chromatographic (HPLC) separation of HPPA as the free form [3,4,9,10] or after the derivatization [1,11–15]. However, these methods lack specificity in varying degrees as quantitative techniques, because the degradation of HPPA has not been taken into consideration. Therefore, in this paper we describe a reliable method for the determination of HPPA by HPLC.

EXPERIMENTAL

Materials

HPPA was purchased from Sigma (St. Louis, MO, USA) and HBA and hydroxylamine hydrochloride from Tokyo Kasei (Tokyo, Japan). HPLC-grade acetonitrile was obtained from Wako (Osaka, Japan). All of the other chemicals used were of reagent-grade purity.

0021-9673/91/$03.50

Preparation of the oxime of the keto form

The oxime of the keto form was prepared with hydroxylamine hydrochloride as described by Lancaster *et al.* [16]. A mixture of sodium hydroxide (4 g), HPPA (125 mg) and hydroxylamine hydrochloride (1 g) in 50 ml of water was heated at 60°C for 30 min. After acidification to pH 1–2 with concentrated hydrochloric acid, crude powder was obtained by slow partial evaporation of the ether extract and purified by recrystallization from a mixture of acetone and chloroform: yellow powder, m.p. 149–152°C; analysis, calculated for $C_9H_9O_4N$, C 55.39, H 4.65, N 7.18; found, C 55.15, H 4.61, N 7.23%; λ_{max}, 275; ε, 1560 in the mobile phase.

Preparation of the oxime of HBA

A mixture of HBA (100 mg) and hydroxylamine hydrochloride (1.2 g) in 50 ml of water was treated in a similar way to the preparation of the keto-form oxime; yellow powder, m.p. 115–120°C; analysis, calculated for $C_7H_7O_2N$, C 61.31, H 5.11, N 10.22; found, C 61.02, H 5.15, N 10.08%; λ_{max}, 266; ε, 13 616 in the mobile phase.

High-performance liquid chromatography

A model 5A high-performance liquid chromatograph (Shimadzu, Kyoto, Japan) equipped with a UV spectrophotometric detector set at 283 nm and a model 7125 syringe-loading sample injector with a 20-μl loop (Rheodyne, Cotati, CA, USA) were used. The quantitative HPLC separations were performed at ambient temperature on a 250 × 4.6 mm I.D. Cosmosil C_{18}-5 (Nacalai Tesque, Kyoto, Japan) with a mobile phase consisting of acetonitrile–acetic acid–water (18:1:81, v/v/v) at a flow-rate of 1.5 ml/min. The components were determined by an absolute calibration method.

RESULTS AND DISCUSSION

We have already reported the vibrational spectroscopic study of phenylpyruvic acids including HPPA [17]; HPPA exists in the enol form in the solid state and in organic media. On the other hand, HPPA in aqueous medium is gradually converted into the ketonic tautomer, and the degradation to HBA also takes place simultaneously. The changes are rapid in alkaline solutions. These phenomena are observed in UV spectra (Fig. 1). At pH values greater than 7.4, the conversion of the enol to keto form and the degradation to HBA requires only a few minutes, while the spectral change is relatively slow in acidic solutions.

The liquid chromatogram of HPPA in an aqueous solution of pH 3.0 shows three peaks corresponding to the keto and enol forms and the decomposition product HBA, as in Fig. 2A. The solution was treated with a large excess of hydroxylamine hydrochloride to give the oximes of the keto form and HBA, and subjected to HPLC (Fig. 2B). In Fig. 2A, peak E is observed as a single peak on injection of a freshly prepared methanolic solution of HPPA and does not disappear on addition of hydroxylamine hydrochloride. From these results, we may conclude that peak E corresponds to the enol form.

The retention time of peak A in Fig. 2A agreed with that of the HBA standard. In addition, peak A disappeared on addition of hydroxylamine hydrochloride, resulting in another peak, A-O (Fig. 2B), the retention of which agreed with that of the authentic HBA oxime. Thus peak A was identified as HBA.

The eluate corresponding to peak K in Fig. 2A was pooled and evaporated to a small volume. The solution again gave the same three peaks as those in Fig. 2A. On the other hand, when peak K was pooled in a vial containing a hydroxylamine hydrochloride solution and chromatographed again, only one peak, K-O, which has the same retention as that of the authentic keto-form oxime, was observed. Thus peak K was identified as the keto form.

Yu and Bailey [1] observed two peaks corresponding to the keto form of HPPA and its oxime derivative on their chromatograms. However, it seems that the keto form reported by them was HBA and its oxime was HBA oxime. It was impossible to prepare the keto-form standard because of tautomerism and instability in an aqueous solution. Besides, the absorption of the keto form is low, and the peak on the chromatogram is overlapped by that of an unknown impurity. Therefore, it was necessary to determine the keto form as its oxime derivative by comparing with the oxime standard. The reaction yield with hydroxylamine by using an HBA solution (10 μg/ml) was examined and a complete conversion of HBA to the oxime was achieved in a few minutes at pH 3 when an equal volume of

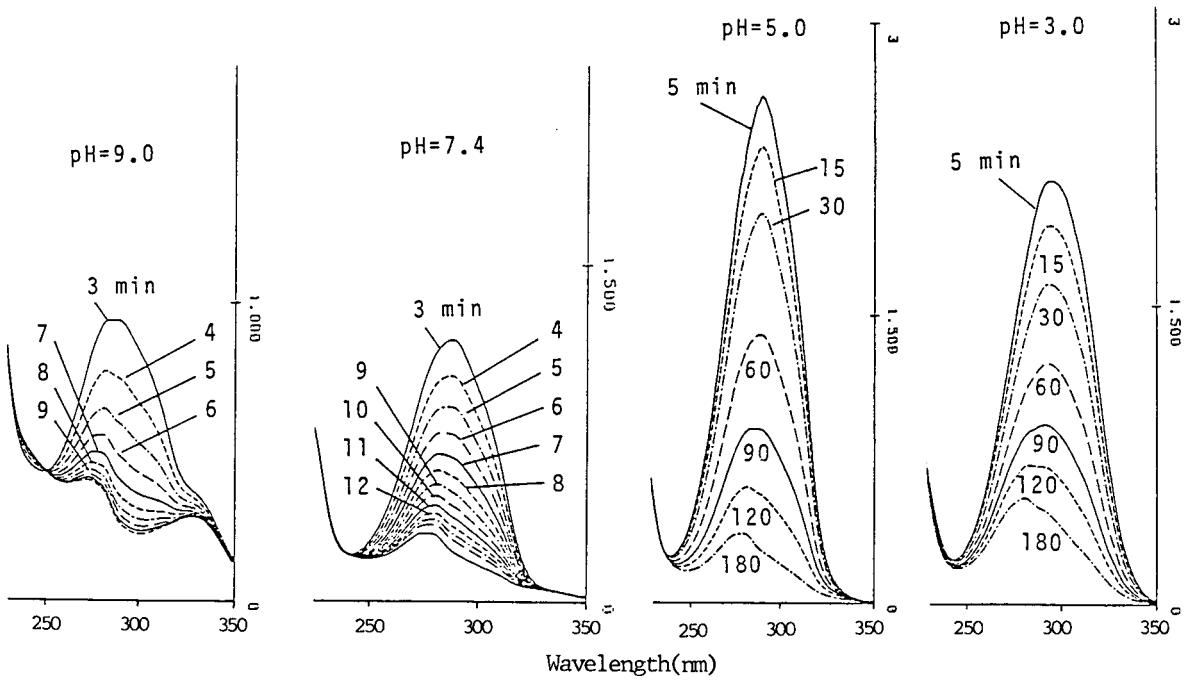

Fig. 1. Changes in UV spectra of HPPA in aqueous solutions (25 μg/ml) due to tautomerism and decomposition. The solutions were prepared using various buffers (pH 9.0, 7.4, 0.1 *M* phosphate; 5.0, 3.0, 0.1 *M* acetate). The values represent the time (min) after the preparation of solutions.

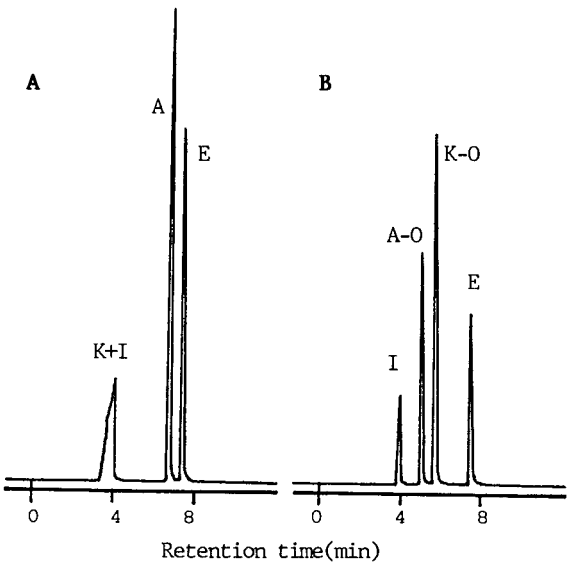

Fig. 2. Chromatograms of HPPA in an aqueous solution of pH 3 (A) and after addition of hydroxylamine hydrochloride (B). Chromatographic conditions: see text. Peaks: A = HBA; A-O: HBA oxime; E = enol form; I = impurity; K = keto form; K-O = keto-form oxime.

hydroxylamine hydrochloride solution (10 mg/ml) was added. At pH 9 the reaction proceeded rather slowly. The keto form is considered to react with hydroxylamine in the same manner as with HBA.

We propose the following equations:

$$\left.\begin{matrix}[E_0] \rightleftarrows [E] \\ [K_0] \searrow [K^*] \\ [A_0] \searrow [A^*]\end{matrix}\right] \xrightarrow{+NH_2OH} \left[\begin{matrix}[E] \\ [K_0\text{-}O]+[K^*\text{-}O]=[K\text{-}O] \\ [A_0\text{-}O]+[A^*\text{-}O]=[A\text{-}O]\end{matrix}\right]$$

where $[E_0]$, $[K_0]$ and $[A_0]$ are the initial concentrations of the enol form, the keto form and HBA in the sample solution, respectively. $[K^*]$ and $[A^*]$ are concentrations produced from E_0 during the period from initial injection to next one after the reaction with hydroxylamine.

$$[K_0] = [K_0\text{-}O] = [K\text{-}O] - [K^*\text{-}O]$$
$$[E_0] = [E] + [K^*\text{-}O] + [A^*\text{-}O] = \quad [E] + [K^*\text{-}O] + [A^*\text{-}O]$$

$$[A^*\text{-}O] = [A\text{-}O] - [A_0\text{-}O] = [A\text{-}O] - [A_0]$$
$$[K^*\text{-}O] = [E_0] - [E] - [A^*\text{-}O] =$$
$$[E_0] - [E] - ([A\text{-}O] - [A_0])$$

$[K_0]$ is defined by the following equation

$$[K_0] = [K\text{-}O] - ([E_0] - [E]) + ([A\text{-}O] - [A_0])$$

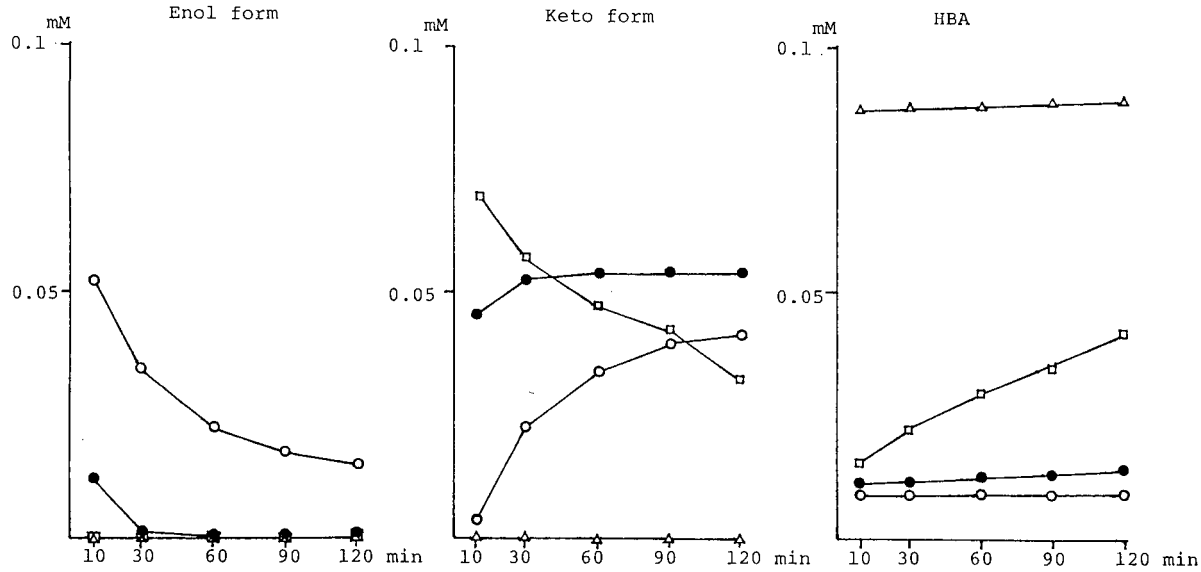

Fig. 3. Effect of pH on the stability of HPPA. ○ = pH 3.0; ● = pH 7.4; □ = pH 10.0; △ = pH 12.0. The sample solutions (0.1 m*M*) of HPPA in 0.05 *M* buffers of several pH values were prepared, and the amounts of the enol and keto forms and HBA were determined.

Thus, $[E_0]$ and $[A_0]$ were measured from their peak heights in Fig. 2A by comparison with those of known amounts of the enol form and HBA. $[K_0]$ was calculated from this equation. Strictly, the enol form is considered to be converted to the keto form or to be decomposed to HBA during running of HPLC. Consequently the values for the enol form tend to be slightly lower.

The effect of pH on the stability of HPPA in aqueous solution was investigated by the present method. An HPPA–methanol solution (450 μg/ml, 2.5 m*M*) was diluted to 0.1 m*M* with 0.05 *M* buffers of several pH values (3.0, acetate; 4.4, 10.0 and 12.0, phosphate). The time dependence of the enol and keto forms and HBA was measured for these solutions. The results are summarized in Fig. 3, from which it can be seen that the conversion from the enol to the keto form proceeds slowly in an acidic solution (pH 3.0) and rapidly in a neutral medium (pH 7.4). HPPA decomposes to HBA gradually at pH 10.0 and instantly at 12.0. A decrease in the amount of the keto form is simultaneously observed at pH 10.0, although no keto form is detected at pH 12.0.

REFERENCES

1 P. H. Yu and B. A. Bailey, *J. Chromatogr.*, 362 (1986) 55.
2 G. Medes, *Biochem. J.*, 26 (1932) 917.
3 H. Todoriki, T. Hayashi and H. Naruse, *J. Chromatogr.*, 310 (1984) 273.
4 G. Rumsby, J. Belloque, R. S. Ersser and J. W. T. Seakines, *Clin. Chim. Acta*, 163 (1987) 171.
5 H. A. Painter and S. S. Zilva, *Biochem. J.*, 41 (1947) 520.
6 K. Schwarz, *Arch. Biochem. Biophys.*, 92 (1961) 168.
7 R. Haavaldsen and T. Norseth, *Anal. Biochem.*, 15 (1966) 536.
8 T. I. Diamondstone, *Anal. Biochem.*, 16 (1966) 395.
9 S. R. Binder and G. Sivorinovsky, *J. Chromatogr.*, 336 (1984) 173.
10 M. L. R. Ramnaraine and M. Tuchman, *J. Chromatogr. Sci.*, 24 (1985) 549.
11 T. Hayashi, H. Tsuchiya, H. Todoriki and H. Naruse, *Anal. Biochem.*, 122 (1982) 173.
12 D. J. Kieber and K. Mopper, *J. Chromatogr.*, 281 (1983) 135.
13 S. Hara, M. Yamaguchi, M. Nakamura and Y. Ohkura, *Chem. Pharm. Bull.*, 33 (1985) 3493.
14 S. Hara, Y. Takemori, M. Yamaguchi, M. Nakamura and Y. Ohkura, *J. Chromatogr.*, 344 (1985) 33.
15 M. Nakamura, S. Hara, M. Yamaguchi, Y. Takemori and Y. Ohkura, *Chem. Pharm. Bull.*, 35 (1987) 687.
16 G. Lancaster, P. Lamm, C. R. Scriver, S. S. Tjoa and O. A. Mamer, *Clin. Chim. Acta*, 48 (1973) 279.
17 K. Hanai, A. Kuwae, S. Kawai and Y. Ono, *J. Phys. Chem.*, 93 (1989) 6013.

Journal of Chromatography, 585 (1991) 322–323
Elsevier Science Publishers B.V., Amsterdam

CHROM. 23 585

Short Communication

Rapid and quantitative separation of nicotinamide and its N^1-methylated metabolite by Dowex AG50-X4 chromatography

Jim R. Kuykendall and Ray Cox*

Cancer Research Laboratory, Veterans Administration Medical Center, 1030 Jefferson Avenue, Memphis, TN 38104 and Department of Biochemistry, University of Tennessee–Memphis, 800 Madison Avenue, Memphis, TN 38163 (USA)

(First received April 3rd, 1991; revised manuscript received June 25th, 1991)

ABSTRACT

The use of column chromatography with Dowex AG50-X4 resin has allowed the quantitative separation of nicotinamide from its primary metabolite, N^1-methylnicotinamide. Although the sensitivity is similar to earlier high-performance liquid chromatographic methods, this procedure allows multiple assays to be carried out simultaneously in a matter of minutes. This method should be useful to study nicotinamide methyltransferase activity in either whole cells or extracts, and is particularly well suited to screen column fractions for enzyme purification purposes.

INTRODUCTION

Although the use of nicotinamide (NA) to decrease cholesterol levels has gained widespread clinical acceptance, in isolated cases, acute liver toxicity results from chronic high dose niacin treatment [1]. NA has been shown to decrease DNA synthesis and cell growth of isolated hepatocytes [2]. Excess NA is primarily metabolized in the liver and kidney to form N^1-Methylnicotinamide (N^1-MN) by enzymatic methylation catalyzed by nicotinamide methyltransferase (NAMTase, E.C. 2.1.1.1). To facilitate the study of NAMTase, we developed a rapid, sensitive chromatographic separation of NA from N^1-MN. Previous chromatographic methods [3–6] are either very time consuming or lack sensitivity.

EXPERIMENTAL

To obtain purified ^{14}C-labeled N^1-MN, we enzymatically methylated [^{14}C]NA using rat liver NAMTase prepared and assayed by a modification of an existing procedure [6]. Changes included using 1 m*M* [^{14}C]NA (specific activity 0.5 mCi/mmol) and unlabeled S-adenosylmethionine (AdoMet), instead of [^{3}H]AdoMet and unlabeled NA in the 200 μl reaction mixture. [^{14}C]N^1-MN was separated from [^{14}C]NA by high-performance liquid chromatography (HPLC) on a Partisil SXC column as described previously [6]. Samples (1 ml) containing either 3000 cpm of [^{14}C]NA or 600 cpm of 1-MN (50 nmol; purified as above by HPLC) were made 0.1 *M* with respect to NH_3COO^- (pH 8.9) and loaded onto Dowex AG50-X4 (mesh size 200–400) columns (5 g pre-swollen) pre-equilibrated with 0.1 *M*

0021-9673/91/$03.50

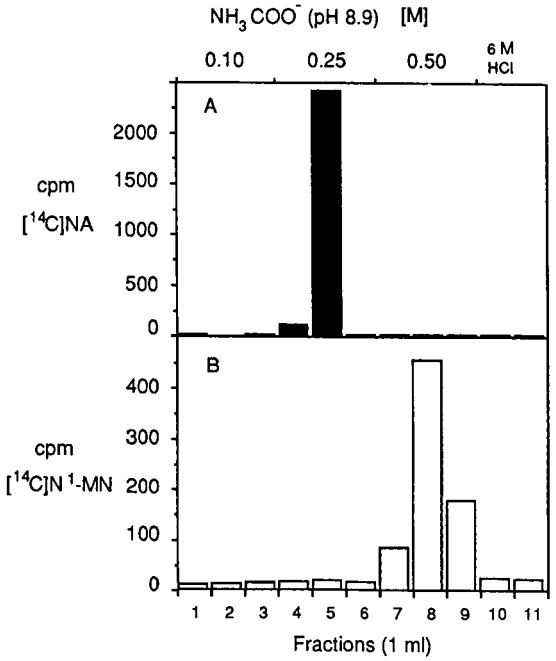

Fig. 1. Separation of NA and N^1-MN by Dowex AG50-X4 column chromatography. Purified [^{14}]N^1-MN (600 cpm or nmoles) or [^{14}C]NA (3000 cpm or 250 nmoles) were loaded as 1-ml samples in 0.1 *M* NH_3COO^- (pH 8.9) on Dowex AG50-X4 columns equilibrated with 0.1 *M* NH_3COO^- (pH 8.9). The columns were eluted with 3-ml step gradients of increasing NH_3COO^- (pH 8.9) at 0.1, 00.25 and 0.5 *M* [^{14}C]NA (A) and [^{14}]N^1-MN (B) were each completely eluted by 0.1 and 0.5 *M* NH_3COO^-, respectively. An additional 2 ml of 6 *M* HCl was unable to further elute any radioactivity.

NH_3COO^- (pH 8.9). The column was sequentially washed with 3-ml aliquots of 0.10, 0.25 and 0.50 *M* NH_3COO^- (pH 8.9) with gravity flow to collect 1-ml fractions and radioactivity determined by scintillation counting. NA and 1-MN were each completely eluted by 0.25 and 0.5 *M* NH_3COO^- (pH 8.9), respectively (Fig. 1), in a time frame of only minutes. Application of an acid-extracted NAMNTase reaction to the column allowed similar separation of the ^{14}C-labeled NA and N^1-MN [7].

RESULTS AND DISCUSSION

By taking advantage of the higher affinity of the positively charged 1-MN for Dowex AG50-X4 resin at high pH we have been able to effectively separate the product (N^1-MN) and substrate (NA) of the NAMTase reaction using differential buffer strength. Since all of the counts in the [^{14}]N^1-MN sample loaded on the column were recovered using this procedure, we offer it as a very sensitive measure of nmol amounts of this nicotinamide metabolite. The major advantage of Dowex chromatography over Partisil SXC HPLC is that it takes 5 min to perform multiple assays, where each HPLC column takes over 1 h to elute each sample [6]. Because of the high sensitivity and rapid nature of this procedure, it would be particularly useful to screen cytoplamic extracts for NAMTase activity in order to purify the enzyme or to study its kinetics. In addition, since this method employs labeled NA, rather than AdoMet, preliminary steps separating labeled AdoMet from the sample can be omitted.

REFERENCES

1 J. A. Etchason, T. D. Miller, R. W. Squires, T. G. Allison, T. G. Gau, J. K. Marttila and B. A. Kottke, *Mayo Clin. Proc.*, 66 (1991) 23.
2 J. Hoshino, U. Kuhne and H. Kroger, *Biochem. Biophys. Res. Comm.*, 105 (1982) 1446.
3 S. Chaykin, M. Dagani, L. Johnson and J. Samli, *Biol. Chem.*, 240 (1956).
4 Y. C. Lee, R. M. McKenzie, R. K. Gholson and N. Raica, *Biochim. Biophys. Acta, 264 (1972) 59.*
5 *W. Christ, G. Arndt and G. Shulze, J. Chromatogr.*, 106 (1975) 418.
6 R. Cox, *Cancer Lett.*, 17 (1983) 295.
7 J. R. Kuykendall, *Ph. D. Thesis,* University of Tenessee, Memphis, TN, 1988.

Journal of Chromatography, 585 (1991) 324–328
Elsevier Science Publishers B.V., Amsterdam

CHROM. 23 542

Short Communication

Determination of acephate by liquid chromatography in the presence of aqueous soil extracts

E. Rodríguez-Gonzalo☆, M. J. Sánchez-Martín and M. Sánchez-Camazano*

Instituto de Recursos Naturales y Agrobiología, C.S.I.C., Cordel de Merinas 40-52, 37071 Salamanca (Spain)

(First received February 5th, 1991; revised manuscript received May 31st, 1991)

ABSTRACT

A liquid chromatographic method has been developed for the determination of acephate in aqueous extracts of agriculture soils. Aqueous extracts of spiked soil samples were used. The lower detection limit was 1 μg/ml; the relative standard deviation for repeatability (R.S.D.) based on peak area measurement ranged from 0.2 to 4.5%. Recoveries from spiked samples ranged from 93.6 to 104.3%. The method used a C_{18} reversed-phase column, a mobile phase of 5% (v/v) methanol–water and UV detection at 215 nm. The application of the proposed method to the study of the adsorption of acephate in aqueous medium by a selected group of soils yielded satisfactory results.

INTRODUCTION

Acephate (O,S-dimethyl acetylphosphoramidothioate) is a systemic insecticide of moderate persistence in soils [1] that is widely used in agriculture. Study of the adsorption of this insecticide by soils and their constituents in aqueous media is of great interest since the high solubility of this compound in water (650 g/l) [1] increases the possible risk of environmental contamination.

Accordingly, we have developed an analytical method using high-performance liquid chromatography (HPLC) with UV detection that will permit the determination of acephate rapidly, simply and with great precision. This method will be used in the systematic study of the adsorption of acephate in aqueous extracts of soils used for agricultural purposes.

Currently, gas chromatography (GC) is the most widely used procedure for the analysis of this insecticide and its residues [2], but there are very few references in the literature concerning the application of liquid chromatography (LC) in the determination of the compound [3,4]. However, the high solubility of acephate in water suggests that reversed-phase HPLC might be a suitable technique for such determination because it permits direct injection of aqueous extracts. This technique of direct injection is more rapid than gas chromatography, which requires extraction with organic solvents and further clean-up procedures. Detection limits of acephate by GC [2] and by LC [4] are 0.02 and 0.05 μg/ml, respectively.

In the present work we report on the analytical characteristics of the proposed LC method and its application to the determination of acephate in the

☆ Present address: Departamento de Química Analítica, Nutrición y Bromatología, Facultad de Química, Universidad de Salamanca, 37008 Salamanca, Spain.

0021-9673/91/$03.50

presence of aqueous extracts of various soils which differ in the content and plant origin of organic matter. The aim was to determine the applicability of the proposed LC method for the study of the soil–water equilibrium of acephate.

The structural formula of acephate is as follows:

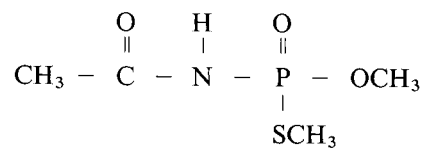

EXPERIMENTAL

Apparatus

The chromatographic system was a Waters chromatograph (Waters Assoc., Chromatography Division, Millipore, Milford MA, USA) equipped with a Waters Model U6K universal liquid chromatography injector) two Model 501 HPLC pumps for solvent delivery attached to a Model 680 automated gradient controller, and a Model 481 LC spectrophotometer. A computerized integrator (Waters 740 data module) was used for area and height measurements of peak. The column was a stainless-steel Nova-Pak C_{18} (Waters Assoc.) column (150 mm × 3.9 m I.D.). Millex-HV_{13} filters (Millipore) used for the samples and Magna nylon membrane filters (MSI) used for solvents had a pore size of 0.45 μm. The Hamilton syringe was of 25 μl, and a 2-ml volume sample loading loop was used.

Reagents

HPLC-grade methanol (Carlo Erba, Milan, Italy) was used in preparing the mobile phase. The water used for the preparations was distilled in glass in the laboratory. The acephate (98% purity) was obtained from Chevron (Richmond, CA, USA). All other chemicals were of analytical-reagent grade.

Soil samples

Seven samples from uncultivated soils were used. The clay, organic carbon and nitrogen contents of the soils were determined [5] and the organic matter content (percentage carbon × 1.72) and the carbon–nitrogen relationship (C/N) were calculated (Table II). The C/N relationship is generally considered to be an index of the degree of organic matter humification [6]. The value decreases with the degree of humification. Before being used, the soils were equilibrated in an atmosphere of 35% relative humidity.

Procedure

HPLC operating conditions. The optimum chromatographic conditions were as follows: eluent, 10% (v/v) methanol–water; flow-rate, 1.0 ml/min; injection volume, 25 μl; wavelength, 215 nm (UV absorption maximum of acephate). Column temperature was ambient.

The solvents were filtered through a 0.45 μm pore nylon membrane filter and degassed daily before use.

Stock solutions of 100 and 500 μg/ml acephate were prepared by dissolving the solid product in distilled water. Working standard solutions were obtained by dilution of suitable aliquots in distilled water which were then filtered through a 0.45-μm Millex-HV_{13} filter. A 25-μl aliquot of each sample was injected into the chromatograph to obtain the calibration curve.

Determinations in aqueous soil extracts. To obtain a solution of extractable matter 1 g of soil was shaken with 10 ml of water at a constant temperature (25.0 ± 0.5°C) over 48 h; this was then centrifuged at 5045 *g* for 30 min and the aqueous extract was separated.

From 100 and 500 μg/ml stock solutions of acephate, aliquots ranging between 0.05 and 0.5 ml were taken and brought up to a final volume of 5 ml with the aqueous extract of the corresponding soil. The resulting solutions, with concentrations ranging from 1 to 50 μg/ml, were filtered through Millex-HV_{13} filters and injected into the chromatograph. Samples were prepared in triplicate and quantified using the external standard method, measuring the area of the peak eluted as a mean value of three injections made.

Adsorption isotherm. Aliquots of 10 ml of aqueous stock solutions of acephate at a concentration between 10 and 50 μg/ml were added to 1.0 g of soil. After 24 h at 20.0 ± 0.5°C with intermittent periods of shaking, the suspensions were centrifuged at 5045 *g* for 30 min and an aliquot of the supernatant fluid filtered through Millex−HV_{13} filters of 0.45 μm pore size. Samples were prepared in duplicate and the value of the area of the peak obtained was

the mean of three injections carried out for each solution.

RESULTS AND DISCUSSION

The chromatographic behaviour of acephate was examined using methanol–water as the eluent. It was observed that the use of a 10% (v/v) methanol–water mixture as the mobile phase with isocratic elution yielded a suitable separation of the acephate peak from that produced by the non-retained species. An increase in the proportion of methanol in the mobile phase eluted the insecticide too fast and hence provided a poor resolution of the corresponding chromatographic peak. For the same reason, the flow-rate used was 1.0 ml/min. Under these conditions, the retention time of acephate was 3.2 min.

The pH of standard solutions was adjusted to between 6 and 8 (normal pH range in aqueous extracts of agriculture soils) by the addition of hydrochloric acid or 0.01% sodium hydroxide. The addition of buffer solutions is not considered to be necessary because no changes were observed in the chromatograms.

Straight calibration lines were obtained by triplicate injection of aqueous solutions of acephate at concentrations ranging between 1 and 100 μg/ml. The area and height of the peaks were plotted in the calibration. The response was linear throughout the concentration range tested and least-squares linear regression analyses of the data provided excellent correlation coefficients (Fig. 1). As may be seen, the sensitivity of the method was greater when peak areas were evaluated.

The proposed method was used to analyse six identical samples containing 10 μg/ml acephate. The analysis showed that a relative standard deviation of 3.1% was obtained for peak-area calculation and 0.8% for peak-height calculation. The relative standard deviation at a concentration level of 1 μg/ml was 5.2 and 3.8% for areas and heights, respectively.

Because of these observations it was considered appropiate to use the peak area for the calculation of the results.

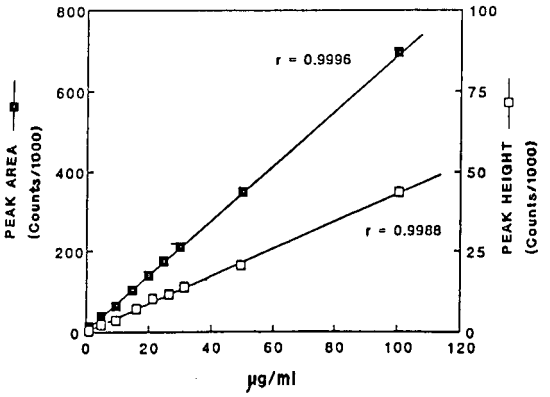

Fig. 1. Calibration graphs for acephate. Mobile phase, 10% (v/v) methanol–water; flow-rate, 1.0 ml/min; UV detection, 215 nm; injected volume, 25 μl.

Determination of acephate in the presence of aqueous soil extracts

Before being spiked, none of the aqueous extracts of the soil samples gave any extraneous peaks which might interfere with the determination of the insecticide.

The aqueous extracts were spiked as stated above. Samples were injected in triplicate and bracketed with injections of the standards. The results were calculated based on the average peak area of the sample and the standard.

In all the aqueous extracts of the soils studied, it is possible to determine acephate levels at a concentration equal to or greater than 10 μg/ml with a relative standard deviation of less than 5%. However, the determination of lower concentrations was only possible in soils with low or medium contents of organic matter (Table I).

Although cultivated soils do not have high contents of organic matter, the determination of acephate at concentrations less than 10 μg/ml in those soils in which strong interferences are seen is possible when using a mobile phase of 5% (v/v) methanol–water. It delays the elution of acephate from 3.2 to approximately 5 min, and allows the quantification of even 1 μg/ml with an acceptable degree of precision (Table I). Fig. 2 shows the chromatograms obtained for samples containing 1 μg/ml acephate in the different soils studied when a mobile phase of 5% (v/v) methanol–water was used.

From the studies carried out in aqueous extracts of soils it may be inferred that the minimum

TABLE I

ACEPHATE DETERMINATION IN AQUEOUS EXTRACTS OF SOIL SAMPLE

Soil	Organic matter (%)	C/N	5 ppm[a]		1 ppm[b]	
			Recovery (%)	R.S.D.[c] (%)	Recovery (%)	R.S.D.[c] (%)
1[d]	6.1	22.6	102.8	1.6	104.3	1.1
2[d]	7.3	21.1	95.6	3.5	96.2	3.4
3[d]	10.2	28.3	87.2	3.2	–	–
4[e]	1.1	12.0	100.6	1.4	102.9	4.5
5[e]	1.9	16.8	97.4	0.3	97.5	0.2
6[e]	5.2	20.0	85.8	4.6	93.6	3.8
7[f]	6.3	10.1	86.4	5.8	94.6	1.4

[a] Mobile phase, 10% (v/v) methanol–water.
[b] Mobile phase, 5% (v/v) methanol–water.
[c] Relative standard deviation of three determinations.
[d] Predominant vegetation holm-oak.
[e] Predominant vegetation heather.
[f] Predominant vegetation grassland.

amount of acephate that can be detected depends not only on the content of organic matter in the soil but also on its nature. Thus, in soils with organic matter from the same source (holm-oak or heather) the degree of interference increases as the organic matter content increases and the degree of humification decreases (soils 3 and 6). This finding is logical if one considers that a low degree of humification implies a predominance of fulvic acids over humic acids. The former are the components of the organic matter with a lower molecular weight and a greater polarity, and hence are more easily extractable in aqueous solution. Soils with the same content of organic matter but from different sources cannot be compared to one another.

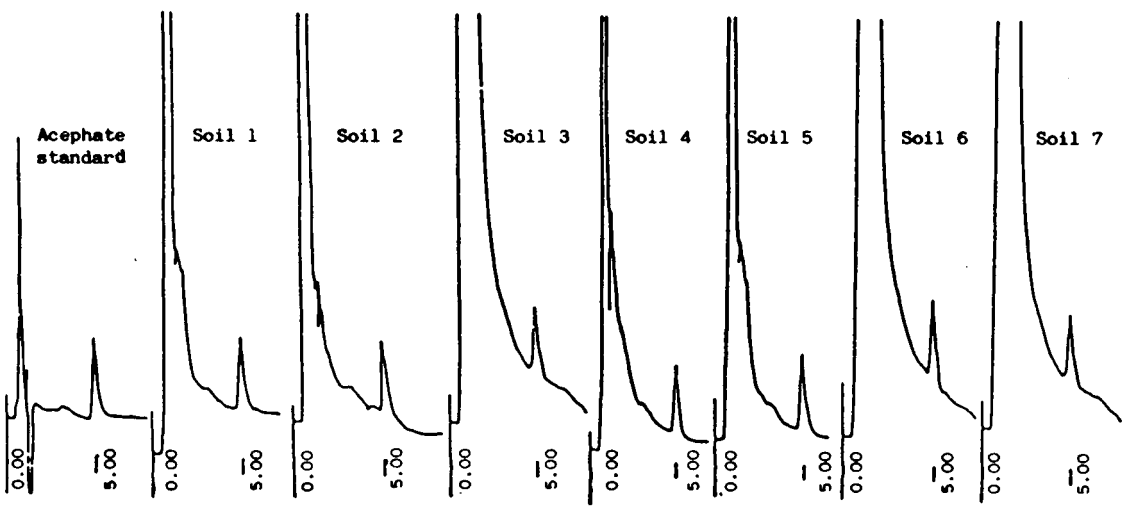

Fig. 2. Chromatograms resulting from the analysis of 1 μg/ml acephate in aqueous extracts of different soil samples. Mobile phase, 5% (v/v) methanol–water; flow-rate, 1.0 ml/min; UV detection, 215 nm; injected volume, 25 μl; attenuation, 4.

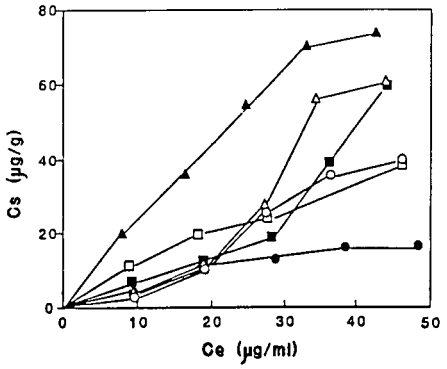

Fig. 3. Adsorption isotherms of acephate by soils. Ce = equilibrium concentration; and Cs = amount spiked − Ce. Equilibrium time, 24 h; temperature, 20°C; soil/solution ratio, 1.0 g: 10.0 ml. Key: ■ = soil 1; □ = soil 2; ○ = soil 4; ▲ = soil 7; △ = soil 8; ● = soil 9.

Application to the study of the adsorption of acephate by soils

The application of the proposed method to the study of the adsorption of acephate by a selected group of soils yielded satisfactory results; the isotherms obtained (Fig. 3) fit the Freundlich equation [7] (with r values $\geqslant 0.097$). The highest values of K, the Freundlich constant, correspond to samples 2 and 7 with a high organic matter content (Table II) and the lowest ones to samples 4 and 8 with a low content in this fraction. This observation suggests that organic matter, as in the case of other organic chemicals [8], is a determinant parameter in the adsorption of acephate. A broader study of the adsorption–desorption process of acephate by cultivated soils is currently under investigation at this laboratory. The statistical study of the results will allow the parameters of the adsorption process to be determined.

TABLE II

CHARACTERISTICS OF THE SOIL SAMPLES AND K ADSORPTION CONSTANTS OF FREUNDLICH

Soil	Organic matter (%)	C/N	Clay (%)	K
1	6.1	22.6	22.0	0.313
2	7.3	21.1	19.3	2.281
4	1.1	12.0	10.6	0.046
7	6.3	10.1	50.9	3.558
8	0.76	5.8	20.7	0.056
9	0.50	3.8	12.1	0.890

ACKNOWLEDGEMENTS

This work was supported by the "Dirección General de Investigación Científica y Técnica" (Spain) under Project No. PB87-0240. The authors thank Chevron for kindly supplying the chemical employed.

REFERENCES

1 C. R. Worthing and S. B. Walker, *The Pesticide Manual*, Lavenham Press, Suffolk, 8th ed., 1987, p. 10.
2 J. B. Leary, in J. Sherma and G. Zweig (Editors), *Analytical Methods for Pesticides and Plant Growth Regulators*, Vol. 7, Academic Press, New York, 1973, p. 363.
3 J. A. Lubkowitz and L. R. Petit, *J. Chromatogr.*, 121 (1976) 161.
4 M. A. Alawi, *Fresenius Z. Anal. Chem.*, 315 (1983) 358.
5 C. A. Black, *Methods of Soil Analysis*, American Society of Agronomy, Madison, WI, 1965.
6 Ph. Duchaufour, *Pedologie*, Masson, Paris, 1984, p. 33.
7 S. U. Khan, *Pesticides in the Soil Environment*, Elsevier, Amsterdam, 1980, p. 39.
8 F. J. Stevenson, *Humus Chemistry. Genesis, Composition, Reactions*, Wiley, New York, 1982, p. 403.

Journal of Chromatography, 585 (1991) 329–332
Elsevier Science Publishers B.V., Amsterdam

CHROM. 23 642

Short Communication

Direct separation of the enantiomers of propafenone, diprafenone and their major metabolites by high-performance liquid chromatography on modified cellulose and amylose chiral stationary phases☆

Th. Hollenhorst and G. Blaschke*

Institute of Pharmaceutical Chemistry, University of Münster, Hittorfstrasse 58–62, 4400 Münster (Germany)

(First received February 26th, 1991; revised manuscript received July 16th, 1991)

ABSTRACT

The enantiomers of propafenone, diprafenone and their major metabolites, N-desalkylpropafenone, 5-hydroxypropafenone and 5-hydroxydiprafenone, were separated on a cellulose tris-3,5-dimethylphenylcarbamate column (Chiralcel OD) and an amylose tris-3,5-dimethylphenylcarbamate column (Chiralpak AD).

INTRODUCTION

The chiral antiarrhythmic drug propafenone (Fig. 1) is used in therapy as the racemate. The sodium antagonistic acitivity of the enantiomers of propafenone is about equal [1]. However, owing to the partial structure of a β-blocking agent, the enantiomers differ in their affinity for the β-adrenergic receptor. Thus, *S*-(+)-propafenone is a hundred times more potent at the β-receptor than *R*-(−)-propafenone [1]. The metabolites N-desalkylpropafenone and 5-hydroxypropafenone (Fig. 1) have similar electrophysiological effects as the parent drug but their β-adrenergic activity is negligible [2]. The increase in the plasma levels of propafenone may cause serious β-adrenergic side-effects as a result of the *S*-(+)-enantiomer. Poor metabolizers lacking the cytochrome P-450 isoenzyme which catalyzes the metabolic conversion of the drug are particularly susceptible to these adverse reactions. Side-effects may also occur in extensive metabolizers when high initial doses are given because the hydroxylating P-450 enzyme system is saturable. Thus, a simple assay for the monitoring of the enantiomeric ratio of propafenone in body fluids is required.

The enantiomers of propafenone have been prepared [3,4]. Circular dichroism (CD) measurements assigned the *R*-configuration to the levorotatory base and the dextrorotatory hydrochloride salt [3,4]. The configuration has recently been confirmed by X-ray analysis [5]. Following derivatization with optically pure isocyanates the resulting diastereomers can be separated by high-performance liquid chromatography (HPLC) [3,4].

☆ Dedicated to Professor Dr. Dr. E. Mutschler on the occasion of his 60th birthday.

0021-9673/91/$03.50

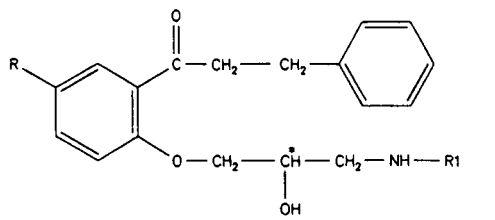

Propafenone R = H ; R1 = $-CH_2-CH_2-CH_3$
N-desalkylpropafenone R = H ; R1 = H
5-hydroxypropafenone R = OH ; R1 = $-CH_2-CH_2-CH_3$

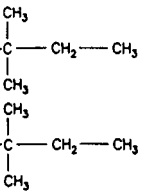

Diprafenone R = H ; R1 = $-C(CH_3)_2-CH_2-CH_3$

5-hydroxydiprafenone R = OH ; R1 = $-C(CH_3)_2-CH_2-CH_3$

Fig. 1. Structures of compounds.

In this communication we would like to describe the first direct resolution of the enantiomers of propafenone, diprafenone and their major metabolites (Fig. 1) on a cellulose tris-3,5-dimethyl–phenylcarbamate column (Chiralcel OD) and an amylose tris-3,5-dimethylphenylcarbamate column.

EXPERIMENTAL

Apparatus

The HPLC system consisted of a Beckman 110B solvent-delivery module (Beckmann, Fullerton, CA, USA), a Lambda 1000 detector (Bischoff, Munich, Germany) operated at 254 nm if not stated otherwise and a CR3-A Chromatopac integrator (Shimadzu, Columbia, MD, USA). A Chiralcel OD column and a Chiralpak AD column containing cellulose tris-3,5-dimethylphenylcarbamate coated on silica gel and amylose tris-3,5-dimethylphenylcarbamate coated on silica gel (each 25 cm × 0.46 cm I.D. particle size 10 μm, both purchased from J. T. Baker, Gross-Gerau, Germany) were used.

Chemicals

Propafenone and its metabolites were obtained from Knoll (Ludwigshafen, Germany). The enantiomers of propafenone were prepared as previously published [3,4]. Diprafenone were purchased from Helopharm (Berlin, Germany). *n*-Hexane, 2-propanol, 2-butanol and diethylamine were purchased from Merck (Darmstadt, Germany) in the highest purity available.

Chromatographic conditions

The concentrations of the compounds were 20 μg/ml in *n*-hexane–2-propanol (90:10) (propafenone and diprafenone) or 2-propanol (hydrophilic metabolites). A 100-μl aliquot was injected into the HPLC system. For mobile phase compositions see Table I.

Preparation of blood samples

To 1.0 ml of plasma were added 200 μl of a *M* sodium hydroxide solution to give pH ⩾ 12. Following addition of 5.0 ml of dichloromethane, the samples were mixed for 10 min and centrifuged for 10 min at 2500 *g*. The organic layer was transferred into a clean glass tube and evaporated under a stream of nitrogen. The residue was dissolved in 100 μl of hexane–2-propanol (90:10) and injected into the chromatographic system B (see Table I).

RESULTS AND DISCUSSION

The direct separation of the enantiomers of β-blocking drugs has been successfully accomplished on a Chiralcel OD column [6]. Thus, this chiral stationary phase was also applied for the resolution of propafenone and its metabolites. The results are summarized in Table II. The use of the standard mobile phase of the Chiralcel OD column, *n*-hexane–2-propanol (90:10), resulted in only an incomplete separation of the enantiomers which was unsuitable for quantitative analysis. Complete resolution was achieved by substituting 2-butanol for 2-propanol. Moreover, the concentration of the modifier was reduced to 7%. The addition of diethylamine suppressed the tailing of the peaks.

The best results for the metabolite N-desalkylpropafenone were obtained by increasing the 2-butanol content of the eluent to 15%. Additionally, the diethylamine concentration was reduced (Fig. 2b). No separation of the enantiomers of 5-hydroxypropafenone was achieved using an alkaline eluent.This can be explained by the fact that the phenolate anion which is formed in alkaline media inhibits sufficient interaction of the enantiomers

TABLE I

MOBILE PHASES

System	*n*-Hexane	2-Butanol	2-Propanol	Diethylamine	Acetic acid	Flow-rate (ml/min)
A	93	7	0	0.2	0	1.0
B	75	0	25	0.2	0	1.0
C	75	0	25	0.2	0	1.5
D	85	15	0	0.1	0	2.0
E	80	20	0	0	0.85	1.0
F	90	0	10	0	0	1.0
G	84	0	16	0	0	1.0

with the chiral stationary phase. In contrast, good resolution resulted under acidic conditions, with the addition of 0.85% acetic acid instead of diethylamine. The concentration of the acid has to be kept within tight limits because small changes cause a significant loss of the resolution of the enantiomers. Trichloroacetic acid was not superior to acetic acid.

The analogue diprafenone and its major metabolite 5-hydroxydiprafenone were resolved under similar conditions (Fig. 2c and Tables I and II). In comparison with the Chiralcel OD column the use of a Chiralpak AD column resulted in an improvement of the resolution of propafenone and a simultaneous reduction in the retention times (Fig. 2a) and Tables I and II). With the exception of diprafenone the other compounds could not be separated on this stationary phase. The separation of the enantiomers of propafenone and N-desalkylpropafenone and unresolved 5-hydroxypropafenone in a single run was achieved by directly connecting the Chiralcel OD and the Chiralpak AD columns (Fig. 2d).

Both chiral stationary phases have been used on a daily basis for more than one year under the conditions described without any loss of performance.

The assay described is suitable for the analysis of the enantiomeric ratio of propafenone in body fluids. Fig. 3 shows representative chromatograms of plasma samples. The stereoselective metabolism of propafenone has been demonstrated using an indirect method after derivatization with isothiocyanates [1]. In accordance with this report the stereoselective metabolism of propafenone can also be shown with the direct method of the separation of the enantiomers of propafenone (Fig. 3c).

TABLE II

SEPARATION OF RACEMATES

Racemate	Column	System	Capacity factors		Selectivity (α)	Resolution factor (R)
			k'_1	k'_2		
Propafenone	OD	A	6.45	8.05	1.24	2.16
Propafenone	AD	A	5.78	7.9	1.36	3.59
Propafenone	AD	B	1.57	2.81	1.79	5.56 (Fig. 2a)
Propafenone	AD	C	1.45	2.54	1.75	4.35
N-Desalkylpropafenone	OD	D	1.0	5.4	5.4	10.13 (Fig. 2b)
5-Hydroxypropafenone	OD	E	5.75	8.25	1.43	1.0
Diprafenone	OD	F	2.12	3.75	1.77	4.72 (Fig. 2c)
5-Hydroxydiprafenone	OD	E	4.3	5.8	1.35	1.28

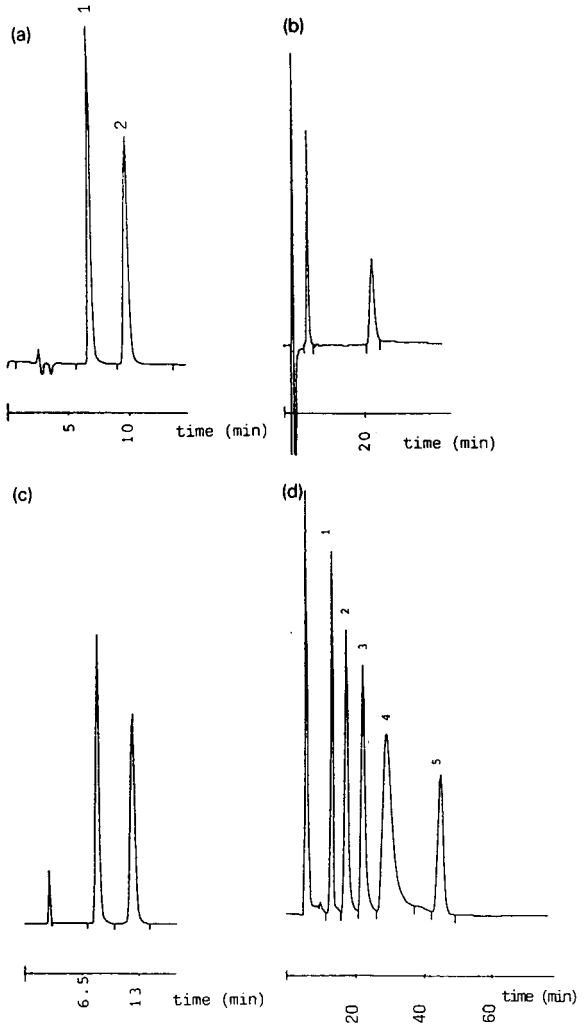

Fig. 2. Chromatograms of separations of the racemates. (a) Separation of propafenone on Chiralpak AD, mobile phase system B: peak 1 = *R*-(−)-propafenone; peak 2 = *S*-(+)-propafenone. (b) Separation of N-desalkylpropafenone on chiralcel OD, mobile phase system D. (c) Separation of diprafenone on Chiralcel OD, mobile phase system F. (d) Mixture of racemic propafenone, N-desalkylpropafenone and 5-hydroxypropafenone, mobile phase system G; column, Chiralcel OD and Chiralpak AD directly connected; wavelength of detection, 222 nm; peaks 1 and 5 = N-desalkylpropafenone; peak 2 = -*R*-(−)-propafenone; peak 3 = *S*-(+)-propafenone; peak 4 = unresolved 5-hydroxypropafenone. For all chromatograms 2 μg of the compounds were injected. For the compositions of the mobile phases see Table I.

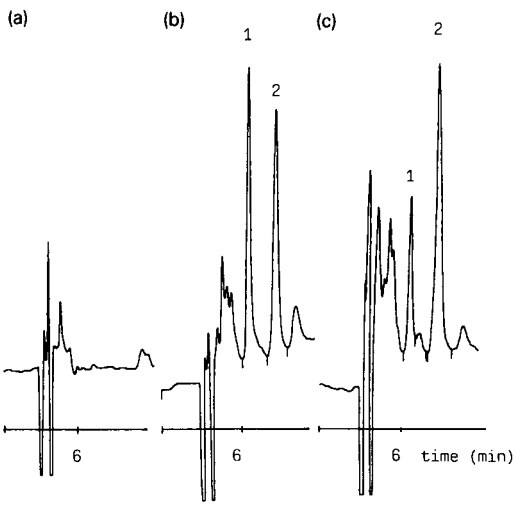

Fig. 3. Chromatograms of plasma samples. (a) Blank plasma; (b) blank plasma spiked with 200 ng/ml of each enantiomer of propafenone; (c) sample 2 h after oral administration of 300 mg of racemic propafenone to humans. Peaks: 1 = *R*-(−)-propafenone; 2 = *S*-(+)-propafenone. Chromatographic conditions: mobile phase, *n*-hexane–2-propanol–diethylamine (75:25:0.2); flow-rate, 1.0 ml/min; column, Chiralpak AD.

ACKNOWLEDGEMENTS

The authors thank Professor Eichelbaum for plasma samples, Dr. G. Scriba for helpful discussions during the preparation of the manuscript, and the Deutsche Forschungsgemeinschaft and the Fonds der Chemischen Industrie for financial support.

REFERENCES

1 H. Kroemer, Ch. Funck-Brentano, D. J. Silberstein, A. J. J. Wood, M. Eichelbaum, R. L. Woosley and D. Roden, *Circulation*, 79 (1989) 1068.
2 H. Kroemer, *Arzneimitteltherapie*, 7 (1989) 4.
3 G. Blaschke and B. Walther, *Liebigs Ann. Chem.*, (1987) 561.
4 B. Walther, *Dissertation*, University of Münster, Münster, 1985.
5 D. Weckert and H. Burzlaff, University of Erlangen, Erlangen, personal communication.
6 Y. Okamoto, M. Kawashima, R. Aboratani, K. Hatada, T. Nishiyama and M. Nasoda, *Chem. Lett.*, (1986) 1237.

Journal of Chromatography, 585 (1991) 333–336
Elsevier Science Publishers B.V., Amsterdam

CHROM. 23 569

Short Communication

Analysis of ε-caprolactam and its cyclic oligomers by high-performance liquid chromatography

Luisa Bonifaci, Donatella Frezzotti, Gianfranco Cavalca, Edgardo Malaguti and Gian Paolo Ravanetti*

Enichem Polimeri, Mantua Research Centre, Via G. Taliercio 14, 46100 Mantua (Italy)

(First received April 18th, 1991; revised manuscript received June 17th, 1991)

ABSTRACT

A high-performance liquid chromatographic method for the determination of ε-caprolactam and its cyclic oligomers is presented. The method uses a methanol–water mixture as eluent. The separation of peaks is well defined and their quantitative determination is performed by calibration with known purity standards. By comparing the ultraviolet and refractive index detection responses, a disagreement with the reported data regarding ε-caprolactam dimer and trimer extinction coefficients was observed and the tetramer and pentamer extinction coefficients were estimated.

INTRODUCTION

The problem of separation of ε-caprolactam cyclic oligomers has existed since the early 1950s. The reported methods use fractional sublimation [1], paper chromatography [2], gas chromatography [3] and gel permeation chromatography [4]. Although suitable, all of them have some limitations of application due to either the substances' nature (higher oligomers are not sublimable) or the analysis length or the low resolution.

Most recently, the introduction of high-performance liquid chromatography (HPLC) has brought an appreciable improvement in ε-caprolactam oligomer analysis, since a large range of efficient columns are available and there is a choice of pure solvents and mixtures.

Krajnik *et al.* [5] proposed the use of reversed-phase (RP)-HPLC on C_{18}-type columns and a methanol–aqueous acetic acid (30:70) mixture as eluent and obtained a good separation between the dimer and the monomer, the most critical point of the whole analysis.

With the same type of columns, but using a methanol–water (35:65) mixture, Tai and Tagawa [6] succeeded in obtaining good separation of higher oligomers, but failed in the dimer–monomer separation.

Guaita [7], using an RF-8 5-μm column and a trifluoroethanol–water (40:60) mixture at 50°C, obtained a good separation of ε-caprolactam cyclic oligomers up to decamer. All these authors used UV detection at a wavelength at which the eluent absorption is negligible (typically 205 or 210 nm).

The method presented in this paper uses a reversed-phase C_{18}-type column and a methanol–water 40:60) mixture as eluent at 25°C. This technique is very efficient for dimer–monomer separation and allows the quantitative determination of oligomers, without using fluorinated solvents.

0021-9673/91/$03.50

EXPERIMENTAL

Equipment

The HPLC analyses were performed using a GPC-ALC 150C Waters chromatograph equipped with a differential refractive index (RI) detector and a UV detector (Waters Model 490) at 210 nm.

A Spherisorb RP-18 Phase Sep (25 cm × 4.6 mm I.D.) column and a methanol–water (40:60) mixture at 25°C as eluent were used. The solvent flow-rate was 0.5 ml/min; the sample concentration and the injected volume were 0.01% (w/v) and 20 μl, respectively.

Materials

For the calibration curves of the UV and RI detectors, ε-caprolactam, dried in a vacuum oven at 40°C for 120 h, and nine fractions of cyclic dimer and trimer obtained from fractional sublimation of a oligomer mixture were used. All the products were supplied by the Enichem nylon 6 industrial plant (Porto Marghera, Italy). The same mixture was successively characterized by HPLC after ethanol extraction.

In order to obtain standard samples of dimer and trimer, fractional sublimation according to Heikens [1] was used. The compositions of the obtained fractions were evaluated by HPLC. The purity of the standard fractions used for the calibrations ranged between 96.7 and 94.7% for the dimer and between 97.5 and 98.5% for the trimer.

RESULTS AND DISCUSSION

The HPLC experimental conditions chosen in the present paper afford a good separation of the cyclic oligomers of ε-caprolactam, especially of the dimer. We also found, as previously reported [5–7], that the dimer is eluted before the monomer. Figs. 1 and 2 show the results of separation for both detectors. The retention times measured by the UV detector were: ε-caprolactam, 11.75 min; dimer, 11.00 min; trimer, 17.37 min; tetramer, 31.25 min; pentamer, 60.63 min. The analysed mixture did not appear to have higher oligomers.

For the quantitative analysis of the chromatographic peaks, the calibration curves of monomer, dimer and trimer for both detectors were determined. All the curves are linear with regression correlation coefficients higher than 0.995.

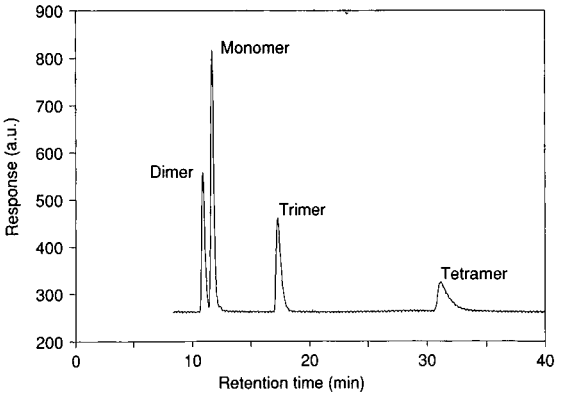

Fig. 1. UV chromatogram of oligomer mixture (pentamer is omitted for clarity).

With RI detection, the dimer and the trimer have a single calibration curve which was used also for the determination of tetramer and pentamer. Fig. 3 shows this curve together with the ε-caprolactam one.

With UV detection each component has its own calibration curve (Fig. 4). Contrary to what was expected on the basis of the extinction coefficient values at 210 nm [4,8], the dimer appears to have a lower response than the trimer. This finding is also strengthened by the fact that the ratios of the UV to RI peak areas are systematically lower for the dimer in all the samples.

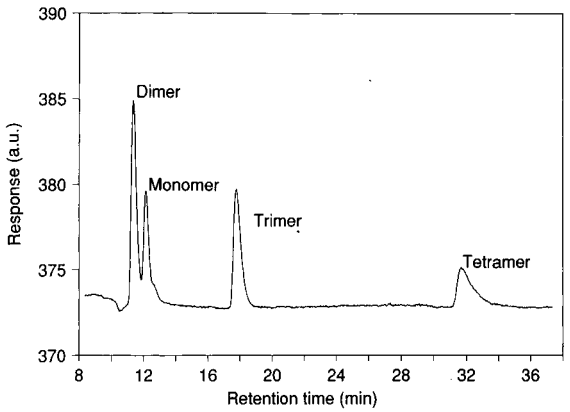

Fig. 2. RI chromatogram of oligomer mixture (pentamer is omitted for clarity).

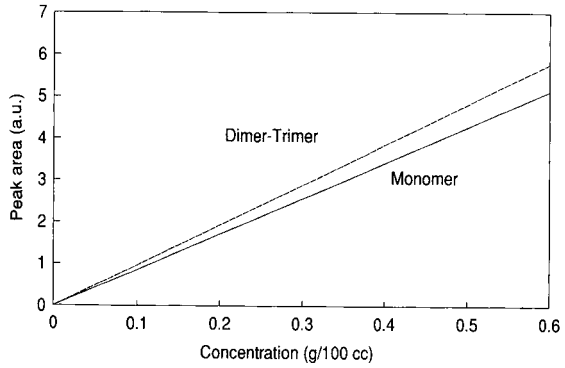

Fig. 3. RI calibration of ε-caprolactam, dimer and trimer.

TABLE I

EXTINCTION COEFFICIENTS OF ε-CAPROLACTAM AND ITS CYCLIC OLIGOMERS AT λ = 210 nm

Compound	ε (l/mol repeating unit · cm)			
	Calculated	Experimental	Ref. 8	Ref. 4
ε-Caprolactam		3160	3325	2800
Dimer	1080	900	1070	980
Trimer	1170	1060	970	970
Tetramer	1100		970	970
Pentamer	1130		970	970

Spectrophotometric measures at 210 nm on these samples have confirmed the above observations. As shown in Table I, in which the extinction coefficient values are reported, there is clearly a lack of agreement with the literature data. Also shown in Table I are the extinction coefficient values calculated from the previously determined calibration curves. The agreement between the spectrophotometric and calculated data can be regarded as satisfactory, mainly for their trend.

Finally, for the determination of tetramer and pentamer via UV, the extinction coefficients from Table I and the ε-caprolactam calibration as reference were used.

An estimation of extinction coefficient values of tetramer and pentamer was attempted, by taking as a reference ε-caprolactam and the calibration curves previously determined. For both compounds a value of about 1100 l/mol · cm was obtained, higher than those previously reported (970 l/mol · cm) [4,8]. Experimental confirmation of the calculated values was not attempted, since pure tetramer and pentamer were unavailable.

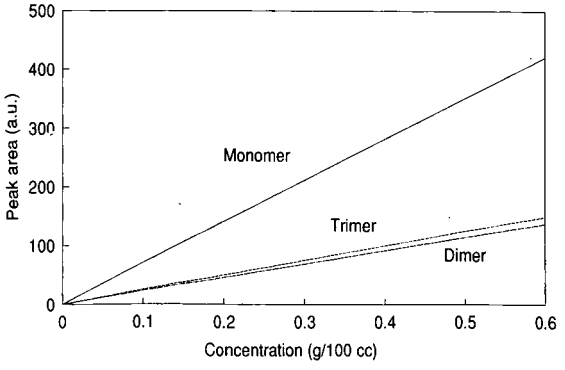

Fig. 4. UV calibration of ε-caprolactam, dimer and trimer.

The use of the dual detection (UV and RI) allows a direct comparison of the determinations of the component concentrations in the mixture. The agreement between the data is satisfactory, therefore differential refractive index detection can be fruitfully used for such analyses, although no example of its use has been reported in the literature. Moreover, in our particular case, RI detection allowed us to verify the extinction coefficient values for dimer and trimer.

CONCLUSION

The proposed HPLC method is effective in the determination of the cyclic oligomers of ε-caprolactam, allowing a good separation between monomer and dimer. Differential refractive index detection appears to be as reliable as the UV detection using the reported experimental conditions. By comparing the UV and RI detector responses, some disagreement with the reported data regarding the extinction coefficients at 210 for dimer and trimer was found.

ACKNOWLEDGEMENTS

The authors are indebted to their department for the permission to publish this work. They also thank Manuela Tommasi and Giovanni Sterzi for the extinction coefficient measurements, and Aldo

Gramostini and Cesare Baldini for continuous assistance during the whole work.

REFERENCES

1 D. Heikens, *Rec. Trav. Chim. Pays-Bas*, 75 (1956) 1199.
2 M. Rothe, *Makromol. Chem.*, 35 (1960) 183.
3 J. M. Andrews, F. R. Jones and J. A. Semlyen, *Polymer*, 15 (1974) 420.
4 S. Mori and T. Takeuchi, *J. Chromatogr.*, 49 (1970) 230.
5 V. Krajnik, P. Bozek, J. Kondelikova and J. Kralicek, *J. Chromatogr.*, 240 (1982) 539.
6 K. Tai and T. Tagawa, *J. Appl. Polym. Sci.*, 27 (1982) 2791.
7 C. Guaita, *Makromol. Chem.*, 185 (1984) 459.
8 S. Russo, *La Chimica e l'Industria*, 63 (1981) 412.

Journal of Chromatography, 585 (1991) 337–341
Elsevier Science Publishers B.V., Amsterdam

CHROM. 23 599

Short Communication

Rapid optical resolution of electrically neutral cobalt(III) chelate complexes by gel permeation chromatography

Milan Strašák* and Pavol Novomeský*

Department of Analytical Chemistry and Laboratory of Structural Biocoordination Chemistry, Faculty of Pharmacy, Comenius University, Odbojárov 10, 832 32 Bratislava (Czechoslovakia)

Slavomír Bystrický

Institute of Chemistry, Slovak Academy of Science, 842 38 Bratislava (Czechoslovakia)

(First received April 26th, 1991; revised manuscript received July 2nd, 1991)

ABSTRACT

Three geometrical isomers of electrically neutral [Co(EBAA)(aa)] [EBAA = ethylenebis(aminoacidate); aa = an amino acidate] complexes have been synthesized and characterized. They have been resolved into the enantiomers, except for symmetrical *cis-mer*-[Co(EBAA)(aa)] isomers, by gel permeation chromatography on a Sephadex G-10 column with water as the eluent, and their absolute configurations have been determined based on their circular dichroism spectra. It has been revealed that, except for [Co(EBG)(β-ala)] [EBG = ethylenebis(glycinate)], the *Δ* enantiomers have a substantially greater optical purity.

INTRODUCTION

Linear tetradentate ligands provide a variety of stereochemical permutations, and linear EBAA ligands [EBAA = ethylenebis(amino acidate)], $^{-}OOCCH(R)NR'CH_2CH_2NR'CH(R)COO^{-}$, are of particular interest for studies of Co(III) and Cr (III) [1]. The interest is not only in their stereochemistry, but also their use as probes of the structure–function relationships of proteins [2]. The complexes can be used for this purpose as they are inert to substitution.

For the neutral [Co(EBAA) (aa)] system (aa = amino acidate) three geometrical isomers are possible (Fig. 1) and there are also the optical *Λ* and *Δ* isomers for the *cis*-α and both *cis*-β forms.

The separation and isolation of these geometrical isomers have been carried out by column chromatography on an anion-exchange resin (Dowex 1-X8, Cl^{-}) and on a cation-exchange column (SP Sephadex C-25, Na^{+}) [3].

Neutral complexes so far completely resolved into enantiomers are limited to tris-chelates. Nakazawa *et al.* [3] have reported that when the bis (μ-*d*-tartrato)diantimonate(III) anion, $[Sb_2(d\text{-tart})_2]^{2-}$, form of QAE-Sephadex is used with water as the eluent, some geometrical isomers of [Co(EBG) (aa)], where EBG is ethylenebis(glycinate) and aa = glycinate (gly) and β-alaninate (β-ala), have been completely resolved into the enantiomers. In the course of studies of metal complexes of amino acid

* Author deceased.

0021-9673/91/$03.50

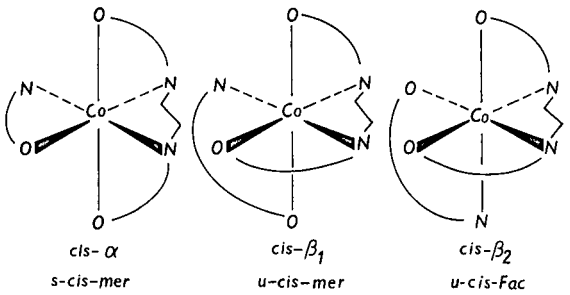

Fig. 1. Three geometrical isomers for a [Co(EBAA) (aa)] complex (both notation are used). s = Symmetrical; u = unsymmetrical.

derivatives, it has been reported that the partial optical resolution of neutral cobalt(III) metal complexes is more difficult than the resolution of cationic or anionic complexes because they do not form diastereoisomers with an optically active resolving agent. However, the optical resolution of such neutral complexes can be obtained chromatographically [7]. Some neutral complexes have been reported to be partially resolved into the enantiomers using a quartz powder column [8] and *mer*- and *fac*-[Co $(gly)_3$] and *cis*-α-[Co(EBG) (gly)] by using a potato starch column [9]. The first complete resolution of neutral complexes was reported by Yoneda and Yoshizawa [10] for *fac*-[Co(β-ala)$_3$] on the Na^+ form of a CM-Sephadex cation exchanger with an ethanol–water solution of sodium *d*-tartrate, Na_2(*d*-tart), as the eluent. Thereafter, the complete resolution of a series of enantiomeric pairs of *fac*-[Co(D/L-ser)$_{3-n}$(β-ala)$_n$] (n = 0 to 3; ser = serinate) was achieved on the Na^+ form of the TSK-211 cation exchanger with an $Na_2[Sb_2$(*d*-tart)$_2]$ aqueous solution as the eluent [11].

Anion-exchange columns have also been used to resolve neutrale complexes into enantiomers [12–14]. Neutral complexes, other than tris(aa) complexes, have also been partially resolved using a *d*-lactose column [15], a quartz column [16] or a Δ-[Ni $(phen)_3$]-montmorillonite (phen = 1,10-phenantroline) column [17]. Recently, [Co$(acac)_3$] and [Cr $(acac)_3$] (acac = acetate) were completely resolved by high-performance liquid chromatography on a (+)-poly(triphenylmethyl methacrylate) column [18]. No resolution of the optical isomers of neutral metal complexes on molecular sieves has yet been described. This method was used here to resolve [Co (EBAA) (aa)] complexes.

The degree of resolution which can be achieved on one passage through chelate cationic [4] and anionic [5] complexes by gel permeation chromatography (GPC) was reported. The object of this study is the rapid optical resolution of neutral cobalt(III) complexes by GPC on a column of the molecular sieve Sephadex G-10.

EXPERIMENTAL

The complexes were prepared by a method analogous to that previously reported [3] for [Co(EBG) (aa)]. All the new compounds gave satisfactory elemental analyses. The geometrical isomers were assigned to *cis*-α and *cis*-β, respectively, according to their absorption spectra and ^1H and ^{13}C NMR spectra [6].

Optical resolution

The racemic neutral complex (20–40 mg) dissolved in an appropriate amount of water (2–5 ml) was loaded onto the column (60 cm × 1 cm I.D.) of Sephadex G-10. The elution was performed with water at a flow-rate of 0.1–0.2 ml/min. During elution the neutral complex was partially separated into enantiomers. The eluates obtained were subjected to absorption (AB) and circular dichroism (CD) measurements.

CD spectra were recorded on a Jobin-Yvon Dichrograph III. The concentrations of the solutions (10^{-4}–10^{-2} mol/l) were determined from their absorption spectra recorded on a Specord M-40 spectrophotometer or by atomic absorption spectrometry (AAS).

RESULTS AND DISCUSSION

The optical resolution of electrically neutral cobalt(III) complexes achieved on one passage through the column is given in Table I. Figs. 2 and 3 show the typical AB and CD spectra. The ligand field symmetry of the *u-cis-fac* isomer is higher than that of the *u-cis*-mer isomer. The decrease in symmetry from facial to meridional is expected to cause a splitting, or at least a broadening, of the lowest energy absorption band in the visible spectra. In both [Co(EBA) (gly)] and [Co(EBV) (gly)] [EBA = ethylenebis(α-alaninate); EBV = ethylenbis(valinate)], broadening is seen clearly in the low-energy

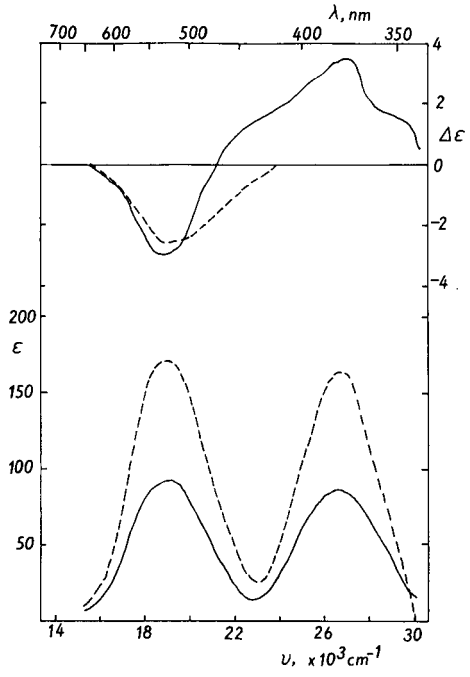

Fig. 2. Absorption spectra (lower) and CD spectra (upper) of Δ-[Co(EBA) (gly)]; (——) *u-cis-mer*; (--) *u-cis-fac*.

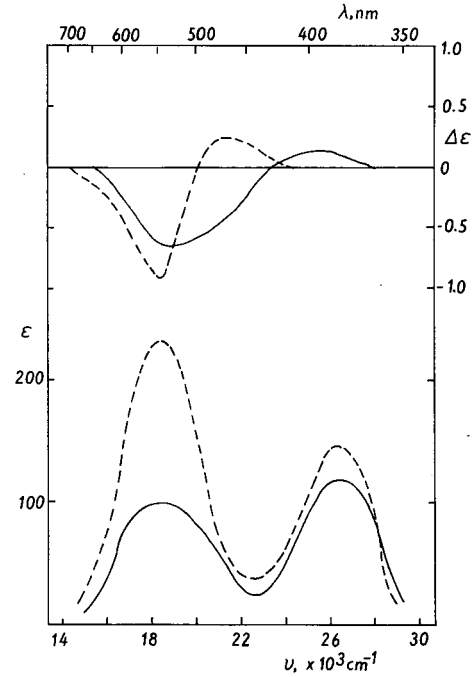

Fig. 3. Absorption spectra (lower) and CD spectra (upper) of Δ-[Co(EBV) (gly)]; (——) *u-cis-mer*; (--) *u-cis-fac*.

absorption band for the first eluted isomer. In [Co (EBG) (β-ala)], a marginal shoulder is observed for the first eluted isomer. In contrast, the last eluted isomer exhibits a relatively sharp absorption band. Therefore, the first and second eluted isomers can be assigned to the *u-cis-mer* and *u-cis-fac* isomers, respectively.

The assignment is consistent with the chromatographic behaviour. Although both isomers are electrically neutral, the *fac* isomer has a greater dipole moment than the *mer* isomer. Thus the former is considered to interact more effectively with the functional group of the SP Sephadex C-25 cation exchanger than the latter. Therefore, the *fac* isomer is expected to be eluted later than the *mer* isomer. This has been observed experimentally.

Partial optical resolution of the complexes has been attained and their absolute configuration has been established based on the fact that the sign of the dominant peak in the first d–d transition region of the CD spectrum can generally be related to the net chirality of the complex [19,20]. A Δ configuration of chelate rings is expected to produce a negative dominant peak in the d–d transition region whereas a Λ configuration produces a positive dominant peak [19]. The CD spectra shown in Figs. 2 and 3 resemble those of [Co(EBG) (β-ala)]. The $\Delta\varepsilon$ values obtained for the optical isomers of [Co (EBG) (β-ala)] (Table I) can be compared with those of the pure isomers [3]. Remarkable differences can be seen. On the $[Sb_2(d\text{-tart})_2]^{2-}$ form of QAE Sephadex the *s-cis-mer* and *u-cis-mer* isomers have been completely resolved into the enantiomers, whereas GPC on Sephadex G-10 does not resolve the *s-c is-mer*.

Some other observations can be made on the resolution of these complexes on the Sephadex G-10. It is interesting that, with all the cationic [4] and anionic [5] complexes studies, the Δ enantiomers have a substantially greater optical purity; this is also true for neutral complexes, except [Co(EBG) (β-ala)]. The relationship between the absolute configurations and the order of elution is given in Table II. An examination of the CD spectra of the eluates shows that the first eluted enantiomers have a Δ configuration, except for [Co(EBG) (β-ala)]. In spite of the results from the optical resolution of the cationic $[CoN_4O_2]^+$-type complexes [4], where the enantiomers with the Λ configuration are eluted

TABLE I

ABSORPTION (AB) AND CIRCULAR DICHROISM (CD) DATA FOR THE FIRST ELUTED ENANTIOMER OF COBALT (III) COMPLEXES

Complex	AB		CD	
	λ (nm)	ε (l mol^{-1} cm^{-1})	λ (nm)	$\Delta\varepsilon$ (l mol^{-1} cm^{-1})
s-cis-mer-[Co(EBG)) (β-ala)]	562	sh[a]	Unresolved	
	504	114	Unresolved	
	373	127	Unresolved	
u-cis-mer[Co(EBG) (β-ala)]	586	sh	554	(+)[b]
	508	80	477	(−)
	373	92		
u-cis-fac-[Co(EBG) (β-ala)]	524	248	560	+1.42
	374	153	480	−1.35
s-cis-mer-[Co(EBA) (gly)]	552	108	Unresolved	
	520	sh	Unresolved	
	374	110	Unresolved	
u-cis-mer-[Co(EBA) (gly)]	529	92	538	−2.91
	374	86	372	+3.52
u-cis-fac-[Co(EBA)(gly)]	531	172	535	−2.61
	373	164	Unresolved	
s-cis-*mer*-[Co(EBV)(gly)]	543	111	Unresolved	
	510	sh	Unresolved	
	373	141	Unresolved	
u-cis-mer-[Co(EBV)(gly)]	513	100	537	−0.62
	374	117	390	+0.14
u-cis-fac-[Co(EBV)(gly)]	529	232	541	−0,93
	373	144	460	+0.24

[a] sh = Shoulder.
[b] Partially resolved.

TABLE II

CORRELATION BETWEEN THE SIGN OF THE DOMINANT CD PEAK OF THE FIRST ELUTED ENANTIOMERS AND THEIR ABSOLUTE CONFIGURATIONS

Isomer	Sign of the longer wavelength CD peak	Absolute configuration	Reference[a]
s-cis-mer-[Co(EBG)(gly)]	+	Λ	3
u-cis-mer-[Co(EBG)(gly)]	+	Λ	3
u-cis-fac-[Co(EBG)(gly)]	+	Λ	3
s-cis-mer-[Co(EBG)(β-ala)]	+	Λ	3
u-cis-mer-[Co(EBG) (β-ala)]	+	Λ	3
u-cis-fac-[Co(EBG)(β-ala)]	+	Λ	3
u-cis-mer-[OC(EBG)(β-ala)]	+	Λ	This work
u-cis-fac-[Co(EBG)(β-ala)]	+	Λ	This work
u-cis-mer-[Co(EBA)(gly)]	−	Δ	This work
u-cis-fac-[Co(EBA)(gly)]	−	Δ	This work
u-cis-mer-[Co(EBV)(gly)]	−	Δ	This work
u-cis-fac-[Co(EBV)(gly)]	−	Δ	This work

[a] Chromatographic conditions: $[Sb_2(D\text{-tart})_2]^{2-}$ form of QAE Sephadex anion exchanger with water for Ref. 3; on Sephadex G-10 with water for this work.

TABLE III

ADJUSTED RETENTION VOLUMES AND SEPARATION FACTORS OBTAINED ON ELUTION WITH WATER

Complex	Retention volume (ml)	Separation factor
Λ-u-cis-mer-[Co(EBG)(β-ala)]	–	[a]
Δ Isomer		
Λ-u-cis-fac-[Co(EBG)(β-ala)]	4.65	1.060
Δ Isomer	4.93	
Λ-u-cis-mer-[Co(EBA)(gly)]	5.02	1.035
Δ Isomer	4.85	
Λ-u-cis-fac-[Co(EBA)(gly)]	4.74	1.019
Δ Isomer	4.65	
Λ-u-cis-mer-[Co(EBV)(gly)]	3.84	1.041
Δ Isomer	3.69	
Λ-u-cis-fac-[Co(EBV)(gly)]	4.06	1.028
Δ Isomer	3.95	

[a] Partially resolved.

first, it is difficult to find a simple relationship between the order of elution and the absolute configuration of the anionic $[CoN_2O_4]^-$ [5] and neutral $[CoN_3O_3]$ complexes.

Each elution curve consists of two peaks, a large first peak and a smaller second peak. By repeating the elution procedure several times, fractions of the first and second peaks were collected and used for measurements of the visible and CD spectra. Thus two series of retention volumes of the enantiomeric pairs, *Λ* and *Δ*, were obtained. The separation factor for each enantiomeric pair was obtained from the retention volumes of two peaks in each elution curve because these complexes originally exist as an enantiomeric pair. The results are shown in Table III. It is obvious that the separation factor of the enantiomeric pair is largest with *fac*-[Co(EBG) (β-ala)], which contains a six-membered chelate ring, and decreases with increasing number of five-membered chelate rings. A similar trend had been observed during the separation of neutral cobalt(III) aa complexes on the Na^+ form of the TSK-211 cation exchanger with $Na_2[Sb_2(d\text{-tart})_2]$ as the eluent [11].

From a comparison of the data in Table I, the degree of optical resolution decreases in the order *cis-β* > *cis-α*. This is because both *cis-β* isomers have lower symmetrical chromophore (C_1) than the *cis-α* (C_2) isomer. As the optical resolution determined by column chromatography of chiral (or prochiral) complexes is based on the interactions between a chiral adsorbent and a chiral complex, the symmetry-dependent chiral discriminations (chirodiastaltic interactions) are greater for complexes with low symmetry.

This chromatographic method can be used to obtain the partial resolution of racemic amino acids and related compounds in the form of cobalt(III) complexes. The separation of optical isomers on the molecular sieve Sephadex G-10 is convenient and appears to be generally applicable for the optical resolution of non-labile metal chelate compounds. The method is rapid and simple and the molecular sieve in the column is stable for several years.

REFERENCES

1 D. J. Radanovič, *Coord. Chem. Rev.*, 54 (1984) 159.
2 M. S. Urdea and J. I. Legg, *J. Biol. Chem.*, 254 (1979) 11868.
3 H. Nakazawa, H. Ohtsuru and H. Yoneda, *Bull. Chem. Soc. Jpn.*, 60 (1987) 525.
4 M. Strašák and S. Bystrický, *J. Chromatogr.*, 403 (1987) 331.
5 M. Strašák and S. Bystrický, *J. Chromatogr.*, 450 (1988) 284.
6 P. Novomeský and M. Strašák, unpublished results.
7 H. Yoneda, *J. Chromatogr.*, 313 (1985) 59.
8 R. Tsuchida, M. Kobayashi and A. Nakamura, *Bull. Chem. Soc. Jpn.*, 11 (1936) 38.
9 J. I. Legg, D. W. Cooke and B. E. Douglas, *Inorg. Chem.*, 6 (1967) 700.
10 H. Yoneda and T. Yoshizawa, *Chem. Lett.*, (1976) 707.
11 S. Yamazaki, T. Yukimoto and H. Yoneda, *J. Chromatogr.*, 175 (1979) 317.
12 T. Yukimoto and H. Yoneda, *J. Chromatogr.*, 222 (1981) 477.
13 S. Yamazaki and H. Yoneda, *Inorg. Nucl. Chem. Lett.*, 15 (1979) 195.
14 H. Yoneda, T. Yukimoto, Y. Kushi and H. Nakazawa, *J. Liq. Chromatogr.*, 9 (1986) 573.
15 R. C. Fay, A. Y. Girgis and U. Klabunde, *J. Am. Chem. Soc.*, 92 (1970) 7056.
16 T. S. Piper, *J. Am. Chem. Soc.*, 83 (1961) 3908.
17 A. Yamagishi and R. Ohnishi, *Inorg. Chem.*, 21 (1982) 4233.
18 Y. Okamoto, S. Honda, E. Yashima and H. Yuki, *Chem. Lett.*, (1983) 1221.
19 A. J. McCaffery, S. F. Mason and B. J. Norman, *J. Chem. Soc.*, (1965) 5094.
20 J. I. Legg and B. E. Douglas, *J. Am. Chem. Soc.*, 88 (1966) 2697.

Journal of Chromatography, 585 (1991) 342–344
Elsevier Science Publishers B.V., Amsterdam

CHROM. 23 577

Short Communication

Regeneration of column activity after the gas chromatographic separation of membrane lipids on thermostable SE-52 phase

Marco Vincenzo Piretti* and Giampiero Pagliuca

Dipartimento di Biochimica, Sezione di Biochimica Veterinaria, Università di Bologna, Via Zanolini 3, 40126 Bologna (Italy)

(First received April 3rd, 1991; revised manuscript received June 18th, 1991)

ABSTRACT

The phosphoglyceride/cholesterol ratio of membrane lipids can be approximately determined by gas chromatography by direct injection into a short capillary column of the lipid material extracted from tissues according, for instance, to the Folch procedure. However, as a result of the pyrolysis of the injected material, in the course of the separation acidic substances are produced that deactivate the stationary phase. With the aid of a suitable scavenger, such as diethylenetriamine, it is possible to regenerate the column activity.

INTRODUCTION

Changes in the lipid composition of cellular membranes, such as those observed in some pathological conditions [1], may be indicated by variations in the phosphoglyceride/cholesterol ratio. This ratio can be rapidly determined by gas chromatography (GC) using a short capillary column coated with a highly thermostable phase such as SE-52 [2,3]. However, as a result of the pyrolysis of the injected material, in the course of the separation [2,3] substances are produced during continuous use that modify the stationary phase and lead to deactivation. With the aid of a suitable scavenger, however, it is possible to regenerate the column activity.

EXPERIMENTAL

A Carlo Erba Model 4160 HRGC gas chromatograph with a Mega SE-52 fused-silica column (10 m × 0.32 mm I.D.; film thickness 0.1 μm) was used. The injection temperature was initially 40°C, programmed at 20°C/min to 340°C, the final temperature being maintained for 10 min. The carrier gas was hydrogen at a flow-rate of 8 ml/min. On-column injection of 1 μl of a 0.2% benzene solution of membrane lipid extract, *i.e.*, a mixture of cholesterol and phosphoglyceride, was applied.

RESULTS AND DISCUSSION

Extraction of membrane lipids by the method of Folch *et al.* [4] and injection into a new column programmed rapidly to 340°C gave a chromatogram similar to that shown at the top of Fig. 1. The peak at 11 min corresponded to cholesterol and those between 13 and 20 min were ascribable to the diglycerides arising from the decomposition of the corresponding phosphoglycerides [2,3] in the course of the separation.

0021-9673/91/$03.50

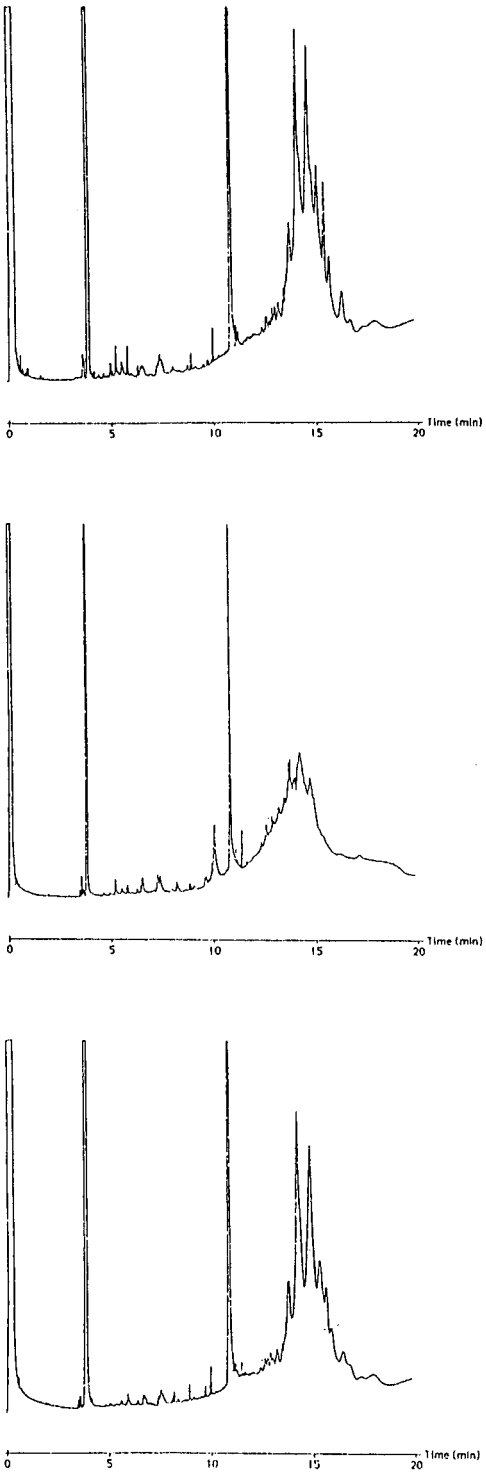

According to the relationship

area of cholesterol peak/100 = area of diglyceride peaks/x

it is possible to relate the composite area of the diglyceride peaks to the single cholesterol peak area normalized at 100 and obtain indirect information about the variation in the lipid composition of the cellular membranes of a tissue in the course of recurring experiments.

When samples are being continuously analysed, progressive deactivation of the stationary phase is observed as a result of adsorption of acidic, non-volatile products arising from decomposition of the phosphoglyceride components. Comparisons between consecutive chromatograms during continuous use may not give rise to any observable change. However, analytical comparisons between chromatograms obtained on consecutive days show considerable differences as the lack of use of the column during the overnight period allows the firm deposition of the acidic breakdown material with a consequential extensive effect on separation (see the middle chromatogram in Fig. 1).

Our investigations have shown that the interfering, non-volatile, acidic compounds that contaminate the column can be satisfactorily eliminated by the use of diethylenetriamine (m.p. = −39°C; b.p. = 207°C). A 1-μl volume of diethylenetriamine in the free state was injected into the column on completion of daily use, under conditions identical with those used for the separation of the membrane lipid fractions. An injection temperature of 40°C resulted in uniform application of the reagent throughout the stationary phase. Increasing the column temperature at 20°C/min resulted in complete elimination of the reagent in 5 min, i.e., at a column temperature of 140°C. Therefore, the

Fig. 1. Chromatograms produced by on-column injection of 1 μl of a 0.2% benzene solution of membrane lipid into a short capillary column coated with SE-52 under the described conditions. Top, chromatogram produced from a new column; middle, chromatogram produced from the same column deactivated by lack of use during the overnight period; bottom, chromatogram produced from the same column after reactivation by injecting 1 μl of the scavenger diethylenetriamine. The peak at 3.6 min corresponds to butylhydroxytoluene.

reagent in the liquid state washes the surface layers of the stationary phase. The effectiveness of such a treatment in the regeneration of the separation ability of the column can be seen in the bottom chromatogram in Fig. 1. In addition to maintaining the optimum separation, the overall working life of the column is also considerably extended.

ACKNOWLEDGEMENT

The authors are grateful to Dr. Raymond Noble (Scottish Agricultural College, Auchincruive, Ayr, Scotland, UK) for assistance in preparing the manuscript.

REFERENCES

1 L. Masotti, E. Casali, N. Gesmundo, G. Sartor, T. Galeotti, S. Borrello, M. V. Piretti and G. Pagliuca, *Ann. N.Y. Acad. Sci.*, 551 (1988) 47–58.
2 S. Hrelia, G. Lercker, P. L. Biagi, A. Bordoni, F. Stefanini, P. Zunarelli and C. A. Rossi, *Biochem. Int.*, 12 (1986) 741–750.
3 A. Bordoni, P. L. Biagi, G. Parenti Castelli, S. Hrelia, C. A. Rossi, G. Lercker, J. C. Izpisua, T. Barber, J. Cabo and G. Lenaz, *Membr. Biochem.*, 8 (1989) 11–18.
4 J. Folch, M. Lees and G. H. Sloane Stanley, *J. Biol. Chem.*, 226 (1957) 497–509.

Journal of Chromatography, 585 (1991) 345–347
Elsevier Science Publishers B.V., Amsterdam

CHROM. 23 637

Short Communication

Determination of succinic acid by pyrolysis–gas chromatography in the presence of sodium sulfite and iron powder

M. Hida and T. Mitsui*

Criminal Science Laboratory Aichi Prefecture, 2-1-1, Sannomaru, Naka-ku, Nagoya 460 (Japan)

Y. Fujimura

Department of Industrial Chemistry, Faculty of Engineering, University of Chubu, 1200, Matsumoto-cho, Kasugai 487 (Japan)

(First received June 11th, 1990; revised manuscript received July 10th, 1991)

ABSTRACT

The determination of succinic acid was studied by Curie-point pyrolysis–gas chromatography. The recommended procedure is as follows: sample solution was added to 40 mg of the mixed powder (iron powder–sodium sulphite = 1:1), placed on a pyrolysis foil with a microsyringe and dried on a hot plate (100°C). Pyrolysis was carried out by using a gas chromatograph fitted with a Curie-point pyrolysis unit (the pyrolysis foil was maintained at 445°C for 5 s). The peak area of dimethyl sulphoxide was used for the determination of succinic acid. The measurement range was 2–102 μg and the calibration curve was a straight line with a correlation coefficient of 0.998. The relative standard deviation for the pyrolysis of succinic acid (41 μg) was 2.2% ($n=4$).

INTRODUCTION

Pyrolysis–gas chromatography (Py–GC) has been used to characterize polymers, high-boiling-point compounds and non-volatile materials [1]. This technique has been employed mainly for qualitative analysis since it is difficult to obtain sufficient reproducible pyrolysis. We have also shown that when the sample is pyrolysed in the presence of a mixture of metal powder and an inorganic salt not only are the observed peak areas larger than in the absence of the mixture but also the pyrolysis is reproducible on repeated runs. In a series of articles we have demonstrated that several amines can be determined by means of Py–GC. For example, glyphosate [2], alkaloid narcotics [3] and aromatic amines [4] were determined by their pyrolysis products with good reproducibility and sensitivity. Further, paraquat [5] was pyrolysed in the presence of nickel powder and potassium iodide. Methyl iodide, which was obtained from the reaction of the methyl radical produced by paraquat and potassium iodide, was used to measure paraquat. Aliphatic amines [6] were determined as the corresponding alkyl chlorides that were obtained from alkyl radicals and metal chlorides. In this paper we describe the application of this technique for the determination of succinic acid, which was pyrolysed in the

0021-9673/91/$03.50

presence of a mixture of iron powder and sodium sulphite. The dimethyl sulphoxide formed was used to determine succinic acid in a similar manner as above.

EXPERIMENTAL

A Curie-point pyrolyser (Japan Analytical Industry, Model JHP-2) was directly coupled to a gas chromatograph (Hitachi Model 163) equipped with a flame ionisation detector. Flame ionisation detection signals were processed using a Hewlett-Packard 3390A integrator. The temperatures of the pyrolyser unit and the tube connecting the pyrolyser and gas chromatograph were maintained at 150 and 200°C, respectively. The separations were performed on a 2 m × 3 mm I.D. stainless-steel column packed with 10% polyethylene glycol (PEG) 20M on Chromosorb W AW-DCMS (80–100 mesh). The pyrolysis products were eluted isothermally at 80°C. All chemicals used were obtained through Wako (Osaka, Japan). They were of high purity and used without further purification. Succinic acid and adipic acid were used as aqueous solutions and other acids were used as methanolic solutions.

Procedure

Equal amounts of iron powder and sodium sulphite were mixed thoroughly in an agate mortar. A 40-mg sample of the mixed powder was placed onto a piece of pyrolysis foil (about 9 mm × 22 mm, 0.05 mm thick) using a microspatula. Then 20 μl of sample solution containing about 40 μg of sample were added using a microsyringe. The solvent on the pyrolysis foil was evaporated to dryness on a hot plate at about 100°C. The pyrolysis foil was carefully folded and placed in a quartz sample tube. The tube was loaded into the pyrolyzer. About 40 μg of sample were used for each experimental determination.

RESULTS AND DISCUSSION

The pyrolysis products were separated by GC, as shown in Fig. 1. The dimethyl sulfoxide formed from the pyrolysis product of succinic acid and sodium sulfite was used for the determination of succinic acid. Sodium carbonate deca-hydrate, potassium iodide and nickel chloride hexa-hydrate, which were

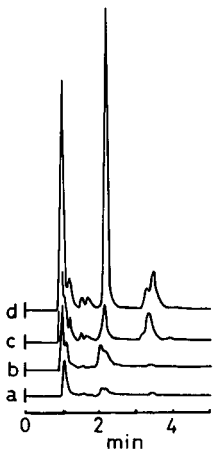

Fig. 1. Typical pyrograms of succinic acid (a) without any additives, (b) with 20 mg of sodium sulphite, (c) with 20 mg of iron powder and (d) with a mixture of sodium sulphite and iron powder. The pyrolysis temperature was 445°C. The amount of succinic acid was 41 μg.

useful salts in previous investigations, and sodium sulphite were studied in this work. The salts served as pyrolysis temperature controllers and sample supports. In the presence of the mixed powder of sodium sulphite and iron powder (through 100 mesh, electrolytic), the dimethyl sulphoxide peak area was about twenty times higher than in its absence. The metal powder was mixed with sodium sulphite in order to improve the conduction of heat from the pyrolysis foil to the sample. The metals used were aluminum, chromium, manganese, iron, nickel and zinc. The maximum total production was observed when chromium or iron powder was used. The effect of the mixed ratio of inorganic salt and metal powder on the peak area of dimethyl sulphoxide was studied using a mixture of 3–30 mg of sodium sulphite and 15 mg of chromium or iron powder. The optimum added mixture was sodium sulphite and iron (1:1, w/w). The amount of the mixture added to the pyrolysis foil varied from 10 to 60 mg. The peak area of dimethyl sulphoxide considerably increased up to 20 mg and slightly increased in the range of 20 mg up to 60 mg. The optimal sensitivity and handling were obtained from addition of 40 mg. With further addition of mixture it was difficult to fold the foil without spilling powder. The pyrolysis temperature was studied by using different Curie-point pyrolysis foils (333, 386,

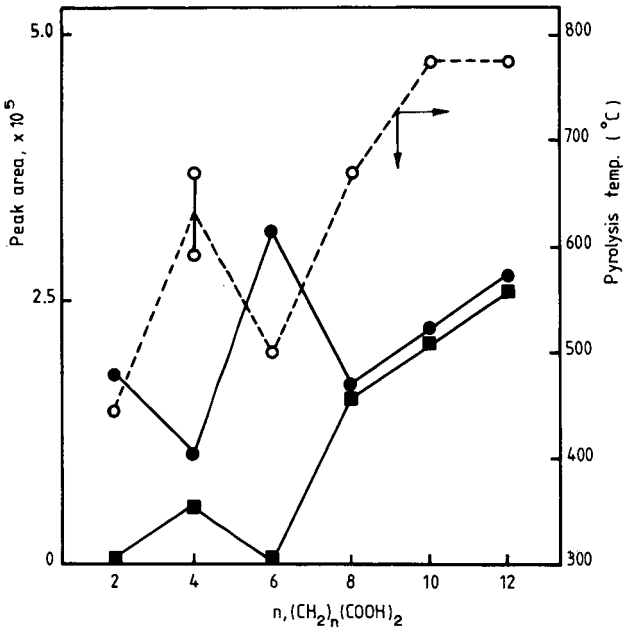

Fig. 2. Effect of additives on succinic acid and its homologues. ■ = no additives; ● = 40 mg of iron powder and sodium sulphite (1:1); ○ = optimal pyrolysis temperature.

445, 500, 590, 670 and 764°C) which are commercially available. The maximum peak was observed when succinic acid was pyrolyzed at 445°C.

The peak area of dimethyl sulphoxide was used to study the effect of addition of succinic acid and its homologues, as shown in Fig. 2. The peak areas of dimethyl sulphoxide pyrolysis of succinic acid and suberic acid in the presence of iron powder–sodium sulphite (1:1, w/w) were about 20 and 35 times greater than without additives. This effect related to the pyrolysis temperature of each acid. Succinic acid and suberic acid were pyrolysed below 500°C and the others above 500°C. Because sodium sulphite decomposed at a higher temperature, improvements in sensitivity were not observed with adipic acid, sebasic acid 1,10-decanedicarboxylic acid and 1,12-dodecanedicarboxylic acid. Adipic acid formed the anhydride.

The pyrolysis of succinic acid was therefore carried out as follows: pyrolysis temperature was 445°C; the mixture ratio of sodium sulphite and iron was 1:1 (w/w); the amount of mixture was 40 mg. The measurement range was 2–102 μg and the calibration curve was a straight line with a correlation coefficient of 0.998. The relative standard deviation for the pyrolysis of succinic acid (41 μg) was 2.2% ($n = 4$). Using Py–GC the quantitative analysis of succinic acid was established.

REFERENCES

1 S. Tsuge and H. Ohtani, *Pyrolysis–Gas Chromatography of Polymers: Fundamentals and Data Compilation*, Tekunoshi-sutem, Japan, 1989.
2 M. Hida, T. Mitsui and Y. Fjimura, *Bunseki Kagakaku*, 38 (1989) 87.
3 T. Mitsi, M. Hida and Y. Fujimura, *J. Anal. Appl. Pyrolysis*, 17 (1989) 83.
4 M. Hida, T. Mitsui and Y. Fujimura, *J. Anal. Appl. Pyrolysis*, 17 (1990) 181.
5 T. Mitsui, Y. Minami and Y. Fujimura, *Bunseki Kagakaku*, 36 (1987) 821.
6 M. Hida, T. Mitsui and Y. Fujimura, *J. Anal. Appl. Pyrolysis*, 17 (1990) 371.

Journal of Chromatography, 585 (1991) 348–352
Elsevier Science Publishers B.V., Amsterdam

CHROM. 23 679

Short Communication

Determination of methylboronic acid in teboroxime by capillary gas chromatography

Douglas A. Both*, Michael Ribick and Mohammed Jemal

Bristol-Myers Squibb Company, Bristol-Myers Squibb Pharmaceutical Research Institute, P.O. Box 191, 1 Squibb Drive, New Brunswick, NJ 08903-0191 (USA)

(First received May 31st, 1991; revised manuscript received August 9th, 1991)

ABSTRACT

A capillary gas chromatographic method has been developed to quantitate the methylboronic acid in a lyophilized formulation. The formulation is first dissolved in 1 *M* hydrochloric acid. Next a tetrahydrofuran solution of the internal standard, 1-butaneboronic acid, and a methylene chloride solution of the derivatizing reagent, pinacol (2,3-dimethyl-2,3-butanediol), are added. The two-phase mixture is shaken for 3 h at 60°C during which time the methylboronic acid is extracted into the methylene chloride phase and reacted with pinacol to form the cyclic pinacol-boronate ester. The product formed in methylene chloride is injected in the split mode onto a capillary gas chromatographic system equipped with a flame ionization detector. Quantitation is achieved by an external standard method.

INTRODUCTION

Methylboronic acid is an essential ingredient in [^{99m}Tc] teboroxime (CardioTec), a new technetium-99m based imaging product developed by Bristol-Myers Squibb for non-invasive diagnosis of myocardial infarction [1–3]. The imaging product is prepared *in situ* from a lyophilized formulation by the addition of a solution of pertechnetate containing 10 to 100 mCi of technetium-99m followed by heating at 100°C for 15 min. CardioTec is the methylboronic acid adduct of chloro, triscyclohexyl dioxime technetium and is formed from its member parts of methylboronic acid, cyclohexanedione dioxime, sodium chloride and technetium. In addition to these ingredients, the lyophilized formulation contains pentetic acid, γ-cyclodextrin, citric acid and stannous chloride. The methylboronic acid content in the formulation is 2.0 mg/vial. The specification allows the methylboronic content to vary between 1.7 and 2.3 mg/vial. The total content of all ingredients in the formulation is 165 mg/vial; thus, the methylboronic acid content is only 1.2% of the total formulation.

A capillary gas chromatographic (GC) method has been developed to quantitate the methylboronic acid in the lyophilized formulation. The sample preparation part of the method involves dissolving the formulation in 1 *M* hydrochloric acid, adding a tetrahydrofuran solution of the internal standard, 1-butaneboronic acid, adding a methylene chloride solution of the derivatizing reagent, pinacol (2,3-dimethyl-2,3-butanediol), and shaking the two-phase mixture for 3 h at 60°C. The methylboronic acid is extracted into the methylene chloride phase and reacted with pinacol to form the cyclic pinacol-boronate ester (Fig. 1). The product formed is hydrolytically and chromatographically stable, and the excess pinacol does not interfere in the chromatography.

0021-9673/91/$03.50

EXPERIMENTAL

Reagents and chemicals

Methylboronic acid was a characterized product obtained from Bristol-Myers Squibb Pharmaceutical Research Institute (Diagnostics Research and Development Department, Princeton, NJ, USA). Anhydrous pinacol (2,3-dimethyl-2,3-butanediol), 1-butaneboronic acid (gold label) and tetrahydrofuran (anhydrous, gold label) were obtained from Aldrich Chemical. Methylene chloride (HPLC grade) and hydrochloric acid (ACS grade) were obtained from Fisher Scientific. Silyl-8 and Sylon-CT were purchased from Pierce Chemical and Supelco, respectively.

A derivatizing solution was made by dissolving 4.0 g of pinacol in 500 ml of methylene chloride. A methylboronic acid standard stock solution was prepared by dissolving 20 ± 2 mg of methylboronic acid in tetrahydrofuran and diluting to 2.0 ml. An internal standard stock solution was prepared by dissolving 20 ± 2 mg of 1-butaneboronic acid in tetrahydrofuran and diluting to 2.0 ml.

Working standard preparation

A 10-ml portion of the derivatizing solution was added to a 20-ml headspace vial (Hewlett-Packard, No. 9301-0716) containing 400 μl of 1 *M* hydrochloric acid. Next, 300 μl of the methylboronic acid stock solution was added, followed by 200 μl of the internal standard stock solution. The vial was crimp-capped and placed into a heating block set at 60°C. The block was then placed on its side into a mechanical shaker. The shaking and heating was allowed to proceed for three hours. After cooling, a portion of the lower methylene chloride layer was transferred to fill an autoinjector vial. A 1.0-μl portion of this solution was then injected into the GC system described below.

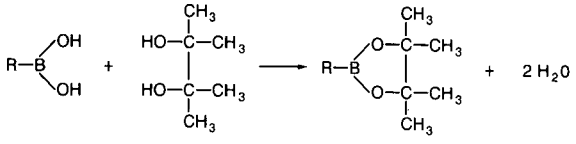

I, II *III* *IV*

Compound	R
Methylboronic acid ***(I)***	CH_3
1-Butaneboronic acid ***(II)***	$CH_3(CH_2)_3$
Pinacol ***(III)***	–
Pinacol-boronate Ester ***(IV)***	–

Fig. 1. Reaction of the alkylboronic acids with pinacol.

Sample preparation

To the crimp-capped vial containing the lyophilized sample powder, 400 μl of 1 *M* hydrochloric acid was added and the sample was dissolved. Next, 200 μl of the internal standard stock solution and 300 μl of tetrahydrofuran were added and mixed carefully, allowing the vial to vent by inserting a syringe without plunger through the rubber septum. The rubber septum was removed and the vial contents were then transferred to a 20-ml headspace vial. After adding 10 ml of the derivatizing solution, the vial was crimp-capped and then treated as described under *Working standard preparation.*

Blank preparation

A 10-ml portion of the derivatizing solution was added to a 20-ml headspace vial containing 400 μl of 1 *M* hydrochloric acid and 300 μl of tetrahydrofuran. The vial was crimp capped and then treated as described under *Working standard preparation.*

Gas chromatography

A Hewlett-Packard 5890 capillary gas chromatograph, equipped with a split/splitless injection port, a flame ionization detector and 7673A autosampler injector, was used. The fused-silica capillary column used was a HP-5 (5% diphenyl and 95% dimethylpolysiloxane, Hewlett-Packard), 25 m × 0.32 mm I.D. and 1.0 μm stationary phase film thickness. The oven temperature was maintained at 120°C for 10 min and then ballistically programmed at 70°C/min to 210°C and held there for 4 min. The injector and detector temperatures were maintained at 200°C and 290°C, respectively. Injection was carried out in the split mode, with a split flow of 50 ml/min. The split port liner was a 4 mm I.D. open tube packed with a short glass wool plug (Hewlett-Packard, No. 19251-60540) and Sylon-CT treated after packing. The helium carrier gas head pressure was maintained at 69 kPa (10 p.s.i.g.) and the flow-rate of the helium make up gas for the flame ionization detector was 30 ml/min. The GC sensitivity was set at a range of 2^2 and attenuation of 2^2.

The analysis was carried out by injecting 1.0 μl of the blank, working standard and sample preparations. The preparations are stable at room temperature in capped autoinjector vials for at least 24 h. It is important to condition the column and deactivate the inlet with Silyl-8. This is performed each time the column or the injection liner is changed. The conditioning is performed by setting the oven temperature to 200°C and column head pressure to 103 kPa (15 p.s.i.g) and injecting 5 μl of Silyl-8 with the split off. The signal is allowed to return to its normal level before lowering the oven temperature and head pressure.

Quantitation

For quantitation the following equation was used:

$$\text{mg of methylboronic acid per vial} = \frac{C_s R_u}{R_s}$$

Where C_s = mg of methylboronic acid in the working standard preparation vial; R_u = area ratio of methylboronic acid to the internal standard in the sample chromatogram; R_s = area ratio of methylboronic acid to the internal standard in the standard chromatogram.

RESULTS AND DISCUSSION

Organic boronic acids have been used for the analysis of bifunctional compounds by GC or GC–mass spectrometry (MS) [4–13]. Alkaneboronic acids react with a variety of 1,2- and 1,3-diols, diamines and aminoalcohols to yield five- or six-membered cyclic boronates. On the other hand, characterization of alkaneboronic acids is difficult due to the facile conversion of the acid to the trimeric cyclic anhydride under mild conditions [7,8]. Thus, to determine methylboronic acid in the formulation by GC, a derivatizing reagent was required that would react quantitatively and give a volatile, thermally and hydrolytically stable product with good chromatographic properties. Ethanolamine and diethanolamine derivatives are chromatographically unsuitable while trimethylsilyl esters and alkyl esters are hydrolytically unstable [6]. The method presented in this paper utilizes the reaction (Fig. 1) of methylboronic acid with pinacol, a 1,2-diol, as the basis for the quantification of methylboronic acid in a formulation that contains several other components.

TABLE I

EFFECT OF TIME ON THE EXTRACTION OF METHYLBORONIC ACID FROM THE FORMULATION AND FORMATION OF THE DERIVATIVE

In this experiment, 1.0 *M* hydrochloric acid was used instead of 400 μl of 1 *M* hydrochloric acid used under *Sample preparation*.

Time (min)	Area ratio[a]	Time (min)	Area ratio[a]
5	0.499	90	1.311
15	0.902	105	1.372
25	1.093	120	1.410
35	1.216	150	1.450
45	1.325	180	1.466
60	1.315	360	1.470
75	1.326		

[a] Area ratio = the area of the methylboronic acid to that of the internal standard.

The addition of hydrochloric acid as described under *Sample preparation* is imperative. Without the acid, (water only), methylboronic acid was only 20% recovered after 3 h at 60°C. The recovery did not improve after allowing the reaction to proceed overnight at room temperature. Table I illustrates the effect of time on the extraction and subsequent derivatization in the presence of 0.1 *M* hydrochloric acid. The recovery of methylboronic acid was complete after 3 h. At room temperature the reaction went to completion in approximately 20 h. The use of a smaller volume (400 μl) of a more concentrated (1 *M*) hydrochloric acid gave a more reproducible recovery than the 0.1 *M* hydrochloric acid. An added benefit to the use of the stronger acid was that the extraction mixture looked cleaner and, in fact, after the heating period, the two phases were nearly indiscernible. It is believed that this strongly acidic reaction condition causes the hydrolysis of cyclodextrin to maltosaccharides and glucose, eliminating the possibility of cyclodextrin-methylboronic acid inclusion complex formation [14].

It is important to use fresh tetrahydrofuran of high purity in the preparation of the standard stock solutions. Low-quality tetrahydrofuran can cause the blank to show a large number of peaks, some of which could interfere with the 1-butaneboronic acid derivative. It is advisable that the tetrahydrofuran

be purchased in small bottles sealed with PTFE-lined rubber septa and screw caps. The small volumes reduce the possibility of oxidation of the tetrahydrofuran and make purging of the bottles with nitrogen after use more practical. Protic solvents such as methanol could not be used because they react with boronic acids. Dimethoxypropane, which is commonly used as a water scavenger for moisture sensitive compounds, gives a peak that interferes with the methyl boronic acid derivative. Dimethoxypropane also forms methanol as a result of its reaction with water and the methanol is likely to react with methylboronic acid. Acetone could not be used because of incomplete solubility of 1-butaneboronic acid.

The accuracy of the method was established by analyzing portions of a placebo formulation (*i.e.* the formulation without methylboronic acid) spiked with varying amounts of methylboronic acid. As shown in Table II, added methylboronic acid was quantitatively recovered. The table also shows that the precision of replicate preparations is excellent. As shown in Table III for two levels of spiking, excellent precision was obtained for replicate injections of the same sample preparation.

Figs. 2–4 show typical chromatograms for a blank preparation (without the internal standard), working standard preparation and a typical sample preparation respectively. The retention times for methylboronic acid derivative, pinacol and 1-butaneboronic acid derivative are 3.3, 4.1 and 10.5 min, respectively.

TABLE II

RECOVERY OF METHYLBORONIC ACID FROM THE FORMULATION

The two values shown for each level of spiking represent replicate preparations, as each level was spiked in duplicate.

Added (mg/vial)	Found (mg/vial)	Recovered (%)
1.00, 1.00	1.06, 1.06	106.0, 106.0
2.00, 2.00	2.03, 1.99	101.5, 99.5
3.00, 3.00	3.05, 2.97	101.7, 99.0
4.00, 4.00	4.06, 4.08	101.5, 102.0
5.00, 5.00	5.00, 5.01	100.0, 100.2

TABLE III

REPRODUCIBILITY OF REPLICATE INJECTIONS AT TWO LEVELS OF SPIKING

Replicate No.	mg/vial found for level 1	mg/vial found for level 2
1	2.00	4.03
2	2.01	3.97
3	2.01	3.93
4	2.01	3.93
5	2.01	3.91
Mean	2.01	3.95
R.S.D.[a]	0.2%	1.2%

[a] R.S.D. = relative standard deviation.

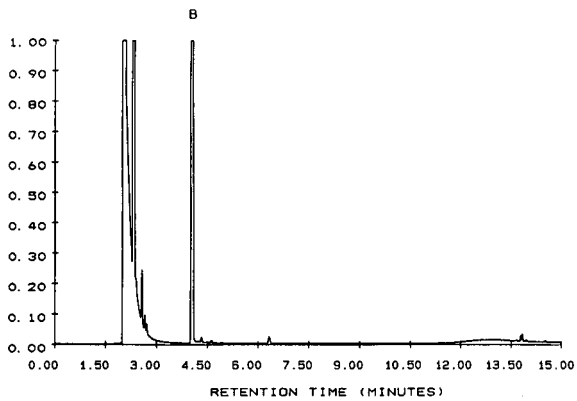

Fig. 2. A chromatogram of a blank preparation without the internal standard. Peak B is due to pinacol.

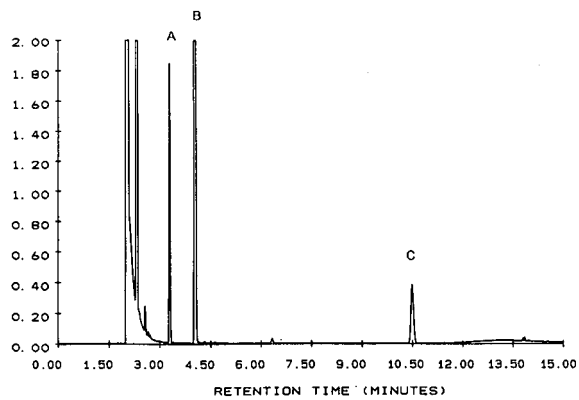

Fig. 3. A chromatogram of a working standard preparation. Peaks A, B and C are due to the methylboronic acid derivative, pinacol and 1-butaneboronic acid derivative, respectively.

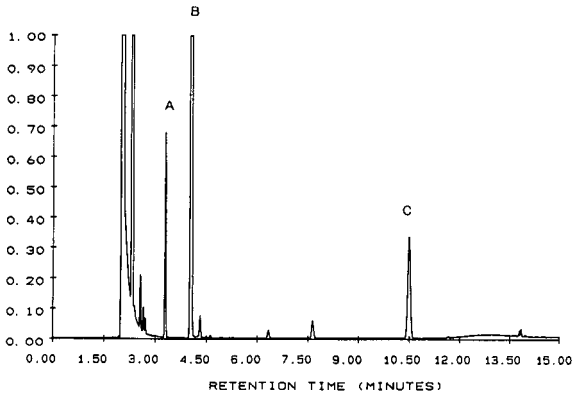

Fig. 4. A chromatogram of a typical sample preparation. Peaks A, B and C are due to the methylboronic acid derivative, pinacol and 1-butaneboronic acid derivative, respectively.

ACKNOWLEDGEMENT

The authors would like to acknowledge the technical assistance provided by Mrs. Betty Fodor.

REFERENCES

1 R. K. Narra, A. D. Nunn, B. L. Kuczynski, T. Feld, P. Wedeking and W. C. Eckelman, *J. Nucl. Med.*, 30 (1989) 1830.
2 E. N. Treher, J. Z. Gougoutas, M. F. Malley, A. D. Nunn and S. E. Unger, *J. Label. Comp. Radiopharm.*, 23 (1986) 118.
3 E. N. Treher, L. C. Francesconi, J. Z. Gougoutas, M. F. Malley and A. D. Nunn, *Inorg. Chem.*, 28 (1989) 3411.
4 G. M. Anthony, C. J. Brooks, I. Maclean and I.Sangster, *J. Chromatogr. Sci.*, 7 (1969) 623.
5 C. J. W. Brooks and I. Maclean, *J. Chromatogr. Sci.*, 9 (1971) 18.
6 S. Singhawangcha, L-E. Chen Hu, C. F. Poole and A. Zlatkis, *J. High Resolut. Chromatogr. Chromatogr. Commun.*, 6 (1978) 304.
7 C. F. Poole and A. Zlatkis, *J. Chromatogr.*, 184 (1980) 99.
8 W. C. Kossa, in R. W. Frei and J. F. Lawrence (Editors), *Chemical Derivatization in Analytical Chemistry*, Plenum Press, New York, 1981.
9 T. Yamaguchi, Y. Morimoto, Y. Sekine and M. Hashimoto, *J. Chromatogr.*, 239 (1982) 609.
10 C. J. W. Brooks and W. J. Cole, *J. Chromatogr.*, 399 (1987) 207.
11 C. Giachetti, G. Zanolo, A. Assandri and P. Poletti, *Biomed. Environ. Mass Spectrom.*, 18 (1989) 592.
12 T. Takano, S. Abe and S. Hata, *Biomed. Environ. Mass Spectrom.*, 19 (1990) 577.
13 J. Zamecnik, *J.Anal. Toxicol.*, 14 (1990) 132.
14 J. Szejtli, *Cyclodextrins and their Inclusion Complexes*, Akademiai Kiado, Budapest, 1982.

Journal of Chromatography, 585 (1991) 353–358
Elsevier Science Publishers B.V., Amsterdam

CHROM. 23 648

Short Communication

Near-continuous measurement of hydrogen sulfide and carbonyl sulfide by an automatic gas chromatograph

Eric R. Lindgren and David W. Pershing*

Chemical Engineering Department, University of Utah, Salt Lake City, UT 84112 (USA)

David A. Kirchgessner and Dennis C. Drehmel

U.S. Environmental Protection Agency, Air and Energy Engineering Research Laboratory, Research Triangle Park, NC 27711 (USA)

(First received February 20th, 1990; revised manuscript received July 19th, 1991)

ABSTRACT

An automatic gas chromatograph with a flame photometric detector that samples and analyzes hydrogen sulfide and carbonyl sulfide at 30-s intervals is described. Temperature programming was used to elute trace amounts of carbon disulfide present in each injection from a Supelpak-S column in a single peak at the end of 15-min runs. The system was used to study the high-temperature fuel-rich sulfur capture reactions of hydrogen sulfide and carbonyl sulfide with injected calcium oxide sorbent, necessitating the nearly continuous measurement of these gaseous sulfur species. The hydrogen sulfide concentration ranged from 300 ppm to 3000 ppm and the carbonyl sulfide from 30 ppm to 300 ppm. The system was also used to monitor sulfur dioxide levels under fuel lean conditions, and the results compared very closely with sulfur dioxide measurements made simultaneously with continuous UV sulfur dioxide instrumentation.

INTRODUCTION

The combustion of coal produces acid rain precursors such as SO_2. Dry calcium based sorbent injection is a potential method for reducing SO_2 emissions from existing coal-fired boilers. A great deal of study has been devoted to the fuel lean SO_2 reaction [1–3]:

$$CaO(s) + SO_2 + \tfrac{1}{2} O_2 \rightarrow CaSO_4(s)$$

The study of this reaction is facilitated by use of continuous analyzers for the measurement of SO_2 which is the predominant sulfur species present at the high temperatures usually studied. Although the reaction is very fast, the high molar volume of calcium sulfate ($CaSO_4$) quickly plugs the porous CaO structure, and utilization of calcium is theoretically limited to *ca.* 50%.

The fuel rich reactions:

$$CaO(s) + H_2S \rightleftharpoons CaS(s) + H_2O$$

$$CaO(s) + COS \rightleftharpoons CaS(s) + CO_2$$

are kinetically faster than the SO_2 reaction [4] and the molar volume of CaS is so much less than $CaSO_4$ that complete calcium utilization is possible. The fuel rich reactions have not been extensively studied particularly under combustion conditions. One difficulty in studying the fuel rich reactions is having to continuously analyze the reduced sulfur species at the concentration levels of interest (up to 3000 ppm or higher).

0021-9673/91/$03.50

Reduced sulfur species have been continuously measured with the Barton coulometric titrator and the DuPont Model 460 UV SO_2 analyzer. The Barton instrument uses bromine as the active reagent; however, erroneously high readings are possible because of reactions with other materials such as terpenes and other hydrocarbons [5]. With the DuPont instrument, the reduced sulfur species are oxidized and measured as SO_2. Thus, information about the relative amounts of various reduced sulfur species is lost.

Gas chromatography (GC) offers a reliable and accurate method for measuring concentrations of various sulfur gases. The use of grab samples, however, provides only periodic analyses, which are not well-suited for the study of sulfur capture reactions. Variations in sorbent feed rate result in fluctuating final sulfur levels requiring multiple samples to obtain an average value. Automatic gas chromatographs have been described in the literature. Huber and Obbens [6] and De Souza [7] have both described automatic GC techniques for monitoring reduced sulfur species. These techniques were designed for lower sulfur levels (1 to 100 ppm), and a complex mix of sulfur species such that 6 to 10 min were required to complete the analysis. The present paper describes an automatic GC technique for measuring moderate levels (up to 3000 ppm) of H_2S and COS at 30-s intervals. Temperature programming was used to elute trace amounts of CS_2 present in each injection in a single peak at the end of 15-min runs.

EXPERIMENTAL

The top portion of a natural gas fueled (26.4 kW) furnace was operated substoichiometrically to study high temperature (1100 °C) sulfur capture reactions of entrained limestone particles under fuel rich conditions at various levels of sulfur concentration and calcium to sulfur molar ratio (Ca/S). Twenty-five per cent excess air was added to the bottom portion of the furnace, and the ultimate fuel lean sulfur capture was simultaneously measured. A detailed description of the furnace and an analysis of the results can be found elsewhere [8].

An automatic GC sampling system was constructed which allowed nearly continuous monitoring of H_2S and COS levels in the rich zone and is depicted in Fig. 1. The GC apparatus used was a Varian 3700 equipped with a dual flame Aerograph Flame Photometric Detector and a pneumatically controlled gas sample valve. The dual flame photometric detector separates the region of sample decomposition from the region of light emission to be measured. The response from this type of flame photometric detector is independent of the molecular form of the sulfur species and much less susceptible to hydrocarbon quenching than single flame photometric detectors [9].

The high temperature gas sample was taken from the furnace through a 0.75 m × 1.6 cm O.D. stainless steel, water-cooled phase discrimination probe. The core flow was 10 to 15 times the sample flow. The probe tip was designed so that the sample stream would have to flow back against the core flow direction as shown in Fig. 2; thus, most of the sorbent particles stayed in the core flow. The sample stream flowed along a water-cooled wall, which quickly quenched any reaction with remaining sorbent particles. The temperature of the sample stream was monitored and maintained above 120°C to prevent any condensation. The stream was then thoroughly filtered through heated submicron filters so that no sorbent or carbon black particles would contaminate the GC analytical system. The gas sample was delivered to the GC system via a 10 m × 0.4 cm heated PTFE tube. As much PTFE as possible was used in the sulfur gas sampling systems; however, the use of stainless steel in the probe construction and filter housings was unavoidable. Problems of H_2S adsorption on the stainless steel were minimized by heating the stainless surfaces (above 120°C) and sampling at a moderately high rate (1.4 std l/min dry; the flow was measured after the water was condensed out and corrected to 0°C and 1 atm). A small sample (*ca.* 25 ml/min) was drawn by vacuum through the GC sampling system from the main sample stream. The GC sampling and calibration system was made entirely of PTFE including all valves, fittings, and sample loop. H_2S adsorption was not a problem and, after a few minutes of sampling, the H_2S level would stabilize.

The GC sampling system consisted of three PTFE solenoid valves and a sample valve actuator all under timer controle. Solenoid valve V1a (see Fig. 1) was used when calibrating the GC (V1b closed), and V1b was used when sampling from the

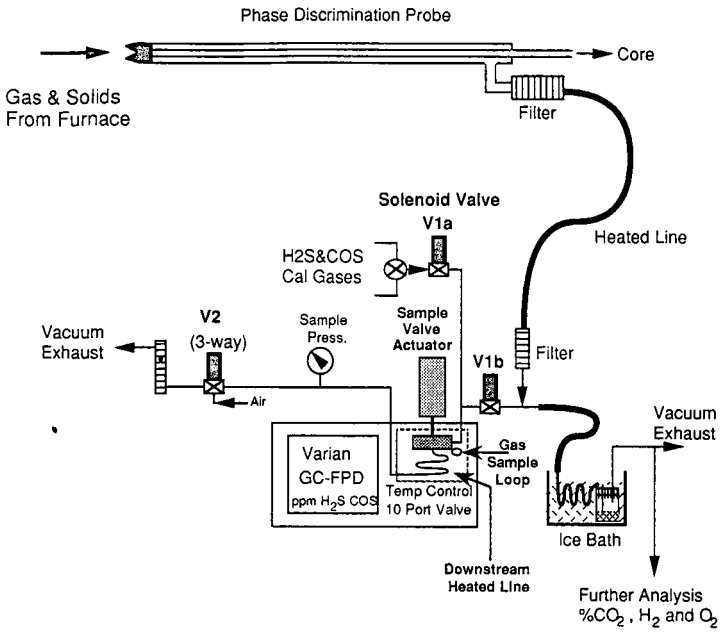

Fig. 1. Schematic of the fuel rich sampling system showing the phase discrimination sampling probe and the automated GC sampling system.

furnace (V1a closed). The distance between V1b and the gas sample valve was only 15 cm of 3.2 mm O.D. (1.6 mm I.D.) PTFE tubing so that very little flow was needed to get fresh sample into the sample loop.

The sampling cycle proceeded as follows: V1b and V2 would both be open for 10 s to allow fresh sample to be drawn into the gas sample loop (*ca.* 0.03 ml). Then V1b would close and V2 would switch allowing air to flow back toward the sample loop and pressurize the loop from about 660 mmHg to atmospheric (760 mmHg). A piece of 1 m of heated 3.2 mm O.D. PTFE tubing (2.0 ml volume) immediately down stream from the sample loop ensured that the flow back into the sample loop did not modify the sample (the sample loop volume was small compared to the volume of the downstream line; the heated PTFE prevented modification due to reaction, adsorption, or condensation; and the length of the downstream line prevented modification by diffusion). The sample system required 12 s to equilibrate to atmospheric pressure. The sample was then injected into the GC column with the sample valve actuator and 8 s were allowed to sweep out the sample loop. The sample valve would then return to the "load" position and V1b and V2 would open and again allow fresh sample to be drawn into the sample loop. Thus, the gas was sampled every 30 s.

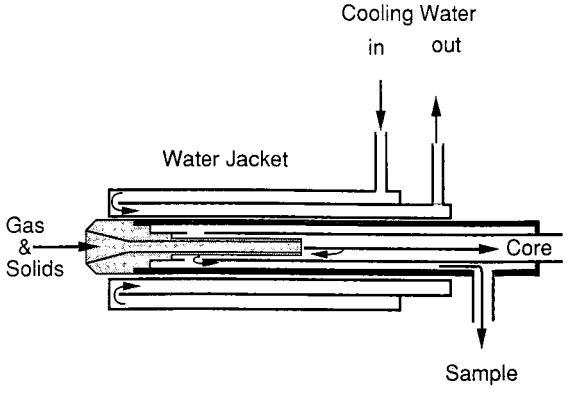

Fig. 2. Detail of phase discrimination probe and water jacket.

Because of the high concentration of H_2S to be measured, a very small sample loop was required. The sample loop used was approximately 6.4 cm × 0.08 cm I.D. for a sample volume of about 0.03 ml. The column used was a Supelco (Bellefonte, PA,

USA) Supelpak-S [46 cm packed (80/100 mesh) × 3.2 mm O.D. PTFE]. This column contains an acetone-washed porous polymer packing which requires no liquid phase. A distinct advantage of this column was that moisture in the sample did not degrade the packing so the analysis could be done on a hot, wet sample [10].

Calibration

Standard calibration gases of H_2S and COS mixtures were obtained from Scott Specialty Gases (Plumsteadville, PA, USA) and were used as received to calibrate the GC–flame photometric detection (FPD) system. Three different mixtures of H_2S/COS were used: 1025 ppm : 310.5 ppm, 1448 : 150.6, and 2980 : 75.39. These gases were certified to ± 1% except for the 1025 : 310.5 gas which was ±2%. Barometric pressure was monitored and corrections were made for any changes measured assuming the concentration in the sample loop was the same as that in the bottle when the sample loop pressure was 760 mm Hg absolute.

Table I shows the conditions used in the operation of the GC–FPD. The FPD apparatus was operated at the lowest sensitivity setting available and was set for square-root output mode. For the sample loop used, the highest concentration of H_2S measurable was *ca.* 1500 ppm when using the normal optimal operating conditions for the FPD. To measure H_2S concentrations up to 3000 ppm the sensitivity of the dual flame photometric detector was decreased by increasing the air rate to the upper emission producing flame (air No. 2) from 170 ml/min to *ca.* 190 ml/min. The additional oxygen in the emission flame probably prevented optimal conversion of the sulfur species to the detected excited diatomic sulfur species [9], thus reducing the sensitivity by a factor of 2.

Fig. 3 shows typical calibration curves (peak area *vs.* ppm sulfur gas in the sample loop) for both the normal and low sensitivity settings. For the normal settings using the square-root output mode, there is a linear response passing through zero and both the COS and H_2S data all fall on the same straight line. This indicates that with the dual flame photometric detector at normal operating settings the theoretical square-root FPD response [9] was achieved. For the low sensitivity setting and the square-root output mode, there was a linear response for concentrations 300 ppm and greater; however, the line does not pass through zero and the lower COS concentration data did not show a linear trend. This indicates that the theoretical square-root FPD response was not achieved with the low sensitivity settings.

TABLE I

GC CONDITIONS USED

Carrier gas	30 ml/min N_2
Sample volume	≈0.03 ml
Sample temperature	150°C
Detector temperature	150°C
Detector gas flows (dual flame)	
H_2	140 ml/min
Air No. 1	80 ml/min
Air No. 2	170 ml/min, normal 190 ml/min, low sensitivity
Temperature programme	
H_2S/COS	70°C for 15 min; increase linearly to 140°C over 2 min (35°C/min); hold at 140°C for 1 min
SO_2	90°C for 15 min; increase linearly to 140°C over 2 min (25°C/min); hold at 140°C for 1 min

The GC system was calibrated before and after each series of three sulfur capture runs, which on average took 1½ h to complete. Under normal FPD

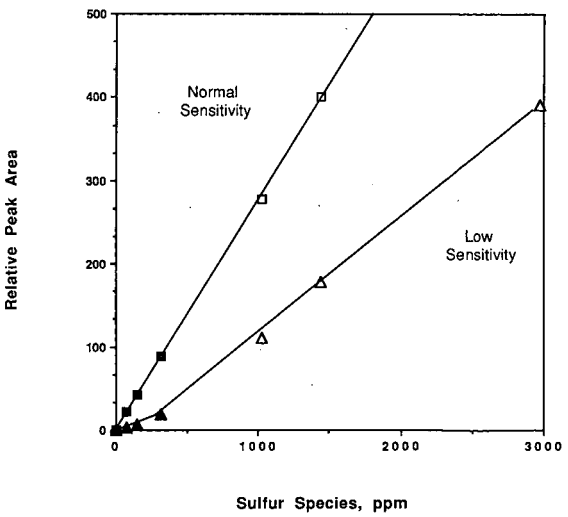

Fig. 3. Typical GC calibration curve. Open symbols: H_2S; solid symbols: COS.

conditions, the calibration for COS was taken as the linear regression fit of the three COS calibration points plus the point (0,0). The H_2S calibration was taken as the linear regression fit of the two H_2S calibration points, the highest COS calibration point and the point (0,0). Under the low sensitivity FPD conditions, the calibration for COS was taken as a cubic fit to the three calibration points, which were forced through the point (0,0). The H_2S calibration was taken as the linear regression fit of the three H_2S calibration points plus the highest COS calibration point. During the 3000 ppm sulfur capture runs, the concentration of H_2S never dropped below *ca.* 800 ppm.

RESULTS AND DISCUSSION

The H_2S and COS peaks were well separated using the Supelpak-S column at 70°C and 30 ml/min N_2 carrier. The retention time for H_2S and COS was 30 and 45 s, respectively. Just under 30 s were required for both peaks to completely elute which allowed multiple sample injections at 30-s intervals. Fig. 4 shows a typical GC trace for a sulfur capture run. There are 11 H_2S peaks before sorbent injection, 10 peaks during sorbent injection, and 10 peak after. The small, broad peak at the end is CS_2. The small amount of CS_2 in each injection did not elute during the 15 min of 70°C isothermal operation. At the end of each run a temperature program was started: 35°C/min for 2 min. The CS_2 from each injection eluted at this time.

The GC sampling and analysis technique could also be used to monitor SO_2 levels in the lean zone where SO_2 was the only sulfur species present. Fig. 5 shows a typical GC trace for SO_2 samples from the lean zone *ca.* 0.1 s after the addition of the excess air. This trace shows 8 peaks before, 12 peaks during and 8 peaks after sorbent injection. The retention time for SO_2 was 47 s, and a 30-s sampling interval allowed adequate time for each peak to elute. The same GC conditions as before were used for this analysis except that the initial isothermal temperature was raised to 90°C.

The lean SO_2 level was also measured simultaneously by a continuous UV analyzer that sampled from a point *ca.* 0.9 s after the addition of the excess air. Fig. 6 shows a comparison of the SO_2 levels as measured by each technique during simultaneous measurements. There is good agreement in the two curves in both the absolute level of SO_2 measured and trends due to variation in the sorbent feed rate. Very similar results were obtained in five other runs. These tests indicate that the rapid sample GC technique used in this study is an accurate method for nearly continuous monitoring of H_2S/COS or SO_2 in high temperature flue gases. The simultaneous lean SO_2 results also indicate that the fuel rich to fuel lean transition reactions are complete in less than 0.1 s.

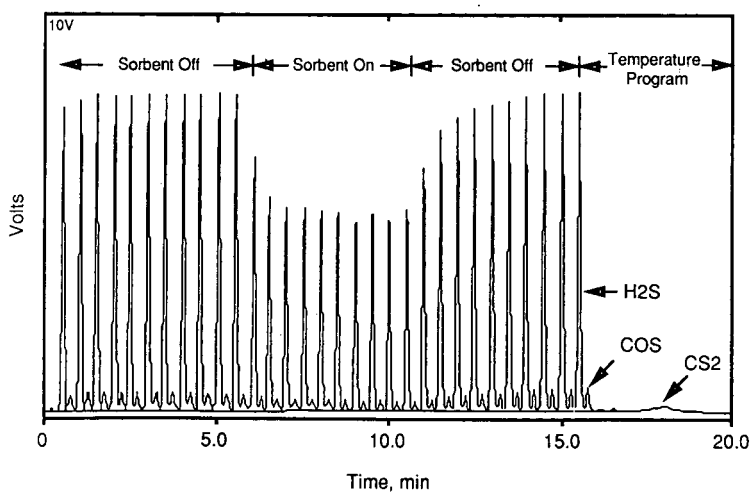

Fig. 4. Typical GC trace for a fuel rich sulfur capture run at Ca/S = 3.0. The H_2S and COS concentrations are reduced from 1430 ppm and 105 ppm to 910 ppm and 60 ppm, respectivley, for an overall fuel rich sulfur reduction of 37%. The GC conditions used are shown in Table I for H_2S/COS measurement at normal sensitivity.

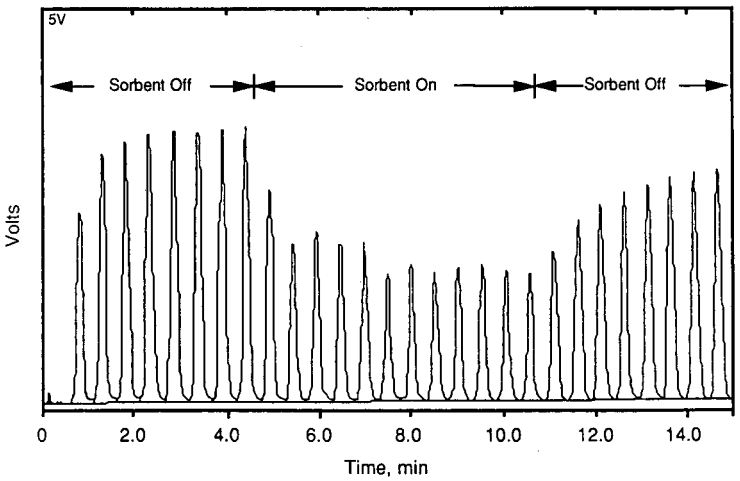

Fig. 5. Typical GC trace for measurement of fuel lean sulfur capture for Ca/S = 3.0. The SO_2 concentration is reduced from 1050 ppm to 475 ppm for an ultimate sulfur reduction of 55 percent. The GC conditions used are shown in Table I for SO_2 measurement at normal sensitivity.

ACKNOWLEDGEMENTS

The research summarized in this paper was supported by the U.S. EPA under Cooperative Agreement CR-811001. The furnace and analytical systems described in this paper are located at the EPA's Environmental Research Center in Research Triangle Park, NC, USA. The authors sincerely thank James H. Abbot and G. Blair Martin for making it possible to use this equipment. We also gratefully acknowledge the support and assistance of Robert H. Borgwardt and Brian K.Gullett, and thank them for the use of their support personnel and analytical equipment.

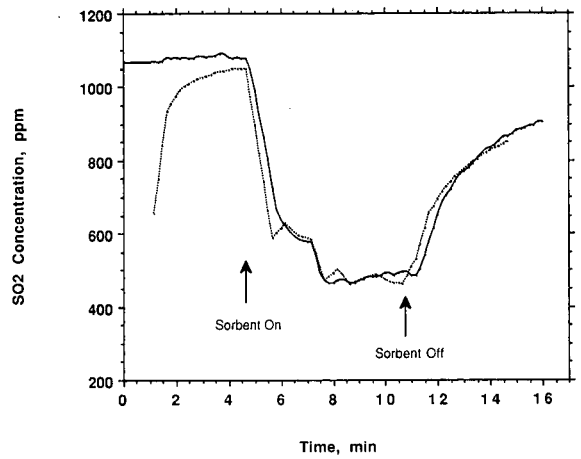

Fig. 6. Comparison of simultaneous SO_2 sulfur capture measurements. —— = Continuous analyzer; ---- = by GC.

REFERENCES

1 R. H. Borgwardt, K. R. Bruce and J. Blake, *Ind. Eng. Chem. Res.*, 26 (10), (1987) 1993.
2 G. D. Silcox, D. M. Slaughter and D.W. Pershing, *20th Symposium (International) on Combustion*, The Combustion Institute, Pittsburgh, PA, 1985.
3 G. Newton, *PhD Thesis*, University of Utah, Salt Lake City, 1987.
4 R. H. Borgwardt, *Environmental Progress*, 3 (2) (1984) 129.
5 T. L. C. de Souza, D. C. Lane and S. P. Bhatia, *Pulp Paper Can.*, 76 (1975) 73.
6 L. Huber and H. Obbens, *J. Chromatogr.*, 349 (1985) 465.
7 T. L. C. de Souza, *J. Chromatogr.*, 395 (1987) 413.
8 E. R. Lindgren, *Ph.D. Thesis*, University of Utah, Salt Lake City, 1990.
9 D. A. Ferguson and L.A. Luke, *Chromatographia*, 12 (1979) 197.
10 T. L. C. de Souza, *J. Chromatogr. Sci.*, 22 (1984) 470.

Journal of Chromatography, 585 (1991) 359–363
Elsevier Science Publishers B.V., Amsterdam

CHROM. 23 611

Short Communication

Effect of the substituents of β-diketonato ligands on R_F values of tris(chelate) transition metal complexes obtained by normal- and reversed-phase thin-layer chromatography on unmodified silica gel

Ž. Lj. Tešić, T. J. Janjić and M. B. Ćelap*

Faculty of Chemistry, University of Belgrade, P.O. Box 550, 11001 Belgrade (Yugoslavia)

(First received May 6th, 1991; revised manuscript received July 5th, 1991)

ABSTRACT

Three series of tris(β-diketonato) complexes of cobalt(III), chromium(III) and ruthenium(III), in which acetylacetonato ligands were successively replaced with dibenzoylmethanato ligands, were chromatographed on silica gel thin layers and the corresponding mechanisms were considered. The R_F values increased with non-aqueous and decreased with aqueous solvent systems. It was established that unmodified silica gel can be used as a sorbent for both normal- and reversed-phase chromatography of metal complexes. The earlier rule of a linear dependence between the R_M values of tris(chelate) transition metal complexes and the number of substituted chelate ligands by others was extended.

INTRODUCTION

In previous work [1] we studied the effect of the composition of coordinated β-diketonato ligands on the R_F values of transition metal complexes obtained by thin-layer chromatography (TLC) on silica gel. The investigations were carried out with complexes of Co(III), Cr(III), Ru(III) and Rh(III) of the non-electrolyte type containing three identical β-diketonato ligands. On the basis of the results obtained, it was concluded that the complexes investigated, using non-aqueous one- and two-component solvent systems, exhibited the higher R_F values the smaller was the electron density on the oxygen ligator atoms. This was explained by the mechanism of hydrogen bond formation between the oxygen ligator atoms and hydrogen atoms of the silanol groups of silica gel. However, when the solvent system was acetone–water (60:40, v/v), a reversed elution order of the complexes investigated was obtained, but no adequate explanation has so far given for this phenomenon. Continuing these studies, in this work we investigated, using non-aqueous and aqueous solvent systems, the chromatographic behaviour of three series of tris(chelate) β-diketonato complexes of Co(III), Cr(III) and Ru(III) in which acetylacetonato ligands were successively replaced with dibenzoylmethanato ligands. In this way we wanted to check the earlier established rule [2–5], valid for both paper chromatography [2,3] and TLC [4,5], of a linear dependence between the R_M values and the number n in the series of complexes of the type $[M(chel_1)_n(chel_2)_{3-n}]$, where M denotes an atom of Co(III),

0021-9673/91/$03.50

TABLE I

R_F VALUES OF THE COMPLEXES INVESTIGATED BY TLC USING ONE- AND MULTI-COMPONENT SOLVENT SYSTEMS

No.	Complex[a]	Ref.	$R_F \times 100$[b]																		
			1	2	3	4	5	6	7	8	9	10	11	12	13	14	15	16	17	18	19
1	$[Co(acac)_3]$	6,7	0	0	4	6	0	30	0	24	2	45	0	5	15	14	4	88	81	84	81
2	$[Co(acac)_2dibzac]$	6,7	3	3	15	16	2	64	2	68	5	59	2	16	45	40	10	65[c]	54[c]	73[c]	72[c]
3	$[Coacac(dibzac)_2]$	6,7	11	10	46	38	5	85	4	96	11	74	7	39	90	76	20	46[c]	22[c]	55[c]	52[c]
4	$[Co(dibzac)_3]$	6,7	41	34	77	68	12	95	8	F	21	84	20	65	F[d]	94	39	0	0	0	0
5	$[Cr(acac)_3]$	8,7	2	0	9	6	0	43	0	32	2	50	0	9	25	19	7	93	77	75	84
6	$[Cr(acac)_2dibzac]$	8,7	6	4	22	16	2	75	2	86	5	64	3	24	60	55	13	68[c]	51[c]	64[c]	67[c]
7	$[Cracac(dibzac)_2]$	8,7	18	14	53	37	6	86	5	F	12	78	10	50	97	86	23	38[c]	19[c]	44[c]	50[c]
8	$[Cr(dibzac)_3]$	8,7	40	44	77	68	24	F	10	F	25	87	28	75	F	97	45	0	0	0	0
9	$[Ru(acac)_3]$	9,7	0	0	7	22	0	40	0	30	0	42	5	7	20	14	6	90	87	81	86
10	$[Ru(acac)_2dibzac]$	9,7	14	11	33	35	4	96	3	96	4	64	11	23	62	76	13	70[c]	50[c]	71[c]	78[c]
11	$[Ruacac(dibzac)_2]$	9,7	34	22	76	50	9	F	5	F	13	80	20	48	90	98	25	46[c]	15[c]	56[c]	59[c]
12	$[Ri(dibzac)_3]$	9,7	59	41	94	66	24	F	9	F	29	88	35	71	F	F	49	0	0	0	0

[a] acac = 2,4-Pentanedionato ion; dibzac = 1,3-diphenyl-1,3-propanedionato ion.
[b] The compositions of the solvent systems are given in Table III.
[c] Small degree of fronting.
[d] F = front.

TABLE II

SLOPES OF THE REGRESSION LINES REPRESENTED FOR THE INVESTIGATED Co(III) CHELATES IN FIG. 2

Central atom	Solvent system																		
	1	2	3	4	5	6	7	8	9	10	11	12	13	14	15	16	17	18	19
Co(III)	2.41	1.17	2.35	1.86	1.52	2.00	1.16	1.74	1.36	1.00	2.01	1.90	3.17	2.44	1.44	−1.71	−2.17	−1.17	−0.55
Cr(III)	1.82	2.32	1.85	1.81	2.17	1.63	1.33	–	1.45	1.00	1.99	1.77	3.64	2.55	1.22	−2.40	−2.10	−1.07	−1.30
Ru(III)	1.28	1.01	2.31	0.82	1.18	–	0.68	–	1.34	1.00	0.99	1.50	2.10	3.35	1.14	−1.43	−2.14	−0.71	−0.85

Cr(III) or Ru(III), $chel_1$ and $chel_2$ represent chelate ligands of the same charge and n = 0–3. In addition, we wanted to give an explanation for the reversed elution order of complexes observed previously [1]. Finally, the aim of this work was also to compare the results obtained here with those reported previously [5] in which these complexes were chromatographed on polyacrylonitrile layers.

EXPERIMENTAL

Syntheses

All complexes investigated were obtained by direct synthesis, *i.e.*, by the action of a mixture of acetylacetone and dibenzoylmethane on the corresponding metal ion, whereby in each reaction all four possible complexes of a metal were obtained [6–9].

Chromatography

Chromatographic separations were carried out on silica gel plates (5 × 5 cm) (HPTLC Fertigplatten 60 für die Nano-DC; Merck, Darmstadt, Germany). Standard solutions (2 mg/cm^3) of the tris (β-diketonato) complexes investigated were prepared in chloroform and the plates were spotted with 0.2-μl aliquots of freshly prepared solutions. Before development, the spotted plates were placed for 30 min in a chromatotographic chamber (4 × 6 × 10 cm) saturated with vapour of the solvent system being used. All solvents were of analytical-reagent grade. After development, the spots of individual complexes were visible, owing to their natural colours.

TABLE III

SOLVENT SYSTEMS USED

No.	Composition	Proportions (v/v)
1	Benzene	
2	Toluene	
3	Dichloromethane	
4	Chloroform	
5	Xylene	
6	*n*-Butyl acetate	
7	1,1-Dichlorethylene	
8	*n*-Amyl acetate	
9	1,2,3,4-Tetrahydronaphthalene	
10	Toluene–tetrahydrofuran	85:15 (v/v)
11	Toluene–*n*-hexane	70:30 (v/v)
12	Toluene–dichloromethane	50:50 (v/v)
13	*n*-Butyl acetate–carbon tetrachloride	30:70 (v/v)
14	*n*-Butyl acetate–chloroform	30:70 (v/v)
15	Chloroform-carbon tetrachloride	60:40 (v/v)
16	Acetone–water	60:40 (v/v)
17	Ethanol–water	65:35 (v/v)
18	Dioxan–water	60:40 (v/v)
19	Methanol–water	75:25 (v/v)

RESULTS AND DISCUSSION

As can be seen from Table I, twelve tris(chelate) complexes of Co(III), Cr(III) and Ru(III), of the non-electrolyte type, containing acetylacetonato and/or dibenzoylmethanato ligands, were chromatographed on thin layers of silica gel, with nine one- and ten two-component solvent systems (Table III). The results obtained show that with non-aqueous one-component solvent systems (Table I, Nos. 1–9) the R_F values of metal complexes increase with increasing number of acetylacetonato ligands substituted by dibenzoylmethanato ligands. The same order of complexes was also obtained with slightly polar non-aqueous two-component solvent systems (Table I, Nos. 10–15). These results are in accordance with a specific interaction of these complexes with the sorbent, which involves the formation of hydrogen bonds between the electronegative oxygen ligator atoms of the chelate and hydrogen atoms of the silanol groups of silica gel. Owing to a negative inductive effect of the phenyl group, the electron density on the oxygen atoms of dibenzoylmethane is smaller than those of acetylacetone, which is why in the former instance the hydrogen bonds formed with the sorbent are weaker, causing a greater mobility of these complexes.

If the order of these complexes obtained by TLC on silica gel with slightly polar non-aqueous solvent systems is compared with that obtained on polyacrylonitrile [5], it may be concluded that this order is reversed. The reason is probably that in the former instance the separtion is due to the formation of hydrogen bonds, as already described, whereas in the latter the separation mechanism involves the interaction of π-electrons of aryl-β-diketonato ligands with cyano groups of the sorbent.

When chromatographic separations were carried out with solvents systems containing 25–40% of water, a reversed elution order of complexes relative

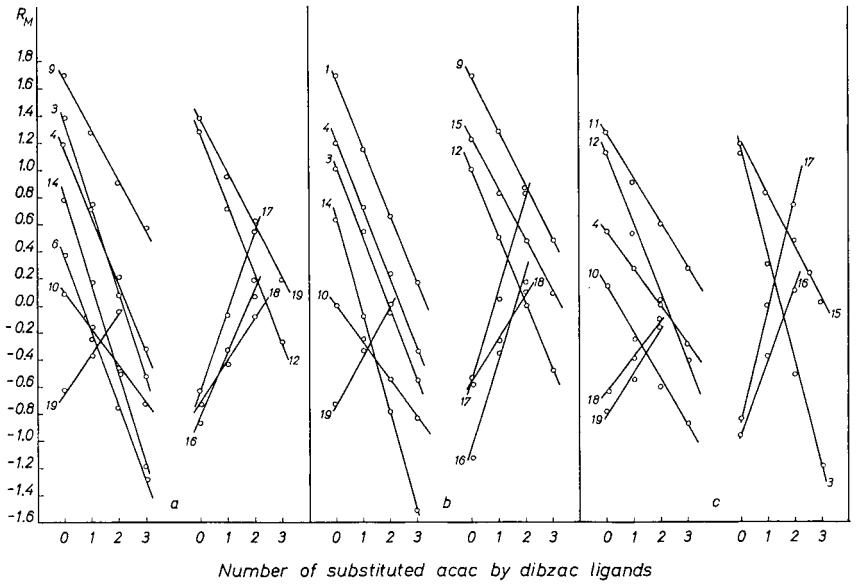

Fig. 1. Dependence of R_M values on the number of 2,4-pentanedionato ligands (acac) substituted by 1,3-diphenyl-1,3-propanedionato ligands (dibzac) in the $[M(acac)_n(dibzac)_{3-n}]$-type complexes ($n$ = 0–3). (a) Cobalt(III); (b) chrominum(III); (c) ruthenium (III). The numbers on the lines refer to the solvent system used (see Table III).

to that found when using non-aqueous solvent systems was obtained (Table I, Nos. 16–19). The latter is in accordance with the fact that more polar solutes elute later in normal-phase systems because the stationary phase is more polar than the mobile phase, and polar solutes elute first in reversed-phase systems because the stationary phase is less polar. In this way it was established for the first time that unmodified silica gel can be used as the sorbent for the reversed-phase chromatography of metal complexes.

The same order of complexes was also obtained in previous work [5] on TLC on polyacrylonitrile by the application of aqueous solvent systems, which was also ascribed to non-specific hydrophobic interactions.

This work also extends the above-mentioned rule [2–5] of a linear dependence between the R_M values of tris(chelate) transition metal complexes and the number of substituted chelate ligands by others in chromatographic separations with both non-aqueous and aqueous solvent systems on silica gel (Fig. 1).

In order to represent quantitatively the selectivity differences between some of the solvent systems

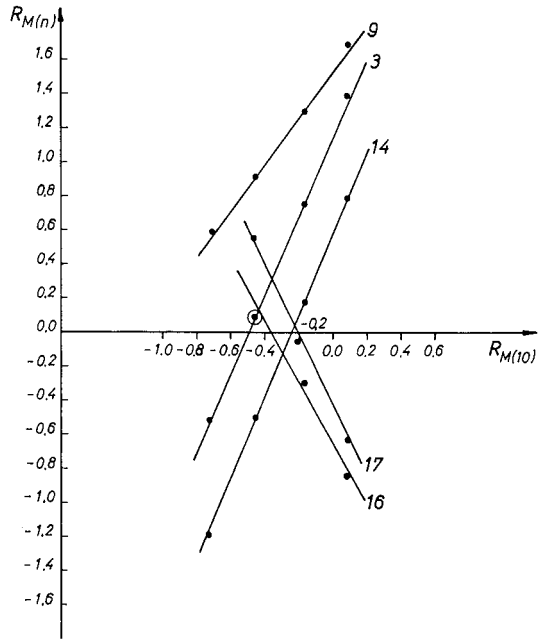

Fig. 2. Correlation between the R_M values of the investigated Co(III) chelates obtained on a thin layer of silica gel with a given solvent system and solvent system 10. $R_{M(n)}$ = R_M values obtained with the solvent system shown by the number on the line; see Table III; $R_{M(10)}$ = the same for solvent system 10.

used in this paper, in Fig. 2 the plots of the correlation between the R_M values of the investigated Co(III) complexes, obtained with solvents 3, 9, 14, 16 and 17 (see Table III), and their R_M values obtained with solvent system 10 are given [10]. In addition, in Table II the corresponding slopes for all three of the applied metals are given. As can be concluded from these data, in normal-phase chromatography the highest selectivity is achieved with solvents 13 and 14, and in reversed-phase chromatography with solvent systems 16 and 17.

ACKNOWLEDGEMENTS

The authors are grateful to the Serbian Republic Research Fund for financial support and to Dr. Ružica Tasovac and Mrs. Zorica Lukanić for elemental microanalyses.

REFERENCES

1 Ž. Lj. Tešić, T. J. Janjić, G. N. Vučković and M. B. Ćelap, *J. Chromatogr.*, 456 (1988) 346.
2 M. Lederer, *J. Chromatogr.*, 119 (1976) 285.
3 M. B. Ćelap, M. J. Malinar, S. Sarić, T. J. Janjić and P. N. Radivojša, *J. Chromatogr.*, 139 (1977) 45.
4 M. B. Ćelap, G. Vučković, M. J. Malinar, T. J. Janjić and P. N. Radivojša, *J. Chromatogr.*, 196 (1980) 59.
5 T. J. Janjić, D. M. Milojković, Ž. Lj. Tešić and M. B. Ćelap, *J. Planar Chromatogr.*, 3 (1990) 495.
6 J. Saar, *Inorg. Chim. Acta*, 122 (1986) 229.
7 Ž. Lj. Tešić, T. J. Janjić and M. B. Ćelap, *Izvodi Radova XXXII Savetovanje Hemičara SR Srbije*, Srpsko Hemijsko Društvo, Beograd, 1990, p. 16.
8 T. Sekine, M. Sano and K. Yoshihara, *Radiochim. Acta*, 48 (1989) 17.
9 L. Wolf, E. Butter and H. Weinelt, *Z. Anorg. Allg. Chem.*, 306 (1960) 87.
10 K. Saitoh, M. Kobayashi and N. Suzuki, *Anal. Chem.*, 53 (1981) 2309.

Journal of Chromatography, 585 (1991) 364–368
Elsevier Science Publishers B.V., Amsterdam

CHROM. 23 574

Short Communication

Electrophoretic mobility and dissociation constants of tripeptides evaluated by isotachophoresis

Takeshi Hirokawa*, Ryuji Sugino and Yoshiyuki Kiso

Applied Physics and Chemistry, Faculty of Engineering, Hiroshima University, Kagamiyama 1, Higashi-Hiroshima 724 (Japan)

(Received April 23rd, 1991)

ABSTRACT

Ionic mobilities and dissociation constants of twenty peptides (seventeen tripeptides and a few oligoglycines) were evaluated on the basis of the observed isotachophoretic qualitative indices R_E in the pH range 8.1–9.5 by the use of a least-squares method. Good correlation was obtained among the mobilities of amino acids, dipeptides and tripeptides when the clay ball model and the conventional formula weight were adopted.

INTRODUCTION

Ionic mobility and dissociation constants of ionic substances are the essential physico-chemical constants for the theoretical treatment of electrophoresis, including separation optimization. As discussed previously [1], isotachophoresis itself is a useful method for the evaluation of the mobility, dissociation constant and ion-pair formation constant when the pH dependence of the qualitative indices are measured accurately and data reduction software is available. The unique feature of the method in comparison with conventional techniques is that a sample mixture can be treated and the necessary amount for the measurement is very small (less than 1 μmol).

As reviewed by Pospichal *et al.* [2], the number of samples for which the mobility has been obtained is not more than about 500. We have evaluated a considerable number of absolute mobilities (m_0) and pK_a values by the use of isotachophoresis, including those of 25 amino acids [3] and 28 dipeptides [4].

In this work, the m_0 and pK_a values of twenty peptides (seventeen tripeptides and a few oligoglycines) were evaluated on the basis of the observed isotachophoretic qualitative indices R_E in the pH range 8.1–9.5. The least-squares method was used, utilizing a simulation technique of the isotachophoretic steady state. The correlation of the mobility among amino acids, dipeptides and tripeptides is briefly discussed on the basis of the clay ball model [4] and the conventional formula weight dependence.

EXPERIMENTAL

Samples

The twenty peptides used are summarized in Table I together with their abbreviations and formula weights. Oligoglycines were purchased from Tokyo Kasei Kogyo (Tokyo, Japan) and the other peptides from Sigma (St. Louis, MO, USA). Sample solutions (5 mM) were prepared by dissolving these dipeptides in distilled water. When the

0021-9673/91/$03.50

TABLE I

PEPTIDE SAMPLES, ABBREVIATIONS AND MOLECULAR WEIGHTS

Peptide	Abbreviation	Molecular weight
L-Alanyl-L-alanyl-L-alanine	$(Ala)_3$	231.2
DL-Alanylglycylglycine	AlaGlyGly	203.2
DL-Alanyl-DL-leucylglycine	AlaLeuGly	259.3
Diglycine	$(Gly)_2$	132.1
Triglycine	$(Gly)_3$	189.2
Tetraglycine	$(Gly)_4$	246.2
Pentaglycine	$(Gly)_5$	303.3
Hexaglycine	$(Gly)_6$	360.3
Glycylglycyl-L-isoleucine	GlyGlyIle	245.3
Glycylglycyl-D-leucine	GlyGlyLeu	245.3
Glycylglycyl-L-phenylalanine	GlyGlyPhe	279.3
Glycylglycyl-L-valine	GlyGlyVal	231.3
Glycyl-L-histidylglycine	GlyHisGly	269.3
Glycyl-DL-leucyl-DL-alanine	GlyLeuAla	259.3
Glycyl-L-leucyl-L-tyrosine	GlyLeuTyr	351.4
Glycyl-L-prolyl-L-alanine	GlyProAla	243.3
Glycyl-D-phenylalanyl-L-phenylalanine	GlyPhePhe	369.4
L-Leucylglycylglycine	LeuGlyGly	245.3
DL-Leucylglycyl-DL-phenylalanine	LeuGlyPhe	335.4
L-Leucyl-L-leucyl-L-leucine	$(Leu)_3$	357.5
L-Seryl-L-seryl-L-serine	$(Ser)_3$	279.3

solubility was low, a small amount of sodium hydroxide solution was added. The internal standards used to correct the asymmetric potential of PGD [5] were butyric acid, glycine and diglycine.

Operational electrolyte system

The leading electrolyte was 10 m*M* hydrochloric acid and the pH of leading electrolyte (pH_L) was adjusted to 8.10 (No. 1) and 8.41 (No. 2) by adding tris(hydroxymethyl)aminomethane, 8.80 (No. 3) and 8.92 (No. 4) by adding 2-amino-2-methyl-1,3-propanediol and to 9.50 (No. 5) by adding ethanolamine. The above pH_L range was determined on the basis that the pK_a values of dipeptides are in the range *ca.* 8–9 [4] and the pK_a values of tripeptides will not be much different from these values. All of the leading electrolytes contained 0.1% of hydroxypropylcellulose (HPC) to suppress electrode reactions and electroendosmosis.

The terminating electrolytes used were 10 m*M* β-alanine and 10 m*M* glycine. The pH of the terminating electrolyte was adjusted to *ca.* 10 by adding barium hydroxide in order to reduce the dilution effect caused by HCO_3^- [6,7]. pH measurements were carried out using a Horiba Model F7ss expanded pH meter.

Isotachopherograms were obtained using a Shimadzu IP-2A isotachophoretic analyser equipped with a potential gradient detector (PGD). The temperature was thermostated at 25°C. The PTFE separating tube used was 40 cm × 0.5 mm I.D. The driving current applied was 50 μA. Fig. 1 shows typical isotachopherograms for several peptides observed with the use of electrolyte system No. 3 (pH_L = 8.8).

The computer program SIPS-LSQ developed by us was used for the evaluation of m_0 and/or pK_a. The method is based on the simulation of an isotachophoretic zone to evaluate the isotachophoretic qualitative indices R_E; the difference between the observed and the simulated R_E values was minimized by varying m_0 and/or pK_a repeatedly. The program was written in Fortran 77. A typical calculation took 1 min on an NEC PC-9801RA microcomputer (80386–80387, clock 20 MHz).

RESULTS AND DISCUSSION

Evaluated mobility and pK_a

The observed R_E values are summarized in Table II together with the R_E values of the internal standards. The asymmetric potential of PGD was corrected using mainly the simulated values for butyric acid [5]. The step heights in the isotachopherogram might be decreased by the dilution effect of carbonate from the terminating zone [6,7]. Therefore, the observed R_E values might be affected to some extent, although not seriously.

Table III summarizes the absolute mobility (m_0) and pK_a values for twenty peptides at 25°C evaluated by the least-squares method using the R_E values in Table II. The mean deviation between the observed and the best-fitted R_E values was 0.5–1.5% (maximum 2.4% for GlyPhePhe). Table III also shows the mobility and pK_a values of the constituent amino acids of the peptides and the internal standards. The pK_a values of oligopeptides were considerably different from those of the constituent amino acids [3]. However, the pK_a values of homologous oligopeptides of $(Gly)_2$–$(Gly)_6$ were

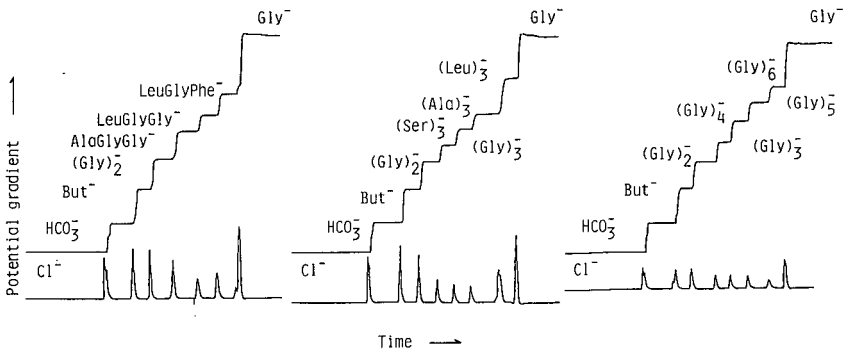

Fig. 1. Observed isotachopherograms of butyric acid, $(Gly)_2$, AlaGlyGly, LeuGlyGly, LeuGlyPhe, $(Gly)_3$, $(Ser)_3$, $(Ala)_3$, $(Leu)_3$, $(Gly)_4$, $(Gly)_5$ and $(Gly)_6$. Butyric acid (But) and $(Gly)_2$ were the internal standards. The leading electrolyte was 10 m*M* hydrochloric acid buffered by ammediol at $pH_L = 8.80$. The terminator was 10 m*M* glycine (pH $\approx$ 10 by adding barium hydroxide).

TABLE II

OBSERVED R_E VALUES OF PEPTIDES AT DIFFERENT pH_L VALUES

Sample	Electrolyte system and pH_L				
	No. 1, 8.10	No. 2, 8.41	No. 3, 8.80	No. 4, 8.92	No. 5, 9.50
β-Ala[a]	19.69	15.83	9.67	8.98	5.15
$(Ala)_3$	5.49	4.67	4.22	4.09	3.95
AlaGlyGly	4.86	4.21	3.73	3.71	3.40
AlaLeuGly	5.72	5.01	4.40	4.30	4.10
Butyric acid[a]	2.43	2.43	2.43	2.43	2.42
Gly[a]	10.77	8.75	5.64	5.27	3.37
$(Gly)_2$[a]	4.19	3.64	3.09	3.00	2.70
$(Gly)_3$	4.29	3.91	3.49	3.42	3.22
$(Gly)_4$	4.91	4.35	3.97	3.89	3.61
$(Gly)_5$	5.50	4.74	4.38	4.31	4.03
$(Gly)_6$	5.88	5.07	4.72	4.65	4.51
GlyGlyIle	5.12	4.58	4.19	4.12	3.88
GlyGlyLeu	5.10	4.66	4.21	4.11	3.83
GlyGlyPhe	4.95	4.59	4.17	4.08	3.83
GlyGlyVal	4.95	4.59	4.05	3.97	3.73
GlyHisGly	5.47	4.74	4.18	4.07	3.87
GlyLeuAla	5.72	4.97	4.48	4.36	4.06
GlyLeuTyr	6.15	5.34	4.67	4.59	4.03
GlyProAla	6.13	5.21	4.39	4.24	3.95
GlyPhePhe	6.13	5.07	4.39	4.61	4.45
LeuGlyGly	5.04	4.48	4.11	4.09	4.04
LeuGlyPhe	5.54	4.88	4.60	4.58	4.54
$(Leu)_3$	5.64	5.21	5.05	4.94	4.90
$(Ser)_3$	4.22	3.93	3.89	3.75	3.95

[a] Standards or terminators for R_E evaluation: the simulated R_E values are listed.

almost identical with each other. It should be noted that the possible divalent ion of GlyLeuTyr was not taken into account in the present evaluation and therefore the evaluated m_0 and pK_a values of GleuLeuTyr might contain considerable errors.

Determination of mobility of oligopeptides by the clay ball model

We have reported previously a simple equation to calculate the mobilities of dipeptides from those of the constituent amino acids [4], based on the assumption that the ions are spherical and the ionic volume of the dipeptides is equal to the sum of the volumes of the constituent amino acids, as if two clay balls merged into a larger ball. This model was applied to calculate the absolute mobilities of oligopeptides (ABC...), where A, B, C,... denote the constituent amino acids. The Stokes radii of the oligopeptides ($r_{ABC...}$) and the mobilities ($m_{ABC...}$) can be described on the basis of the present assumption as

$$r_{ABC...} = [3(V_A + V_B + V_C + ...)/4\pi]^{1/3} = (r_A^3 + r_B^3 + r_C^3 + ...)^{1/3} \quad (1)$$

and

$$m_{ABC...} = (m_A^{-3} + m_B^{-3} + m_C^{-3} + ...)^{1/3} \quad (2)$$

For oligoglycines $(Gly)_n$ (n = 2–6), the absolute mobilities calculated by the use of eqn. 2 were $29.7 \cdot 10^{-5}$, $25.9 \cdot 10^{-5}$, $23.6 \cdot 10^{-5}$, $21.9 \cdot 10^{-5}$ and

TABLE III

ABSOLUTE MOBILITIES (m_0) AND pK_a VALUES OF PEPTIDES, THE CONSTITUENT AMINO ACIDS AND THE INTERNAL STANDARDS

Sample	m_0		pK_a Observed
	Observed	Estimated	
$(Ala)_3$	22.2	22.3	8.245
AlaGlyGly	25.0	24.5	8.254
AlaLeuGly	21.3	21.3	8.272
$(Gly)_3$	26.1	25.9	8.102
$(Gly)_4$	23.3	23.6	8.142
$(Gly)_5$	21.2	21.9	8.167
$(Gly)_6$	19.3	20.6	8.107
GlyGlyIle	21.9	22.3	8.096
GlyGlyLeu	21.9	22.1	8.116
GlyGlyPhe	21.9	22.3	8.041
GlyGlyVal	22.6	23.0	8.125
GlyHisGly	22.5	23.0	8.279
GlyLeuAla	21.1	21.3	8.259
GlyLeuTyr[a]	21.0	17.1	8.405
GlyProAla	22.5	20.9	8.492
GlyPhePhe	19.7	20.2	8.216
LeuGlyGly	21.5	22.1	7.992
LeuGlyPhe	19.3	20.0	7.938
$(Leu)_3$	17.6	18.3	7.730
$(Ser)_3$	22.0	23.3	7.385
	m_0		pK_a
Butyric acid	33.8		4.820
Glycine	37.4		9.780
$(Gly)_2$	31.5		8.400
β-Alanine	30.8		10.241
Ala	32.2		9.857
Gly	37.4		9.780
Ileu	26.7		9.765
Leu	26.4		9.728
Phe	26.9		9.262
Val	28.4		9.710
Tyr	20.0		8.405
	40.0		10.189
Ser	33.6		9.302

[a] Analysed as a monovalent anion.

$20.6 \cdot 10^{-5}$ cm^2 V^{-1} s^{-1}. The mean deviation was 3.6%. Although the maximum deviation for $(Gly)_6$ of 6.3% may suggest that the estimate for the higher oligopeptides will be poor, the clay ball model gives a simple rule for calculating rough mobilities of such peptides. The good feature of this model is the applicability to heterogeneous oligopeptides as described previously [4]. The mean deviation for the twenty oligopeptides except for GlyLeuTyr was 1.2%. The worst deviation was found for GlyProAla and $(Ser)_3$ as −7.3 and 5.9%, respectively. By the least-squares method for the nineteen peptides, the following equation between the observed m_0 and the estimated $m_{ABC...}$ was obtained:

$$m_0 = 1.076 m_{ABC...} - 2 \cdot 10^{-5} \quad (3)$$

The coefficient in eqn. 3 suggests that the estimated $m_{ABC...}$ values were slightly underestimated in comparison with the observed values and the situation was the same as for dipeptides. The correlation coefficient between the observed m_0 and the estimated $m_{ABC...}$ values was 0.95 and the mean deviation between the estimated and the observed m_0 values was 1.8%.

On the other hand, it has been well established that the mobility can be correlated with formula weight. For all of the oligopeptides treated, the following equation was obtained by the least-squares method:

$$m_0 = (293.2/\sqrt{FW} + 3.78) \cdot 10^{-5}\ cm^2\ V^{-1}\ s^{-1} \quad (4)$$

where m_0 is the absolute mobility of the monovalent ion and FW the formula weight. The mean deviation between the estimated and the observed mobilities was 3.5% for the twenty peptides. The deviation for $(Leu)_3$ and GlyLeuTyr was as high as −9.6% and 7.5%, respectively. If these were omitted, the mean deviation decreased to 2.9%. By the least-squares method for the nineteen peptides, the following equation between the observed m_0 and the estimated $m_{ABC...}$ values was obtained when eqn. 4 was used:

$$m_0 = 0.989 m_{ABC...} - 2.3 \cdot 10^{-6} \quad (5)$$

The correlation coefficient was 0.89.

For oligoglycines, a better mobility was obtained by the use of the conventional formula weight. The following equation expresses the mobility of oligoglycines, Gly_n (n = 1–6):

$$m_0 = (291.39/\sqrt{FW} + 4.66) \cdot 10^{-5}\ cm^2\ V^{-1}\ s^{-1} \quad (6)$$

The mean deviation for $(Gly)_n$ (n = 1–6) was 2.2% and the correlation coefficient was 0.992.

REFERENCES

1 T. Hirokawa and Y. Kiso, *J. Chromatogr.*, 252 (1982) 33.
2 J. Pospichal, P. Gebauer and P. Bocek, *Chem. Rev.*, 89 (1989) 419.

3 T. Hirokawa, T. Gojo and Y. Kiso, *J. Chromatogr.*, 369 (1986) 59.
4 T. Hirokawa, T. Gojo and Y. Kiso, *J. Chromatogr.*, 390 (1987) 201.
5 T. Hirokawa, M. Nishino, N. Aoki, Y. Kiso, Y. Sawamoto, T. Yagi and J. Akiyama, *J. Chromatogr.*, 271 (1983) D1.
6 Th. P. E. M. Verheggen, J. C. Reijenga and F. M. Everaerts, *J. Chromatogr.*, 260 (1983) 471.
7 T. Hirokawa, T. Taka, Y. Yokota and Y. Kiso, *J. Chromatogr.*, 555 (1991) 247.

Journal of Chromatography, 585 (1991) 369–372
Elsevier Science Publishers B.V., Amsterdam

CHROM. 23 555

Short Communication

Studies of the electrophoretic behaviour of *p*-dihydroxyborylphenylalanine and related compounds by the three-spot method

Yoshinori Kitaoka*, Mitsue Kobayashi and Yowri Ujeno

Research Reactor Institute of Kyoto University, Kumatori-cho, Sennan-gun, Osaka 590-04 (Japan)

(First received April 8th, 1991; revised manuscript received June 7th, 1991)

ABSTRACT

The effects of capillary action and electro-osmotic flow on the electrophoretic migration of *p*-dihydroxyborylphenylalanine (BPA) and related compounds were determined by spotting a sample solution at three different positions on the support. The zone electrophoretic behaviour of phenylalanine analogues was studied in support solutions of various pH values. A specific interaction between BPA and oxalate ions was found, which will be useful in the isolation of BPA from phenylalanine analogues.

INTRODUCTION

The zone electrophoretic behaviour of a compound gives useful information on its chemical state in solution. However, the observed migration distance is usually a summation of capillary action, electro-osmotic flow and electrophoretic movement [1–3]. Thus on each run it is essential to measure the factors which affect the electrophoretic mobility. Capillary action and electro osmotic flow were determined in this work by spotting a sample solution at three different positions on a support.

During studies of the physicochemical nature of BPA, which has recently been used for boron neutron capture therapy [4], a specific electrophoretic interaction was found between BPA and oxalate ions. This interaction will be useful in isolating compounds with dihydroxyboryl groups.

EXPERIMENTAL

BPA (^{10}B-enriched) was purchased from Eagle-Picher Research Laboratory (Miami, FL, USA). Amino acids of guaranteed grade were purchased from Wako (Osaka, Japan). Supporting solutions [0.05 *M* potassium oxalate (pH 1.68 at 25°C), 0.05 *M* hydrogen potassium phthalate (pH 4.01), phosphate buffer (pH 6.68), 0.01 *M* sodium borate (pH 9.18) and carbonate buffer (pH 10.02)] were also purchased from Wako. The support was Toyoroshi No. 51A filter paper (51 A, 2 × 40 cm), which was cut into pieces of 1 × 40 cm.

The apparatus and procedures used were similar to those described previously [3]. To reduce the analysis time, the electric voltage was usually applied to the spotting strips (1 × 40 cm) soon after spotting. The temperature of the migration chamber was kept constant by circulating thermostatically controlled water in a glass tube in *n*-hexane. Sodi-

um chloride solutions (0.1 *M*) were used as the electrode cell solutions. First, a spotting strip was dipped in the supporting solution and the excess of supporting solution removed by another filter paper. A 3–5 μl volume of sample solution (about $5 \cdot 10^{-3}$ *M*) was spotted at the three different positions (A, 5 cm to the cathodic side from the centre of the strip; B, the centre; C, 5 cm to the anodic side) on the strip and wetted with the support solution. Six strips (three pairs) were set in parallel in *n*-hexane in the migration chamber and the electrode cells.

A constant electric voltage was applied to two pairs for 30 min at constant temperature. One pair was allowed to stand in the migration chamber without application of the electric voltage and was used to estimate the effect of capillary action. The amino acids on the strip were detected by spraying with ninhydrin solution.

RESULTS AND DISCUSSION

The movements due to capillary action under the electrophoresis conditions used (51 A filter paper, 30 min at about 15°C) were $+0.7 \pm 0.1$, 0.0 ± 0.1 and -0.7 ± 0.1 cm at the A, B and C positions, respectively (positive movement is towards the anode, negative movement towards the cathode). The movements depended mainly on the distances from the centre of a strip and did not vary with pH. The sample spotted at the centre of the strip did not move. The relationship between the migration distance of picric acid (PA) or phenylalanine (Phe) and the voltage gradient at the three spotting positions (A, B and C) is shown in Fig. 1. The observed migration distances of PA were proportional to the voltage gradients. The movements at zero voltage gradient are due to capillary action. As the support (Toyoroshi No. 51A) contains carboxy groups which dissociate in 0.1 *M* sodium chloride solution, all the migrants were affected by an electro-osmotic flow [5].

The pK_a values of Phe were 1.83 and 9.13 [6]. Thus the small migration distances of Phe are considered to be due to its zwitterions. When discussing chemical species, capillary action and electro-osmotic flow should be taken into account. Unless stated otherwise, the following data are taken from the observed migration distances spotted at the centre of the support.

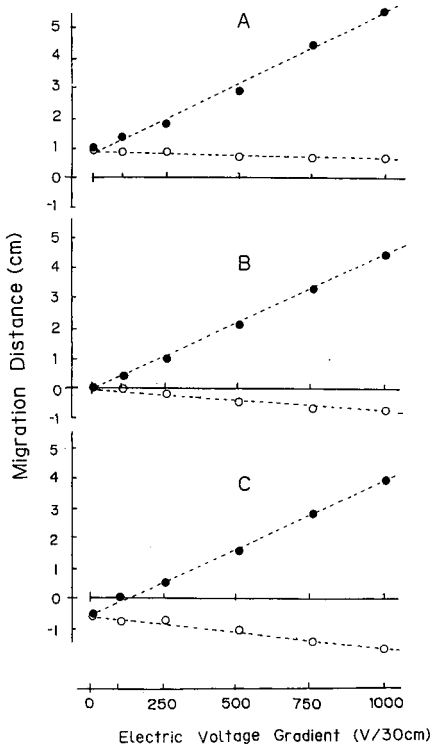

Fig. 1. Relationship between migration distance and voltage gradient. Sample solution: (●) $5 \cdot 10^{-3}$ *M* PA; (○) $5 \cdot 10^{-3}$ *M* Phe. Spotting positions: A, B and C. Electrophoresis conditions: support, Toyoroshi No. 51A; supporting solution, 0.1 *M* sodium chloride; migration temperature, about 15°C.

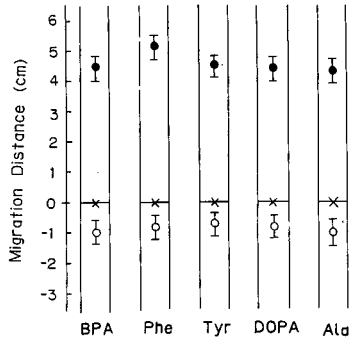

Fig. 2. Migration distances of phenylalanine analogues and picric acid in 0.1 *M* sodium chloride solution. Migrants: (●) PA; (○) sample (BPA, Phe, Tyr, DOPA and Ala). Electrophoresis conditions: 1000 V per 30 cm; time 30 min; migration temperature, 15°C; support, Toyoroshi No. 51A; starting position, ×; spotting position, B.

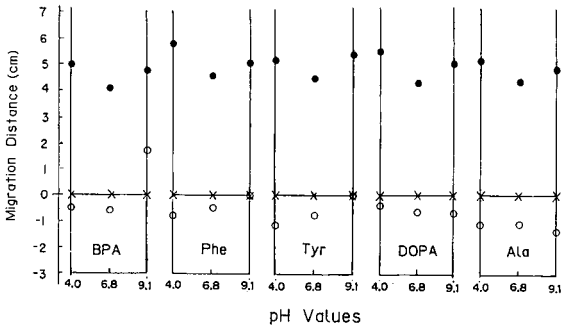

Fig. 3. Migration distances for various pH values of the supporting solution. Electrophoresis conditions and symbols as in Fig. 2. The pH values of the supporting solutions were 4.0, 6.8 and 9.1, respectively.

Fig. 2 shows the migration distances of phenylalanine analogues [BPA, Phe, tyrosine (Tyr), 3,4-dihydroxyphenylalanine (DOPA), alanine (Ala)] and PA. All the amino acids showed similar migration distances. The reproducibilities of the observed migration distances in a 0.1 *M* sodium chloride solution were not good because of its weak buffering capacity [7].

The migration distances in supporting solutions of various pH values are shown in Fig. 3. The observed migration distances of PA varied with the supporting solutions as a result of differences in the electric currents and pH values. The migration distances were similar, except for BPA at pH 9.1. The anionic migration of BPA at pH 9.1 seems to be due to the deprotonation of $-NH_3^+$ and/or the addition of OH^- to $-B(OH)_2$ groups in BPA molecules.

The electrophoresis was carried out in a strong acid solution containing oxalate ions. Surprisingly, an anionic migration of BPA was observed in the acid solution. In general, in acidic solution, the amino groups in amino acids should be protonated and the carboxy groups do not dissociate. Consequently, all the usual amino acids should behave as cations. Phe, Tyr, DOPA and Ala showed the usual cationic movements whereas BPA showed anionic movement (Fig. 4). To study this further, electrophoresis was performed in a mixture of oxalate and 0.1 *M* sodium chloride solution (Fig. 5). Results similar to those in Fig. 4 were obtained. When a hydrochloric acid solution was used instead of oxalate, this anionic movement was not observed. This means that the peculiar movement of BPA is closely related to the presence of oxalate anions. Considering the electron-deficient nature of boron atoms, it can be reasonably assumed that the dihydroxyboryl groups complex with the oxalate anions [8,9]. It was concluded that the anionic movement of BPA was due to the specific interaction between BPA and oxalate anions.

When the dissociation constant and molecular weight of the migrants are similar, it is difficult to separate them by normal electrophoresis methods.

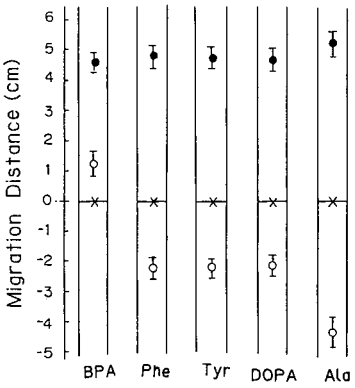

Fig. 4. Migration distances in potassium oxalate solution. Electrophoresis conditions and symbols as in Fig. 2. Supporting solution, 0.05 *M* potassium oxalate (pH 1.68 at 25°C).

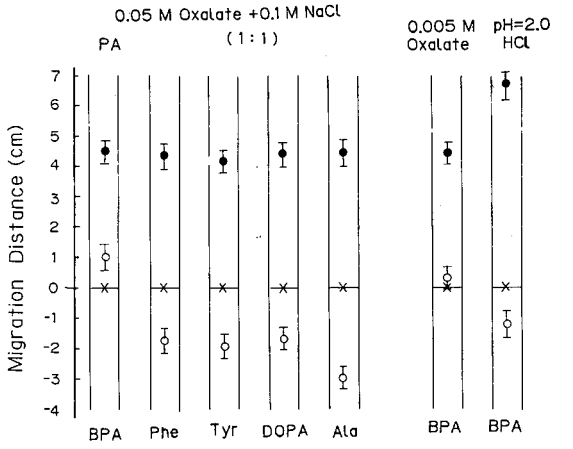

Fig. 5. Migration distances in diluted oxalate and hydrochloric acid solutions. Electrophoresis conditions and symbols as in Fig. 2. Supporting solutions: 0.05 *M* potassium oxalate–0.1 *M* sodium chloride (1:1, v/v); 0.005 *M* potassium oxalate; 0.001 *M* hydrochloric acid.

However, a dihydroxyboryl compound can easily be isolated from a mixture by using a supporting solution containing oxalate ions.

REFERENCES

1 J. R. Whitaker, *Paper Chromatography and Electrophoresis*, Vol. 1, Academic Press, New York, London, 1968.
2 Y. Kitaoka, *Bull. Chem. Soc. Jpn.*, 55 (1982) 2281.
3 Y. Kitaoka, *J. Chromatogr.*, 252 (1982) 301.
4 F. Barth, A. H. Soloway and R. G. Fairchild, *Sci. Am.*, Oct. (1990) 69.
5 Y. Kitaoka, *Annu. Rep. Res. Reactor Inst. Kyoto Univ.*, 19 (1986) 60.
6 T. Yamakawa (Editor), *Biochemical Data Book*, Vol. 1, Tokyokagakudoujin, Tokyo, 1979, p. 31.
7 Y. Kitaoka, *J. Chromatogr.*, 168 (1979) 241.
8 E. L. Muetterties, *The Chemistry of Boron and its Compounds*, Wiley, New York, 1967.
9 K. Kustin and R. Pizer, *J. Am. Chem. Soc.*, 91 (1969) 317.

Journal of Chromatography, 585 (1991) 373–375
Elsevier Science Publishers B.V., Amsterdam

CHROM. 23 589

Short Communication

Isolation and purification of bacterial proteinases by means of autofocusing

Vladimír Sitkey*, Ivana Travěncová and Martin Minárik

Research Institute LIKO, Miletičovà, P.O. Box 4, 820 06 Bratislava (Czechoslovakia)

(First received March 18th, 1991; revised manuscript received June 28th, 1991)

ABSTRACT

Autofocusing was used for the isolation and purification of neutral and alkaline proteinases from fermentation broth, after separation of cells. The yield of proteinases achieved was 19–78%, and was inversely proportional to the degree of purification, which varied from 3.0 to 7.9. Because of considerable losses of enzyme activity and the long duration of the process, autofocusing seems to be a non-economic technique for industrial isolation of relatively cheap enzymes.

INTRODUCTION

Attention has been drawn previously [1] to the possibility of industrial autofocusing as a new method for large-scale isoelectric separation of various substances and also of whole cells. Autofocusing is defined [2] as a modification of isoelectric focusing without carrier ampholytes. The pH gradient is created automatically during autofocusing by the substrate itself. The efficiency of the process depends on the conductivity of the working solution and on the concentration of the material to be separated.

We have tested autofocusing as a potential technique for isolation of bacterial proteinases.

EXPERIMENTAL

Instrumentation and conditions

An autofocuser of 1.1 dm^3 volume containing twenty cells (Technology Center of the Slovak Academy of Sciences, Košice, Czechoslovakia) was connected to a constant power supply (type VN, Development Workshops of Czechoslovak Academy of Sciences, Prague, Czechoslovakia).

For pH and conductivity measurements a Model OK 104 pH–conductivity meter (Radelkis, Budapest, Hungary) was used.

Autofocusing was carried out at 5°C, at a power of 3 W with a variable field strength from 200 to 1000 V until the current decreased to zero. The liquid concentrate of proteinases was dissolved in pure distilled water, so that the conductivity of the solution was less than 500 μS.

Preparation of proteinases

Neutral proteinase was obtained by cultivating *Bacillus cereus* CCM 3993 in submerged culture [3]. After treatment with flocculant [4], the cells were separated by centrifugation and the supernatant containing dissolved proteinase was concentrated in a Model DC-2 ultrafilter (Amicon, Lexington, KY, USA) on an H1P10-20 Diaflo hollow fiber cartridge having a molecular weight cut-off of 5000.

0021-9673/91/$03.50

Alkaline proteinase was prepared by cultivation of *Bacillus subtilis* CCM 3701 [5] and treated in the same way as neutral proteinase.

Analytical assays

The activity of neutral proteinase (PU/ml) was determined according to Keay and Wildi [6], and the activity of alkaline proteinase (FU/ml) was assayed by the FOLP method [7] using Hammarsten casein (Serva, Heidelberg, Germany) as a substrate in both cases.

Proteins were determined by the method of Lowry *et al.* [8], using bovine serum albumin (Serva) as a standard.

RESULTS AND DISCUSSION

Autofocusing of neutral proteinase

Fig. 1 shows the separation of neutral proteinase from the filtrate of fermentation broth. Along the step-like pH gradient created during autofocusing there are two main peaks corresponding to the maximum content of proteins and to the maximum proteolytic activity. The maximum specific activity of neutral proteinase (15 000 PU/mg) was in fractions 12 and 13 with pH values from 9.8 to 10.5. The degree of purification achieved in these fractions was approximately 5.0, but the yield of enzyme was only 42% as compared with the starting activity. After analysis of all fractions we found that the loss

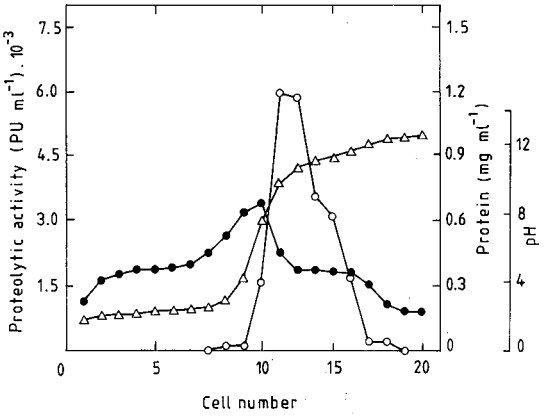

Fig. 1. Autofocusing of neutral proteinase. Processing conditions were: starting pH of the solution, 5.37; proteolytic activity, $1.7 \cdot 10^3$ PU/ml; conductivity 430 μS; time of autofocusing, 46 h. △ = pH gradient; ○ = proteolytic activity; ● = proteins.

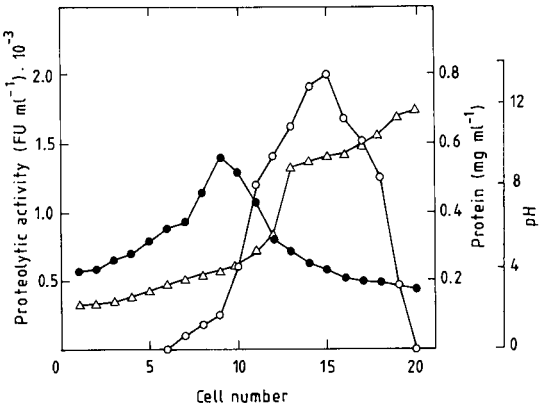

Fig. 2. Autofocusing of alkaline proteinase. Processing conditions were: starting pH of the solution, 7.44; proteolytic activity, $1.5 \cdot 10^3$ FU/ml; conductivity, 480 μS; time of autofocusing, 50 h. △ = pH gradient; ○ = proteolytic activity; ● = proteins.

of proteolytic activity due to inactivation during autofocusing was up to 19%. This phenomenon was caused by the extreme values of pH in the fractions on the border of the autofocuser, as neutral proteinase is inactivated at the pH values below 5 or above 10.

Autofocusing of alkaline proteinase

As follows from Fig. 2, the shift of the peaks corresponds to the partial separation of ballast proteins from the alkaline proteinase. However, the separation of alkaline proteinase is worse than in the case of neutral proteinase. This can be caused by large pI − pH differences in the pH gradient steps. The maximum specific activity was reached in fractions 14–16 (16 035 FU/mg) with a degree of purification of 7.9, the yield being only 19%. The pH values of this area lay in the interval from 9.2 to

TABLE I

COMPARISON OF THE AUTOFOCUSING EFFECT ON THE SEPARATION OF NEUTRAL AND ALKALINE PROTEINASES

Type of proteinase	Degree of purification	Yield (%)
Neutral	3.0	78
	5.6	42
Alkaline	5.6	40
	7.9	19

10.0 near the isoelectric point (9.4). Total loss of proteolytic activity caused by inactivation of enzyme owing to the long (50 h) effect of low pH in the fractions situated near the anode was up to 52%.

CONCLUSIONS

The results of the experiments, summarized in Table I, illustrate that autofocusing has different effects on the purification and the yield of neutral and alkaline proteinases. Partial separation of ballast proteins and the purification of both enzymes (from 3 to 7.9 times) were positive features of this process. In both cases colored impurities were focused to opposite sides of the box, so that fractions with the maximum proteolytic activity remained uncolored. Because of considerable losses of enzyme activity during this time-consuming process and the need to dialyze or to dilute the samples before separation, autofocusing seems to be an unsuitable technique for industrial recovery and purification of comparatively cheap enzymes like proteinases.

REFERENCES

1 O. Sova, *J. Chromatogr.*, 320 (1985) 213–218.
2 O. Sova, *J. Chromatogr.*, 320 (1985) 15–22.
3 E. Kuzmová, V. Sitkey and D. Majerčíková, *Czech. Patent*, 260 378 (1987).
4 V. Sitkey, E. Kuzmová and S. Krčmar, *Czech. Patent*, 270 124 (1987).
5 A. Šnajdrová, E. Kuzmová, V. Sitkey and J. Rojeková, *Czech. Patent*, 234 180 (1983).
6 L. Keay and B. S. Wildi, *Biotechnol. Bioeng.*, 12 (1970) 179–212.
7 L. M. Lupova, L. G. Federova and R. N. Grebeshova, *Prikl. Biochim. Mikrobiol.*, 9 (1973) 629–633.
8 O. H. Lowry, N. J. Rosebrough, A. L. Farr and R. Randall, *J. Biol. Chem.*, 193 (1951) 265–275.

Journal of Chromatography, 585 (1991) 376–377
Elsevier Science Publishers B.V., Amsterdam

CHROM. 23 622

Discussion

Comments on the Note "Liquid chromatographic determination of planar aromatic sulphur compounds in crude oil", *J. Chromatogr.*, 475 (1989) 421

Jan T. Andersson

Abteilung Analytische Chemie, Universität Ulm, Postfach 4066, W-7900 Ulm (Germany)

(Received February 22nd, 1991)

In a Note by Sinkkonen [1], some efforts were reported on the attempted separation of polycyclic aromatic sulphur heterocycles (PASHs) from polycyclic aromatic hydrocarbons (PAHs). This is not a trivial problem, and efforts have been made for several decades to accomplish this separation in many laboratories, but no completely satisfactory procedure is known to date. In the Note, three methods were tested, all of them having been described previously in the literature, and no new results of use were presented.

The three methods mentioned are (1) thin-layer chromatography (TLC), (2) ligand-exchange chromatography (LEC) and (3) "oxidation of dibenzothiophenes to sulphones and analysis by high-performance liquid chromatography (HPLC)".

Thin-layer chromatography. Biphenyl and dibenzothiophene were used on silica and alumina as test substances to check whether a PAH and a PASH can be separated by normal-phase chromatography. It is well known that this separation does not succeed and in general that PAHs and PASHs of the same number of aromatic carbon atoms cannot be usefully separated on silica [2].

It was stated that they are separable on alumina; however, this is not necessarily very significant for the ultimate goal of the work, which is the separation of the two *classes* of compounds from each other from a very complex mixture such as a crude oil. In such a mixture there may be, *e.g.*, fluorenes and acenaphthylenes present which elute in the similar range to the above compounds. Further, such samples consist of mixtures of a large number of alkylated derivatives of all parent structures, obscuring any small separation that may be observed using parent compounds. Those limitations were not mentioned.

Normal-phase chromatography on silica or alumina is widely used (also in the Note) for the separation of aromatic compounds from alkanes in mixtures such as crude oils. Obviously no useful class separation of PAHs and PASHs has ever been observed by the literally hundreds of workers who have used this separation method.

Ligand-exchange chromatography. That dibenzothiophenes can easily be separated from PAHs, as reported in the Note, is already well documented in the literature (see, *e.g.*, the four references to LEC in the Note and ref. 2 here). This result is therefore far from new.

It is now well known that LEC on palladium(II) chloride–silica discriminates against those PASHs which contain a terminal thiophene [3], such PASHs elute in the PAH fraction. This method

0021-9673/91/$03.50

therefore does not provide a general method of separating PASHs from PAHs. This fact was not mentioned in the Note.

It is stated that the PASHs "partly eluted as PASH–$PdCl_2$ complexes which cannot be analysed by conventional means". A very simple remedy for this problem, involving the use of a small amount of aminopropyl-substituted silica, was described in 1987 [3].

The use of silver nitrate–silica was mentioned as an alternative; a closer examination has already shown it not to be a very useful alternative for the desired separation [4].

Oxidation. The statement that sulphones of PASHs cannot be analysed by gas chromatography is not true, there is absolutely no problem in doing this [5,6]. Hundreds of such sulphones have been routinely analysed by gas chromatography. The oxidation–reduction procedure is singularly ill-suited for the analysis of PASHs as the finally isolated PASH fraction frequently shows very little similarity to the starting mixture [7]. This was also indicated by the workers who introduced the procedure [8].

It is difficult to say whether the reversed-phase HPLC of the oxidized fraction of a Russian crude oil, described in the Note, is relevant or not, but as it is known that the oxidation method used in producing the sample for this chromatographic step so drastically alters the sample components (and not only effects the oxidation of PASHs to their dioxides), it is not very plausible that it is of any use for the determination of the aromatic sulphur components, which was the aim of the whole work.

REFERENCES

1 S. Sinkkonen, *J. Chromatogr.*, 475 (1989) 421.
2 J. T. Andersson, *Fresenius' Z. Anal. Chem.*, 326 (1987) 425.
3 J. T. Andersson, *Anal. Chem.*, 59 (1987) 2207.
4 J. T. Andersson, *Fresenius' Z. Anal. Chem.*, 327 (1987) 38.
5 J. T. Andersson, *J. High Resolut. Chromatogr. Chromatogr. Commun.*, 7 (1984) 334.
6 J. T. Andersson, *J. Chromatogr.*, 354 (1986) 83.
7 J. T. Andersson, poster presented at the *15th International Symposium on Chromatography, Nürnberg, October 1–5, 1984.*
8 R. C. Kong, M. L. Lee, M. Iwao, Y. Tominaga, R. Pratap, R. D. Thompson and R. N. Castle, *Fuel*, 63 (1984) 702.

Journal of Chromatography, 585 (1991) 378
Elsevier Science Publishers B.V., Amsterdam

CHROM. 23 560

Book Review

Analytical Biotechnology —Capillary electrophoresis and chromatography (ACS Symposium Series, No. 434), edited by Cs. Horváth and J. N. Nikely, American Chemical Society, Washington, DC, 1990, X + 213 pp., price US$ 49.95, ISBN 0-8412-1819-6.

This book contains eleven contributions, namely: (1) High-resolution nanotechnique for separation, characterization and quantitation of micro- and macromolecules: capillary electrophoresis, by N. A. Guzman, L. Hernandez and S. Terabe; (2) Applications of capillary zone electrophoresis to quality control, by R. G. Nielsen and E. C. Rickard; (3) Analysis of cyclic nucleotides by capillary electrophoresis using ultraviolet detection, by L. Hernandez, B. H. Hoebel and N. A. Guzman; (4) On-column radioisotope detection for capillary electrophoresis, by S. L. Pentoney, Jr., R. N. Zare and J. F. Quint; (5) Strategies for an analytical examination of biological pharmaceuticals, by E. Canova-Davis, G. M. Teshima, T. J. Kessler, P.-J. Lee, A. W. Guzetta and W. S. Hancock; (6) Analytical chemistry of therapeutic proteins, by R. M. Riggin and N. A. Farid; (7) Improvement and experimental validation of protein impurity immunoassays for recombinant DNA products, by V. Anicetti; (8) Minimum variance purity control of preparative chromatography with simultaneous optimization of yield: using HPCL as an on-line species-specific detector, by D. D. Frey; (9) Amino acid sequence–mass spectrometric analyses of mating pheromones of the ciliate *Euplotes raikovi*, by R. A. Bradshaw, S. Raffioni, P. Luporini, B. Chait, T. Lee and J. Shively; (10) Micropellicular sorbents for rapid reversed-phase chromatography of proteins and peptides, by Cs. G. Horváth; and (11) Displacement chromatographic separations on β-cyclodextrin–silica columns, by G. Vigh, G. Quintero and G. Farkas.

At first glance, the book looks like a collection of diverse contributions only, ranging from a comprehensive survey of a field (10), via an overall introduction to the methodology of a technique (1) and a mathematical–statistical recipe for the optimization of the yield of a preparative technique (8), to a contribution that is in fact a short original note (3), as presented at the *196th National Meeting of the American Chemical Society, Los Angeles, CA, September 25–30, 1988.*

However, a more detailed examination of the book shows that the articles are very inspirative and the collection presented may provide a good orientation for bioanalytical chemists, separation scientists and genetic engineers involved in process development and monitoring in the biotechnology industry.

The drawback of the book is that the latest literature included relates to first part of 1989, which for capillary electrophoresis means that two great international symposia held since then are not covered.

Concerning presentation, the book is really diverse, with camera-ready reproductions ranging from high quality (5) up to hard-to-read pages covered with the maximum density of type (11).

The reviewer concludes that the book should be available in all biotechnology laboratories using chromatography and electrophoresis.

Bethesda, MD (USA) Petr Boček

Journal of Chromatography, 585 (1991) 379
Elsevier Science Publishers B.V., Amsterdam

CHROM. 23 602

Book Review

A practical guide to the care, maintenance and troubleshooting of capillary gas chromatographic systems, by D. Rood, Hüthig, Heidelberg, 1991, VIII + 191 pp., price DM 78.00, ISBN 3-7785-1898-4.

This book, as the title indicates, is a practical manual and is quite excellent. The first five or six chapters present background material regarding columns, their installation, carrier gases, basic definitions, test mixtures and so forth in a clear, descriptive way that should be intelligible to even the merest novice. Succeeding chapters deal at length with column damage, sample induced problems, operation and maintenance of injectors and detectors and an illuminating concluding chapter on troubleshooting.

The coverage is so comprehensive, and the presentation so explicit that one is left feeling that, with this book to hand, one can cope with anything that arises in the daily round of the gas chromatographic laboratory. I cannot recommend this volume too highly. A book of this kind has long been needed and the author is to be complimented on producing a manual that sets the standard for future essays into this area of laboratory practice.

Swansea (UK) Howard Purnell

Journal of Chromatography, 585 (1991) 380
Elsevier Science Publishers B.V., Amsterdam

CHROM. 23 675

Book Review

Unified separation science, by J. C. Giddings, Wiley, Chichester, 1991, XXIV + 320 pp., price £ 43.65, ISBN 0-471-52089-6.

This unique book is based on a series of lecture notes from the University of Utah. It treats the science of analytical separations as a unified discipline rather than as a collection of chapters on seemingly unrelated topics. Giddings' very successful approach is based on the physical–mathematical description of the mass transport phenomena underlying all separation processes. This gives a common basic theory, allowing the optimization and comparison of different separation methods. The very difficult tasks of integration and unifying the theory of all different branches of analytical separations is accomplished in a unique way. Many chapters are based on the formidable list of related publications by the author and his co-workers.

The text can be divided into two main parts. Part 1 (six chapters) includes the fundamental background of separations: flow, diffusion and equilibrium phenomena. Concepts such as Gaussian zone formation, band broadening, statistics of overlapping peaks and more dimensional separations are also discussed.

In Part 2, the general principles discussed in the theoretical Part 1 are applied to give a better understanding of specific methods. Three chapters cover chromatography, one is devoted to electrophoresis and sedimentation and one to several variants of field-flow fractionation. Also in Part 2 the emphasis is on the fundamental basis of separation. One can hardly find a description of apparatus, and recipes are altogether absent. Scientists interested in a specific application area will have to select a different book.

This book is intended for graduate students and working scientists interested in the fundamentals behind the analytical methods of separation. Exercises help the reader to develop and test the obtained physical insights.

Eindhoven (Netherlands) C. A. Cramers

Author Index

Erratum

J. Chromatogr., 557 (1991) 469–479
Page 473, eqn. 9 should read $q_1^2 = p_o / D$.

PUBLICATION SCHEDULE FOR 1992

Journal of Chromatography and Journal of Chromatography, Biomedical Applications

MONTH	O 1991	N 1991	D 1991	
Journal of Chromatography	25 585/1	1 585/2 8 586/1 22 586/2 29 587/1	20 587/2 27 588/1 + 2	The publication schedule for further issues will be published later
Cumulative Indexes, Vols. 551–600				
Bibliography Section				
Biomedical Applications				

INFORMATION FOR AUTHORS

(Detailed *Instructions to Authors* were published in Vol. 558, pp. 469–472. A free reprint can be obtained by application to the publisher, Elsevier Science Publishers B.V., P.O. Box 330, 1000 AH Amsterdam, The Netherlands.)

Types of Contributions. The following types of papers are published in the *Journal of Chromatography* and the section on *Biomedical Applications:* Regular research papers (Full-length papers), Review articles and Short Communications. Short Communications are usually descriptions of short investigations, or they can report minor technical improvements of previously published procedures; they reflect the same quality of research as Full-length papers, but should preferably not exceed six printed pages. For Review articles, see inside front cover under Submission of Papers.

Submission. Every paper must be accompanied by a letter from the senior author, stating that he/she is submitting the paper for publication in the *Journal of Chromatography*.

Manuscripts. Manuscripts should be typed in double spacing on consecutively numbered pages of uniform size. The manuscript should be preceded by a sheet of manuscript paper carrying the title of the paper and the name and full postal address of the person to whom the proofs are to be sent. As a rule, papers should be divided into sections, headed by a caption (*e.g.*, Abstract, Introduction, Experimental, Results, Discussion, etc.). All illustrations, photographs, tables, etc., should be on separate sheets.

Introduction. Every paper must have a concise introduction mentioning what has been done before on the topic described, and stating clearly what is new in the paper now submitted.

Abstract. All articles should have an abstract of 50–100 words which clearly and briefly indicates what is new, different and significant.

Illustrations. The figures should be submitted in a form suitable for reproduction, drawn in Indian ink on drawing or tracing paper. Each illustration should have a legend, all the *legends* being typed (with double spacing) together on a *separate sheet.* If structures are given in the text, the original drawings should be supplied. Coloured illustrations are reproduced at the author's expense, the cost being determined by the number of pages and by the number of colours needed. The written permission of the author and publisher must be obtained for the use of any figure already published. Its source must be indicated in the legend.

References. References should be numbered in the order in which they are cited in the text, and listed in numerical sequence on a separate sheet at the end of the article. Please check a recent issue for the layout of the reference list. Abbreviations for the titles of journals should follow the system used by *Chemical Abstracts.* Articles not yet published should be given as "in press" (journal should be specified), "submitted for publication" (journal should be specified), "in preparation" or "personal communication".

Dispatch. Before sending the manuscript to the Editor please check that the envelope contains four copies of the paper complete with references, legends and figures. One of the sets of figures must be the originals suitable for direct reproduction. Please also ensure that permission to publish has been obtained from your institute.

Proofs. One set of proofs will be sent to the author to be carefully checked for printer's errors. Corrections must be restricted to instances in which the proof is at variance with the manuscript. "Extra corrections" will be inserted at the author's expense.

Reprints. Fifty reprints of Full-length papers and Short Communications will be supplied free of charge. Additional reprints can be ordered by the authors. An order form containing price quotations will be sent to the authors together with the proofs of their article.

Advertisements. The Editors of the journal accept no responsibility for the contents of the advertisements. Advertisement rates are available on request. Advertising orders and enquiries can be sent to the Advertising Manager, Elsevier Science Publishers B.V., Advertising Department, P.O. Box 211, 1000 AE Amsterdam, Netherlands; courier shipments to: Van de Sande Bakhuyzenstraat 4, 1061 AG Amsterdam, Netherlands; Tel. (+31-20) 515 3220/515 3222, Telefax (+31-20) 6833 041, Telex 16479 els vi nl. *UK*: T. G. Scott & Son Ltd., Tim Blake, Portland House, 21 Narborough Road, Cosby, Leics. LE9 5TA, UK; Tel. (+44-533) 753 333, Telefax (+44-533) 750 522. *USA and Canada*: Weston Media Associates, Daniel S. Lipner, P.O. Box 1110, Greens Farms, CT 06436-1110, USA; Tel. (+1-203) 261 2500, Telefax (+1-203) 261 0101.

This comprehensive book covers all important separation methods

Chromatography Today

by **C.F. Poole** and **S.K. Poole**, Wayne State University, Detroit, MI, USA

Chromatography Today provides an extensive coverage of all important chromatographic methods in a single text. Gas, liquid, thin layer and supercritical fluid chromatographic and capillary electrophoretic methods are handled with an emphasis on the contemporary practice.
Particular attention is given to the optimization of these techniques. Method selection then becomes a more logical process.
As an integral part of the total analytical technique, sample preparation methods as well as preparative scale separations are treated fully. The most common hyphenated techniques used for sample identification are also discussed.

Scope and level of **Chromatography Today** make the book suitable for:
- graduate level students as a textbook in separation science;
- professional institutes offering short courses in chromatography;
- chromatographers who may use the book to refresh their knowledge in the field.

Chromatography Today offers:
- a comprehensive collation of all relevant equations, physical constants and general information used by chromatographers;
- extensive bibliography of recent literature to facilitate the location of specific items or areas of interest.

Chromatography Today is illustrated with over 200 figures, 110 tables and contains more than 3,330 references to contemporary literature.

Contents:

1991 x + 1026 pages
Price: US $ 147.50 / Dfl. 295.00
ISBN 0-444-88492-0

Paperback:
Price: US $ 75.00 / Dfl. 150.00
ISBN 0-444-89161-7

Elsevier Science Publishers

P.O. Box 211, 1000 AE Amsterdam, The Netherlands
P.O. Box 882, Madison Square Station, New York, NY 10159, USA